



Palladium-Catalyzed Arene Functionalization via Single-Electron Reduction of Selectfluor

Citation

Mazzotti, Anthony Renato. 2016. Palladium-Catalyzed Arene Functionalization via Single-Electron Reduction of Selectfluor. Doctoral dissertation, Harvard University, Graduate School of Arts & Sciences.

Permanent link

<http://nrs.harvard.edu/urn-3:HUL.InstRepos:33840680>

Terms of Use

This article was downloaded from Harvard University's DASH repository, and is made available under the terms and conditions applicable to Other Posted Material, as set forth at <http://nrs.harvard.edu/urn-3:HUL.InstRepos:dash.current.terms-of-use#LAA>

Share Your Story

The Harvard community has made this article openly available.
Please share how this access benefits you. [Submit a story](#).

[Accessibility](#)

Palladium-Catalyzed Arene Functionalization *via* Single-Electron Reduction of Selectfluor

A dissertation presented

by

Anthony Renato Mazzotti

to

The Department of Chemistry and Chemical Biology

In partial fulfillment of the requirements

for the degree of

Doctor of Philosophy

in the subject of

Chemistry

Harvard University

Cambridge, Massachusetts

July 2016

© Anthony Renato Mazzotti

All Rights Reserved.

Palladium-Catalyzed Arene Functionalization *via* Single-Electron Reduction of Selectfluor**Abstract**

Palladium-catalysis is commonly used in the functionalization of aromatic rings, ranging from prefunctionalized substrates such as aryl metals or aryl (pseudo)halides to the direct functionalization of aromatic C–H bonds. Palladium-catalyzed functionalizations typically proceed through a (trans)metallation step to generate an organometallic intermediate. The work in this thesis describes two palladium-catalyzed arene functionalization methodologies that forego the formation of an organometallic species. Instead, the catalysts reduce Selectfluor by a single electron to generate reactive intermediates: Selectfluor radical cation, which retains the fluoride and is an active fluorinating reagent, and TEDA²⁺, which loses the fluoride and is an active reagent for the functionalization of arene C–H bonds.

Chapter 1 describes the development of a method for the palladium(III)-catalyzed fluorination of arylboronic acid derivatives. The reaction is tolerant of air and moisture, able to be carried out in an open flask and was successfully performed on up to decagram scale. The reaction tolerates protic functional groups and bulky *ortho,ortho'*-disubstitution, and can be applied to the synthesis of natural product derivatives. We observe single electron oxidation of a bis-terpyridyl palladium(II) complex to generate a mononuclear palladium(III), the first mononuclear palladium(III) catalyst in the literature. Fluorination *via* a radical pathway renders the reaction tolerant of protic functionality and circumvents formation of protodeborylated side product commonly observed in other transition metal-mediated fluorination reactions.

Chapter 2 describes the development of an arene C–H functionalization method for

the incorporation of the doubly cationic residue of Selectfluor, TEDA, with high *para*-selectivity. The substitution of arene C–H bonds by TEDA selectively creates a protected aniline moiety and is tolerant of air and moisture, able to be performed with substrate as the limiting reagent and up to decagram scale without loss of yield. Subsequent reduction of the aryl-TEDA species by sodium thiosulfate provides pharmaceutically-relevant aryl piperazines directly in a one-pot, two-step sequence from the starting arene C–H bond. In the vast majority of cases, aryl piperazines are furnished as a single constitutional isomer across a wide variety of carboarene and heteroarene substrates.

TABLE OF CONTENTS

Acknowledgements	ix
Introduction.....	1
Fluorine in Organic Molecules	1
Impact of Aryl Fluorides in Medicinal Chemistry.....	2
Nucleophilic Arene Fluorination.....	5
Electrophilic Arene Fluorination	7
Radical Fluorination.....	12
C-H Bond Functionalization	14
Arene C-H Bond Functionalization: Chelation Assistance	15
Arene C-H Bond Functionalization: Electronically Biased Arenes	18
Arene C-H Bond Functionalization: Electronically Neutral Arenes.....	21
Chapter 1 – Palladium(III)-Catalyzed Fluorination of Arylboronic Acid Derivatives	25
Chapter 2 – Charge-Transfer-Directed Radical Substitution Enables <i>Para</i>-Selective C–H Functionalization	35
Chapter 3 – Experimental Methods.....	47
Materials and Methods.....	47
Experimental Procedures and Compound Characterization for Chapter 1¹⁰⁹	48
I. Representative Procedure for the Pd-Catalyzed Fluorination Reaction	48
II. Synthesis and Characterization of Palladium Complexes.....	49
III. Synthesis and Characterization of Non-Commerically Available Starting Materials	55
IV. Synthesis and Characterization of Aryl Fluorides	69
Evaluation of other [Pd] pre-catalysts (Data pertaining to Table 1.2).....	85

Evaluation of other arylboron reagents (Data pertaining to Scheme 1.2)	87
Evaluation of other nitrogenous ligands	89
Evaluation of other single-electron redox catalysts.....	91
Evaluation of radical clock substrates	92
Reaction Kinetics¹¹⁴	93
Kinetic Profile of Catalytic Reaction	93
Discussion of the structure of [(terpy)₂Pd][BF₄]₂ (1.5)	101
Binding Constant Analysis.....	103
In-Situ ¹H NMR of Pd-Catalyzed Fluorination Reaction	104
Derivation of the Rate Law for the Catalytic Reaction	106
Isotopic Labeling Experiment	109
Radiochemistry General Methods and Procedures	109
DFT Calculations.....	112
X-ray Crystallographic Analysis	117
[(terpy)Pd(MeCN)][BF ₄] ₂ (1.1) (CCDC 935776)	117
[(terpy) ₂ Pd][BF ₄] ₃ •[NaBF ₄] (3.1) (CCDC 935778)	123
[(terpy) ₂ Pd][BF ₄] ₂ (3.2) (CCDC 935779).....	126
EPR Data	130
EPR Spectrum of 1.2 with Simulated Spectrum. Frozen MeCN solution, 77 K.....	130
EPR Spectrum of 1.2 with Simulated Spectrum. Single Crystals, 298 K.....	130
Discussion of EPR Data	131
UV-vis/NIR Data	132
UV-vis Spectrum of 1.1 (DMF, 23 °C)	132
UV-vis/NIR Spectrum of 1.2 (MeCN, 23 °C)	133
UV-vis/NIR Spectrum of 3.2 (MeCN, 23 °C)	134
Electrochemical Data	134
General Methods.....	134

CV of [(terpy) ₂ Pd][BF ₄] ₃ (1.2)	135
CV of [(terpy)Pd(MeCN)][BF ₄] ₂ (1.1) with added terpyridine	136
CV of terpyridine.....	136
Discussion of electrochemical data.....	136
Experimental Procedures and Compound Characterization for Chapter 2¹²⁴.....	137
Synthesis and Characterization of Complex 1.....	137
General considerations for aromatic C–H TEDAylation reactions	138
Procedure for aromatic C–H TEDAylation reactions (1 equiv arene)	140
Procedure for aromatic C–H TEDAylation reactions (excess arene)	152
Fluoro-N,N,N-trimethylanilinium cations.....	161
Aromatic TEDAylation trials with 1.05 equivalents of Selectfluor	164
Selectivity of TEDAylation with Resonance Electron-withdrawing Substituents.....	166
Evidence for TEDA²⁺ radical dication as the C–N bond forming species	168
Observation of aliphatic C–H fluorination under TEDAylation conditions.....	169
Observation of Aryl–TEDA formation under copper catalysis	170
Positional Selectivity as a Function of Electron Affinity: A Discussion	172
Aromatic substitution of fluorobenzene by phthalimidyl radical	173
Synthesis of authentic samples of 3.14, 3.15, and 3.16	174
Aromatic substitution of fluorobenzene by piperidine aminium radical	176
Synthesis of authentic samples of 3.17, 3.18, and 3.19	177
Procedures for the preparation of aryl piperazines ¹²⁶	180
Positively Charged Oxyl Radicals.....	209
DFT Calculations.....	210
Calculation and visualization of Fukui indices.....	210
Electron affinity calculations	215
TEDA ²⁺ aminium radical electron affinity.....	216
Piperadine aminium radical electron affinity	218

Dimethylamine radical cation electron affinity	220
Phthalimide radical electron affinity	221
Propyloxyl radical electron affinity	223
2-(trimethylammonium)ethyl-oxyl radical electron affinity	224
2-(trimethylammonium)-1-(trimethylammoniummethyl)ethyl-oxyl radical electron affinity	226
References	229

ACKNOWLEDGEMENTS

First and foremost, I want acknowledge my appreciation for the graduate school experience itself. Graduate school has made me realize how little I know and how much I have to learn, especially from my colleagues. I have learned the value of collaboration in solving the truly difficult challenges. While it taught me the meaning of anxiety, it also provided me the tools to overcome it. Furthermore, I learned the skill of story telling, how to craft a narrative and deliver it to a group. It has made me a better scientist and a better human being.

I want to thank my advisor, Professor Tobias Ritter, for teaching me about project development. When I arrived in graduate school, I was bright-eyed and bushy-tailed and eager to change the world. I wanted to tackle the most impactful problems. Tobias taught me that the most important part of solving a problem was in picking the right one to solve. The second most important part was in learning everything in the literature surrounding the problem. While this approach did not initially feel too satisfying or productive, lab work itself is extremely slow. Spending time reading was the most efficient way to learn how to pick a direction without repeating the mistakes of the past.

I want to thank my graduate advising committee, Theodore Betley and Eric Jacobsen. Each have lended an ear when I needed it and have given me incredible advice over the last six years, especially during this past year serving as surrogate advisors while Tobias was in Germany. Both of them have helped me through some challenging times in graduate school and I appreciate it more than I can say. I especially want to thank Ted for helping me out during my second year; he told me what I needed to hear without sugarcoating it, and I'll forever appreciate his words of wisdom.

I want to thank my labmates, with whom I have spent countless hours. I have leaned

on them day in and day out for inspiration, guidance and most important of all, levity. For all they taught me on our joint projects, I thank Pingping Tang, Jennifer Murphy, Michael Campbell, Rob Cooper, Greg Boursalian, and Won Seok Ham. For sharing a laboratory space and tolerating my nonsense on a daily basis, I thank Jochen Brandt, Constanze Neumann, Hang Shi, and Rob Cooper. For their friendship above and beyond the call of duty, to the point of attending my wedding, I thank Charles Reese, Nickeisha Stephenson, Martin Strebl, and our former month-long rotating student Matthew Wilding. For helpful and enjoyable discussions on a nearly daily basis, I thank the entirety of the Ritter lab, both past and present. Graduate school is filled with many ups and many downs, but my labmates have been there with me every day and I sincerely appreciate them for all they have done.

I want to thank my chemistry teachers of the past. I want to thank Mr. Daley for putting up with me for 2 years in high school, for teaching me introductory chemistry and for writing me an overly generous letter of recommendation for the University of Illinois. He was with me during my first lab fire; I had dropped a crucible of burning ethanol down the front of my plastic labcoat. I also want to thank my undergraduate advisor, Professor M. Christina White. Without her second semester undergraduate organic chemistry course, I would probably have gone on to medical school. She made me realize how much organic chemistry was like puzzle solving. I wouldn't be writing this thesis without her support.

Most of all, I want to thank my family. My parents, Jayne and Jack, along with my twin sister, Erica, have been with me quite literally from the beginning. I don't know how I would have gotten through graduate school without their continuous love and support. I would like to thank my wife of two years, Michelle, for being by my side nearly the entire span of graduate school. We met in my second year and I can't think of a single instance in graduate school that wasn't made infinitely better by her in my life. Words can't express how much my family has meant to me throughout this entire process; thank you so much.

List of Abbreviations:

Ac: acyl
Ar: aryl
bipy: 2,2'-bipyridine
CMD: concerted metallation-deprotonation
cod: 1,5-cyclooctadiene
coe: cyclooctene
COSY: ^1H - ^1H Correlation Spectroscopy
 $\text{C}_{\text{S}}\text{Ar}$: concerted nucleophilic aromatic substitution
Cy: cyclohexyl
DCM: dichloromethane
DFT: density functional theory
DG: directing group
DMA: dimethylacetamide
DMF: dimethylformamide
dtbpy: 4,4'-di-*tert*-butyl bipyridine
EA: electron affinity
EPR: electron paramagnetic resonance
ESI-TOF: electrospray ionization – time of flight
Et: ethyl
FDA: Food and Drug Administration
HFIP: 1,1,1,3,3,3-hexafluoro-2-propanol
HOMO: highest occupied molecular orbital
HRMS: high resolution mass spectrometry
KIE: kinetic isotope effect
LC: liquid chromatography
m-CPBA: *meta*-chloroperoxybenzoic acid
Me: methyl
MeOBIPHEP: (6,6'-dimethoxybiphenyl-2,2'-diyl)bis(diphenylphosphine)
MIDA: *N*-methyliminodiacetic acid
MS: mass spectrometry
NFSI: *N*-fluorobenzenesulfonimide
NIR: Near-Infrared Spectroscopy
NMP: *N*-methyl-2-pyrrolidone
NMR: nuclear magnetic resonance spectroscopy
NOE(SY): Nuclear Overhauser Effect (Spectroscopy)
PET: positron emission tomography
pH: numeric scale to specific acidity or basicity of aqueous solution
Ph: phenyl
Phe: phenylalanine
Piv: pivalate
 pK_{a} : $-\log(\text{acid dissociation constant})$
 pK_{aH} : $-\log(\text{conjugate acid dissociation constant})$
S.E.T.: single electron transfer
 $\text{S}_{\text{E}}\text{Ar}$: electrophilic aromatic substitution
Selectfluor: *N*-fluoro-*N'*-(chloromethyl)-triethylenediamine
 $\text{S}_{\text{N}}\text{Ar}$: nucleophilic aromatic substitution
t-Bu: *tert*-butyl
TEDA: *N*-(chloromethyl)-triethylenediamine

terpy: 2,2':6',2''-terpyridine

THF: tetrahydrofuran

TMS: trimethylsilyl

TOCSY: Total Correlation Spectroscopy

Tyr: tyrosine

UV-Vis: Ultraviolet-visible

Publications:

The work in Chapter 1 and portions of Chapter 3 has been reproduced, with permission, from the following publication:

Mazzotti, A. R.;[†] Cambell, M. G.;[†] Tang, P.; Murphy, J. M.; Ritter, T.,
Palladium(III)-Catalyzed Fluorination of Arylboronic Acid Derivatives. *J. Am. Chem. Soc.* 2013, *135*, 14012-14015.

The work in Chapter 2 and portions of Chapter 3 has been reproduced, with permission, from the following publication:

Boursalian, G. B.; Ham, W. S.; **Mazzotti, A. R.**; Ritter, T., Charge-transfer-directed radical substitution enables para-selective C–H functionalization. *Nat Chem* 2016, *advance online publication*.

[†] Denotes equal contribution

INTRODUCTION

Fluorine in Organic Molecules

The fluorination of organic molecules is useful across a variety of industries for the development of agrochemicals,¹ pharmaceuticals,² electrooptics,³ polymers,⁴ and positron emission tomography (PET) radiotracers.⁵ Due to its extremely high electronegativity, the incorporation of fluorine in an organic molecule drastically alters its physical and chemical properties. In the context of the work described herein, the late-stage installation of aryl carbon-fluorine bonds has particular interest in the pharmaceutical and agrochemical industries. Strategic incorporation of fluorine into molecular architectures fine-tunes the oxidative stability, bioavailability, basicity, and binding affinity.⁶ In the 1970s, fluorinated compounds were rarely used in either of these industries. Over the past 40 years, the use of fluorinated molecules in the pharmaceutical⁷ and agrochemical^{1a,8} industries has increased over 20%, causing a drastic increase demand for the development of new methodologies for the installation of fluorine and fluorinated substituents. It should be noted that the late-stage installation of ¹⁸F is incredibly useful for the development of PET tracers, but its discussion falls outside the scope of this thesis. Further discussion will be only in the context of C-¹⁹F bond formation.

Typically, total synthesis process-scale routes to fluorinated compounds utilize synthetic building blocks with the carbon-fluorine bond pre-installed. In these instances, fluorination methods such as S_NAr of electron-poor building blocks or thermal decomposition of diazonium tetrafluoroborate salts offer two of the most industrially-relevant ways of installing aryl fluorides.⁹ However, many instances exist that require the use of milder, more functional group tolerant fluorination methods. A strong case for the late-stage installation of the C-F bond is made when a complex advanced intermediate is readily accessible, such as

during natural product derivatization or medicinal chemistry structural diversification. In these instances, a semisynthesis of the desired product, where the C–F bond is installed at a late stage, is potentially cheaper or far more efficient than a total synthesis from a simple starting material with the C–F bond pre-installed.

For these more specialized purposes, the most general, state-of-the-art methodologies are most important to consider and will thus serve as the bulk of the topics covered in the following sections. A broader coverage of fluorination is described very well in a number of recent reviews of the field.¹⁰

Impact of Aryl Fluorides in Medicinal Chemistry

The development of pharmaceuticals requires fine-tuning the properties of a molecule, balancing the physical and chemical properties to promote a desired outcome for a specific length of time.^{2d} Fluorine substituents on an aromatic molecule provide a handle to very selectively alter the properties of the nearby functionality, thereby modifying both the observed interaction and the stability of the molecule.^{2a}

Biological organisms remove molecules from circulation through oxidative degradation, a mechanism exemplified by cytochrome P450 enzymes in the liver.^{2a} These enzymes act as either oxidases or monooxygenases, targeting the most oxidatively labile positions on pharmaceutical small molecules.¹¹ These modified pharmaceutical small molecules are often less active or inactive forms that are more easily excreted by the organism. One method to increase the metabolic stability of a molecule is through fluorination of the sites prone to oxidation, blocking P450 oxidation at those positions.¹²

One compound where fluorination has had dramatic effects in increasing the metabolic stability of the lead compound is in the cholesterol-absorption inhibitor Ezetimibe.^{12a} Early in development, SCH 48461 was shown to inhibit cholesterol-absorption, albeit in low potency (ED_{50} (hamster) = 2.2 mg kg⁻¹) (Figure I.1). Through degradation

studies, it was found to have two metabolically labile sites: the *para*-position of a phenyl substituent and the methyl ether of one anisole moiety. In combination with other minor changes, substitution of the *para* C-H bond and anisole C-OMe bonds with C-F bonds lead to a more than 50-fold increase in potency and the discovery of Ezetimib (ED_{50} (hamster) = 0.04 mg kg⁻¹).

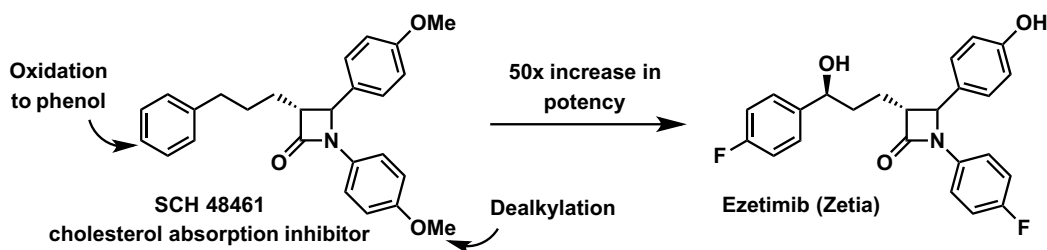


Figure I.1. Fluorination of the oxidation-prone sites on the initial hit SCH 48461 helps to increase the potency of the molecule for cholesterol absorption inhibition by blocking two sites of oxidative metabolism, leading to the discovery of Ezetimib (Zetia).

Fluorine substitution on an aromatic ring has a significant effect on the electronics of that aromatic ring, specifically on the arene binding affinity.¹³ This altered electronic distribution has a significant effect on the preferred molecular interaction of a small molecule pharmaceutical with the structural motifs within the targeted protein binding pocket.¹⁴ To illustrate the difference, it is helpful to consider the pi-pi stacking of two aromatic molecules (Figure I.2). Two electron-rich aromatic rings, such as benzene, prefer to stack either in an off-centered or edge-to-face orientation to promote the best electrostatic overlap. This is due to the innate electronic distribution in the molecule: the electron-rich pi-clouds above and below the aromatic ring bear a strong partial negative charge. However, this charge distribution changes dramatically as electronegative substituents are installed on the arene. A perfluorobenzene molecule bears a strong partial negative charge at the periphery of the ring due to the highly polarized C-F bond, which promotes a face-centered overlap with an electron rich arene. Given that the vast majority of arenes in the body are electron rich benzene- or anisole-derivatives (largely Phe or Tyr residues), the installation of fluorine

substituents on a small molecule pharmaceutical will often promote face-centered arene stacking within the protein target.

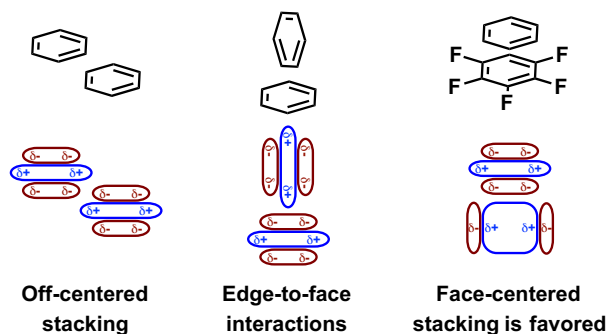


Figure I.2. Energetically-favored stacking orientations of arenes.

As the most electronegative element known, fluorine incorporation alters the pK_a and pK_{aH} of nearby acids and bases, respectively.^{2f, 15} This potentially altered protonation state can have a drastic effect on the ability of a molecule to progress throughout a biological organism. In human beings, the stomach has an average pH of 2-3, which increases to 6-7.4 throughout the intestine.¹⁶ These changes in pH can alter the preferred protonation state of a molecule in different parts of the digestive tract. As a molecule's bioavailability is proportional to, among several things, the charge state of that molecule,^{2a} modifications that increase the charge on the molecule will make it less bioavailable and vice versa.¹⁷ In some cases, this change can be very significant, altering the pH by several orders of magnitude, as in the comparison of pyridine ($pK_{aH} = 5.23$) to 2-fluoropyridine ($pK_{aH} = -0.44$) (Figure I.3).¹⁸ This change in pK_a can also often be roughly correlated to the binding affinity of the functional group, which can alter how the molecule binds to targets within the body.^{17a} Additionally, the installation of fluorine on aromatic rings causes a very minor but noticeable increase in the lipophilicity of the molecule^{15, 19} (this effect is much more pronounced for aliphatic fluorination and polyfluorinated substituents).²⁰

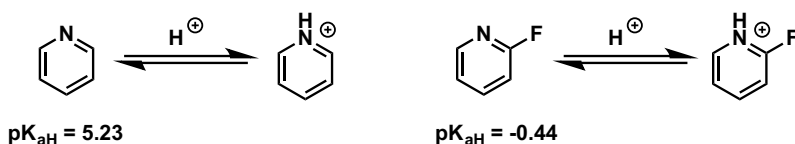


Figure I.3. Fluorination in the 2-position of pyridine lowers the acid dissociation constant by over 5 orders of magnitude, greatly reducing the basicity of the nitrogen heterocycle.

Nucleophilic Arene Fluorination

A review of arene fluorination would be remiss to start at anything but the beginning. The Balz-Schiemann process was pioneered in 1927,²¹ where the heating aryl diazonium tetrafluoroborate salts was shown to cause a nucleophilic attack of fluoride *ipso* to the diazonium and liberate aryl fluoride with concomitant loss of dinitrogen and boron trifluoride (Figure I.4a). Subsequently, nucleophilic aromatic substitution (S_NAr) by fluoride of exceedingly electron poor aryl chloride,²² aryl nitro,²³ and aryl trimethylammonium compounds²⁴ was reported (Figure I.4b). These reactions serve as the foundation for the installation of fluorine via nucleophilic displacement and remain a primary avenue by which most simple aryl fluorides are synthesized today.⁹

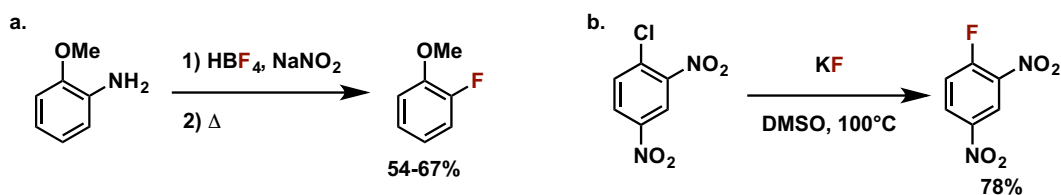


Figure I.4. a. Formation of aryl diazonium tetrafluoroborate, followed by thermal decomposition for the formation of aryl fluorides in the Balz-Schiemann process. **b.** Nucleophilic aromatic substitution by fluoride of electron-poor chloroarene.

Some modern methods for the nucleophilic installation of aryl fluorides are derivatives of this early S_NAr technology. Perhaps the most obvious evolution of this early technology is in our lab's development of Phenofluor (Figure I.5).²⁵ This initial methodology and its derivative²⁶ promote the deoxyfluorination of phenols, ranging from electron rich aniline derivatives to electron poor quinine derivatives. In-depth mechanistic analysis of this

reaction revealed this reaction to proceed through a concerted S_NAr (CS_NAr) pathway.²⁷ Typical S_NAr reactions proceed through formation of a Meisenheimer complex²⁸ and are thus only useful for electron poor substrates. However, phenofluor's imidazolium unit forms a tetrahedral intermediate bound to fluoride and phenol, which promotes a subsequent CS_NAr of the fluoride *ipso* to the phenol and provides the reaction with a fairly general substrate scope.

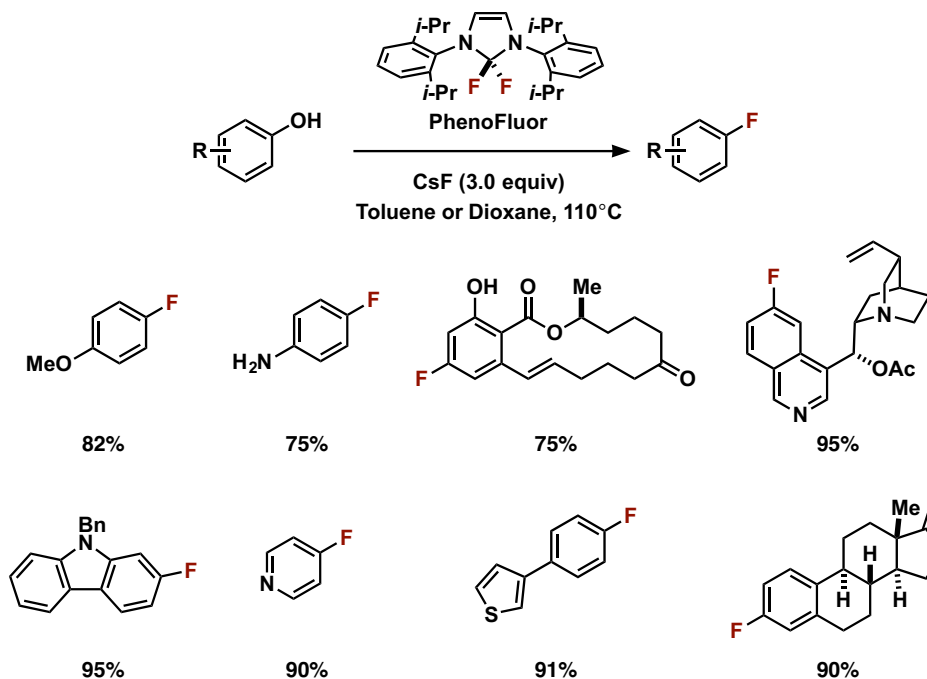


Figure I.5. Phenofluor-mediated deoxyfluorination of phenols.

The most advanced and well-understood method for the transition metal-catalyzed nucleophilic fluorination of aryl electrophiles has been developed in the Buchwald lab. The first iteration of this chemistry utilized the highly advanced biaryl phosphine ligand BretPhos to promote the reductive elimination of the carbon-fluorine bond from palladium through a Pd(0)/Pd(II) cycle (Figure I.6a).²⁹ The bulk of this ligand promotes formation of a monomeric trigonal palladium(II) center that undergoes relatively facile reductive elimination upon heating. The methodology worked extremely well for electron poor aryl triflates, but gave constitutional isomers of aryl fluoride products for electron rich arene substrates.

Thorough mechanistic evaluation of the system over the last several years has resulted in marked improvements in both precatalyst and ligand structures (Figure I.6b).³⁰ The newest generation of the catalyst has eliminated nearly all traces of the isomer production through installation of a fluorinated arene substituent off of the biaryl ligand substituent (Figure I.6c).³¹

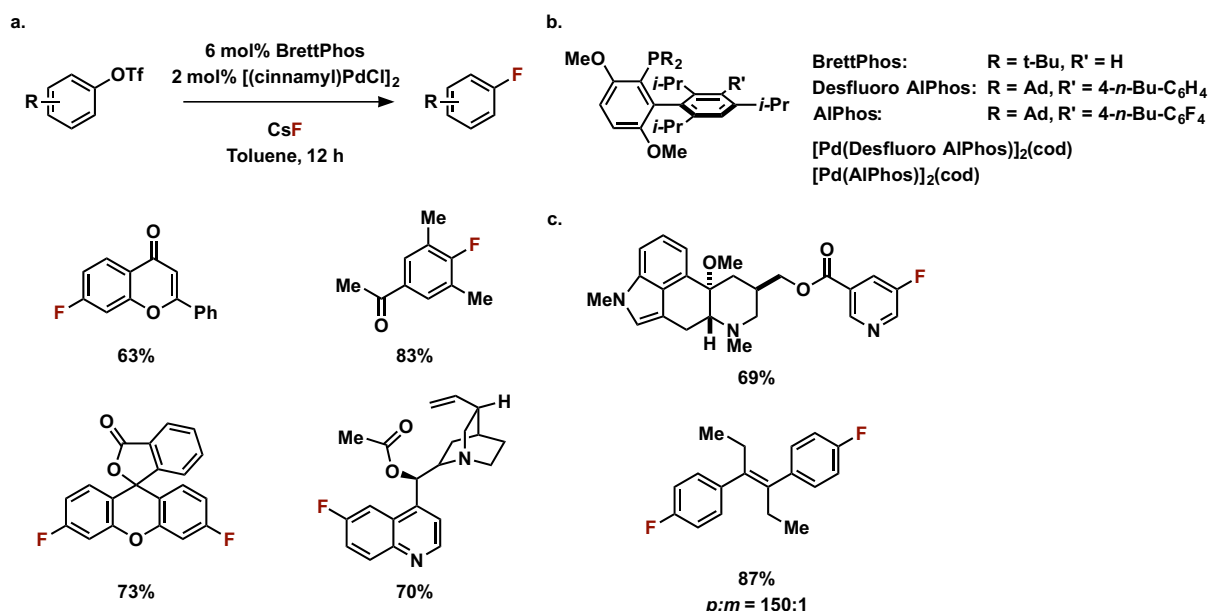


Figure I.6. **a.** Palladium-catalyzed fluorination of aryl triflates. **b.** State-of-the-art phosphine ligands and palladium complexes for fluorination of aryl electrophiles. **c.** Advances made in phosphine derivatives and catalyst precursors allows fluorination of heteroaryl bromides and high selectivity for electron-rich and -neutral aryl electrophiles.

Electrophilic Arene Fluorination

The most fundamental method for electrophilic arene fluorination is direct fluorination of arene C–H bonds. One of the earliest transition metal-mediated methodologies to successfully fluorinate aryl C–H bonds was developed by the Subramanian group, who used CuF₂ as the catalyst in combination with inexpensive HF and O₂ as stoichiometric reagents (Figure I.7).³² The synthetic utility of this reaction is greatly limited by the high temperature of the reaction (450–550°C), the need to vaporize the substrate, and the need to cycle the benzene and HF/O₂ streams to regenerate the catalyst, preventing

catalyst turnover in the presence of the substrate. However, the use of such inexpensive, simple reagents provides an excellent platform on which to build a more general methodology.

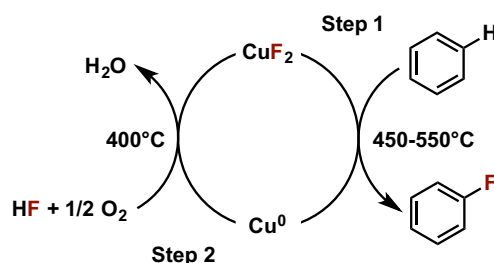


Figure I.7. CuF_2 -mediated fluorination of arene C–H bonds and subsequent CuF_2 regeneration with a stream of O_2/HF .

In an ideal world, cheap and atom economical fluorine gas would serve as an excellent source of electrophilic fluorine. However, the highly reactive nature of fluorine gas makes it challenging to handle and gives it exceptionally poor functional group tolerance. Despite these downsides, several methods have been developed which are successfully able to fluorinate aromatic C–H bonds with moderate selectivity for mono-fluorination on simple aromatic substrates (Figure I.8a).³³ To overcome the challenges associated with highly reactive fluorinating reagents such as fluorine gas and hypofluorite,³⁴ a number of bench stable electrophilic fluorination reagents have been developed over the years including *N*-fluorobis(phenyl)sulfonamide (NFSI),³⁵ *N*-fluoropyridinium salts,³⁶ and 1-chloromethyl-4-fluoro-1,4-diazoniabicyclo-[2.2.2]octane bis(tetrafluoroborate) (Selectfluor, F-TEDA- BF_4) (Figure I.8c).³⁷ These bench stable reagents have been used to develop a variety of electrophilic fluorination methodologies, the most basic of which involve the direct fluorination of main-group organometallic substrates such as Grignard reagents³⁸ (Figure I.8b)^{38d} and aryl lithium reagents.^{38a, 39}

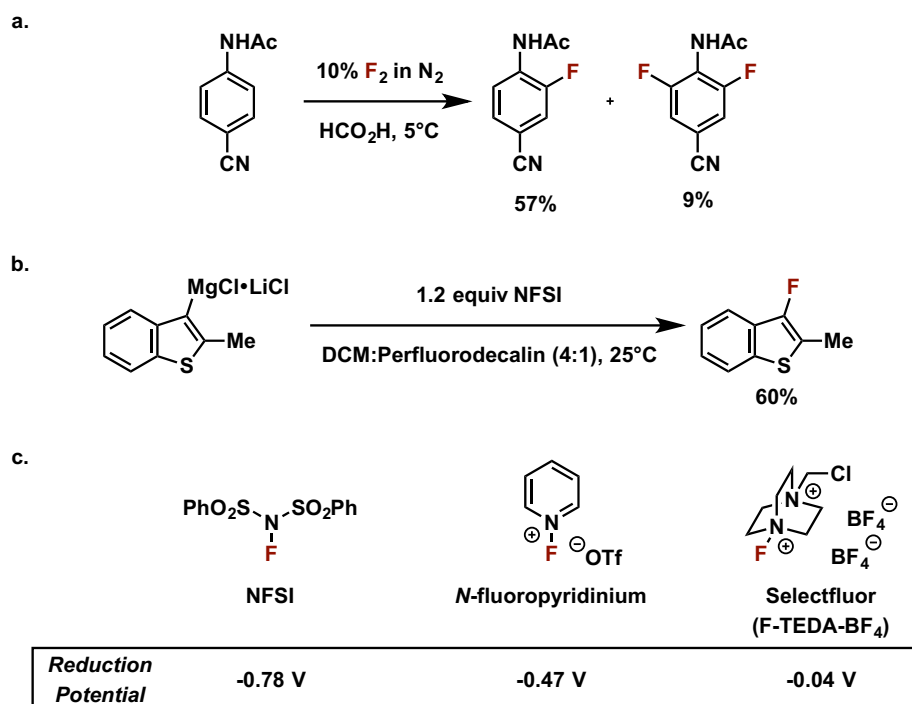
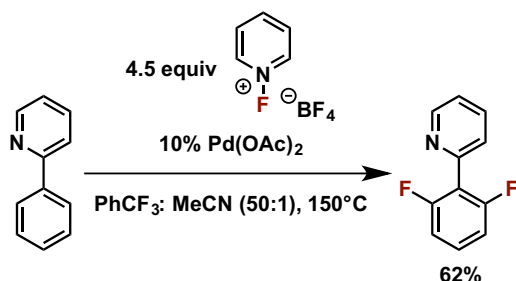


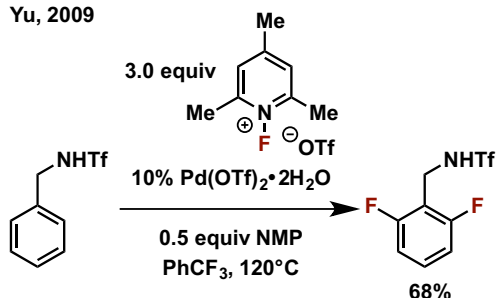
Figure I.8. a. Direct fluorination of arene C–H bonds using fluorine gas. b. Direct fluorination of aryl Grignard reagents using NFSI. c. Bench stable electrophilic fluorination reagents.

The first transition metal-catalyzed reactions for the fluorination of aromatic C–H bonds were palladium-catalyzed methodologies developed by the Sanford⁴⁰ and Yu⁴¹ groups (Figure I.9a). These methodologies utilized coordinating directing groups to enable facile metallation of the nearby arene. Oxidation of the cyclopallidated compound leads to either a high-valent monomeric⁴² or a high-valent multimetallic⁴³ species capable of undergoing C–F bond reductive elimination. Several methodologies have been developed since, including ones that prevent double-fluorination of the substrate (Figure I.9b)⁴⁴ and ones that use a wide variety of alternative directing groups (Figure I.9c).⁴⁵ A palladium-catalyzed methodology that promotes the fluorination of arene C–H bonds without the use of a directing group, however, remains unknown at this time.

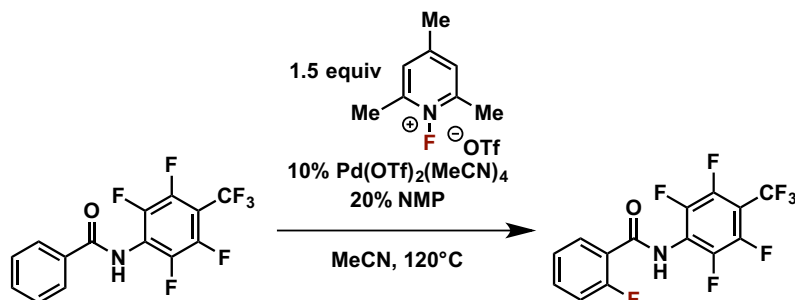
a. Sanford, 2006



Yu, 2009



b.



c.

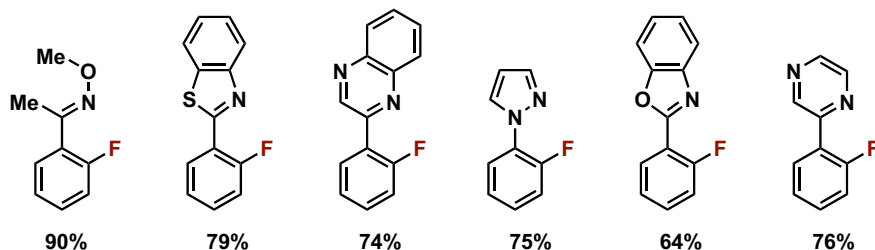


Figure I.9. a. Palladium-catalyzed double-fluorination of arene C–H bonds using coordinating directing groups, demonstrated by the Sanford and Yu groups. b. Palladium-catalyzed fluorination of arene C–H bonds using a directing group and circumventing the previous requirement for a blocking group to prevent observation of double-fluorination. c. Palladium-catalyzed fluorination of arene C–H bonds using a variety of coordinating directing groups.

One of the most general fluorination methodologies to date is a silver-catalyzed fluorination of aryl stannanes using selectfluor developed by our group.⁴⁶ This methodology builds upon early studies for the fluorination of aryl stannanes by XeF_2 ⁴⁷ and greatly broadens the functional group tolerance, enabling the fluorination of complex natural products derivatives (Figure I.10). This chemistry is proposed to proceed through multimetallic high-valent silver intermediates;⁴⁸ it has been shown that multimetallic systems lower the barrier to challenging transformations through a cooperative redox of the metal centers.⁴⁹ This involvement of multiple silver centers is believed to be the origin of the low

energy barrier observed for aryl C–F bond reductive elimination, a transformation that typically has a very high activation barrier. While this transformation necessitates the use of toxic aryl stannanes as substrates, it displays a functional group tolerance and substrate scope far greater than any other currently known fluorination methodology.

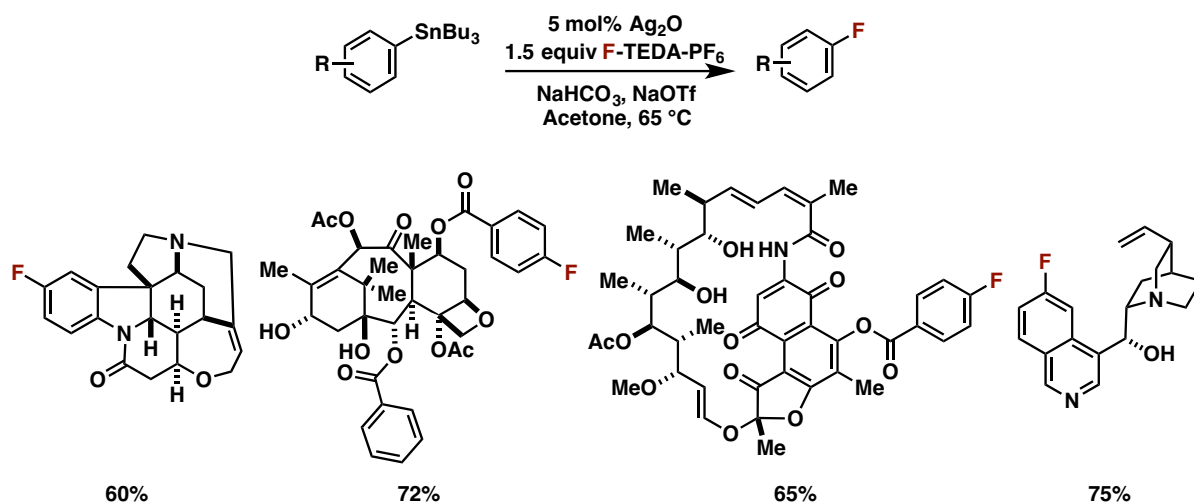


Figure I.10. Silver-catalyzed fluorination of aryl stannanes.

The discussion of most stoichiometric metal-mediated fluorination methodologies falls outside the realm of reactions useful for the preparation of meaningful quantities of aryl fluorides. However, two stoichiometric methodologies exist which should be noted in particular. The first is a method for C–H fluorination at the 2-position of pyridines and diazines with AgF_2 .⁵⁰ The second is a two-step stoichiometric fluorination of arylboronic acids developed early on in our laboratories, which served as a starting point for the catalytic methodology described in Chapter 1. This original methodology utilizes a palladium pyridyl-sulfonamide complex to promote the formation of aryl fluorides after isolation of the intermediate palladium aryl complex and subsequent reaction with Selectfluor (Figure I.11).⁵¹ Mechanistic evaluation of this reaction revealed the intermediacy of a high valent Pd(IV) fluoride.⁵² Dissociation of the weakly coordinated sulfonamide oxygen generates a trigonal bipyramidal structure, which is primed to undergo facile reductive elimination of the C–F

bond.⁵³

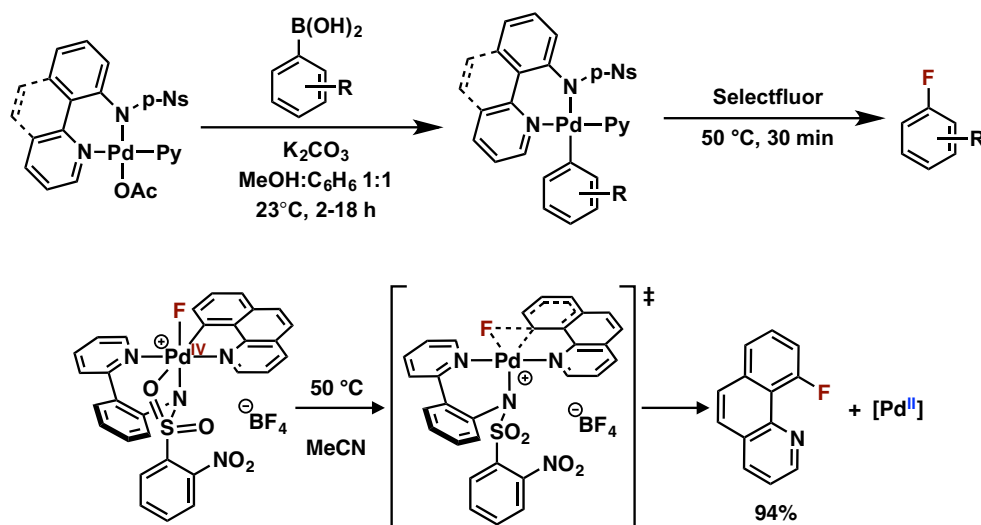


Figure I.11. Two-step stoichiometric fluorination of arylboronic acids mediated by a palladium pyridyl-sulfonamide complex. Mechanistic work reveals the intermediacy of a high-valent Pd(IV)-F which undergoes reductive elimination to form the aryl C–F bond.

Radical Fluorination

In the context of the methodology described in Chapter 1, it is useful to consider fluorination methodologies that proceed via radical mechanisms. Prior to the work performed in Chapter 1, little was known about radical fluorination of arenes. However, the radical fluorination of aliphatic substrates had been shown in several instances.⁵⁴

Radical fluorination of aliphatic carboxylate precursors has been shown to proceed via oxidative decarboxylation.^{54a} Early examples involve simple photolysis or thermolysis of *tert*-butyl peroxy esters in the presence of N-fluorobenzenesulfonimide (NFSI).^{54b} However, later methodologies were able to use carboxylic acid precursors in combination with Selectfluor and either direct photoexcitation^{54c} or a silver catalyst.^{54a} Mechanistic evidence for the silver-catalyzed reaction suggests a silver-mediated decarboxylation occurs to form an aliphatic radical; not only does the reaction show preference for tertiary over primary fluorination (Figure I.12a), but use of a cyclopropane substrate generates the ring-opened product to the exclusion of direct decarboxylation-fluorination product (Figure I.12b).^{54a}

Additionally, the authors perform mechanistic studies with 1-adamantanecarboxylic acid and Ag(II) precursors, showing that despite rapid decarboxylation of the substrate by Ag(II), no decarboxylative fluorination is observed (Figure I.12c). These studies suggest that the aliphatic radical is unable to be fluorinated by Selectfluor; instead, the authors postulate fluorination of the aliphatic radical by Ag(II)-F.

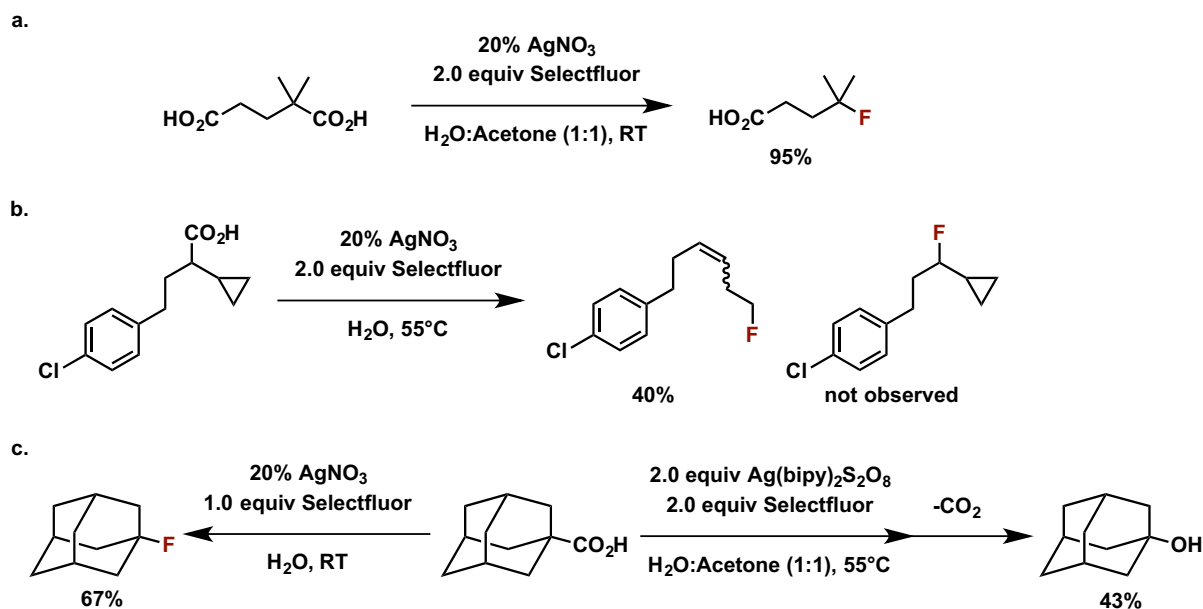


Figure I.12. **a.** Silver-catalyzed decarboxylative fluorination selective for tertiary over primary carboxylate. **b.** Silver-catalyzed decarboxylated fluorination adjacent to cyclopropane ring shows exclusively ring-opened product to the exclusion of the product containing the cyclopropane ring. **c.** Silver-catalyzed fluorination of adamantly carboxylate proceeds efficiently under standard conditions. However, when a silver(II) source is used to cause rapid decarboxylation in the presence of Selectfluor, no desired C–F is formed, suggesting a mechanistic pathway other than aliphatic radical undergoing F[•] abstraction directly from Selectfluor.

Radical fluorination of aliphatic C–H has been demonstrated at benzylic, allylic, and aliphatic positions, initially reported by the Groves⁵⁵ and Lectka⁵⁶ groups and later by several others.⁵⁷ In some cases, mechanistic support is limited to a tolerance of MeCN or a sensitivity to O₂.⁵⁶ However, the manganese porphyrin-catalyzed fluorination published by the Groves group demonstrated a 2:1 mixture of C–H bond fluorination and cyclopropane ring opening when norcarane was used as a substrate (Figure I.13a).⁵⁵ A later report by the Lectka group, describing a photocatalytic fluorination reaction, showed that use of an aryl-

substituted α,β -substituted ester substrate in the reaction resulted in a mixture of the desired benzylic fluorination and ring closure products (Figure I.13b).^{57b}

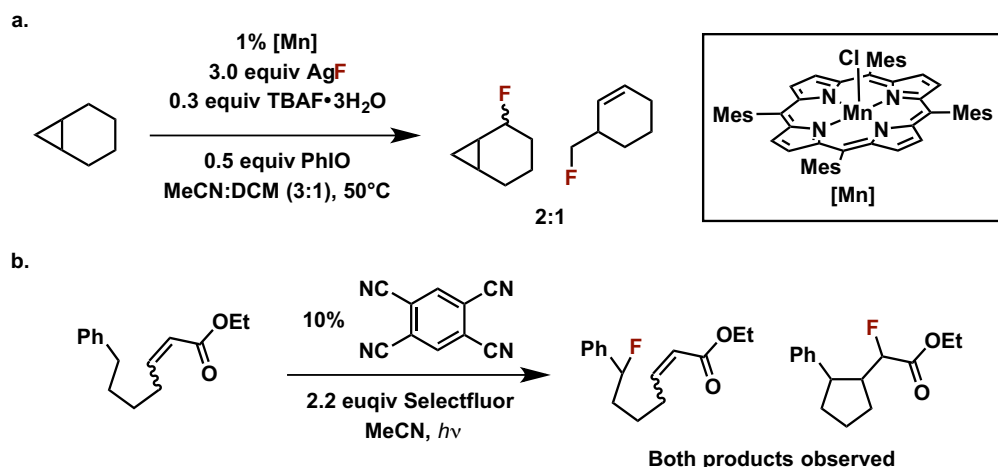


Figure I.13. a. Manganese porphyrin-catalyzed fluorination of aliphatic C–H bonds using norcarane as a substrate, revealing 2:1 ratio of desired fluorination to cyclopropane ring opened product. **b.** Light-mediated tetracyanobenzene-catalyzed fluorination of aliphatic C–H bonds of aryl-substituted α,β -substituted ester substrate results in significant cyclopentane ring closure product forming.

C-H Bond Functionalization

The field of direct C–H bond functionalization has numerous applications in the field of organic synthesis. One of the ideal uses of C–H bond functionalization is eventual elimination of the need for prefunctionalized substrates.⁵⁸ This requirement for prefunctionalization, at its simplest, typically adds at least one additional step in a synthesis. By expanding the field of C–H bond functionalization, chemists will slowly be able to reduce step count in synthetic routes. This reduction often has positive ramifications through an increase in overall yield, reduction in the total time requirement, an improvement in the atom economy of the synthesis, and a reduction in the waste generated in both the reactions and the purifications procedures.⁵⁹

However, the slow acceptance of C–H bond functionalization in total synthesis, along with the relatively slow development of the necessary synthetic methods, makes this desire to

completely supplant prefunctionalized cross-coupling reactions a relatively long-term goal.⁵⁹

The area of study that can be immediately impacted by the area of C-H bond functionalization is in the direct derivatization of natural products and advanced synthetic intermediates.⁶⁰ New C-H bond functionalization reactions that are applicable to complex molecular scaffolds unlock short semisynthetic sequences to novel molecular scaffolds, allowing facile access to molecules that would often otherwise require lengthy total syntheses.^{60c, 60d} In no other area is this straightforward access to derivatives more relevant than in the discovery of bioactive molecules in the agrochemical and pharmaceutical industries.

In the context of the work described herein, it is most useful to focus on C-H functionalization in the context of aromatic C-H bonds. One common route to achieve selective arene C-H functionalization is through the use of transition metal catalysis. Significant work has been done in this area; for a more exhaustive discussion, several reviews have been written on the subject.⁶¹ The following sections will serve as an overview of the types of strategies currently employed in overcoming what is often the challenging step in arene C-H functionalization: cleavage of the C-H bond itself.

Arene C-H Bond Functionalization: Chelation Assistance

One of the more thoroughly explored areas of transition metal-catalyzed arene C-H bond functionalization over the last decade is in the area of chelation assistance.^{61a, 61b, 62} The reactivity and selectivity of the metal catalyst is increased dramatically by tethering the substrate to a ligand, artificially increasing the concentration of the substrate near the catalyst through a proximity effect. To demonstrate this effect, it is helpful to examine the acetoxylation of aromatic C-H bonds. Palladium acetate has been shown to catalyze the acetoxylation of benzene (Figure I.14a), a reaction that is accelerated by the presence of pyridine (Figure I.14b).⁶³ However, when 2-arylpyridines are subjected to similar reaction

conditions in benzene solvent, the acetoxylation of the tethered arene occurs in 77% yield, despite the presence of benzene in a 72-fold excess of the pyridine-tethered substrate (Figure I.14c).⁶⁴ This chelation assistance strategy has allowed a variety of very simple metal salts to serve as highly active and general catalysts for the functionalization of aromatic C–H bonds with a variety of coordinating directing groups.^{61a}

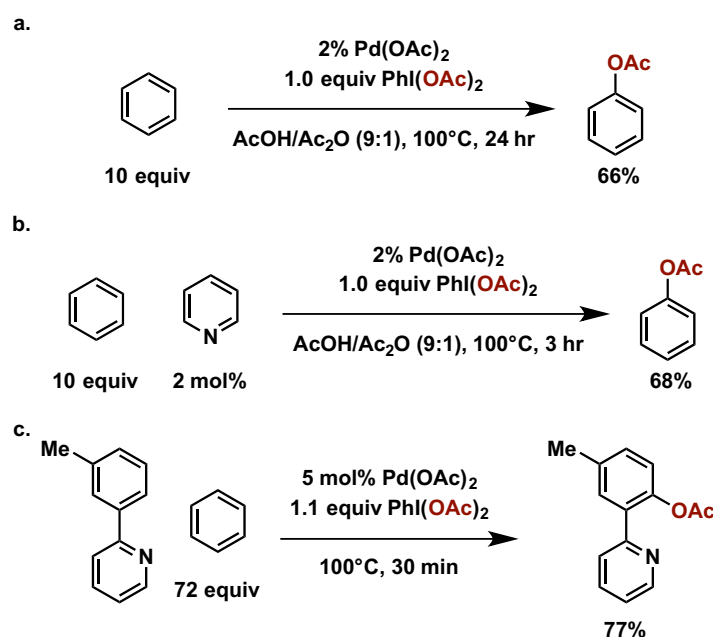


Figure I.14. **a.** Palladium-catalyzed acetoxylation of arene C–H bonds. **b.** Palladium-catalyzed acetoxylation of arene C–H bonds accelerated by pyridine ligand. **c.** Palladium-catalyzed acetoxylation of arene C–H bonds shows remarkably high selectivity for arene tethered to pyridine coordinating directing group in the presence of solvent quantities of benzene.

The first example of transition metal-catalyzed arene C–H functionalization in the literature was developed by Shinji Murai using ketones to direct metallation with $\text{RuH}_2(\text{CO})(\text{PPh}_3)_3$.⁶⁵ This complex was shown to very efficiently add the arene C–H bond across olefins to install alkyl substituents at the *ortho*-position (Figure I.15a). Over the years, $\text{Pd}(\text{OAc})_2$ has become one of the more commonly used catalysts for similar transformations, able to metallate *ortho* to a wide variety of functional groups and install not only carbon substituents, but also halogen, nitrogen, oxygen, among others (Figure I.15b).^{61b, 62}

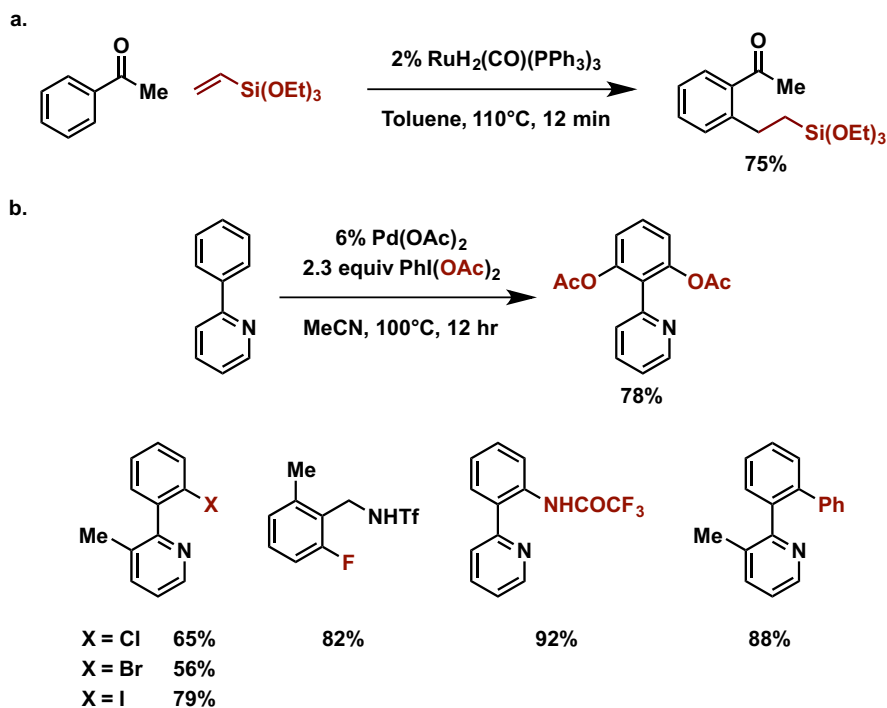


Figure I.15. a. Ruthenium-catalyzed *ortho*-selective alkylation of arene C–H bonds using a ketone coordinating directing group. b. Palladium-catalyzed arene C–H bond functionalization for the installation of acetoxy, halogen, amide, and aryl substituents.

Until quite recently, the directing group strategy was used nearly exclusively for installation of *ortho* functionality. In 2012, Jin-Quan Yu developed the first directing group that favors metallation of a C–H bond *meta* to the directing group (Figure I.16a).⁶⁶ This advance took advantage of a preferred end-on template using a nitrile-based coordinating group. Instead of taking advantage of the preference for metallation in a 5- or 6-membered metallocycle in the case of *ortho*-metallation, this new technology takes advantage of a preference for the new directing group to form cyclophane-like 11-membered metallocycles. In 2015, the Maiti group was able to extend this same concept from *meta*-selective to *para*-selective using a similar but slightly larger nitrile-based directing group template (Figure I.16b).⁶⁷

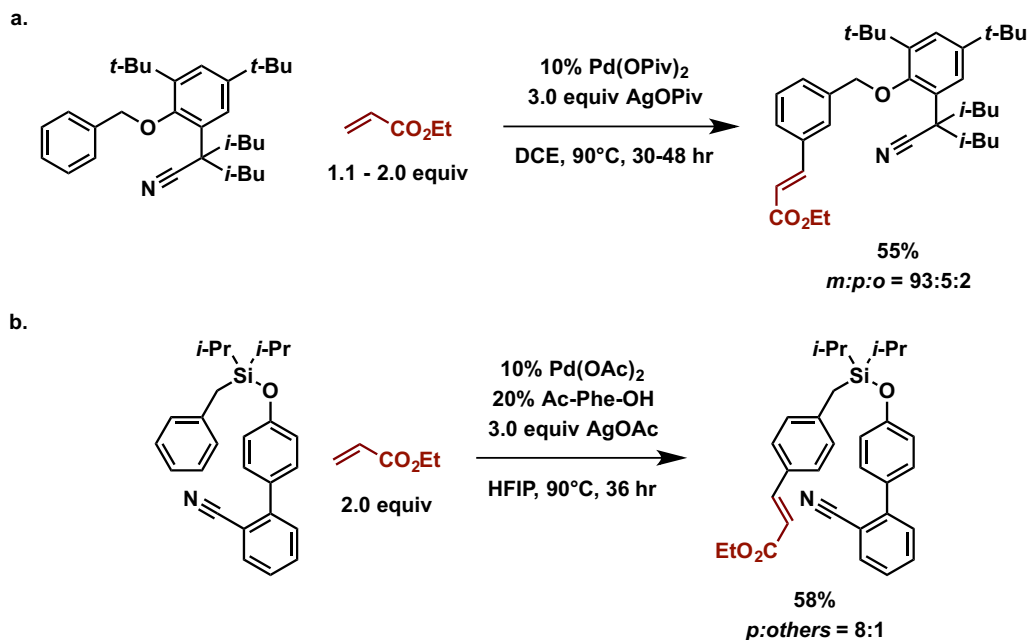


Figure I.16. **a.** Palladium-catalyzed *meta*-selective olefination of arene C–H bonds using a directing group template. **b.** Palladium-catalyzed *para*-selective olefination of arene C–H bonds using a directing group template.

It should be noted that the vast majority of C–H functionalization reactions using chelation assistance require only a single equivalent of arene to realize synthetically useful yields of functionalized product. This is important to note, as any application that targets a natural product or advanced synthetic intermediate will likely require the use of the substrate as the limiting reagent.

Arene C-H Bond Functionalization: Electronically Biased Arenes

Electronic bias on the arene substrate for facile metallation at specific positions has been another attractive method for overcoming the challenging metallation step.^{62b, 68} This section broadly combines two mechanisms of metallation, electrophilic aromatic substitution (S_EAr)⁶⁹ and concerted metallation-deprotonation (CMD).⁷⁰ Both these mechanisms, while they approach the problem from two opposing ends of the reactivity spectrum, take advantage of an electronic bias on the arene substrate to promote the C–H metallation step and often allow for use of a single equivalent of arene substrate.

Electrophilic aromatic substitution by a metal is mechanistically identical to S_EAr by a non-metal: the first step involves reversible formation of a metal-carbon bond and loss of aromaticity, while subsequent deprotonation results in rearomatization and formation of the metal-arene species.⁶⁹ The earliest example of this mechanism is the auration reactions using $AuCl_3$ by the Kharasch group.⁷¹ The observed speed of reactivity is directly proportional to the electron density of the arene; toluene reacts very quickly, methyl salicylate is much slower, and nitrobenzene shows no reaction. Dalibor Sames performed a more thorough mechanistic study on the arylation of indole derivatives, most notably involving a Hammett analysis and a KIE study.⁶⁹ The Hammett analysis revealed a ρ -value of -0.71, supporting a stabilization of positive charge at the 3-position (Figure I.17a). Furthermore, the KIE for both the C2 and C3 positions was investigated. The authors found a KIE of 1.2 for C2 and 1.6 for C3 (Figure I.17b), the latter of which is quite large for a position that does not undergo substitution in the reaction, especially compared to the relatively small KIE for the substituted C2 position. This secondary KIE observed at C3, along with the negative ρ -value from the Hammett analysis, heavily suggests an electrophilic substitution pathway.

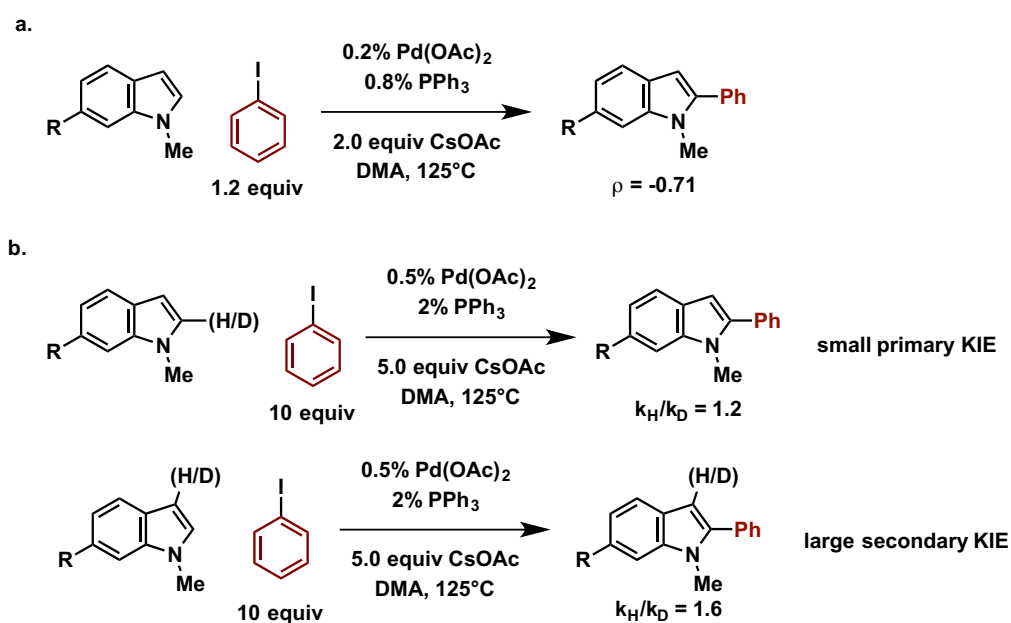


Figure I.17. **a.** Palladium-catalyzed C2-selective arylation of indole C–H bonds. **b.** KIE of C–(H/D) at both C2 and C3 positions of indole.

Concerted metallation-deprotonation (CMD) involves coordination of a metal to the *ipso*-position of the targeted C–H bond.⁷² A base coordinated to the metal center is then well positioned to deprotonate this highly acidified C–H bond. This mechanistic pathway has been thoroughly explored in large part by the Fagnou group in the context of palladium catalysis.^{70, 72-73} The group has developed and studied a variety of reactions believed to proceed through a CMD mechanism. Mechanistic study suggests the involvement of two energetic components: (1) the energy of distortion, which is a combination of the energy required to open a vacant site on the palladium catalyst, and the strain energy associated with out-of-plane bending and elongation of the arene C–H bond (C–H bond acidity and out of plane bending, Figure I.18a) and (2) the electronic interactive energy, which is the positive energetic benefit of binding the distorted arene to palladium bearing the open coordination site (nucleophilicity, Figure I.18a).⁷⁰ Examination of these two factors revealed that for substrates in which the energy of distortion plays a significant role in the selectivity for aromatic C–H bond functionalization, the primary energetic contributor that changes between substrates is not the out-of-plane bending energy, but the C–H bond elongation energy. Furthermore, they found that the C–H bond elongation energy could be approximated using the C–H bond acidity. This trend between C–H acidity and lower energetic barriers is observed in their previous competition study between benzothiophene and 3-fluorobenzothiophene, where they see nearly exclusive arylation of 3-fluorobenzothiophene (Figure I.18b).⁷³ Calculated free energies of activation for a handful of substrates (Figure I.18c) illustrate this trend of lower energetic barriers for substrates with higher C–H bond acidity.

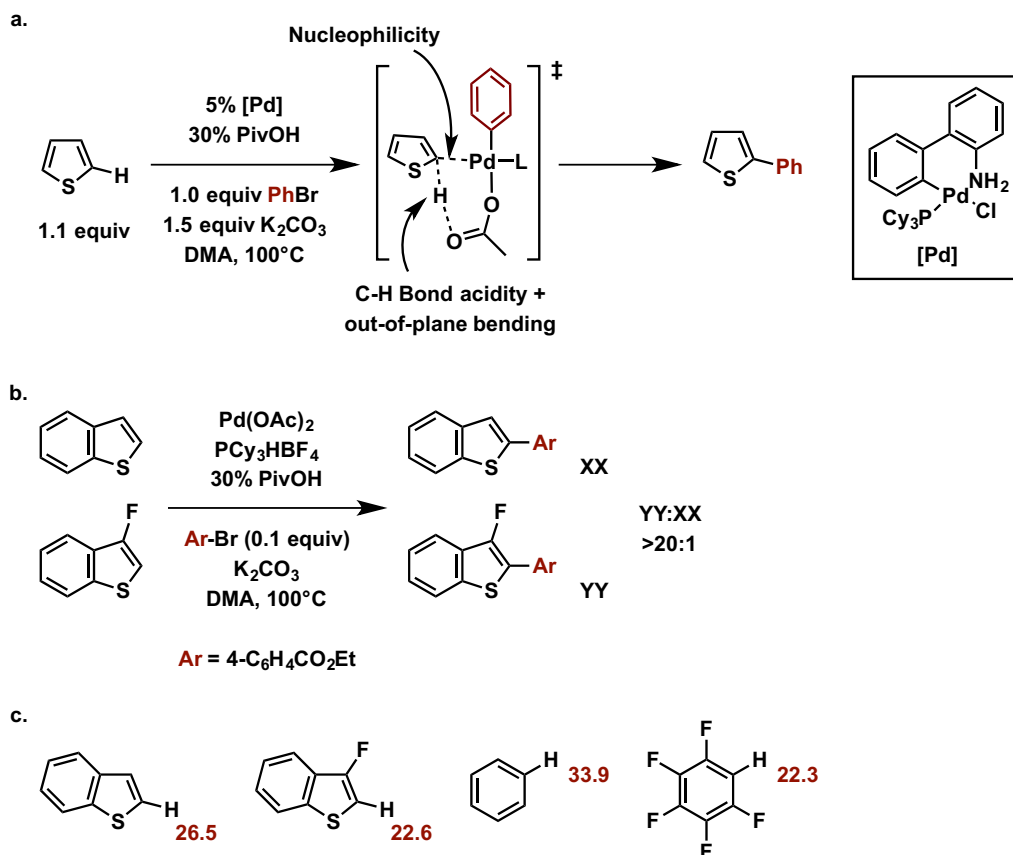


Figure I.18. a. The activation barrier for concerted metallation-deprotonation by Pd(II) is a combination of attractive interaction between the arene and palladium (Nucleophilicity) and an out-of-plane bending and elongation of the C–H bond.⁷⁰ **b.** Palladium-catalyzed arylation of arene C–H bonds shows >20:1 selectivity in competition experiment for 3-fluorobenzothiophene over benzothiophene. **c.** Calculated free energies of activation ($\Delta G^\ddagger_{298\text{K}}$, kcal mol^{–1}) for arene C–H bonds *via* CMD pathway with palladium and an acetate ligand.

It is, however, important to note that S_EAr is not exclusive to electron rich arenes, nor is CMD exclusive to electron poor arenes.^{73–74} Both mechanisms operate on much wider electronic substrate scopes, but tend to be fastest with the respective electronically biased substrates.

Arene C-H Bond Functionalization: Electronically Neutral Arenes

Electronically neutral arenes are typically much slower in arene C–H bond functionalization chemistry without the use of a directing group; they undergo both S_EAr⁷⁴ and CMD,⁷³ albeit slowly. To increase the speed of functionalization, these substrates are often used in cosolvent or solvent quantities, as is the case in the selected acetoxylation

(Figure I.19a)⁶³ and phenylation (Figure I.19b)⁷⁵ examples. A large portion of reported reactions for the functionalization of electronically neutral arenes without a coordinating directing group require the arene to be present in excess for significant yields of the C–H bond functionalized product,^{61c} limiting the synthetic utility of these reactions in the context of complex molecules.

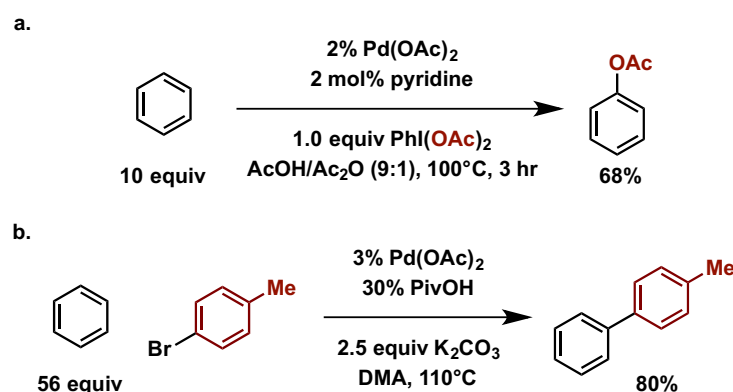


Figure I.19. **a.** Palladium-catalyzed acetoxylation of arene C–H bonds. **b.** Palladium-catalyzed arylation of arene C–H bonds.

One prominent exception to the requirement for excess arene in these electronically neutral C–H functionalizations is the borylation and silylation chemistry pioneered largely by the Hartwig group. The borylation is catalyzed by an [Ir(OMe)(cod)]₂/dtbpy catalyst using B₂pin₂ as the borylating reagent (Figure I.20a),⁷⁶ while the silylation chemistry is catalyzed by a [Rh(coe)₂OH]₂/BIPHEP derivative using HSiMe(OTMS)₂ as a silyating reagent (Figure I.20b).⁷⁷ These reactions are able to very efficiently functionalize a single equivalent of arene while still using arene as the limiting reagent. This chemistry, while highly useful for boryl and silyl installation, is currently limited to the installation of these strongly donating substituents.

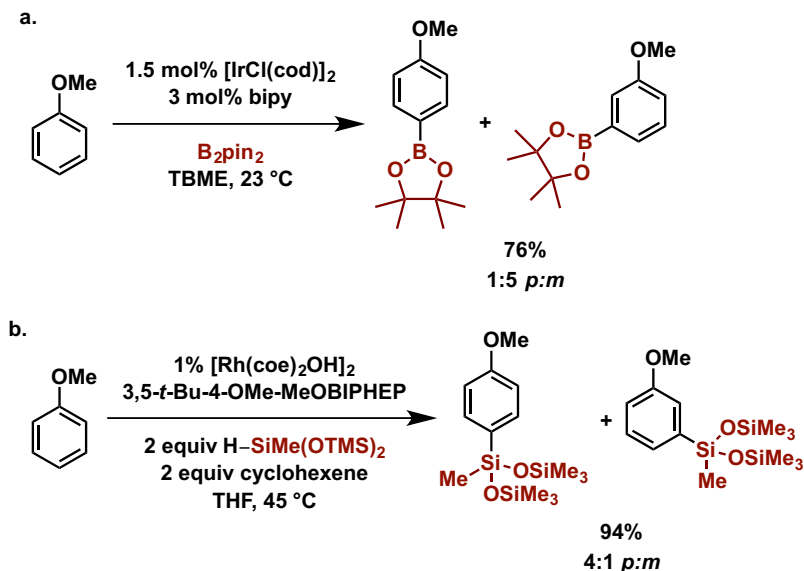


Figure I.20. **a.** Iridium-catalyzed borylation of arene C–H bonds. **b.** Rhodium-catalyzed silylation of arene C–H bonds.

The mechanism has been most thoroughly explored with the borylation; the strongly donating boryl ligands make the iridium center highly electron rich, capable of either oxidative addition into the arene C–H bond or a σ -bond metathesis between the Ir-Bpin bond and arene C–H bond (Figure I.21a).⁷⁸ Under the current mechanistic understanding, the metal center is too electron poor to promote these types of mechanistic pathways without the strongly donating silyl or boryl ligands. It should also be noted that this borylation and silylation chemistry, while efficient across a wide range of arene substrates, creates a mixture of *para*- and *meta*-constitutional isomers when mono-substituted arenes are subjected to the reaction.^{76c} While attempts to favor *para*-selectivity in the borylation have been moderately successful when using steric control with a bulky ligand,⁷⁹ the reaction requires extremely bulky groups, such as TMS or *t*-Bu, to observe high *para*-selectivity on mono-substituted arenes (Figure I.21b).

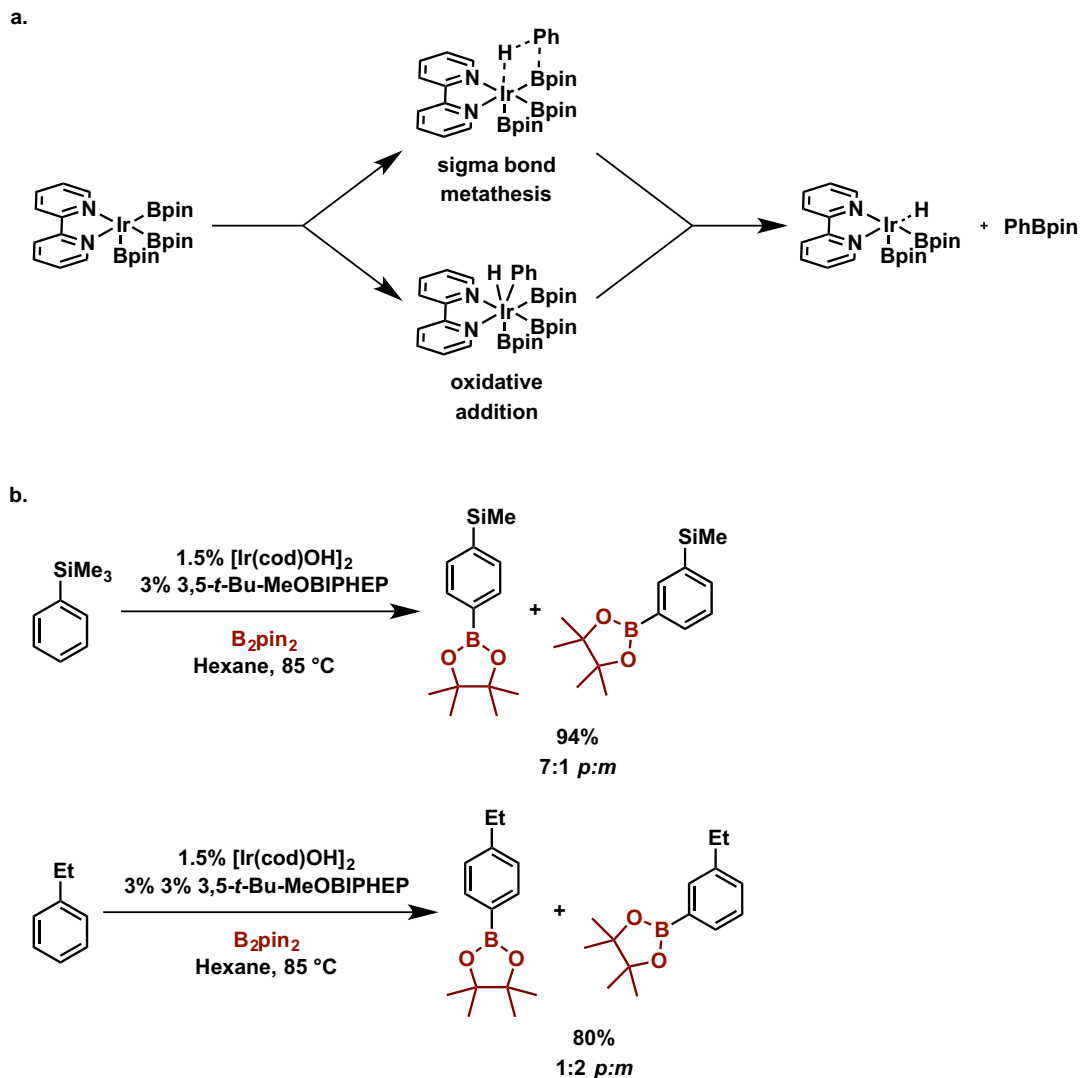


Figure I.21. a. Iridium-catalyzed borylation proposed to proceed through either a σ -bond metathesis between the arene C–H bond and an iridium-Bpin bond, or an oxidative addition into the arene C–H bond followed by reductive elimination to form the borylated arene. b. Iridium-catalyzed borylation reaction using sterically bulky ligand is *para*-selective for mono-substituted arenes with bulky substituents. However, it is *meta*-selective when smaller substituents are present on the arene.

A general strategy to functionalize arenes at the *para*-position remains unknown in the literature. The work put forward in Chapter 2 attempts to establish an initial framework on which a general strategy for *para*-selective arene C–H functionalization might be built.

CHAPTER 1 – PALLADIUM(III)-CATALYZED FLUORINATION OF ARYLBORONIC ACID DERIVATIVES

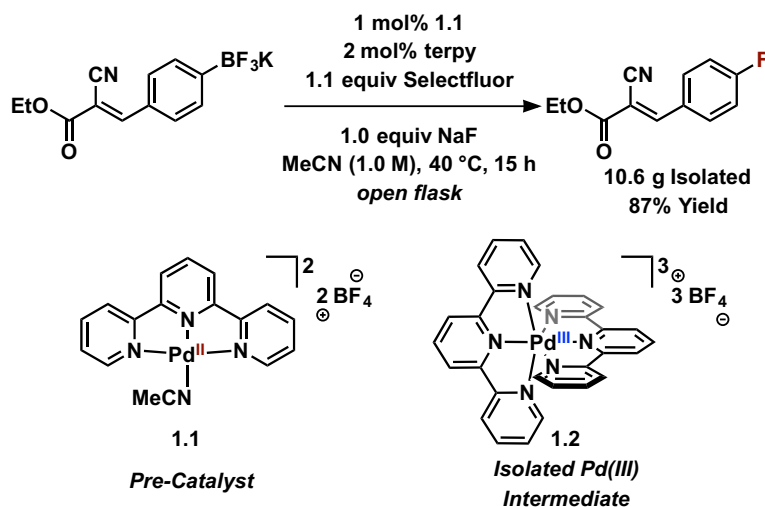
A practical, palladium-catalyzed synthesis of aryl fluorides from arylboronic acid derivatives is presented. The reaction is operationally simple and amenable to multi-gram-scale synthesis. Evaluation of the reaction mechanism suggests a single-electron-transfer pathway, involving a Pd(III) intermediate that has been isolated and characterized.

In the past decade there has been an increase in the number of available methods for the installation of fluorine and fluorine-containing functional groups into organic molecules.^{10a, 80} However, the development of practical carbon–fluorine bond forming reactions to provide aryl fluorides still remains as one of the most challenging transformations in the field of fluorination.^{10a, 80} In this communication, we report a palladium-catalyzed fluorination of arylboronic acid derivatives, which allows for an operationally simple, multi-gram-scale synthesis of functionalized aryl fluorides. A metal-catalyzed fluorination of arylboronic acid derivatives has not previously been reported. Kinetic studies suggest a mechanism distinct from other known arene fluorination reactions, which proceeds through a single-electron-transfer (S.E.T.) pathway without the formation of organopalladium species, and involving an unusual Pd(III) intermediate (**1.2**) that has been isolated and characterized (Scheme 1.1).

To date, only two catalytic reactions have been reported that provide a general route to functionalized aryl fluorides: Buchwald's palladium-catalyzed fluorination of aryl triflates,^{29, 81} and our group's silver-catalyzed fluorination of aryl stannanes.⁴⁶ Our silver-catalyzed reaction requires the preparation and use of toxic aryl stannanes. The palladium-catalyzed nucleophilic fluorination uses more readily available aryl triflates; it currently requires dried fluoride salts and can give mixtures of constitutional isomers for some

substrates due to competing pathways in addition to C–F reductive elimination. Work toward catalytic C–H fluorination has been reported by the groups of Groves,⁵⁵ Sanford,⁸² and Yu.^{44, 83} Direct C–H fluorination is ideal from a perspective of step- and atom-economy, but the development of catalysts that provide selectivity for a broad range of substrates remains challenging.

There are a handful of modern stoichiometric arene fluorination reactions. On gram- and smaller scale, deoxyfluorination with PhenoFluor^{25, 84} is in our opinion currently the most practical method to obtain a large variety of aryl fluorides, but it requires stoichiometric amounts of PhenoFluor. Metal-mediated procedures have been developed for a variety of arene precursors, but frequently require superstoichiometric amounts of transition metal. A copper-mediated fluorination of aryl iodides was reported by Hartwig,⁸⁵ and silver-mediated fluorination reactions have been developed for aryl stannanes, aryl silanes, and arylboronic acids.^{48, 86} There are several other metal-mediated fluorination reactions of arylboronic acid derivatives, using either palladium⁸⁷ or copper.⁸⁸ Further development of the reported metal-mediated reactions to use only catalytic quantities of the transition metal has remained difficult. For arylboronic acid derivatives, slow transmetallation of the arene from boron to the transition metal complex is frequently a hurdle to achieving C–F bond-forming catalysis.^{86b, 87}



Scheme 1.1. Catalytic Fluorination of Aryl Trifluoroborates, and Isolated Pd(III) Intermediate 2.^a ^a terpy = 2,2':6',2''-terpyridine.

Herein we describe a palladium-catalyzed fluorination of arylboronic acid derivatives, using terpyridyl Pd(II) complex **1.1** as a pre-catalyst (Scheme 1.1). We propose a mechanism that proceeds without the formation of organopalladium intermediates, which circumvents the problem of transmetallation from the arylboron reagent. Complex **1.1** has been prepared in one step from Pd(OAc)₂, terpyridine (terpy), and HBF₄ on decagram scale, and all reagents used in the catalytic fluorination reaction including **1.1** are stable to air and moisture. The reaction can be performed in an open flask, and is effective for milligram to at least multi-gram scale synthesis of aryl fluorides, which are readily isolated. Inseparable side products from protodeborylation were not observed for the majority of substrates, which may also be due in part to a mechanism that does not involve organopalladium intermediates. Protodeborylation is a common problem for fluorination reactions of arylboronic acid derivatives.⁸⁸

As shown in Table 1.1, a wide variety of aryl trifluoroborates can be fluorinated, including both electron-rich and electron-poor arenes. DMF was found to be the optimal solvent for most electron-rich and electron-neutral arenes, while acetonitrile typically provided higher yields for arenes with electron-withdrawing substituents. Ketones, primary

amides, carboxylic acids, esters, alcohols, basic heterocycles, aryl bromides, and *ortho*, *ortho*'-disubstitution are tolerated in the reaction.

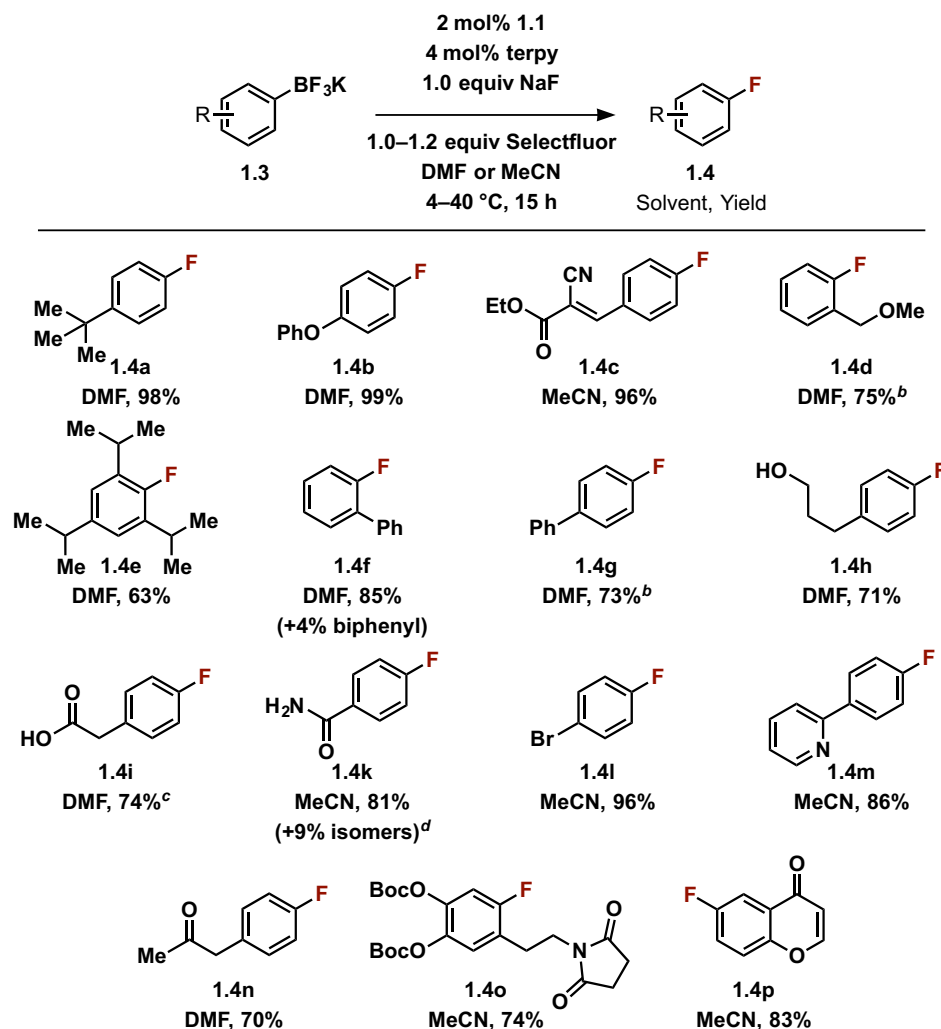
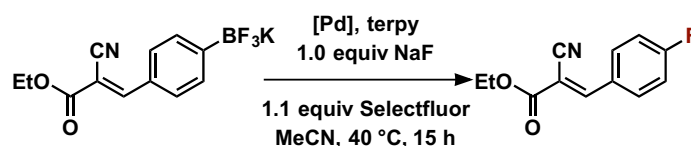


Table 1.1. Fluorination of Aryl Trifluoroborates.^a ^a Yields refer to isolated material of $\geq 98\%$ purity unless otherwise noted. ^b No NaF was used. ^c 5 mol% **1** and 10 mol% terpy were used. ^d 9% of a mixture of constitutional isomers (ortho- and meta-fluorobenzamide).

Competing formation of constitutional isomers is a challenge for metal-catalyzed fluorination reactions.^{29, 81} Such impurities are usually difficult to separate from the desired aryl fluoride product. The majority of the aryl fluorides shown in Table 1.1 were isolated cleanly, with $\geq 98\%$ purity. In particular, electron-rich aryl trifluoroborates generally did not react to form inseparable side products. Substrates with electron-withdrawing substituents are more likely to give constitutional isomers and difluorinated products along with the

expected aryl fluoride product (typically $\leq 10\%$): substrate **1.3k** is a representative example, which reacts to form **1.4k** along with 9% of ortho- and meta-fluorobenzamide. Other electron-poor substrates such as **1.3c** provided clean isolated product. The Pd-catalyzed fluorination reaction is ineffective for fluorination of heterocycles, and arenes bearing methoxy substituents gave significant amounts of side products resulting from demethylation.

A variety of commercially available Pd(II) salts can be used in the fluorination reaction, as shown in Table 1.2. In general, palladium salts with less coordinating anions gave the highest yields. Anion metathesis using NaBF₄ as an additive resulted in higher yields for pre-catalysts with coordinating anions such as acetate. Palladium salts with halide anions were not suitable pre-catalysts for the fluorination reaction. Ultimately, we found **1.1** to be the most convenient pre-catalyst because no additive was needed, and due to its robust stability toward air and moisture as compared to [Pd(MeCN)₄][BF₄]₂. Complex **1.1** can be stored on the benchtop under ambient conditions without observable decomposition or decrease in catalytic reactivity for at least six months.



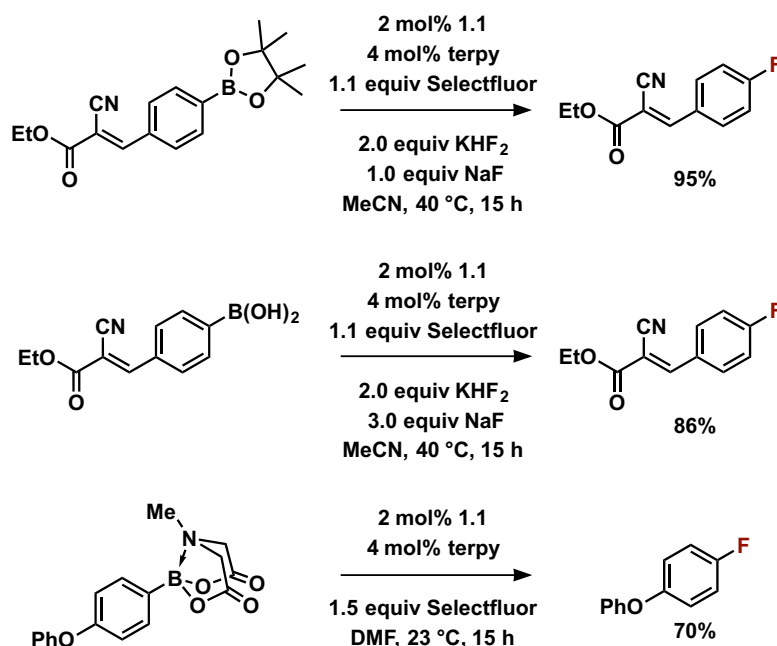
[Pd]	Additive	Yield
1.1	<i>none</i>	96%
1.2	<i>none</i>	95%
[Pd(MeCN) ₄][BF ₄] ₂	<i>none</i>	95%
Pd(OAc) ₂	NaBF ₄ (2.0 equiv)	91%^b
Pd(O ₂ CCF ₃) ₂	NaBF ₄ (1.0 equiv)	91%

Table 1.2. Effectiveness of Other Palladium Pre-Catalysts.^a 2 mol% [Pd] and 4 mol% terpy were used. Yields refer to isolated, purified material. ^b 5 mol% Pd(OAc)₂ and 10 mol% terpy were used.

To highlight the reaction's practical utility, we have demonstrated that other common arylboron reagents are viable substrates. *In situ* formation of aryl trifluoroborates via

addition of a mixture of NaF and KHF_2 allowed for efficient fluorination of pinacol boronic esters and arylboronic acids (Scheme 1.2). The ability to directly use a variety of arylboronic acid derivatives, without the need for prior isolation of the aryl trifluoroborate, allows for fluorination of a greater range of starting materials.

We observed that MIDA esters of electron-rich arylboronic acids can also undergo Pd-catalyzed fluorination, albeit in lower yield and requiring a larger amount of Selectfluor (Scheme 1.2). No aryl fluoride product was obtained when either NaF or KHF_2 was added, suggesting that fluorination proceeds without formation of the aryl trifluoroborate. MIDA esters of electron-poor arylboronic acids did not afford product. The direct fluorination of MIDA boronates, in the absence of exogenous fluoride anion, indicates a mechanism in which the fluorine atom involved in C–F bond formation is derived from Selectfluor, rather than added fluoride anion.



Scheme 1.2. Fluorination of various arylboronic acid derivatives. Yields refer to isolated, purified material.

We propose that the Pd-catalyzed fluorination reaction proceeds via an outer-sphere pathway, involving an unusual mononuclear Pd(III) intermediate. A mechanism that is

consistent with the experimental data, as described below, is shown in Scheme 1.3: first, turnover-limiting oxidation of a bis-terpyridyl Pd(II) complex (**1.5**) by Selectfluor affords Pd(III) **1.2** and a Selectfluor radical cation; F• transfer from the Selectfluor radical cation to an aryl trifluoroborate forms the C–F bond and generates a delocalized radical; finally, S.E.T. from the radical to **1.2** regenerates **1.5**, and provides a delocalized cation, which converts to the aryl fluoride with loss of BF₃. The generated BF₃ can react with fluoride anion or adventitious water, which may be why the addition of one equivalent of NaF typically increases the yield of aryl fluoride. Complexes of palladium in the +III oxidation state are uncommon, and have only recently been identified as relevant intermediates in organic and organometallic reactions.^{43b, 49, 89}

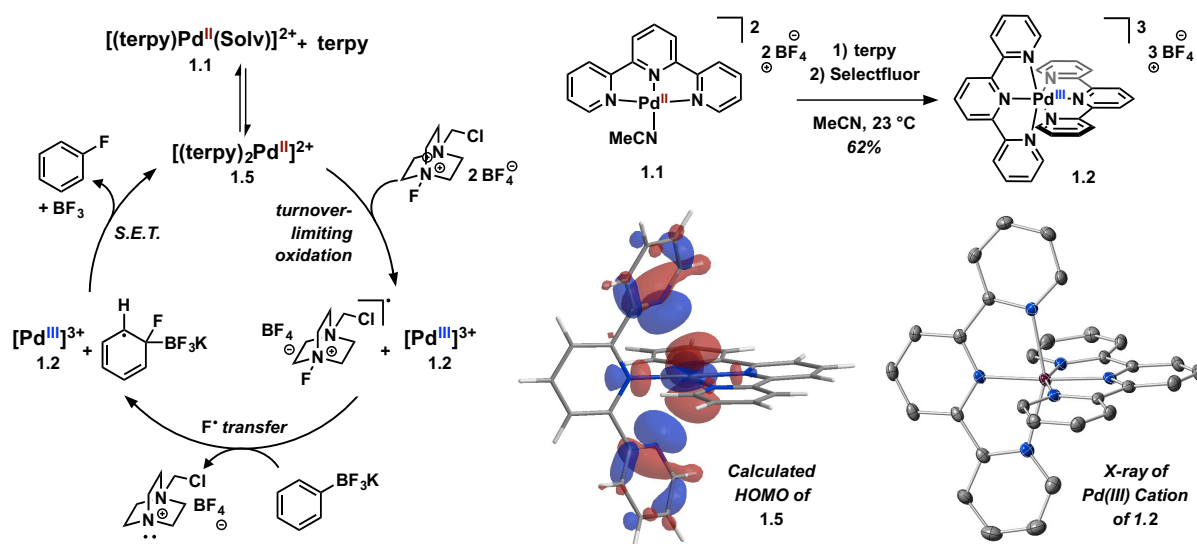
Aryl fluoride formation displayed a well-behaved kinetic profile throughout the course of the catalytic reaction, and no induction period was observed. Therefore, we were able to experimentally determine the rate law using initial rate kinetics, by monitoring aryl fluoride formation via ¹⁹F NMR spectroscopy. The reaction displays first-order kinetic dependence on the palladium catalyst, saturation kinetics with respect to terpyridine, zero-order dependence on aryl trifluoroborate, and a non-integer kinetic order of 1.4 with respect to Selectfluor. The saturation behavior observed for terpyridine, along with *in situ* ¹H NMR spectroscopy of the reaction mixture, indicates a catalyst resting state consisting of an off-cycle equilibrium between bis-terpyridyl Pd(II) complex **1.5** and a terpyridyl Pd(II) solvento complex (e.g. **1.1**). In DMF, the equilibrium of **1.5** with **1.1** and free terpyridine is rapid, with a measured binding constant of $K_a = 3 \times 10^3$. The non-integer kinetic order experimentally determined for Selectfluor suggests that Selectfluor also participates in a rapid equilibrium with **1.5**, prior to turnover-limiting oxidation (*vide infra*).

No reaction was observed between pre-catalyst **1.1** and aryl trifluoroborates in the presence or absence of exogenous terpyridine ligand, and less than 5% background reaction

was observed between Selectfluor and the evaluated aryl trifluoroborates. When **1.1** was treated with one equivalent of terpyridine, followed by one equivalent of Selectfluor, a color change from orange to deep red occurred. The color persisted in MeCN, and crystallization afforded red needles of Pd(III) complex **1.2** in 62% yield. The structure of **1.2** was determined by X-ray crystallography (Scheme 2) and exhibits a Jahn-Teller distorted octahedral geometry. The identity of **1.2** in MeCN solutions was confirmed by EPR spectroscopy, magnetic susceptibility, and UV-vis/NIR spectroscopy. The Jahn-Teller distorted octahedral geometry and the metric parameters of the terpyridine ligands are consistent with a d^7 configuration at Pd with an unpaired electron in a d_{z^2} -based orbital, rather than a ligand-centered radical, which is also supported by the UV-vis/NIR data and DFT calculations. In the solid state, **1.2** is stable for months under ambient conditions. Pd(III) complex **1.2** is a chemically competent catalyst in the fluorination reaction, and was not observed to react with aryl trifluoroborates in the absence of Selectfluor, consistent with the mechanism shown in Scheme 1.3. Additionally, **1.2** was not observed to react further when treated with additional Selectfluor, suggesting that a Pd(IV) intermediate is not accessible under the reaction conditions.

The structure of the initial complex formed by **1.1** and terpyridine, Pd(II) **1.5**, is predicted to have a pseudo-octahedral geometry, which is supported by DFT calculations. The calculated HOMO of **1.5**, shown in Scheme 1.3, is primarily of d_{z^2} parentage with respect to palladium and antibonding between palladium and the apical pyridyl ligands. Removal of one electron from the HOMO results in the Jahn-Teller distorted structure displayed by **1.2**. Selectfluor's ability to act as a single-electron oxidant has been supported through a combination of experimental and theoretical studies.⁹⁰ Electrochemical measurements show that oxidation of Pd(II) **1.5** to Pd(III) **1.2** does not proceed by outer-sphere S.E.T., which suggests the formation of an intermediate adduct between **1.5** and

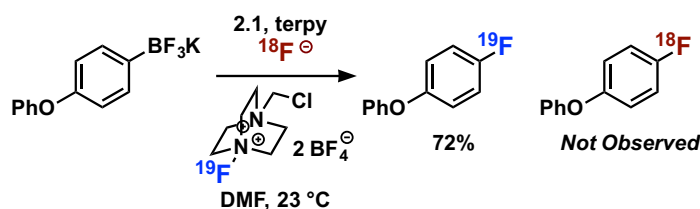
Selectfluor. The formation of such an adduct is also consistent with the non-integer kinetic order measured for Selectfluor (1.4). The specific mode of interaction between the palladium catalyst and Selectfluor is unclear at this point, but is likely critical to the success of the fluorination reaction; we speculate that the fluxional binding of terpyridine in **1.5** is important to the observed reactivity (see Chapter 3 for further discussion).



Scheme 1.3. Proposed Mechanism for Pd-Catalyzed Fluorination, Synthesis and X-ray Structure of Pd(III) Intermediate **1.2, and DFT Calculated Structure of Pd(II) Intermediate **1.5**.**^a ^a terpy = 2,2':6',2''-terpyridine; Solv = solvent (DMF or MeCN); See Supporting Information for details of DFT calculations; X-ray structure of **2** shown with 50% probability ellipsoids; H-atoms, counteranions, and solvent molecules omitted for clarity.

The observation of turnover-limiting oxidation during catalysis prevents us from studying the C–F bond forming step via kinetic analysis. We postulate that C–F bond formation occurs via one of two pathways after initial oxidation of **1.5** by Selectfluor: (1) direct F• transfer to the aryl trifluoroborate; or, (2) S.E.T. from the aryl trifluoroborate to the Selectfluor radical cation, to afford a radical cation, followed by nucleophilic attack of fluoride. In both cases, one-electron oxidation of the resulting radical by Pd(III) **1.2**, as shown in Scheme 2, would afford product and regenerate Pd(II) **1.5**. We carried out an isotopic labeling experiment to distinguish between the two pathways, in which the fluorination reaction was performed in the presence of exogenous [¹⁸F]fluoride. Aryl fluoride

formation proceeded in 72% yield, but no incorporation of the ^{18}F label was observed (Scheme 1.4). While the S.E.T./fluoride attack pathway via a tight solvent cage mechanism cannot be rigorously excluded, the absence of ^{18}F incorporation suggests the $\text{F}\cdot$ transfer pathway for C–F bond formation.



Scheme 1.4. Isotopic Labeling Experiment

In previously reported metal-mediated or -catalyzed arene fluorination reactions, including our group's palladium- and silver-mediated fluorination of arylboronic acids, carbon–fluorine bond formation is proposed to occur via reductive elimination from an aryl–metal fluoride complex.^{52, 91} The palladium-catalyzed fluorination reaction presented here is unusual in that it seems to proceed without the formation of organopalladium intermediates, yet provides high levels of selectivity.

In conclusion, we have reported the first metal-catalyzed fluorination of arylboronic acid derivatives. The reaction proceeds under mild conditions, is tolerant towards moisture and air, and is amenable to multi-gram-scale synthesis of functionalized aryl fluorides. We propose a single-electron-transfer mechanism involving a well-defined Pd(III) intermediate. This reaction provides a level of practicality and operational simplicity not previously achieved by metal-catalyzed or -mediated arene fluorination reactions, and does not generally afford side products from protodemetalation, a common problem for the synthesis of aryl fluorides. Drawbacks of the reaction include the inability to fluorinate heterocycles, and the formation of constitutional isomers for some electron-poor substrates.

CHAPTER 2 – CHARGE-TRANSFER-DIRECTED RADICAL SUBSTITUTION ENABLES *PARA*-SELECTIVE C–H FUNCTIONALIZATION

Efficient C–H functionalization requires selectivity for specific C–H bonds. Progress has been made for directed aromatic substitution reactions to achieve *ortho*- and *meta*-selectivity, but a general strategy for *para*-selective C–H functionalization has remained elusive. Herein, we introduce a previously unappreciated concept which enables nearly complete *para* selectivity. We propose that radicals with high electron affinity elicit arene-to-radical charge transfer in the transition state of radical addition, which is the factor primarily responsible for high positional selectivity. We demonstrate that the selectivity is predictable by a simple theoretical tool and show the utility of the concept through a direct synthesis of aryl piperazines. Our results contradict the notion, widely held by organic chemists, that radical aromatic substitution reactions are inherently unselective. The concept of charge transfer directed radical substitution could serve as the basis for the development of new, highly selective C–H functionalization reactions.

Historically, electrophilic aromatic substitution is perhaps the most important reaction class for the functionalization of aromatic C–H bonds, but typically affords mixtures of products (Figure 2.1a).⁹² Transition-metal catalyzed reactions have generally struggled with the same limitations in positional selectivity, except when a coordinating directing group on the arene substrate is utilized to position the catalyst within close proximity to a specific C–H bond.^{59, 61c} This chelation-assisted approach has been successful in enabling C–H functionalization *ortho*,^{61b, 62a} and in some cases *meta*,⁶⁶ to the coordinating directing group (Figure 2.1b). Steric hindrance has been explored as a strategy to control positional selectivity in C–H functionalization, but product mixtures still result, particularly for monosubstituted arenes.^{77, 79, 93} There have been isolated reports of non-chelation-assisted

aromatic C–H functionalization reactions with anomalously high *para* selectivity for monosubstituted arenes; however, these reactions either require solvent quantities of arene or work only on activated arenes, and the origin of their *para* selectivity is unknown, precluding generalization to the design of other *para* selective functionalization reactions.⁹⁴ Thus, no general strategy currently exists for highly *para* selective C–H functionalization. Such a strategy would constitute a novel complement to the classical electrophilic aromatic substitution paradigm, especially if no particular directing group is required.

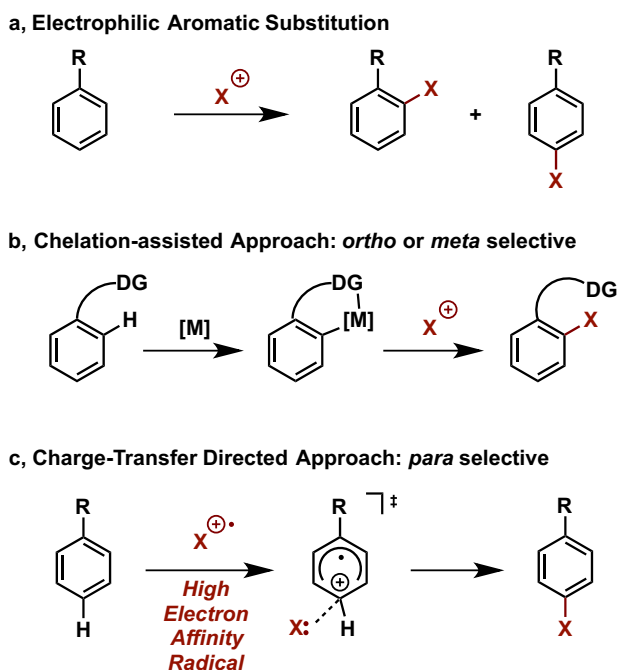


Figure 2.1. Selective C–H functionalization. **a**, Electrophilic Aromatic Substitution generally yields mixtures of isomers. **b**, Lewis basic directing groups direct functionalization to proximal bonds by chelation assistance. DG = Directing Group. **c**, Charge-transfer directed approach: arene-to-radical charge transfer, elicited by highly electrophilic radicals, leads to high *para* selectivity.

Herein, we describe how aromatic substitution by highly electrophilic radicals, which are capable of eliciting significant charge transfer from the arene in the transition state of addition, exhibits high selectivity for positions *para* to substituents on the arene (Figure 2.1c). Radical aromatic substitution reactions normally do not proceed with synthetically useful positional selectivity on substituted arenes. For example, in the 2007 edition of

Advanced Organic Chemistry by Carey and Sundberg, it is claimed that “*there are some inherent limits to the usefulness of such reactions. Radical Substitutions are only moderately sensitive to substituent directing effects, so that substituted reactants usually give a mixture of products. This means that the practical utility is limited to symmetrical reactants, such as benzene, where the position of attack is immaterial.*”⁹⁵ The results reported herein

demonstrate that, contrary to prior assumptions, radical aromatic substitution can furnish novel, useful products with high chemo- and positional selectivity when an appropriately electrophilic radical is used. We show that for most substrates, including monosubstituted arenes, only one of the possible positional isomers is observed in significant amounts. The charge transfer directed concept does not require a coordinating directing group as do chelation-assisted C–H functionalization reactions because selectivity is determined by the electronic structure in the transition state as opposed to enforced proximity of the catalyst.

Results and Discussion:

Charge Transfer Directed Radical Substitution:

The doubly cationic radical TEDA²⁺, derived from single electron reduction of Selectfluor, is capable of engaging in radical aromatic substitution to yield *N*-aryl-*N*'-chloromethyl-diazoniabicyclo[2.2.2]octane salts, which we have termed Ar–TEDA compounds (Figure 2, see page 184–188 in Chapter 3 for evidence implicating TEDA²⁺ as C–N bond forming species). The reaction is enabled by a dual catalyst combination: Pd catalyst **2.1**, which we have introduced in a previous report, and Ru(bipy)₃(PF₆)₂ (Figure 2.2a).⁹⁶ Photoirradiation is not required for reaction, which works equally well when shielded from light. For most arenes only one of the possible positional isomers of the Ar–TEDA product is observed as judged by nuclear magnetic resonance spectroscopy; fluorobenzene, for example, yields the *para* substituted product in >99:1 positional selectivity (Chapter 3 Figure 3.4). All monosubstituted arenes tested give the *para* substituted product as the only

significant isomer. Disubstituted arenes and some heteroarenes likewise undergo clean substitution at the position *para* to the group with the strongest directing effect. Thus, the synthesis of Ar–TEDA compounds described here constitutes a general non-chelation-assisted C–H functionalization reaction, with the arene as the limiting reagent, with nearly exclusive positional selectivity across a broad range of substitution patterns.

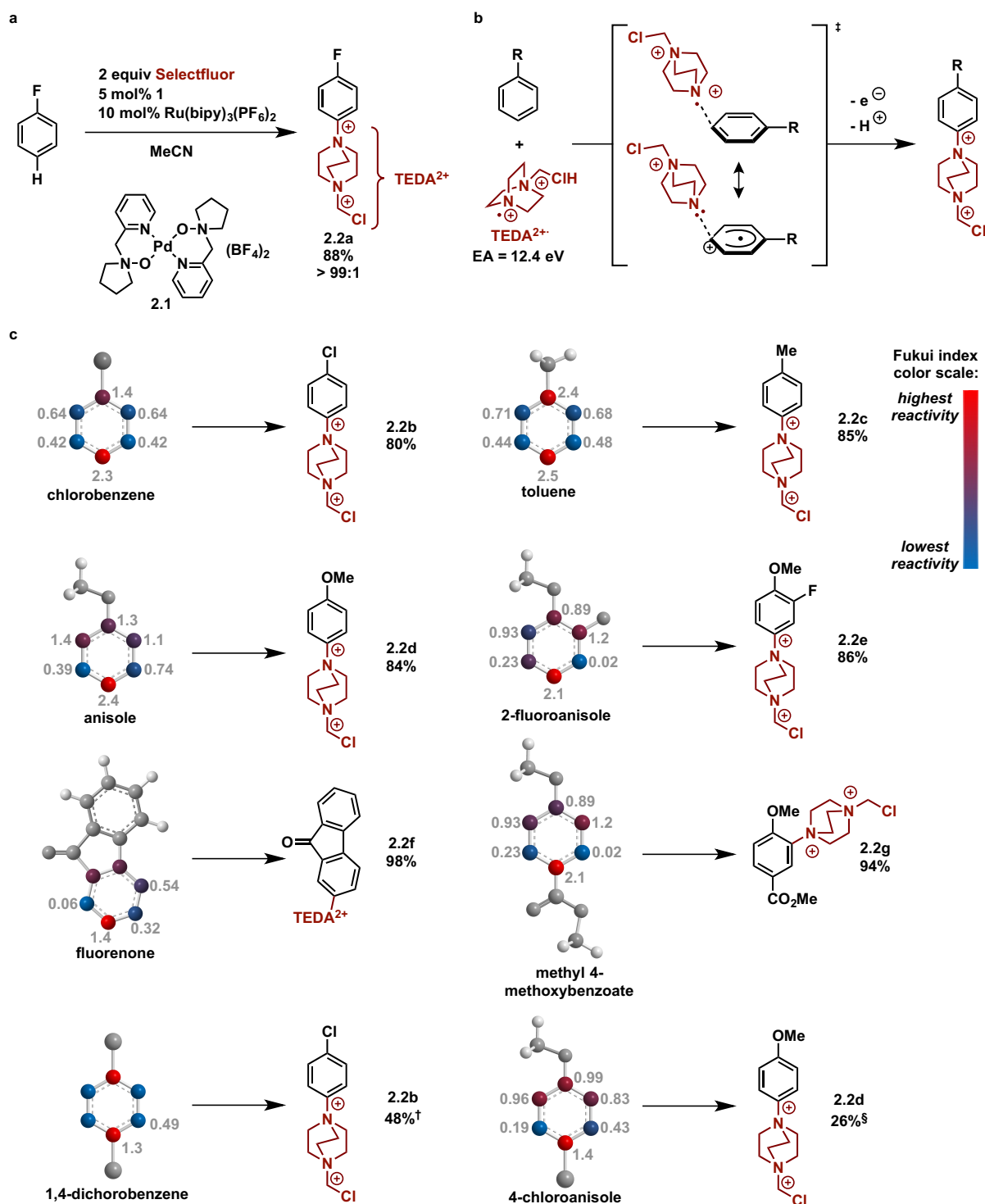


Figure 2.2. Charge transfer directed aromatic substitution. **a**, Conversion of fluorobenzene to the corresponding Ar-TEDA compound **2.2a**. **b**, Positional selectivity of TEDA^{2+} substitution is due to the stabilizing effect of arene-to-radical charge transfer in the transition state of addition. EA = Electron Affinity, refers to gas phase adiabatic electron affinity calculated by DFT. **c**, The position of substitution by TEDA^{2+} is predictable by Fukui indices. Fukui indices depicted are multiplied by ten for simplicity of presentation. DFT computations of Fukui indices and electron affinity of TEDA^{2+} performed at the (U)B3LYP/6-311G(d) level of theory, with continuum polarization solvent model for Fukui index calculations. Note that Fukui indices are computed for one conformation of the molecule, so indices of positions that are symmetrically disposed about a substituent need not be equal. See Chapter 3 for full

computational details. † Substitution in the 2-position was observed in 11% yield in addition to *ipso* substitution (Chapter 3). § Substitution in the 2-position was observed in 10% yield in addition to *ipso* substitution (Chapter 3).

The TEDA²⁺ radical is an electrophilic radical, with an electron affinity of 12.4 eV, calculated by DFT. The high electron affinity of TEDA²⁺ should favor a large contribution of charge-transfer in the transition state of addition (Figure 2.2B), which in turn leads to high selectivity for aromatic substitution at the position from which charge transfer is the greatest.⁹⁷ Therefore, a predictive tool for the positional selectivity of the reaction would be a metric which indicates the greatest extent of charge transfer that can be expected upon attack at a given position. We found Fukui nucleophilicity indices to be well-suited to this purpose. The Fukui nucleophilicity index of an atom, determined by simple quantum chemical calculations, is a measure of how readily electron density is transferred to an incoming electrophilic species attacking at the relevant atom.⁹⁸ Fukui indices are especially convenient as a predictive tool because the Fukui index for all atoms in a given molecule are determined by a pair of simple calculations on the arene itself; there is no need to map the potential energy surface of the reaction by computing the transition states of various pathways.

Figure 2.2C shows several Ar–TEDA products and the corresponding starting material, with each aromatic carbon atom of the starting material labeled with its Fukui nucleophilicity index. The Fukui nucleophilicity index is successful in predicting the site of substitution by TEDA²⁺ in almost all cases. Certain 1,4-disubstituted arenes, including 1,4-dichlorobenzene and 4-chloroanisole, yield *ipso* substitution of the halogen as the primary product.⁹⁹ Gratifyingly, Fukui nucleophilicity indices correctly predict even the observed *ipso* substitution in these cases. If a non-substitutable functional group is present at the site with the highest Fukui index, substitution at the site with the next highest Fukui index is observed, as in methyl 4-methoxybenzoate (**2.2g**). Although steric hindrance to *ortho* attack may serve to further augment the *para* selectivity of the reaction, the fact that even fluorobenzene, with

a single small substituent, gives >99:1 selectivity renders unlikely steric hindrance as the primary factor governing selectivity.

The high degree of positional selectivity we report here is unusual, especially in the context of radical aromatic substitution. A reason may be a lack of studies of substitution reactions by radicals of high electron affinity. While the TEDA^{2+•} radical dication has been proposed as an intermediate in recently reported aliphatic C–H oxidation methodologies utilizing Selectfluor,^{56, 100} to our knowledge addition of this radical to unsaturated systems has not been investigated. The most commonly employed radicals in a synthetic context are uncharged carbon-, oxygen-, nitrogen-, and halogen-based radicals, which have electron affinities in the range of 0.8–3.6 eV, far below the value for TEDA^{2+•} (12.44 eV, Figure 2.3). Aromatic substitution reactions of most neutral radicals are known to proceed with low selectivity.⁹⁵ For example, the phenyl radical has an electron affinity of 1.1 eV, and under conditions reported by Li, undergoes aromatic substitution with fluorobenzene to give an *ortho:meta:para* ratio of 47:16:37.¹⁰¹ The neutral phthalimide radical has a higher electron affinity (EA = 3.66 eV). We have found that the phthalimide radical, when generated under conditions reported by Sanford,¹⁰² undergoes aromatic substitution with fluorobenzene in a 37:11:52 ratio of *ortho*, *meta*, and *para* isomers; the selectivity for the *para* position is higher, though the other isomers still abound.

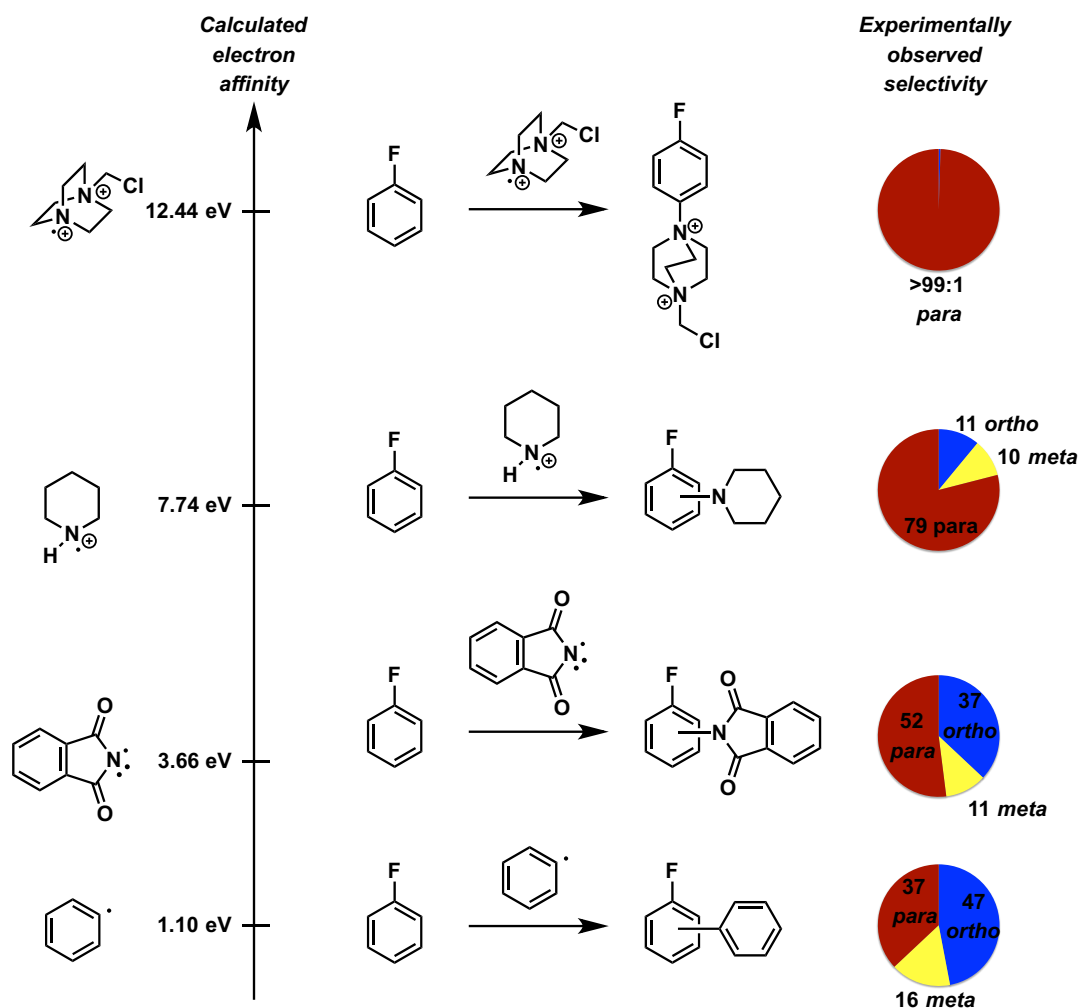


Figure 2.3. Selectivity for *para* substitution increases with increasing electron affinity of the radical. Electron affinities refer to gas phase adiabatic electron affinity calculated at the (U)B3LYP/6-311G(d) level of theory.

Positive charge increases electron affinity, and based on our findings and proposal, positively charged radicals should result in more selective arene substitution reactions. Monocationic aminium radicals have electron-affinities in the range of 7–8 eV, and their aromatic substitution reactivity was thoroughly investigated in seminal work by Minisci, who noted the higher selectivity of aminium radical addition compared to less electrophilic radicals. Under Minisci's conditions, the monocationic aminium radical derived from piperidine (EA = 7.74 eV) adds to fluorobenzene more selectively than the neutral phthalimide radical to afford an *o*:*m*:*p* ratio of 11:10:79. Minisci described the selectivity of monocationic aminium radicals as similar to the selectivity of electrophilic aromatic

substitution, affording products of *ortho* and *para* substitution of monosubstituted arenes bearing electron donating groups.¹⁰³ We have discovered that, for sufficiently electrophilic radicals, charge transfer in the transition state of addition can lead to high selectivity for the *para* position over *ortho*; we have rationalized the phenomenon in terms of charge transfer in the transition state, and have introduced Fukui indices as a tool for predicting the site of substitution. The second positive charge of the TEDA^{2+•} aminium radical increases the electron affinity to 12.44 eV, and at this level, nearly absolute selectivity for the *para* position is observed for monosubstituted arenes.

The general applicability of the charge-transfer directed concept will depend on whether other radicals of comparable electron affinity to TEDA^{2+•} can be designed. The uncommonly high electron affinity of TEDA^{2+•} is due to its two positive charges; doubly cationic organic radicals are rare, presumably because there has been a lack of generally appreciated applications and because strategies for accessing them are unexplored. We anticipate that the correlation between electron affinity and positional selectivity described herein will stimulate research in high electron affinity radicals due to their potential to address the longstanding challenge of positional selectivity in C–H functionalization.

We furthermore note that radicals of electron affinity comparable to TEDA^{2+•} need not in principle be based on cationic aminium radicals. For example, DFT calculations indicate that alkoxyl radicals exhibit a similar trend with increasing positive charge, though the septet oxygen atom itself lacks a formal charge (Chapter 3 Figure 3.14). Thus, in principle, highly electrophilic radicals could be designed for the installation of a variety of functional groups, not just C–N bonds.

Application to the synthesis of aryl piperazines:

As one synthetic application of the charge transfer directed radical substitution concept, we have developed a two-step, one-pot synthesis of aryl piperazines from the

corresponding aryl C–H compounds (Figure 2.4). The procedure involves reduction of the Aryl–TEDA compounds by sodium thiosulfate, which converts the TEDA moiety into a piperazine heterocycle. Piperazines are a common motif in pharmaceuticals and materials; they constitute the third most common heterocycle present in the small molecule pharmaceuticals listed in the FDA Orange Book.¹⁰⁴ Aryl piperazines are commonly synthesized by Buchwald-Hartwig cross coupling reactions of aryl electrophiles with piperazine derivatives.¹⁰⁵ The direct synthesis of aryl piperazines reported here is advantageous because it does not require a pre-functionalized substrate, such as an aryl halide. Importantly, this advantage relies on the high and predictable positional selectivity of the reaction, which enables the high-yield synthesis of a single desired positional isomer. The reaction is operationally simple, and can be performed under air with commercial-quality solvent. Furthermore, the piperazine moiety is obtained with an unprotected secondary amine, ready for subsequent manipulation.

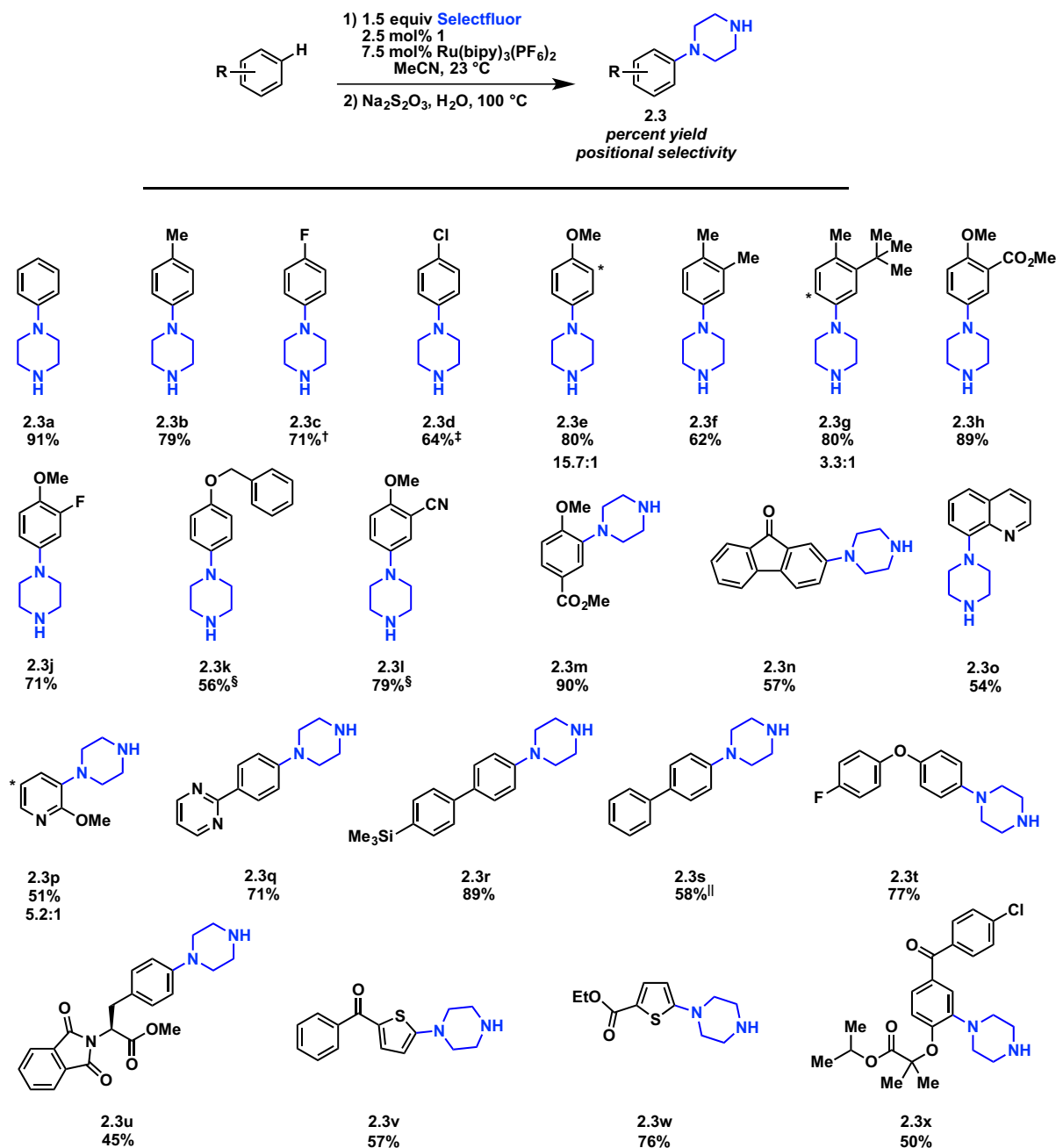


Figure 2.4. Two-step, one-pot synthesis of aryl piperazines by charge transfer directed C–H functionalization. [†] 40 °C reaction temperature in the first step. [‡] 45 °C reaction temperature in the first step. [§] 2.5 equiv Selectfluor, 5.0 mol% **2.1**, and 10 mol% Ru(bipy)₂(PF₆)₂ in first step. ^{||} 1.0 equiv Selectfluor used in first step. * denotes the site of piperazination of the other constitutional isomer.

A variety of arenes, including 5- and 6-membered heteroarenes, undergo piperazination. Generally, attack of TEDA²⁺ *ortho* to substituents is unfavorable, and occurs only for arenes in which the preferred *para* position for substitution is blocked by a group which cannot undergo *ipso* substitution; this observation can be applied to block

piperazination of certain positions, or even entire arene rings, as in substrates **2.3r** and **2.3t**. Product **2.3g** demonstrates the limits of the positional selectivity of the reaction: the two substituents in 2-methyl-tert-butylbenzene differ only slightly in their electron-donating ability, and the product was isolated as a 3.3:1 mixture of isomeric products. Although TEDA^{2+•} is known to engage in sp³ C–H bond cleavage, we have observed no evidence of such side-reactions in our investigations, despite the fact that several substrates contain weak C–H bonds adjacent to aromatic rings (e.g., **2.3f**) or ether oxygen atoms (e.g., **2.3e**, **2.3k**); addition of TEDA^{2+•} to the unsaturated aromatic system outcompetes C–H bond cleavage.

For most substrates, nearly full conversion to the Ar–TEDA compound is observed, and in several cases the yield of the piperazine following the thiosulfate-mediated stage is lower. For example, the anti-cholesterol drug Fenofibrate undergoes Ar–TEDA formation in 88% yield, but upon treatment with sodium thiosulfate at 100 °C the yield of piperazine **2.3x** is 51%. The Ar–TEDA formation reaction exhibits significant functional group tolerance, despite the highly reactive and electrophilic nature of the TEDA^{2+•} radical intermediate; for most substrates in Figure 2.4, the majority of mass balance is lost in the piperazine formation step, not the Ar–TEDA formation step.

We have shown that the doubly cationic nitrogen-based radical TEDA^{2+•} undergoes radical substitution with arenes with higher positional selectivity than any conventional methodology for arene substitution. We put forth a previously underappreciated rationale to explain and predict positional selectivities in charge transfer directed radical aromatic substitution: high selectivity is achieved through a high degree of charge-transfer in the transition state of addition. This charge transfer effect is maximized for radicals with high electron affinity. Our results can rationalize why known electrophilic radical substitution reactions of neutral radicals are typically not selective, and more importantly, they provide a framework to guide the design of new, selective arene substitution chemistry.

CHAPTER 3 – EXPERIMENTAL METHODS

Materials and Methods

Reactions were carried out under ambient atmosphere unless otherwise noted.

Purified compounds were dried under high vacuum (0.01–0.05 Torr). Yields refer to purified and spectroscopically pure compounds. Thin layer chromatography (TLC) was performed using EMD TLC plates pre-coated with 250 μm thickness silica gel 60 F₂₅₄ plates and visualized by fluorescence quenching under UV light and KMnO₄ stain. Flash chromatography was performed using silica gel (230-400 mesh) purchased from Silicycle, Inc., using a forced flow of eluent at 0.3-0.5 bar pressure.¹⁰⁶ Melting points were measured on a Thomas Scientific Uni-Melt capillary melting point apparatus. All melting points were measured in open capillaries and are uncorrected. All air- and moisture-sensitive manipulations were performed using oven-dried glassware, including standard Schlenk and glovebox techniques under an atmosphere of nitrogen. NMR spectra were recorded on either a Varian Unity/Inova 600 spectrometer operating at 600 MHz for ¹H acquisitions, a Varian Unity/Inova 500 spectrometer operating at 500 MHz and 125 MHz for ¹H and ¹³C acquisitions, respectively, or a Varian Mercury 400 spectrometer operating at 400 MHz and 375 MHz for ¹H and ¹⁹F acquisitions, respectively. Chemical shifts are reported in ppm with the solvent resonance as the internal standard (¹H: CDCl₃, δ 7.26; CD₂Cl₂, δ 5.32; (CD₃)₂SO, δ 2.50; CD₃CN, δ 1.94; (CD₃)₂CO, δ 2.05), (¹³C: CDCl₃, δ 77.16; CD₂Cl₂, δ 53.84; CD₃CN, δ 1.32, (CD₃)₂SO, δ 39.52; (CD₃)₂CO, δ 29.84, 206.26),¹⁰⁷ or added 3-nitrofluorobenzene (-112.0 ppm) for ¹⁹F spectra. Data is reported as follows: s = singlet, br = broad, d = doublet, t = triplet, q = quartet, quin = quintet, m = multiplet; coupling constants in Hz; integration. All deuterated solvents were purchased from Cambridge Isotope Laboratories. Solution-state magnetic susceptibility measurements were obtained using the Evans method¹⁰⁸ and are

reported as follows: (field strength, solvent, temperature): μ_{eff} (concentration in mg/mL).

EPR spectra were recorded on a Bruker ElexSys E500 EPR spectrometer operating at X-band frequency (9 GHz). UV-vis/NIR spectra were measured on a PerkinElmer Lambda 750 spectrophotometer. Electrochemical measurements were made using a CH Instruments Model 600E Series Electrochemical Analyzer/Workstation with a glassy carbon working electrode, a Pt wire counterelectrode, and a non-aqueous Ag/Ag⁺ reference electrode. High-resolution mass spectra were obtained using an Agilent ESI-TOF (6210) mass spectrometer or a Bruker q-TOF Maxis Impact mass spectrometer. LC/MS data were obtained using a Shimadzu LCMS-2020.

Reagents and Solvents: All chemicals were used as received unless otherwise noted.

Pd(OAc)₂ was purchased from Strem. HBF₄•OEt₂ was purchased from Alfa Aesar. 1-Chloromethyl-4-fluoro-1,4-diazoniabicyclo[2.2.2]octane bis(tetrafluoroborate) (Selectfluor) and 2,2':6',2''-terpyridine (terpy) were purchased from Strem or SigmaAldrich.

For the reactions described in Chapter 1, DMF was ACS Reagent grade, purchased from SigmaAldrich; MeCN was ACS grade, purchased from BDH. These solvents were used as received without further purification.

Experimental Procedures and Compound Characterization for Chapter 1¹⁰⁹

I. Representative Procedure for the Pd-Catalyzed Fluorination Reaction

Representative Procedure A: Electron Poor Substrates (MeCN)

Palladium precatalyst **1.1** (307 mg, 554 μ mol, 0.010 equiv), terpy (258 mg, 1.11 mmol, 0.040 equiv), aryl trifluoroborate (55.4 mmol, 1.00 equiv), Selectfluor (23.5 g, 66.4 mmol, 1.20 equiv), and sodium fluoride (2.32 g, 55.4 mmol, 1.00 equiv) were added to a round-bottom flask (200 mL), followed by acetonitrile (55.4 mL, 1.0 M) at 23 °C. An air-cooled reflux condenser was fitted to the round bottom flask. The reaction mixture was stirred for 15 hours

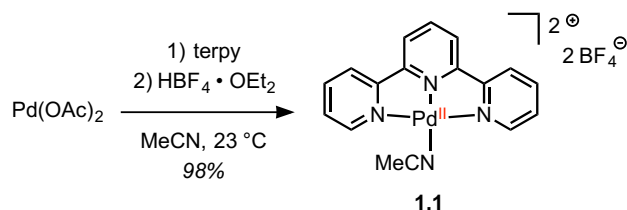
open to air at 40 °C, allowed to cool to 23 °C, and then transferred to a separatory funnel, rinsing the reaction flask with additional acetonitrile (2 × 50 mL). Pentane (250 mL) was added and the organic layer was washed with water (350 mL). The aqueous layer was extracted with dichloromethane (4 × 300 mL). The combined organic layers were washed with brine (500 mL), dried over sodium sulfate, filtered, and concentrated *in vacuo*. The residue was purified by chromatography on silica gel to afford the aryl fluoride product.

Representative Procedure B: Electron Neutral or Electron Rich Substrates (DMF)

Palladium precatalyst **1.1** (201 mg, 362 μmol, 0.010 equiv), terpy (169 mg, 724 μmol, 0.040 equiv), aryl trifluoroborate (36.2 mmol, 1.00 equiv), Selectfluor (14.1 g, 39.8 mmol, 1.10 equiv), and sodium fluoride (1.52 g, 36.2 mmol, 1.00 equiv) were added to a round-bottom flask (100 mL), followed by DMF (36 mL, 1.0 M) at 23 °C. An air-cooled reflux condenser was fitted to the round bottom flask. The reaction mixture was stirred for 15 hours open to air at 23 °C, and then transferred to a separatory funnel. Pentane (250 mL) was added and the organic layer was washed with a 5% aqueous lithium chloride solution (250 mL). The aqueous layer was extracted with pentane (4 × 150 mL). For aryl fluorides that are poorly soluble in pentane, diethyl ether was used as the extraction solvent. The combined organic layers were dried over sodium sulfate, filtered, and concentrated *in vacuo*. The residue was purified by chromatography on silica gel to afford the aryl fluoride product.

II. Synthesis and Characterization of Palladium Complexes

[(terpy)Pd(MeCN)][BF₄]₂ (**1.1**)



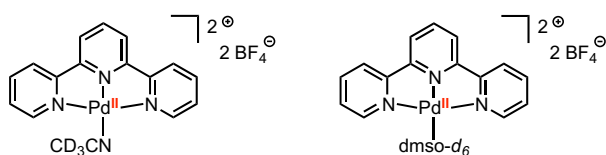
To Pd(OAc)₂ (5.00 g, 20.4 mmol, 1.00 equiv) in MeCN (250 mL) at 23 °C was added terpy (4.77 g, 20.4 mmol, 1.00 equiv). The reaction mixture was stirred for 20 minutes, affording a pink/orange slurry. To this slurry was added HBF₄·OEt₂ (6.05 mL, 7.20 g, 41.9 mmol, 2.05 equiv) via syringe. The reaction mixture was stirred vigorously for 30 min, at which point a suspension of tan solids was observed. The solids were collected by filtration and washed with Et₂O (100 mL). Further precipitation was observed from the filtrate at this point, and the precipitate was collected by a second filtration. The combined solids were washed with additional Et₂O (50 mL), and then dried under vacuum to afford 10.8 g of the title compound as a pale tan solid (98% yield).

X-ray quality crystals were grown as follows: a saturated solution of **1.1** in MeCN was prepared by dissolving approximately 5 mg of **1.1** in 1 mL MeCN at 23 °C, and filtering over a celite plug to remove any remaining solids. A 4 mL glass vial containing the solution was placed, uncapped, into a 20 mL glass vial containing approximately 4 mL of Et₂O. The 20 mL vial was capped, and vapor diffusion of Et₂O into the MeCN solution of **1.1** at 23 °C gave orange crystals after 24 hours.

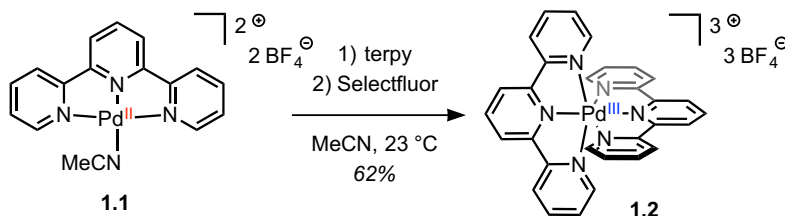
mp: 273–275 °C (decomp). NMR spectroscopy: ¹H-NMR (400 MHz, CD₃CN, 23 °C, δ): 8.57 (d, *J* = 5.6 Hz, 2H), 8.51 (t, *J* = 8.2 Hz, 1H), 8.43 (t, *J* = 7.8 Hz, 2H), 8.34 (d, *J* = 8.0 Hz, 2H), 8.28 (d, *J* = 8.4 Hz, 2H), 7.84 (td, *J* = 6.6 Hz, 1.5 Hz, 2H), 1.96 (s, 3H). ¹H-NMR (400 MHz, dms_o-*d*₆, 23 °C, δ): 8.67–8.60 (m, 5H), 8.54–8.49 (m, 4H), 7.92 (td, *J* = 6.8 Hz, 1.0 Hz, 2H), 2.06 (s, 3H). ¹³C-NMR (125 MHz, dms_o-*d*₆, 23 °C, δ): 157.0, 155.2, 150.5, 143.5, 143.2, 129.0, 125.5, 124.7, 118.1, 1.2. ¹⁹F-NMR (375 MHz, CD₃CN, 23 °C, δ): –151.7 (s). UV-VIS Spectroscopy (DMF, 23 °C): 526 nm (ε = 144 M⁻¹ cm⁻¹); 367 nm (ε = 1.16 × 10⁴ M⁻¹ cm⁻¹); 349 nm (ε = 1.29 × 10⁴ M⁻¹ cm⁻¹); 333 nm (ε = 1.07 × 10⁴ M⁻¹ cm⁻¹). FT-IR Spectroscopy (neat, cm⁻¹): 2323, 1606, 1574, 1483, 1452, 1323, 1029, 828, 781, 724, 517. Anal: calcd for C₁₇H₁₄B₂F₈N₄Pd: C, 36.83; H, 2.55; N, 10.11; found: C, 37.11; H, 2.56; N,

9.97. X-ray data included in X-Ray Data Analysis section.

The acetonitrile ligand in **1.1** is displaced by either CD₃CN or dms-*d*₆ upon dissolution; as a result, free CH₃CN is observed in the ¹H and ¹³C NMR spectra (¹³C-NMR signals were not observed in CD₃CN due to low solubility). Compound **1.1** is poorly soluble in non-coordinating solvents. Accordingly, the solution structures corresponding to the NMR data reported above should be considered as:



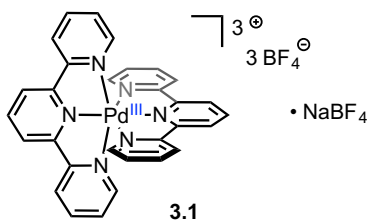
[(terpy)₂Pd][BF₄]₃ (1.2**)**



To a suspension of [(terpy)Pd(MeCN)][BF₄]₂ (**1.1**) (250. mg, 0.451 mmol, 1.00 equiv) in MeCN (10 mL) at 23 °C was added terpy (105 mg, 0.451 mmol, 1.00 equiv) and the mixture was stirred for 1 minute, affording a homogeneous orange solution. To this solution was added Selectfluor (168 mg, 0.474 mmol, 1.05 equiv), and the reaction mixture was stirred vigorously at 23 °C for 20 minutes, at which point a homogeneous deep red solution was observed. The solution was transferred to a 20 mL glass vial, and the vial was placed, uncapped, into a jar containing approximately 50 mL of Et₂O. The jar was capped, and vapor diffusion of Et₂O into the MeCN solution at 23 °C resulted in the growth of large red needle crystals after 24 hours. The following purification procedure was performed to remove residual Selectfluor and TEDA-BF₄: the supernatant from crystallization was decanted, and the crystallized material was dissolved in MeCN (15 mL), filtered over a celite plug, and

crystallized again by vapor diffusion of Et₂O (50 mL) into the MeCN solution. The supernatant from crystallization was decanted, and the crystallized material was again dissolved in MeCN (15 mL), filtered over a celite plug, and crystallized once more by vapor diffusion of Et₂O (50 mL) into the MeCN solution. The final batch of crystals was isolated and dried under vacuum to afford 233 mg of the title compound as deep red needle crystals (62% yield). Crystals grown in this manner were found to be suitable for X-ray diffraction. mp: 220 °C (decomp). NMR Spectroscopy: ¹⁹F-NMR (375 MHz, CD₃CN, 23 °C, δ): −151.3 (s). UV-VIS Spectroscopy (MeCN, 23 °C): 1002 nm (ε = 95.9 M^{−1} cm^{−1}); 419 nm (ε = 1.52 × 10³ M^{−1} cm^{−1}); 340 nm (ε = 2.36 × 10⁴ M^{−1} cm^{−1}). Magnetic susceptibility (500 MHz, CD₃CN, 23 °C): μ_{eff} = 1.74 μ_B (14.3 mg/mL). FT-IR Spectroscopy (neat, cm^{−1}): 3102, 1603, 1502, 1479, 1315, 1245, 1026, 780, 644, 519. Anal: calcd for C₃₀H₂₂B₃F₁₂N₆Pd: C, 43.24; H, 2.66; N, 10.08; found: C, 43.05; H, 2.51; N, 9.85. EPR spectra included in EPR Data section. X-ray data included in X-Ray Data Analysis section. ¹H-NMR and ¹³C-NMR signals were not observed.

Crystallization of [(terpy)₂Pd][BF₄]₃·[NaBF₄] (3.1)



Due to the high level of disorder in the X-ray crystal structure of [(terpy)₂Pd][BF₄]₃ (**2**) (see X-ray data section), we felt that this structure was not suitable to satisfactorily determine the structural metrics or Pd oxidation state. Therefore, compound **1.2** was derivatized as its NaBF₄ adduct, which allowed us to unambiguously characterize the Pd(III) cation. To a solution of **1.2** (15. mg, 0.018 mmol, 1.0 equiv) in MeCN (1 mL) was added NaBF₄ (4.0 mg, 0.036 mmol, 2.0 equiv). The mixture was allowed to stir for 30 minutes at 23 °C, and

was then transferred to a 4 mL glass vial. The vial was placed, uncapped, into a 20 mL glass vial containing approximately 4 mL of Et₂O. The 20 mL vial was capped, and vapor diffusion of Et₂O into the MeCN solution at 23 °C gave dark red plate crystals of **S1** after 24 hours, which were suitable for X-ray analysis. Full details are presented in the X-ray crystallographic data section.

Solutions prepared by dissolving crystals of **3.1** in MeCN displayed spectroscopic properties (¹⁹F-NMR, UV-vis/NIR, EPR) identical to **1.2**.

The X-ray structure of **3.1** allows a determination of the (+III) oxidation state at Pd, and the Pd(III) cation displays a Jahn-Teller distorted octahedral geometry, consistent with the *d*⁷ electronic configuration (Pd–N₁ and Pd–N₃ vs. Pd–N₄ and Pd–N₆, Fig. S1).

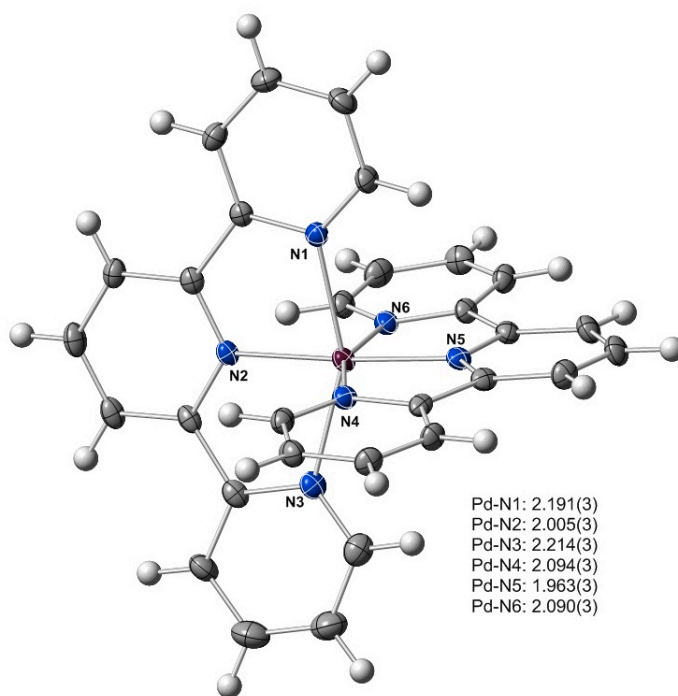
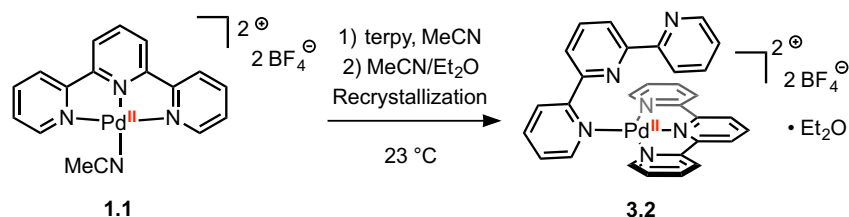


Figure 3.1. X-ray crystal structure of the Pd(III) cation of complex **3.1**, with Pd–N distances (in Å), displaying a Jahn-Teller distorted octahedral structure. Thermal ellipsoids are plotted at the 50% probability level.

Crystallization of [(terpy)₂Pd][BF₄]₂ (**3.2**)



To a suspension of [(terpy)Pd(MeCN)][BF₄]₂ (**1.1**) (20. mg, 0.036 mmol, 1.0 equiv) in MeCN (1 mL) at 23 °C was added terpy (8.4 mg, 0.036 mmol, 1.0 equiv), and the mixture was stirred for 5 minutes, affording an orange solution. The mixture was transferred to a 4 mL glass vial, and the vial was placed, uncapped, into a 20 mL glass vial containing approximately 4 mL of Et₂O. The 20 mL vial was capped, and vapor diffusion of Et₂O into the MeCN solution at 23 °C resulted in the growth of orange/yellow crystals after 24 hours, which were suitable for X-ray diffraction.

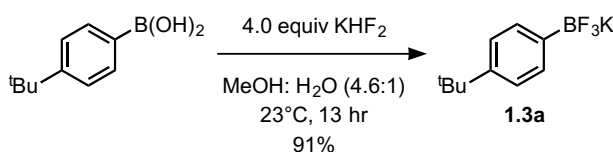
mp: 260–266 °C (decomp). NMR spectroscopy: ¹H-NMR (400 MHz, CD₃CN, 23 °C, δ): 8.8 (br s), 8.5–7.8 (br m), 7.5 (br s). ¹⁹F-NMR (375 MHz, CD₃CN, 23 °C, δ): –151.9 (s). UV-VIS Spectroscopy (MeCN, 23 °C): 526 nm (ε = 102 M^{–1} cm^{–1}); 364 nm (ε = 1.15 × 10⁴ M^{–1} cm^{–1}); 347 nm (ε = 1.08 × 10⁴ M^{–1} cm^{–1}); 331 nm (ε = 7.52 × 10³ M^{–1} cm^{–1}). FT-IR Spectroscopy (neat, cm^{–1}): 3086, 1605, 1563, 1451, 1321, 1249, 1028, 771 520. Anal: calcd for C₃₀H₂₂B₂F₈N₆Pd • 0.5 Et₂O: C, 49.01; H, 3.45; N, 10.75; found: C, 49.06; H, 3.27; N, 10.73. X-ray data included in X-Ray Data Analysis section. ¹³C-NMR signals were not observed due to low solubility of **3.2**. The broad ¹H-NMR signals suggest fluxional behavior, likely due to rotation of the unligated pyridyl groups on the NMR timescale. X-ray crystallographic analysis, along with the ¹H-NMR spectrum of crystals of **3.2** dissolved in CD₃CN, shows that compound **3.2** crystallizes with Et₂O as a solvent of crystallization (1:1 ratio of **3.2**:Et₂O).

Please see the discussion in the Reaction Kinetics section regarding the relevance of **3.2** vs.

1.5 to the Pd-catalyzed fluorination reaction.

III. Synthesis and Characterization of Non-Commerically Available Starting Materials

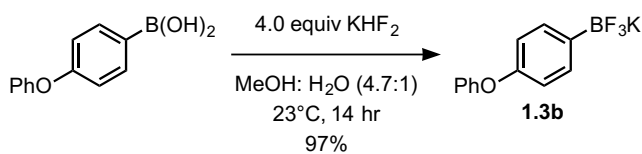
Potassium 4-*tert*-butylphenyl trifluoroborate (1.3a)



To a vigorously stirred suspension of 4-*tert*-butylphenylboronic acid (1.00 g, 5.62 mmol, 1.00 equiv) in methanol (25 mL, c = 0.2 M) was added a solution of potassium bifluoride (1.76 g, 22.5 mmol, 4.00 equiv) in water (5 mL) at 23 °C. The reaction mixture was stirred for 13 hours at 23 °C and then concentrated *in vacuo* to afford a colorless solid that was further dried at 80 °C at 100 mtorr. The solid was stirred in refluxing acetone (50 mL) and the hot supernatant was filtered through celite. The product was further extracted with acetone (2 × 50 mL) at 23 °C and the supernatant was filtered through celite. The combined filtrates were concentrated *in vacuo* to afford the title compound (1.22 g, 5.09 mmol, 91% yield) as a colorless crystalline solid.

NMR Spectroscopy: ¹H NMR (500 MHz, acetone-*d*₆, 23 °C, δ): 7.39 (d, *J* = 8.0 Hz, 2H), 7.13 (d, *J* = 7.6 Hz, 2H), 1.25 (s, 9H). ¹³C NMR (125 MHz, DMSO-*d*₆, 23 °C, δ): 146.9, 131.1, 122.9, 33.9, 31.4. ¹⁹F NMR (375 MHz, acetone-*d*₆, 23 °C, δ): −143.1 (bs). HRMS-FIA(*m/z*) calcd for C₁₀H₁₃BF₃K [M−K][−], 201.1070; found, 201.1070.

Potassium 4-phenoxyphenyl trifluoroborate (1.3b)

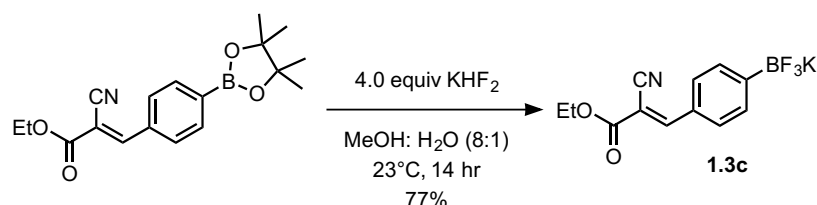


To a vigorously stirred suspension of 4-phenoxyphenylboronic acid (15.0 g, 70.1 mmol, 1.00

equiv) in methanol (280 mL, c = 0.3 M) was added a solution of potassium bifluoride (21.9 g, 280 mmol, 4.00 equiv) in water (60 mL) at 23 °C. The reaction mixture was stirred for 14 hours at 23 °C and then concentrated *in vacuo* to afford a colorless solid that was further dried at 80 °C at 100 mtorr. The solid was suspended in acetone (1 × 180 mL, 4 × 60 mL), stirred vigorously, and the supernatant was filtered through celite. The combined filtrates were concentrated *in vacuo* to afford the title compound (18.7 g, 67.8 mmol, 97% yield) as a colorless crystalline solid.

NMR Spectroscopy: ¹H NMR (500 MHz, acetone-*d*₆, 23 °C, δ): 7.48 (d, *J* = 8.2 Hz, 2H), 7.31-7.27 (m, 2H), 7.00 (tt, *J* = 7.4, 1.0 Hz, 1H), 6.91-6.89 (m, 2H), 6.78-6.77 (m, 2H). ¹³C NMR (125 MHz, acetone-*d*₆, 23 °C, δ): 159.5, 155.5, 133.8, 133.8, 130.3, 122.9, 118.4, 118.4. ¹⁹F NMR (375 MHz, acetone-*d*₆, 23 °C, δ): −143.1 (bs). HRMS-FIA(*m/z*) calcd for C₁₂H₉BF₃OK [M−K][−], 237.0706; found, 237.0712.

Potassium (*E*)-4-(2-cyano-2-ethoxycarbonylvinyl)phenyl trifluoroborate (1.3c)

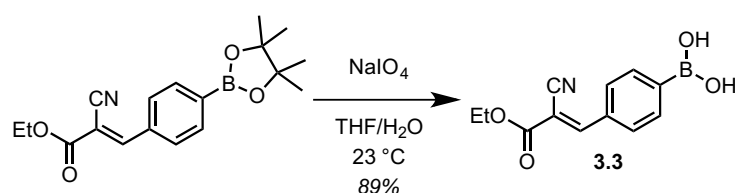


To a vigorously stirred suspension of [(*E*)-4-(2-cyano-2-ethoxycarbonylvinyl)phenyl]boronic acid pinacol ester (25.0 g, 76.4 mmol, 1.00 equiv) in methanol (560 mL, c = 0.1 M) was added a solution of potassium bifluoride (23.9 g, 306 mmol, 4.00 equiv) in water (70 mL) at 23 °C. The reaction mixture was stirred for 14 hours at 23 °C and then concentrated *in vacuo* to afford a colorless solid that was further dried at 80 °C at 100 mtorr. The solid was suspended in acetone (1 × 500 mL, 4 × 100 mL), stirred vigorously, and the supernatant was filtered through celite. The combined filtrates were concentrated *in vacuo* to afford a colorless solid. The solid was purified by the following procedure: the solid was dissolved in

refluxing acetone (300 mL) and the solution was allowed to cool to 23 °C. Pentane (300 mL) was layered on top of the cooled acetone solution at 23 °C. Slow diffusion of the pentane into the acetone solution resulted in the growth of colorless crystals, which were isolated by filtration. The colorless crystals were dissolved in refluxing acetone (300 mL) and the hot solution was filtered through celite. The filtrate was concentrated *in vacuo* to afford a colorless solid. The solid was purified by crystallization using the layering procedure detailed above to afford the title compound (18.1 g, 58.9 mmol, 77% yield) as a colorless crystalline solid.

NMR Spectroscopy: ^1H NMR (600 MHz, DMSO- d_6 , 23 °C, δ): 8.27 (s, 1H), 7.83 (d, J = 7.9 Hz, 2H), 7.51 (d, J = 8.0 Hz, 2H), 4.29 (q, J = 7.1 Hz, 2H), 1.29 (d, J = 14.2 Hz, 3H). ^{13}C NMR (125 MHz, DMSO- d_6 , 23 °C, δ): 162.4, 156.3, 132.2, 129.4, 128.4, 116.1, 99.5, 62.1, 14.0. ^{19}F NMR (375 MHz, acetone- d_6 , 23 °C, δ): -144.6 (bs). HRMS-FIA(m/z) calcd for $\text{C}_{12}\text{H}_{10}\text{BF}_3\text{NO}_2\text{K} [\text{M}-\text{K}]^-$, 268.0764; found, 268.0770.

[(*E*)-4-(2-cyano-2-ethoxycarbonylvinyl)phenyl]boronic acid (3.3)



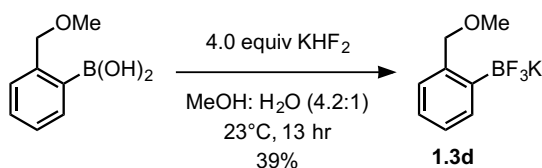
A 50 mL round-bottom flask was charged with [(*E*)-4-(2-cyano-2-ethoxycarbonylvinyl)phenyl]boronic acid pinacol ester (1.00 g, 3.06 mmol, 1.00 equiv), followed by THF (6 mL) and H₂O (6 mL) at 23 °C. To this mixture was added NaIO₄ (1.96 g, 9.18 mmol, 3.00 equiv), and the reaction mixture was stirred for 1 hour at 23 °C, affording a thick white slurry. To this slurry was added 1.0 N HCl (10 mL), and the mixture was allowed to stir for an additional 4 hours. The reaction mixture was transferred to a separatory funnel, and the product was extracted from the aqueous mixture with EtOAc (4 × 50 mL). The

combined organic phases were washed with brine (2 × 50 mL), dried over Na₂SO₄, filtered, and concentrated under vacuum to give an off-white solid. The solid was triturated with hexanes (2 × 30 mL), and then dried under vacuum to afford 668 mg of the title compound as an off-white solid (89% yield).

NMR spectroscopy: ¹H-NMR (400 MHz, dms-*d*₆, 23 °C, δ): 8.37 (s, 1H), 8.31 (br s, 2H), 7.99–7.91 (m, 4H), 4.30 (q, *J* = 7.2 Hz, 2H), 1.29 (t, *J* = 7.0 Hz, 3H). ¹³C-NMR (125 MHz, dms-*d*₆, 23 °C, δ): 161.8, 155.1, 140.3, 134.6, 132.5, 129.6, 115.6, 102.9, 62.4, 14.0. Mass Spectrometry: HRMS (ESI-TOF) (*m/z*): Calcd for [C₁₂H₁₂BNO₄ + Na]⁺, 268.0757. Found, 268.0744.

The ¹H-NMR spectrum of **3.3** in dms-*d*₆ displays a minor set of aromatic peaks, the presence of which are concentration-dependent, corresponding to the boroxine of **3.3**: arylboronic acids are well known to equilibrate with the boroxine form in solution.¹¹⁰ The presence of the boroxine did not have an observable impact on the Pd-catalyzed fluorination of **3.3** (*vide infra*).

Potassium 2-(methoxymethyl)phenyl trifluoroborate (**1.3d**)

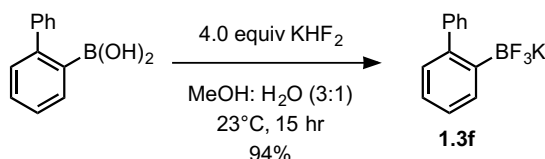


To a vigorously stirred suspension of 2-(methoxymethyl)phenylboronic acid (1.00 g, 6.02 mmol, 1.00 equiv) in methanol (25 mL, *c* = 0.2 M) was added a solution of potassium bifluoride (1.88 g, 24.1 mmol, 4.00 equiv) in water (6 mL) at 23 °C. The reaction mixture was stirred for 13 hours at 23 °C and then concentrated *in vacuo* to afford a colorless solid that was further dried at 80 °C at 100 mtorr. The solid was stirred in refluxing acetone (3 × 50 mL) and the hot supernatant was filtered through celite. The combined filtrates were concentrated *in vacuo* to afford the title compound (535 mg, 2.35 mmol, 39% yield) as a

colorless crystalline solid.

NMR Spectroscopy: ^1H NMR (600 MHz, acetone- d_6 , 23 °C, δ): 7.51 (d, J = 7.1 Hz, 1H), 7.24 (d, J = 7.5 Hz, 1H), 7.01 (td, J = 7.4, 1.4 Hz, 1H), 6.96 (t, J = 7.2 Hz, 1H), 4.68 (s, 2H), 3.29 (s, 3H). ^{13}C NMR (125 MHz, acetone- d_6 , 23 °C, δ): 142.2, 133.0, 133.0, 126.9, 126.2, 126.0, 74.9, 57.6. ^{19}F NMR (375 MHz, acetone- d_6 , 23 °C, δ): -140.2 (bs). HRMS-FIA(m/z) calcd for $\text{C}_8\text{H}_9\text{BF}_3\text{OK}$ [M-K] $^-$, 189.0706; found, 189.0706.

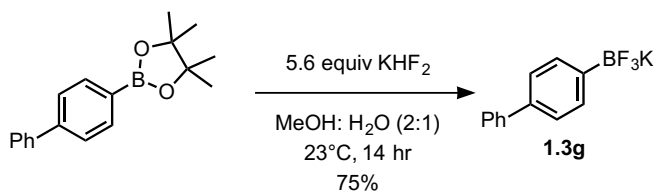
Potassium 2-biphenyl trifluoroborate (1.3f)



To a vigorously stirred suspension of 2-biphenylboronic acid (250 mg, 1.26 mmol, 1.00 equiv) in methanol (3 mL, c = 0.4 M) was added a solution of potassium bifluoride (394 mg, 5.05 mmol, 4.00 equiv) in water (1 mL) at 23 °C. The reaction mixture was stirred for 15 hours at 23 °C and then concentrated *in vacuo* to afford a colorless solid that was further dried at 80 °C at 100 mtorr. The solid was suspended in acetone (3×20 mL), stirred vigorously, and the supernatant was filtered through celite. The combined filtrates were concentrated *in vacuo* to afford the title compound (310 mg, 1.19 mmol, 94% yield) as a colorless crystalline solid.

NMR Spectroscopy: ^1H NMR (600 MHz, acetone- d_6 , 23 °C, δ): δ 7.70 (dd, J = 6.2, 2.5 Hz, 1H), 7.54-7.52 (m, 2H), 7.25-7.22 (m, 2H), 7.16-7.13 (m, 1H), 7.10-7.06 (m, 2H), 7.04-7.01 (m, 1H). ^{13}C NMR (125 MHz, DMSO- d_6 , 23 °C, δ): 146.0, 145.3, 133.0, 133.0, 129.2, 128.8, 126.8, 125.3, 125.1, 125.0. ^{19}F NMR (375 MHz, acetone- d_6 , 23 °C, δ): -136.5 (bs). HRMS-FIA(m/z) calcd for $\text{C}_{12}\text{H}_9\text{BF}_3\text{K}$ [M-K] $^-$, 221.0757; found, 221.0761.

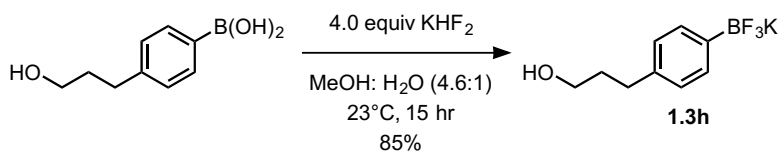
Potassium 4-biphenyl trifluoroborate (1.3g)



To a vigorously stirred suspension of 4-biphenylboronic acid pinacol ester (1.00 g, 3.57 mmol, 1.00 equiv) in methanol (10 mL, $c = 0.4$ M) was added a solution of potassium bifluoride (1.56 g, 20.0 mmol, 5.60 equiv) in water (5 mL) at 23 °C. The reaction mixture was stirred for 14 hours at 23 °C and then concentrated *in vacuo* to afford a colorless solid that was further dried at 80 °C at 100 mtorr. The solid was suspended in water (40 mL) and the suspension was filtered. The filter cake was washed with methanol (2×40 mL), diethyl ether (40 mL), and pentane (40 mL). The residue was dried under vacuum to afford the title compound (699 mg, 2.69 mmol, 75% yield) as a colorless crystalline solid.

NMR Spectroscopy: ¹H NMR (600 MHz, DMSO-*d*₆, 23 °C, δ): 7.59 (dd, $J = 8.2, 1.1$ Hz, 2H), 7.42-7.37 (m, 6H), 7.28 (tt, $J = 7.3, 1.1$ Hz, 1H). ¹³C NMR (125 MHz, DMSO-*d*₆, 23 °C, δ): 141.5, 136.9, 132.0, 128.8, 126.6, 126.3, 124.7. ¹⁹F NMR (375 MHz, DMSO-*d*₆, 23 °C, δ): –141.1. HRMS-FIA(m/z) calcd for C₁₂H₉BF₃K [M–K][–], 221.0757; found, 221.0761.

Potassium 4-(3-hydroxypropyl)phenyl trifluoroborate (1.3h)

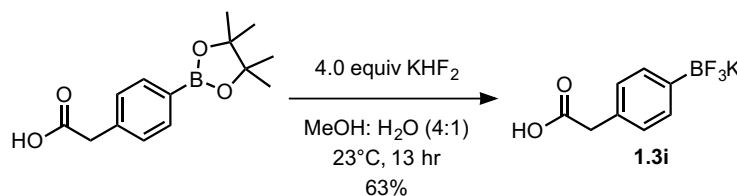


To a vigorously stirred suspension of 4-(3-hydroxypropyl)phenylboronic acid (1.00 g, 5.56 mmol, 1.00 equiv) in methanol (23 mL, $c = 0.2$ M) was added a solution of potassium bifluoride (1.74 g, 22.2 mmol, 4.00 equiv) in water (5 mL) at 23 °C. The reaction mixture was stirred for 15 hours at 23 °C and then concentrated *in vacuo* to afford a colorless solid

that was further dried at 80 °C at 100 mtorr. The solid was stirred in refluxing acetone (4 × 20 mL) and the hot supernatant was filtered through celite. The combined filtrates were concentrated *in vacuo* to afford the title compound (1.14 g, 4.72 mmol, 85% yield) as a colorless crystalline solid.

NMR Spectroscopy: ¹H NMR (600 MHz, acetone-*d*₆, 23 °C, δ): 7.37 (d, *J* = 7.7 Hz, 2H), 6.94 (d, *J* = 7.5 Hz, 2H), 3.55-3.52 (m, 2H), 3.41 (t, *J* = 5.3 Hz, 1H), 2.57 (t, *J* = 7.7 Hz, 2H), 1.79-1.74 (m, 2H). ¹³C NMR (125 MHz, DMSO-*d*₆, 23 °C, δ): 138.4, 131.4, 126.4, 60.4, 34.7, 31.7. ¹⁹F NMR (375 MHz, acetone-*d*₆, 23 °C, δ): −142.9 (bs). HRMS-FIA(*m/z*) calcd for C₉H₁₁BF₃OK [M−K][−], 203.0862; found, 203.0862.

Potassium 4-(carboxymethyl)phenyl trifluoroborate (1.3i)

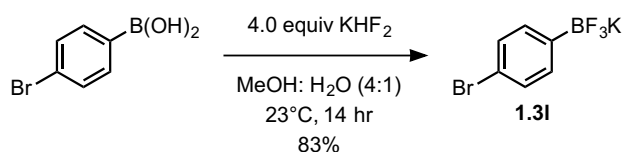


To a vigorously stirred suspension of 4-(carboxymethyl)phenylboronic acid pinacol ester (1.00 g, 3.82 mmol, 1.00 equiv) in methanol (16 mL, *c* = 0.2 M) was added a solution of potassium bifluoride (1.19 g, 15.3 mmol, 4.00 equiv) in water (4 mL) at 23 °C. The reaction mixture was stirred for 13 hours at 23 °C and then concentrated *in vacuo* to afford a yellow solid that was further dried at 80 °C at 100 mtorr. The solid was purified by continuous soxhlet extraction for 72 hours with acetone (200 mL). The filtrate was concentrated *in vacuo* and the residue was triturated with diethyl ether (3 × 10 mL) to afford the title compound (577 mg, 2.38 mmol, 63% yield) as a colorless crystalline solid.

NMR Spectroscopy: ¹H NMR (600 MHz, DMSO-*d*₆, 23 °C, δ): 12.38 (s, 1H), 7.23 (d, *J* = 7.7 Hz, 1H), 6.95 (d, *J* = 7.5 Hz, 1H), 3.38 (s, 1H). ¹³C NMR (125 MHz, DMSO-*d*₆, 23 °C, δ): 173.4, 131.5, 131.3, 127.2, 41.3. ¹⁹F NMR (375 MHz, DMSO-*d*₆, 23 °C, δ): −140.9. HRMS-

FIA(m/z) calcd for $\text{C}_8\text{H}_7\text{BF}_3\text{O}_2\text{K}$ $[\text{M}-\text{K}]^-$, 203.0498; found, 203.0496.

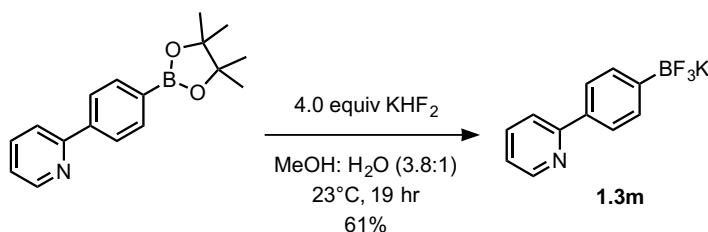
Potassium 4-bromophenyl trifluoroborate (1.3l)



To a vigorously stirred suspension of 4-bromophenylboronic acid (1.00 g, 4.98 mmol, 1.00 equiv) in methanol (20 mL, $c = 0.2$ M) was added a solution of potassium bifluoride (1.56 g, 19.9 mmol, 4.00 equiv) in water (5 mL) at 23 °C. The reaction mixture was stirred for 14 hours at 23 °C and then concentrated *in vacuo* to afford a colorless solid that was further dried at 80 °C at 100 mtorr. The solid was suspended in acetone (4×25 mL), stirred vigorously, and the supernatant was filtered through celite. The combined filtrates were concentrated *in vacuo* to afford the title compound (1.09 g, 4.15 mmol, 83% yield) as a colorless crystalline solid.

NMR Spectroscopy: ^1H NMR (600 MHz, $\text{DMSO}-d_6$, 23 °C, δ): 7.28-7.20 (m, 2H). ^{13}C NMR (125 MHz, $\text{acetone}-d_6$, 23 °C, δ): 134.6, 129.9, 119.7. ^{19}F NMR (375 MHz, $\text{acetone}-d_6$, 23 °C, δ): -143.8 (bs). HRMS-FIA(m/z) calcd for $\text{C}_6\text{H}_4\text{BBrF}_3\text{L}$ $[\text{M}-\text{K}]^-$, 222.9548; found, 222.9547.

Potassium 4-(pyridin-2-yl)phenyl trifluoroborate (1.3m)

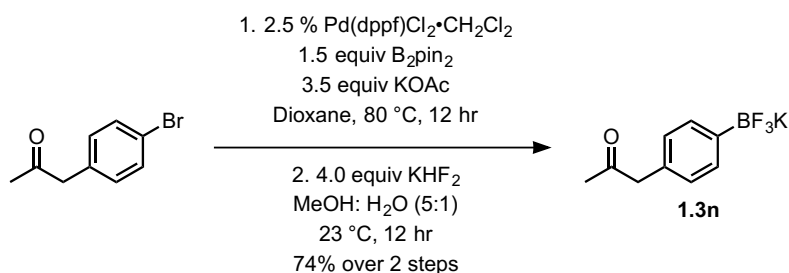


To a vigorously stirred suspension of 4-(pyridine-2-yl)phenylboronic acid pinacol ester (1.00 g, 3.56 mmol, 1.00 equiv) in methanol (15 mL, $c = 0.2$ M) was added a solution of potassium bifluoride (1.11 g, 14.2 mmol, 4.00 equiv) in water (4 mL) at 23 °C. The reaction mixture

was stirred for 19 hours at 23 °C and then concentrated *in vacuo* to afford a yellow solid that was further dried at 80 °C at 100 mtorr. The solid was stirred in refluxing acetone (4 × 30 mL) and the hot supernatant was filtered through celite. The combined filtrates were concentrated *in vacuo* to afford a yellow solid. The solid was purified by the following procedure: the solid was dissolved in refluxing acetone (10 mL) and the solution was allowed to cool to 23 °C. Layering of pentane (10 mL) on top of the cooled acetone solution at 23 °C resulted in the growth of yellow crystals, which were isolated by filtration of the suspension. This layering procedure was repeated twice more to afford the title compound (563 mg, 2.16 mmol, 61% yield) as a colorless crystalline solid.

NMR Spectroscopy: ¹H NMR (600 MHz, acetone-*d*₆, 23 °C, δ): 8.58 (dq, *J* = 4.8, 1.2 Hz, 1H), 7.86 (d, *J* = 7.7 Hz, 2H), 7.82 (dt, *J* = 8.4, 1.2 Hz, 1H), 7.76 (td, *J* = 7.7, 1.9 Hz, 1H), 7.58 (d, *J* = 8.0 Hz, 2H), 7.19 (ddd, *J* = 7.3, 4.8, 1.1 Hz, 1H). ¹³C NMR (125 MHz, acetone-*d*₆, 23 °C, δ): 159.0, 150.2, 137.3, 137.2, 132.8, 135.6, 122.2, 120.4. ¹⁹F NMR (375 MHz, acetone-*d*₆, 23 °C, δ): −143.4 (bs). HRMS-FIA(*m/z*) calcd for C₁₁H₈BF₃NK [M-K][−], 222.0709; found, 222.0710.

Potassium 4-(2-oxopropyl)phenyl trifluoroborate (1.3n)



To a flame-dried Schlenk tube was added bis(pinacolato)diboron (3.58 g, 14.1 mmol, 1.5 equiv) and potassium acetate (3.22 g, 32.9 mmol, 3.5 equiv). The Schlenk tube was evacuated and backfilled with dinitrogen (process repeated three times). Dioxane (40 mL anhydrous, degassed) was added followed by 1-(4-bromophenyl)propan-2-one (2.00 g, 9.39

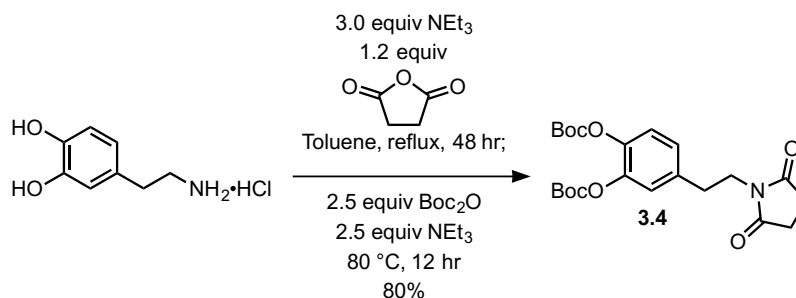
mmol, 1.00 equiv). The reaction mixture was submitted to two freeze-pump-thaw cycles, followed by the addition of [1,1'-bis(diphenylphosphino)ferrocene]dichloropalladium complex in dichloromethane (192 mg, 0.235 mmol, 0.025 equiv). The reaction mixture was submitted to another freeze-pump-thaw cycle and heated at 80 °C for 12 hours. The reaction was allowed to cool to 23 °C and water (30 mL) was added dropwise under a dinitrogen atmosphere. The reaction mixture was transferred to separatory funnel and the aqueous layer was extracted with dichloromethane (3 × 30 mL). The combined organic layers were dried over magnesium sulfate, filtered, and concentrated *in vacuo* to afford an orange oil. The residue was purified by chromatography on silica gel eluting with a solvent mixture of hexanes/dichloromethane (1:4 (v/v)) to afford a yellow oil (3.48 g) containing 4-(2-oxopropyl)phenylboronic acid pinacol ester (2.37 g, 9.10 mmol, 97% yield), dioxane, and pinacol. The purity of the residue was determined by integration of the ¹H NMR spectrum of the mixture. This mixture was carried through to the next reaction without further purification.

The yellow oil obtained from the previous step was diluted with methanol (40 mL, c = 0.2). To this vigorously stirred solution was added a solution of potassium bifluoride (2.84 g, 36.4 mmol, 4.00 equiv) in water (8 mL) at 23 °C. The reaction mixture was stirred for 12 hours at 23 °C and then concentrated *in vacuo* to afford a yellow solid that was further dried at 80 °C at 100 mtorr. The solid was stirred in refluxing acetone (3 × 150 mL) and the hot supernatant was filtered through celite. The filtrate was concentrated *in vacuo* and the residue was triturated with tetrahydrofuran (5 × 12 mL) to afford the title compound (1.65 g, 6.89 mmol, 74% yield for 2 steps) as a colorless crystalline solid.

NMR Spectroscopy: ¹H NMR (600 MHz, DMSO-*d*₆, 23 °C, δ): 7.26 (d, *J* = 7.7 Hz, 2H), 6.91 (d, *J* = 7.5 Hz, 2H), 3.57 (s, 2H), 2.04 (s, 3H). ¹³C NMR (125 MHz, DMSO-*d*₆, 23 °C, δ): 206.8, 131.6, 131.1, 127.5, 50.2, 29.0. ¹⁹F NMR (375 MHz, DMSO-*d*₆, 23 °C, δ): -141.0 (bs).

HRMS-FIA(m/z) calcd for C₉H₉BF₃OK [M-K]⁻, 201.0706; found, 201.0705.

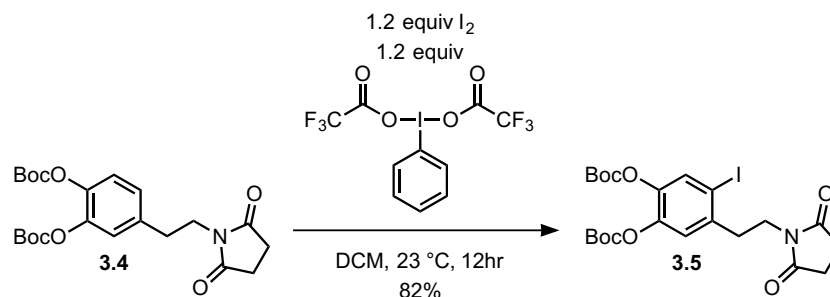
Protected dopamine (3.4)



To a vigorously stirred suspension of dopamine hydrochloride (5.00 g, 26.4 mmol, 1.00 equiv) in toluene (100 mL, 0.3 M) was added triethylamine (10.9 mL, 79.1 mmol, 3.00 equiv) and succinic anhydride (3.17 g, 31.6 mmol, 1.20 equiv) at 23 °C. The reaction mixture was stirred for 48 hours at reflux and allowed to cool to 23 °C. Boc anhydride (15.2 mL, 65.9 mmol, 2.50 equiv) and triethylamine (9.11 mL, 65.9 mmol, 2.50 equiv) were added to the reaction mixture at 23 °C. The reaction mixture was stirred for 12 hours at 80 °C, allowed to cool to 23 °C, and then transferred to a separatory funnel. The organic layer was washed with brine (3 × 50 mL). The combined aqueous layers were extracted with ethyl acetate (50 mL). The combined organic layers were dried over magnesium sulfate, filtered, and concentrated *in vacuo*. The residue was purified by chromatography on silica gel eluting with a solvent mixture of hexanes/ethyl acetate (1:1 (v/v)) to afford the title compound (9.15 g, 21.0 mmol, 80% yield) as a colorless crystalline solid.

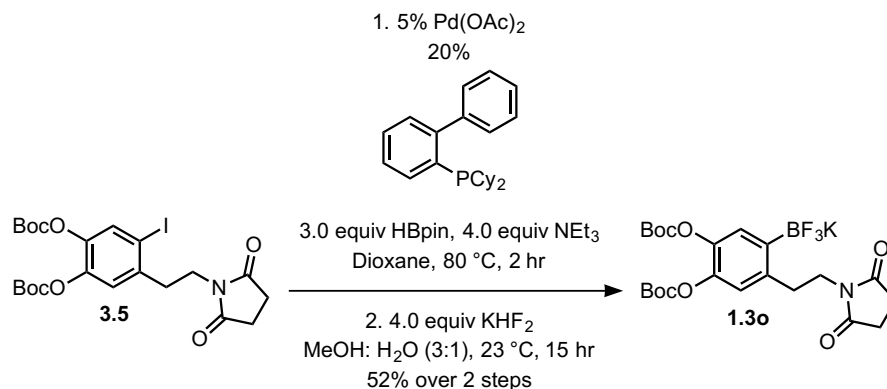
R_f = 0.37 (hexanes/ethyl acetate 1:1 (v/v)). NMR Spectroscopy: ¹H NMR (600 MHz, CDCl₃, 23 °C, δ): 7.17 (d, *J* = 8.3 Hz, 1H), 7.11 (dd, *J* = 8.3, 2.0 Hz, 1H), 7.08 (d, *J* = 2.0 Hz, 1H), 3.73 (dd, *J* = 8.5, 7.0 Hz, 2H), 2.88 (t, *J* = 7.7 Hz, 2H), 2.65 (s, 4H), 1.54 (s, 9H), 1.53 (s, 9H). ¹³C NMR (125 MHz, CDCl₃, 23 °C, δ): 177.0, 150.6, 150.6, 142.2, 141.1, 136.1, 126.6, 123.5, 123.0, 83.6, 83.5, 39.3, 32.6, 27.9, 27.5, 27.5. HRMS-FIA(m/z) calcd for C₂₂H₂₉NO₈ [M+NH₄]⁺, 453.2231; found, 453.2246.

Aryl iodide 3.5



To a vigorously stirred solution of [bis(trifluoroacetoxy)iodo]benzene (2.15 g, 4.99 mmol, 1.20 equiv) and iodine (1.27 g, 4.99 mmol, 1.20 equiv) in dichloromethane (80 mL, $c = 0.06$ M) was added compound **3.4** (1.81 g, 4.16 mmol, 1.00 equiv) at 23 °C. The reaction mixture was stirred for 12 hours at 23 °C, followed by the addition of a saturated aqueous sodium thiosulfate solution (approx. 30 mL) at 23 °C. The reaction mixture was transferred to a separatory funnel and extracted with dichloromethane (3×40 mL). The combined organic layers were dried over magnesium sulfate, filtered, and concentrated *in vacuo*. The residue was purified by chromatography on silica gel eluting with a solvent mixture of hexanes/ethyl acetate (2:1 (v/v)) to afford the title compound (1.90 g, 3.39 mmol, 82% yield) as a yellow oil. $R_f = 0.43$ (hexanes/ethyl acetate 1:1 (v/v)). NMR Spectroscopy: 1H NMR (600 MHz, $CDCl_3$, 23 °C, δ): 7.67 (s, 1H), 7.05 (s, 1H), 3.77 (t, $J = 7.2$ Hz, 2H), 3.01 (t, $J = 7.1$ Hz, 2H), 2.65 (s, 4H), 1.52 (s, 18H). ^{13}C NMR (125 MHz, $CDCl_3-d_6$, 23 °C, δ): 177.1, 150.4, 150.2, 142.5, 141.3, 138.9, 133.5, 124.0, 94.7, 84.1, 84.1, 37.8, 37.5, 28.0, 27.6, 27.5. HRMS-FIA(m/z) calcd for $C_{22}H_{28}INO_8$ $[M+NH_4]^+$, 579.1198; found, 579.1204.

Aryl trifluoroborate 1.3o



To a flame-dried Schlenk tube was added aryl iodide **3.5** (1.00 g, 1.78 mmol, 1.00 equiv).

The Schlenk tube was evacuated and backfilled with dinitrogen (process repeated three

times). Dioxane (5 mL anhydrous, degassed) was added followed by triethylamine (985 μ L,

7.13 mmol, 4.00 equiv) and pinacolborane (775 μ L, 5.35 mmol, 3.00 equiv). The reaction

mixture was submitted to three freeze-pump-thaw cycles, followed by the addition of

palladium acetate (20.0 mg, 89.1 μ mol, 0.0500 equiv) and (2-

biphenyl)dicyclohexylphosphine (125 mg, 356 μ mol, 0.200 equiv). The reaction mixture was

submitted to another freeze-pump-thaw cycle and heated to 80 °C for 2 hours. The reaction

was allowed to cool to 23 °C and a saturated aqueous ammonium chloride solution (5 mL)

was added dropwise under a dinitrogen atmosphere. The reaction mixture was transferred to

a separatory funnel and the aqueous layer was extracted with ethyl acetate (3 \times 20 mL). The

combined organic layers were dried over magnesium sulfate, filtered, and concentrated *in*

vacuo. The residue was purified by chromatography on silica gel eluting with a solvent

mixture of hexanes/ethyl acetate (3:1 (v/v)) to afford a yellow oil (1.00 g).

An aliquot of the yellow oil obtained in the previous step (400 mg) was diluted with

methanol (3 mL). To this vigorously stirred solution was added a solution of potassium

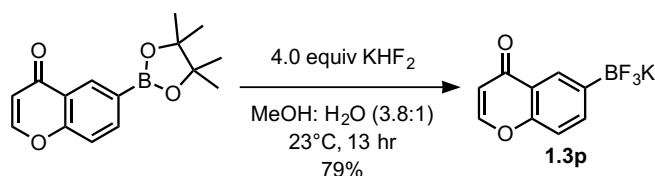
bifluoride (223 mg, 2.85 mmol, 4.00 equiv) in water (1 mL) at 23 °C. The reaction mixture

was stirred for 18 hours at 23 °C and then concentrated *in vacuo* to afford a yellow solid that

was further dried at 80 °C at 100 mtorr. The solid was suspended in acetone (4 × 20 mL), stirred vigorously, and the supernatant was filtered through celite. The combined filtrates were concentrated *in vacuo* to afford a yellow solid. The solid was purified by the following procedure: the solid was dissolved in acetone (4 mL) and the resulting solution was layered with pentane (15 mL). Slow diffusion of pentane into the acetone solution afforded colorless crystals, which were isolated and dried under vacuum to give the title compound (200 mg, 370 μmol, 52% yield over 2 steps) as a colorless crystalline solid.

NMR Spectroscopy: ¹H NMR (600 MHz, DMSO-*d*₆, 23 °C, δ): 7.08 (s, 1H), 6.76 (s, 1H), 3.57 (t, *J* = 7.3 Hz, 2H), 2.88 (t, *J* = 7.3 Hz, 2H), 2.58 (s, 4H), 1.46 (s, 18H). ¹³C NMR (125 MHz, DMSO-*d*₆, 23 °C, δ): 177.5, 150.7, 150.6, 140.2, 139.5, 138.9, 125.6, 121.7, 82.8, 82.6, 31.6, 27.9, 27.2. ¹⁹F NMR (375 MHz, DMSO-*d*₆, 23 °C, δ): −138.9 (bs). HRMS-FIA(*m/z*) calcd for C₂₂H₂₈BF₃NO₈K [M−K][−], 502.1870; found, 502.1879.

Potassium 4-oxo-4*H*-chromen-6-yl trifluoroborate (1.3p)

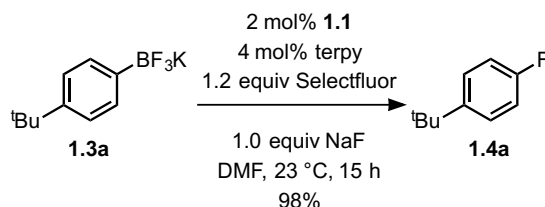


To a vigorously stirred suspension of 4-oxo-4*H*-chromen-6-ylboronic acid pinacol ester (1.00 g, 3.68 mmol, 1.00 equiv) in methanol (15 mL, *c* = 0.2 M) was added a solution of potassium bifluoride (1.15 g, 14.7 mmol, 4.00 equiv) in water (4 mL) at 23 °C. The reaction mixture was stirred for 13 hours at 23 °C and then concentrated *in vacuo* to afford an orange solid that was further dried at 80 °C at 100 mtorr. The solid was purified by continuous soxhlet extraction for 40 hours with acetone (250 mL). Subsequently, the hot extract was filtered through celite, which was rinsed with hot acetone (3 × 20 mL). The filtrate was concentrated *in vacuo* and the residue was triturated with tetrahydrofuran (4 × 5 mL) to afford the title compound (732 mg, 2.90 mmol, 79% yield) as a colorless crystalline solid.

NMR Spectroscopy: ^1H NMR (600 MHz, $\text{DMSO}-d_6$, 23 °C, δ): 8.18 (d, J = 6.0 Hz, 1H), 8.02 (s, 1H), 7.72 (d, J = 8.0 Hz, 1H), 7.34 (d, J = 8.1 Hz, 1H), 6.24 (d, J = 5.9 Hz, 1H). ^{13}C NMR (125 MHz, $\text{DMSO}-d_6$, 23 °C, δ): 177.3, 156.2, 155.0, 137.8, 127.0, 127.0, 122.9, 115.7, 112.1. ^{19}F NMR (375 MHz, $\text{acetone}-d_6$, 23 °C, δ): -143.4. HRMS-FIA(m/z) calcd for $\text{C}_9\text{H}_5\text{BF}_3\text{O}_2 [\text{M}-\text{K}]^-$, 213.0342; found, 213.0340.

IV. Synthesis and Characterization of Aryl Fluorides

1-(*tert*-Butyl)-4-fluorobenzene (1.4a)

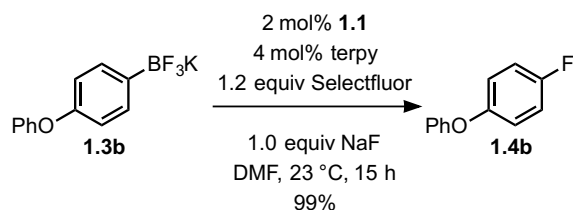


To a mixture of palladium precatalyst **1.1** (7.8 mg, 14 μmol , 0.020 equiv), terpy (6.5 mg, 28 μmol , 0.040 equiv), aryl trifluoroborate **1.3a** (168 mg, 700 μmol , 1.00 equiv), Selectfluor (298 mg, 840 μmol , 1.20 equiv), and sodium fluoride (29.4 mg, 700 μmol , 1.00 equiv) was added dimethylformamide (7.0 mL, 0.1 M) at 23 °C. The reaction mixture was stirred for 15 hours at 23 °C and then transferred to a separatory funnel. Pentane (20 mL) was added and the organic layer was washed with a 5% aqueous lithium chloride solution (3×20 mL). The organic layer was dried over sodium sulfate. The organic layer was filtered through silica gel (approx. 20 g) eluting with pentane (approx. 200 mL) and concentrated *in vacuo* at 0 °C to afford a colorless oil (166 mg) containing the title compound (105 mg, 687 μmol , 98% yield), water, and pentane. The remaining solvent was not removed from the sample due to volatility of the product. The solvent content of the residue was determined by integration of the ^1H NMR spectrum of the mixture. Azeotropic evaporation of the trace solvent with CDCl_3 was performed prior to ^1H and ^{13}C NMR characterization.

R_f = 0.79 (pentane). NMR Spectroscopy: ^1H NMR (600 MHz, CDCl_3 , 23 °C, δ): 7.35–7.32

(m, 2H), 6.99–6.95 (m, 2H), 1.31 (s, 9H). ^{13}C NMR (125 MHz, CDCl_3 , 23 °C, δ): 160.9 (d, J = 242 Hz), 146.7 (d, J = 1.8 Hz), 126.7 (d, J = 7.3 Hz), 114.6 (d, J = 20.0 Hz), 34.3, 31.5. ^{19}F NMR (375 MHz, CDCl_3 , 23 °C, δ): –121.7. HRMS-FIA(m/z) calcd for $\text{C}_{10}\text{H}_{13}\text{F}$ [$\text{M}-\text{CH}_3$] $^+$, 137.0761; found, 137.0760.

1-Fluoro-4-phenoxybenzene (**1.4b**)

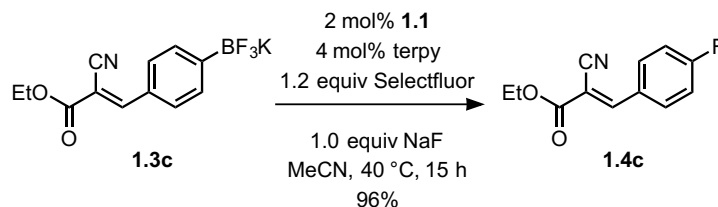


To a mixture of palladium precatalyst **1.1** (7.8 mg, 14 μmol , 0.020 equiv), terpy (6.5 mg, 28 μmol , 0.040 equiv), aryl trifluoroborate **1.3b** (193 mg, 700 μmol , 1.00 equiv), Selectfluor (298 mg, 840 μmol , 1.20 equiv), and sodium fluoride (29.4 mg, 700 μmol , 1.00 equiv) was added dimethylformamide (7.0 mL, 0.1 M) at 23 °C. The reaction mixture was stirred for 15 hours at 23 °C and then transferred to a separatory funnel. Pentane (20 mL) was added and the organic layer was washed with a 5% aqueous lithium chloride solution (20 mL). The aqueous layer was extracted with pentane (3 \times 20 mL). The combined organic layers were dried over sodium sulfate, filtered, and concentrated *in vacuo* at 0 °C to afford a colorless oil. The residue was purified by chromatography on silica gel eluting with pentane to afford a colorless oil (142 mg) containing the title compound (99.2 mg, 700 μmol , >99% yield), water, pentane, diethyl ether, and acetone. The remaining solvent was not removed from the sample due to volatility of the product. The solvent content of the residue was determined by integration of the ^1H NMR spectrum of the mixture. Azeotropic evaporation of the trace solvent with CDCl_3 was performed prior to ^1H and ^{13}C NMR characterization.

R_f = 0.35 (pentane). NMR Spectroscopy: ^1H NMR (600 MHz, CDCl_3 , 23 °C, δ): 7.34–7.31 (m, 2H), 7.09 (tt, J = 7.4, 1.0 Hz, 1H), 7.05–7.01 (m, 2H), 7.00–6.97 (m, 4H). ^{13}C NMR (125

MHz, CDCl₃, 23 °C, δ): 158.8 (d, J = 240 Hz), 157.7, 152.9, 129.8, 123.1, 120.5 (d, J = 8.3 Hz), 118.2, 116.3 (d, J = 23.8 Hz). ¹⁹F NMR (375 MHz, CDCl₃, 23 °C, δ): -123.2. HRMS-FIA(m/z) calcd for C₁₂H₉FO [M]⁺, 188.0632; found, 188.0633.

(*E*)-Ethyl 2-cyano-3-(4-fluorophenyl)acrylate (1.4c) (milligram scale)



To a mixture of palladium precatalyst **1.1** (4.4 mg, 8.0 μ mol, 0.020 equiv), terpy (3.7 mg, 16 μ mol, 0.040 equiv), aryl trifluoroborate **1.3a** (123 mg, 400 μ mol, 1.00 equiv), Selectfluor (170 mg, 480 μ mol, 1.20 equiv), and sodium fluoride (16.8 mg, 400 μ mol, 1.00 equiv) was added acetonitrile (4.0 mL, 0.1 M) at 23 °C. The reaction mixture was stirred for 15 hours at 40 °C, allowed to cool to 23 °C, and then transferred to a separatory funnel, rinsing the reaction vial with additional acetonitrile (2 \times 4 mL). Pentane (20 mL) was added and the organic layer was washed with water (20 mL). The aqueous layer was extracted with pentane (5 \times 20 mL). The combined organic layers were dried over sodium sulfate, filtered, and concentrated *in vacuo* to afford a colorless solid. The solid was purified by chromatography on silica gel eluting with a solvent mixture of pentane/Et₂O (17:3 (v/v)) to afford the title compound (84.5 mg, 385 μ mol, 96% yield) as a colorless crystalline solid. Purity of the product was confirmed via ¹H and ¹⁹F NMR spectroscopy. The spectra were identical to those obtained from the large-scale reaction below.

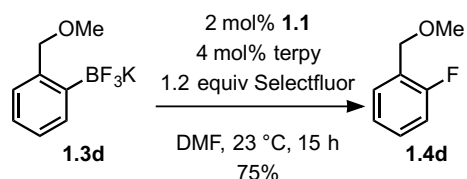
(*E*)-Ethyl 2-cyano-3-(4-fluorophenyl)acrylate (1.4c) (decagram scale)

To a mixture of palladium precatalyst **1.1** (307 mg, 554 μ mol, 0.010 equiv), terpy (258 mg, 1.11 mmol, 0.040 equiv), aryl trifluoroborate **1.3a** (17.0 g, 55.4 mmol, 1.00 equiv),

Selectfluor (23.5 g, 66.4 mmol, 1.20 equiv), and sodium fluoride (2.32 g, 55.4 mmol, 1.00 equiv) were added to a round-bottom flask (200 mL), followed by acetonitrile (55.4 mL, 1.0 M) at 23 °C. An air-cooled reflux condenser was fitted to the round bottom flask. The reaction mixture was stirred for 15 hours open to air at 40 °C, allowed to cool to 23 °C, and then transferred to a separatory funnel, rinsing the reaction vial with additional acetonitrile (2 × 50 mL). Pentane (250 mL) was added and the organic layer was washed with water (350 mL). The aqueous layer was extracted with dichloromethane (4 × 300 mL). The combined organic layers were extracted with brine (500 mL), dried over sodium sulfate, filtered, and concentrated *in vacuo* to afford a yellow solid. The solid was purified by chromatography on silica gel eluting with a solvent mixture of pentane/Et₂O (9:1 (v/v)) to afford the title compound (10.6 g, 48.6 mmol, 88% yield) as a colorless crystalline solid.

R_f = 0.38 (pentane/Et₂O 9:1 (v/v)). NMR Spectroscopy: ¹H NMR (500 MHz, CDCl₃, 23 °C, δ): 8.21 (s, 1H), 8.05–8.01 (m, 2H), 7.22–7.17 (m, 2H), 4.39 (q, J = 7.1 Hz, 2H), 1.40 (t, J = 7.2 Hz, 3H). ¹³C NMR (125 MHz, CDCl₃, 23 °C, δ): 165.2 (d, J = 256 Hz), 162.2, 153.2, 133.4 (d, J = 9.1 Hz), 127.7 (d, J = 3.6 Hz), 116.5 (d, J = 21.9 Hz), 115.3, 102.4 (d, J = 2.8 Hz), 62.6, 14.0. ¹⁹F NMR (375 MHz, CDCl₃, 23 °C, δ): –106.0. HRMS-FIA(m/z) calcd for C₁₂H₁₀FNO₂ [M+H]⁺, 220.0768; found, 220.0769.

1-Fluoro-2-(methoxymethyl)benzene (1.4d)

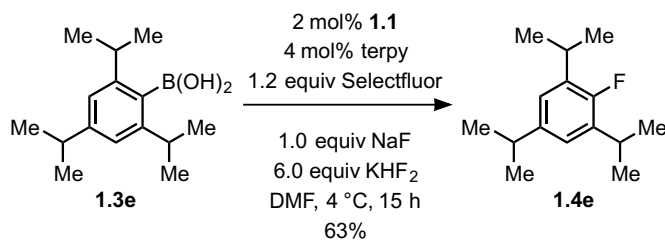


To a mixture of palladium catalyst **1.1** (7.8 mg, 14 μ mol, 0.020 equiv) and terpy (6.5 mg, 28 μ mol, 0.040 equiv) was added dimethylformamide (7.0 mL, 0.1 M) at 23 °C. This suspension was swirled for approx. 20 seconds until it became homogenous. This solution

was transferred via syringe to a mixture of aryl trifluoroborate **1.3d** (160 mg, 700 μmol , 1.00 equiv) and Selectfluor (298 mg, 840 μmol , 1.20 equiv). The reaction mixture was stirred for 15 hours at 23 °C and then transferred to a separatory funnel. Pentane (20 mL) was added and the organic layer was washed with a 5% aqueous lithium chloride solution ($1 \times 20 \text{ mL}$, $2 \times 10 \text{ mL}$). The organic layer was dried over sodium sulfate. The organic layer was filtered through silica gel (approx. 20 g) eluting with a solvent mixture of pentane/Et₂O (9:1 (v/v), approx. 200 mL) and concentrated *in vacuo* at 0 °C to afford a yellow oil (86.3 mg) containing the title compound (74.0 mg, 528 μmol , 75% yield), water, diethyl ether, and pentane. The remaining solvent was not removed from the sample due to volatility of the product. The solvent content of the residue was determined by integration of the ¹H NMR spectrum of the mixture. Azeotropic evaporation of the trace solvent with CDCl₃ was performed prior to ¹H and ¹³C NMR characterization. The ¹H NMR and LRMS data correspond to the data reported in reference 111.¹¹¹ High resolution mass spectrometry could only identify [(M+H)-F], therefore low resolution mass spectrometry was used to confirm the molecular ion of the title compound.

R_f = 0.67 (pentane/Et₂O 9:1 (v/v)). NMR Spectroscopy: ¹H NMR (500 MHz, CDCl₃, 23 °C, δ): 7.41 (t, J = 7.0 Hz, 1H), 7.28 (q, J = 7.5 Hz, 1H), 7.14 (t, J = 7.0 Hz, 1H), 7.05 (t, J = 9.0 Hz, 1H), 4.53 (s, 2H), 3.42 (s, 3H). ¹³C NMR (125 MHz, CDCl₃, 23 °C, δ): 160.8 (d, J = 246 Hz), 130.0 (d, J = 3.6 Hz), 129.3 (d, J = 8.3 Hz), 125.2 (d, J = 14.6 Hz), 124.0 (d, J = 3.6 Hz), 115.2 (d, J = 21.9 Hz), 68.0 (d, J = 3.6 Hz), 58.3. ¹⁹F NMR (375 MHz, CDCl₃, 23 °C, δ): –122.2. LRMS-FIA(m/z) calcd for C₈H₉FO [M]⁺, 140.1; found, 140.1. HRMS-FIA(m/z) calcd for C₈H₉FO [(M+H)-F], 123.0760; found, 123.0756.

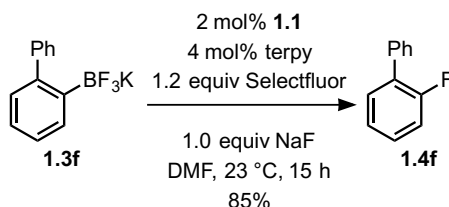
2-Fluoro-1,3,5-triisopropylbenzene (1.4e)



To a mixture of palladium precatalyst **1.1** (7.8 mg, 14 μ mol, 0.020 equiv), terpy (6.5 mg, 28 μ mol, 0.040 equiv), arylboronic acid **1.3e** (175 mg, 700 μ mol, 1.00 equiv), Selectfluor (298 mg, 840 μ mol, 1.20 equiv), sodium fluoride (29.4 mg, 700 μ mol, 1.00 equiv), and potassium bifluoride (328 mg, 4.20 mmol, 6.00 equiv) at 4 °C was added cold dimethylformamide (7.0 mL, 0.1 M) at 4 °C. The reaction mixture was stirred for 15 hours at 4 °C and then transferred cold to a separatory funnel. Pentane (20 mL) was added and the organic layer was washed with a 5% aqueous lithium chloride solution (20 mL). The aqueous layer was extracted with pentane (3 \times 20 mL). The combined organic layers were dried over sodium sulfate, filtered, and concentrated *in vacuo* at 0 °C to afford a yellow oil. The residue was purified by preparative thin layer chromatography on silica gel eluting with perfluorohexanes to afford a colorless oil (148 mg) containing the title compound (98.6 mg, 443 μ mol, 63% yield), water, pentane, and dichloromethane. The remaining solvent was not removed from the sample due to volatility of the product. The solvent content of the residue was determined by integration of the ¹H NMR spectrum of the mixture. Azeotropic evaporation of the trace solvent with CDCl₃ was performed prior to ¹H and ¹³C NMR characterization. *R_f* = 0.10 (perfluorohexanes). NMR Spectroscopy: ¹H NMR (600 MHz, CDCl₃, 23 °C, δ): 6.91 (d, *J* = 6.8 Hz, 2H), 3.22 (hept, *J* = 6.9 Hz, 2H), 2.86 (hept, *J* = 7.1 Hz, 1H), 1.26 (d, *J* = 7.0 Hz, 12H), 1.24 (d, *J* = 6.9 Hz, 6H). ¹³C NMR (125 MHz, CDCl₃, 23 °C, δ): 156.6 (d, *J* = 240 Hz), 143.8 (d, *J* = 3.6 Hz), 134.5 (d, *J* = 15.4 Hz), 122.2 (d, *J* = 5.5 Hz), 33.9, 27.4 (d, *J* = 2.6 Hz), 24.3, 22.8. ¹⁹F NMR (375 MHz, CDCl₃, 23 °C, δ): -133.4. HRMS-FIA(*m/z*) calcd

for $\text{C}_{15}\text{H}_{23}\text{F} [\text{M}]^+$, 222.1778; found, 222.1773.

2-Fluoro-1,1'-biphenyl (1.4f)

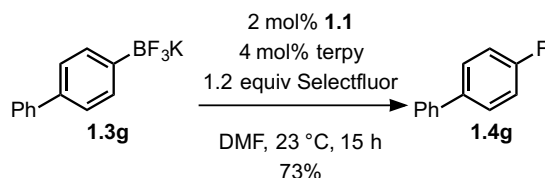


To a mixture of palladium catalyst **1.1** (7.8 mg, 14 μmol , 0.020 equiv) and terpy (6.5 mg, 28 μmol , 0.040 equiv) was added dimethylformamide (7.0 mL, 0.1 M) at 23 °C. This suspension was swirled for approx. 20 seconds until it became homogenous. This solution was transferred via syringe to a mixture of aryl trifluoroborate **1.3f** (182 mg, 700 μmol , 1.00 equiv), Selectfluor (298 mg, 840 μmol , 1.20 equiv), and sodium fluoride (29.4 mg, 700 μmol , 1.00 equiv). The reaction mixture was stirred for 15 hours at 23 °C and then transferred to a separatory funnel. Pentane (20 mL) was added and the organic layer was washed with a 5% aqueous lithium chloride solution (20 mL). The aqueous layer was extracted with pentane (4 \times 20 mL). The combined organic layers were dried over sodium sulfate. The organic layer was filtered through silica gel (approx. 20 g) eluting with pentane (approx. 200 mL) and concentrated *in vacuo* at 0 °C to afford a colorless solid (106.6 mg) containing the title compound (102 mg, 592 μmol , 85% yield) and biphenyl (4.6 mg, 29.8 μmol , 4% yield).

Purity of the residue was determined by integration of the ^1H NMR spectrum of the mixture. R_f = 0.62 (pentane). NMR Spectroscopy: ^1H NMR (600 MHz, CDCl_3 , 23 °C, δ): 7.57–7.54 (m, 2H), 7.46–7.43 (m, 3H), 7.39 (tt, J = 7.5, 1.4 Hz, 1H), 7.32 (dddd, J = 8.2, 7.3, 5.2, 1.9 Hz, 1H), 7.21 (td, J = 7.5, 1.2 Hz, 1H), 7.16 (ddd, J = 10.8, 8.2, 1.2 Hz, 1H). ^{13}C NMR (125 MHz, CDCl_3 , 23 °C, δ): 159.7 (d, J = 247 Hz), 135.8, 130.7 (d, J = 3.6 Hz), 129.1 (d, J = 5.3 Hz), 129.0 (d, J = 2.8 Hz), 128.9 (d, J = 8.3 Hz), 128.4, 127.6, 124.3 (d, J = 3.6 Hz), 116.0 (d, J = 22.8 Hz). ^{19}F NMR (375 MHz, CDCl_3 , 23 °C, δ): –121.1. HRMS-APCI(m/z) calcd for

$\text{C}_{12}\text{H}_9\text{F} [\text{M}]^+$, 172.0683; found, 172.0688.

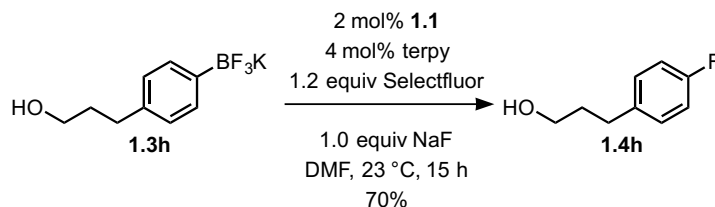
4-Fluoro-1,1'-biphenyl (1.4g)



To a mixture of palladium catalyst **1.1** (7.8 mg, 14 μmol , 0.020 equiv) and terpy (6.5 mg, 28 μmol , 0.040 equiv) was added dimethylformamide (7.0 mL, 0.1 M) at 23 °C. This suspension was swirled for approx. 20 seconds until it became homogenous. This solution was transferred via syringe to a mixture of aryl trifluoroborate **1.3g** (182 mg, 700 μmol , 1.00 equiv) and Selectfluor (298 mg, 840 μmol , 1.20 equiv). The reaction mixture was stirred for 15 hours at 23 °C and then transferred to a separatory funnel. Pentane (20 mL) was added and the organic layer was washed with a 5% aqueous lithium chloride solution (20 mL). The aqueous layer was extracted with pentane (4×20 mL). The combined organic layers were dried over sodium sulfate. The organic layer was filtered through silica gel (approx. 20 g) eluting with pentane (approx. 200 mL) and concentrated *in vacuo* at 0 °C to afford the title compound (88.4 mg, 513 μmol , 73% yield) as a colorless crystalline solid.

R_f = 0.62 (pentane). NMR Spectroscopy: ^1H NMR (600 MHz, CDCl_3 , 23 °C, δ): 7.56–7.53 (m, 4H), 7.45–7.42 (tm, J = 7.8 Hz, 2H), 7.36–7.33 (m, 1H), 7.15–7.11 (m, 2H). ^{13}C NMR (125 MHz, CDCl_3 , 23 °C, δ): 162.4 (d, J = 246 Hz), 140.2, 137.3 (d, J = 3.6 Hz), 128.8, 128.6 (d, J = 8.3 Hz), 127.2, 127.0, 115.6 (d, J = 21.9 Hz). ^{19}F NMR (375 MHz, CDCl_3 , 23 °C, δ): –118.9. HRMS-FIA(m/z) calcd for $\text{C}_{12}\text{H}_9\text{F} [\text{M}]^+$, 172.0683; found, 172.0685.

3-(4-Fluorophenyl)propan-1-ol (**1.4h**)

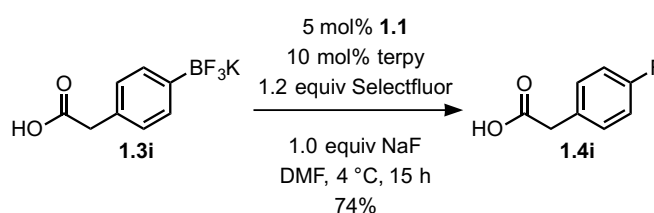


To a mixture of palladium precatalyst **1.1** (5.5 mg, 10 μmol , 0.020 equiv), terpy (4.7 mg, 20 μmol , 0.040 equiv), aryl trifluoroborate **1.3h** (121 mg, 500 μmol , 1.00 equiv), Selectfluor (213 mg, 600 μmol , 1.20 equiv), and sodium fluoride (21.0 mg, 500 μmol , 1.00 equiv) was added dimethylformamide (5.0 mL, 0.1 M) at 23 °C. The reaction mixture was stirred for 15 hours at 23 °C and then transferred to a separatory funnel. Diethyl ether (20 mL) was added and the organic layer was washed with a 5% aqueous lithium chloride solution (20 mL). The aqueous layer was extracted with diethyl ether (2×20 mL). The combined organic layers were dried over sodium sulfate, filtered, and concentrated *in vacuo* at 0 °C to afford a yellow oil. The residue was purified by chromatography on silica gel eluting with a solvent mixture of pentane/Et₂O (11:9 (v/v)) to afford a colorless oil (97.2 mg) containing the title compound (54.7 mg, 355 μmol , 71% yield), water, pentane, diethyl ether, and dichloromethane. The remaining solvent was not removed from the sample due to volatility of the product. The solvent content of the residue was determined by integration of the ¹H NMR spectrum of the mixture. Azeotropic evaporation of the trace solvent with CDCl₃ was performed prior to ¹H and ¹³C NMR characterization. The ¹H and ¹³C NMR spectroscopic data correspond to the data reported in reference 112.¹¹² High resolution mass spectrometry could only identify [(M+H)-F], therefore low resolution mass spectrometry was used to confirm the molecular ion of the title compound.

R_f = 0.24 (pentane/Et₂O 11:9 (v/v)). NMR Spectroscopy: ¹H NMR (500 MHz, CDCl₃, 23 °C, δ): 7.17–7.13 (m, 2H), 6.99–6.94 (m, 2H), 3.67 (t, J = 6.4 Hz, 2H), 2.69 (t, J = 7.7 Hz, 2H),

1.90–1.84 (tdd, $J = 8.6, 6.8, 5.3$ Hz, 2H), 1.32 (s, 1H). ^{13}C NMR (125 MHz, CDCl_3 , 23 °C, δ): 161.2 (d, $J = 242$ Hz), 137.4 (d, $J = 2.8$ Hz), 129.7 (d, $J = 7.4$ Hz), 115.0 (d, $J = 20.9$ Hz), 62.0, 34.2, 31.2. ^{19}F NMR (375 MHz, CDCl_3 , 23 °C, δ): –120.7. LRMS-FIA(m/z) calcd for $\text{C}_9\text{H}_{11}\text{FO} [\text{M}]^+$, 154.1; found, 154.1. HRMS-FIA(m/z) calcd for $\text{C}_9\text{H}_{11}\text{FO} [(\text{M}+\text{H})-\text{F}]$, 136.0883; found, 136.0882.

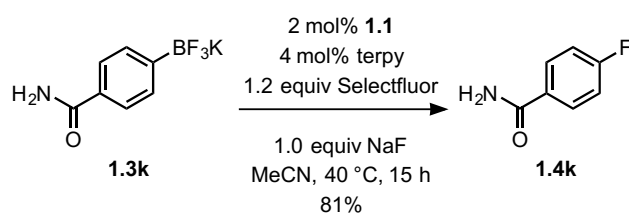
2-(4-Fluorophenyl)acetic acid (**1.4i**)



To a mixture of palladium precatalyst **1.1** (13.9 mg, 25.0 μmol , 0.0500 equiv), terpy (11.7 mg, 50.0 μmol , 0.100 equiv), aryl trifluoroborate **1.3i** (121 mg, 500 μmol , 1.00 equiv), Selectfluor (213 mg, 600 μmol , 1.20 equiv), and sodium fluoride (21.0 mg, 500 μmol , 1.00 equiv) was added dimethylformamide (5.0 mL, 0.1 M) at 23 °C. The reaction mixture was stirred for 15 hours at 4 °C and then transferred to a separatory funnel. Diethyl ether (20 mL) was added and the organic layer was washed with a 1 N aqueous HCl solution (20 mL). The aqueous layer was extracted with diethyl ether (3 \times 20 mL). The combined organic layers were dried over sodium sulfate, filtered, and concentrated *in vacuo* to afford a yellow solid. The solid was purified by chromatography on silica gel eluting with a solvent mixture of pentane/ Et_2O /AcOH (70:30:1 (v/v)) to afford a colorless solid (60.1 mg) containing the title compound (57.1 mg, 370 μmol , 74% yield) and dichloromethane. The remaining solvent was not removed from the sample due to volatility of the product. The solvent content of the residue was determined by integration of the ^1H NMR spectrum of the mixture. Azeotropic evaporation of the trace solvent with CDCl_3 was performed prior to ^1H and ^{13}C NMR characterization.

$R_f = 0.36$ (pentane/Et₂O/AcOH 70:30:1 (v/v)). NMR Spectroscopy: ¹H NMR (600 MHz, CDCl₃, 23 °C, δ): 10.31 (bs, 1H), 7.27–7.24 (m, 2H), 7.05–7.01 (m, 2H), 3.64 (s, 2H). ¹³C NMR (125 MHz, CDCl₃, 23 °C, δ): 178.1, 162.1 (d, $J = 245$ Hz), 130.9 (d, $J = 8.3$ Hz), 128.9 (d, $J = 3.6$ Hz), 115.5 (d, $J = 21.9$ Hz), 40.2. ¹⁹F NMR (375 MHz, CDCl₃, 23 °C, δ): –118.2. HRMS-FIA(m/z) calcd for C₈H₇FO₂ [M–H][–], 153.0357; found, 153.0353.

4-Fluorobenzamide (1.4k)



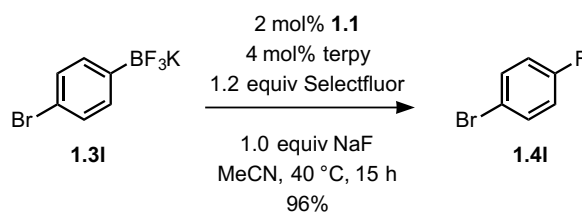
To a mixture of palladium precatalyst **1.1** (5.5 mg, 10 μmol, 0.020 equiv), terpy (4.7 mg, 20 μmol, 0.040 equiv), aryl trifluoroborate **1.3k** (114 mg, 500 μmol, 1.00 equiv), Selectfluor (213 mg, 600 μmol, 1.20 equiv), and sodium fluoride (21.0 mg, 500 μmol, 1.00 equiv) was added acetonitrile (5.0 mL, 0.1 M) at 23 °C. The reaction mixture was stirred for 15 hours at 40 °C, allowed to cool to 23 °C, and then transferred to a separatory funnel.

Dichloromethane (20 mL) was added and the organic layer was washed with water (20 mL). The aqueous layer was extracted with dichloromethane (3 × 20 mL). The combined organic layers were dried over sodium sulfate, filtered, and concentrated *in vacuo* to afford a yellow solid. The solid was purified by chromatography on silica gel eluting with a solvent mixture of dichloromethane/methanol (99:1 (v/v)) ramping to a solvent mixture of dichloromethane/methanol (97:3 (v/v)) to afford a colorless solid (64.2 mg) containing the title compound (56.0 mg, 403 μmol, 81% yield), 3-fluorobenzamide (3.88 mg, 27.9 μmol, 6% yield), 2-fluorobenzamide (2.22 mg, 15.9 μmol, 3% yield), water, pentane, and dichloromethane. The remaining solvent was not removed from the sample due to volatility of the product. The solvent content of the residue was determined by integration of the ¹H

NMR spectrum of the mixture. Azeotropic evaporation of the trace solvent with CDCl_3 was performed prior to ^1H and ^{13}C NMR characterization.

$R_f = 0.20$ (dichloromethane/methanol 19:1 (v/v)). NMR Spectroscopy: ^1H NMR (600 MHz, CDCl_3 , 23 °C, δ): 7.85–7.81 (m, 2H), 7.15–7.11 (m, 2H), 5.98 (bs, 1H), 5.67 (bs, 1H). ^{13}C NMR (100 MHz, $\text{DMSO}-d_6$, 23 °C, δ): 167.2, 163.9 (d, $J = 249$ Hz), 130.3, 129.8 (d, $J = 9.1$ Hz), 114.6 (d, $J = 21.4$ Hz). ^{19}F NMR (375 MHz, CDCl_3 , 23 °C, δ): –110.3. HRMS-FIA(m/z) calcd for $\text{C}_7\text{H}_6\text{FNO}$ $[\text{M}+\text{H}]^+$, 140.0506; found, 140.0508.

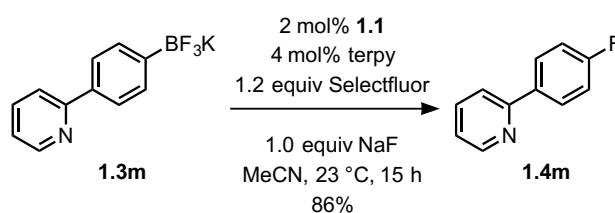
1-Bromo-4-fluorobenzene (1.4I)



To a mixture of palladium precatalyst **1.1** (5.5 mg, 10 μmol , 0.020 equiv), terpy (4.7 mg, 20 μmol , 0.040 equiv), aryl trifluoroborate **1.3I** (131 mg, 500 μmol , 1.00 equiv), Selectfluor (213 mg, 600 μmol , 1.20 equiv), and sodium fluoride (21.0 mg, 500 μmol , 1.00 equiv) was added acetonitrile (5.0 mL, 0.1 M) at 23 °C. The reaction mixture was stirred for 15 hours at 40 °C, allowed to cool to 23 °C, and then transferred to a separatory funnel. Pentane (20 mL) was added and the organic layer was washed with water (20 mL). The aqueous layer was extracted with pentane (3×20 mL). The combined organic layers were dried over sodium sulfate. The organic layer was filtered through silica gel (approx. 20 g) eluting with pentane (approx. 200 mL) and concentrated *in vacuo* at 0 °C to afford a colorless oil (130 mg) containing the title compound (84.4 mg, 482 μmol , 96% yield), pentane, and water. The remaining solvent was not removed from the sample due to volatility of the product. The solvent content of the residue was determined by integration of the ^1H NMR spectrum of the mixture.

$R_f = 0.84$ (pentane). NMR Spectroscopy: ^1H NMR (500 MHz, CDCl_3 , 23 °C, δ): 7.47–7.42 (m, 1H), 6.98–6.93 (m, 1H). ^{13}C NMR (125 MHz, CDCl_3 , 23 °C, δ): 161.8 (d, $J = 245$ Hz), 132.9 (d, $J = 7.4$ Hz), 117.2 (d, $J = 22.8$ Hz), 116.5 (d, $J = 3.6$ Hz). ^{19}F NMR (375 MHz, CDCl_3 , 23 °C, δ): –118.4. HRMS-FIA(m/z) calcd for $\text{C}_6\text{H}_4\text{BrF} [\text{M}]^+$, 175.9455; found, 175.9452.

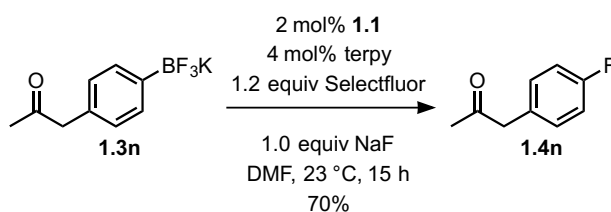
2-(4-Fluorophenyl)pyridine (**1.4m**)



To a mixture of palladium precatalyst **1.1** (5.5 mg, 10 μmol , 0.020 equiv), terpy (4.7 mg, 20 μmol , 0.040 equiv), aryl trifluoroborate **1.3m** (131 mg, 500 μmol , 1.00 equiv), Selectfluor (213 mg, 600 μmol , 1.20 equiv), and sodium fluoride (21.0 mg, 500 μmol , 1.00 equiv) was added acetonitrile (5.0 mL, 0.1 M) at 23 °C. The reaction mixture was stirred for 15 hours at 23 °C and then transferred to a separatory funnel, rinsing the reaction vial with additional acetonitrile (2×4 mL). Pentane (20 mL) was added and the organic layer was washed with water (20 mL). The aqueous layer was extracted with pentane (6×20 mL). The combined organic layers were dried over sodium sulfate, filtered, and concentrated *in vacuo* to afford a yellow solid. The solid was purified by chromatography on silica gel eluting with a solvent mixture of pentane/ Et_2O (4:1 (v/v)) to afford a colorless solid (78.0 mg) containing the title compound (74.9 mg, 432 μmol , 86% yield), water, and pentane. The remaining solvent was not removed from the sample due to volatility of the product. The solvent content of the residue was determined by integration of the ^1H NMR spectrum of the mixture. Azeotropic evaporation of the trace solvent with CDCl_3 was performed prior to ^1H and ^{13}C NMR characterization.

$R_f = 0.41$ (pentane/diethyl ether 4:1 (v/v)). NMR Spectroscopy: ^1H NMR (600 MHz, CDCl_3 , 23 °C, δ): 8.68 (ddd, $J = 4.8, 1.7, 0.9$ Hz, 1H), 7.98 (q, $J = 7.5$ Hz, 2H), 7.75 (td, $J = 7.7, 1.8$ Hz, 1H), 7.23 (ddd, $J = 7.4, 4.8, 1.1$ Hz, 1H), 7.18–7.14 (m, 2H). ^{13}C NMR (125 MHz, CDCl_3 , 23 °C, δ): 163.4 (d, $J = 249$ Hz), 156.4, 149.6, 136.7, 135.5, 128.6 (d, $J = 7.3$), 122.0, 120.1, 115.6 (d, $J = 20.0$ Hz). ^{19}F NMR (375 MHz, CDCl_3 , 23 °C, δ): –116.2. HRMS-FIA(m/z) calcd for $\text{C}_{11}\text{H}_8\text{FN}$ $[\text{M}+\text{H}]^+$, 174.0714; found, 174.0722.

1-(4-Fluorophenyl)propan-2-one (**1.4n**)

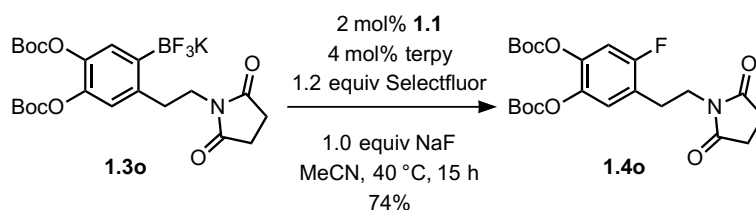


To a mixture of palladium precatalyst **1.1** (7.8 mg, 14 μmol , 0.020 equiv), terpy (6.5 mg, 28 μmol , 0.040 equiv), aryl trifluoroborate **1.3n** (168 mg, 700 μmol , 1.00 equiv), Selectfluor (298 mg, 840 μmol , 1.20 equiv), and sodium fluoride (29.4 mg, 700 μmol , 1.00 equiv) was added dimethylformamide (7.0 mL, 0.1 M) at 23 °C. The reaction mixture was stirred for 15 hours at 23 °C and then transferred to a separatory funnel. Pentane (20 mL) was added and the organic layer was washed with a 5% aqueous lithium chloride solution (20 mL). The aqueous layer was extracted with pentane (3×20 mL). The combined organic layers were dried over sodium sulfate, filtered, and concentrated *in vacuo* at 0 °C to afford a yellow oil. The residue was purified by chromatography on silica gel eluting with a solvent mixture of pentane/ Et_2O (17:3 (v/v)) to afford a colorless oil (104 mg) containing the title compound (74.9 mg, 493 μmol , 70% yield), dichloromethane, pentane, and water. The remaining solvent was not removed from the sample due to volatility of the product. The solvent content of the residue was determined by integration of the ^1H NMR spectrum of the mixture. Azeotropic evaporation of the trace solvent with CDCl_3 was performed prior to ^1H and ^{13}C

NMR characterization.

R_f = 0.28 (pentane/diethyl ether 17:3 (v/v)). NMR Spectroscopy: ^1H NMR (600 MHz, CDCl_3 , 23 °C, δ): 7.18–7.14 (m, 2H), 7.04–7.00 (m, 2H), 3.68 (s, 2H), 2.17 (s, 3H). ^{13}C NMR (125 MHz, CDCl_3 , 23 °C, δ): 206.0, 161.9 (d, J = 244 Hz), 130.9 (d, J = 8.3 Hz), 129.9 (d, J = 3.6 Hz), 115.5 (d, J = 21.0 Hz), 49.8, 29.2. ^{19}F NMR (375 MHz, CDCl_3 , 23 °C, δ): –118.8. HRMS-FIA(m/z) calcd for $\text{C}_9\text{H}_9\text{FO}$ [$\text{M}+\text{H}$] $^+$, 153.0710; found, 153.0709.

Aryl Fluoride 1.4o



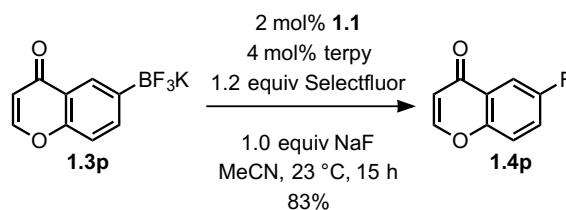
To a mixture of palladium precatalyst **1.1** (2.2 mg, 4.0 μmol , 0.020 equiv), terpy (1.9 mg, 8.0 μmol , 0.040 equiv), aryl trifluoroborate **1.3o** (108 mg, 200 μmol , 1.00 equiv), Selectfluor (85.0 mg, 240 μmol , 1.20 equiv), and sodium fluoride (8.40 mg, 200 μmol , 1.00 equiv) was added acetonitrile (2.0 mL, 0.1 M) at 23 °C. The reaction mixture was stirred for 15 hours at 40 °C, allowed to cool to 23 °C, and then transferred to a separatory funnel.

Dichloromethane (20 mL) was added and the organic layer was washed with water (20 mL). The aqueous layer was extracted with dichloromethane (4×20 mL). The combined organic layers were washed with brine (20 mL), dried over sodium sulfate, filtered, and concentrated *in vacuo* to afford a yellow solid. The solid was purified by chromatography on silica gel eluting with a solvent mixture of hexanes/ethyl acetate (1:1 (v/v)) to afford the title compound (67.1 mg, 148 μmol , 74% yield) as a colorless crystalline solid.

R_f = 0.44 (hexanes/ethyl acetate 1:1 (v/v)). NMR Spectroscopy: ^1H NMR (600 MHz, CDCl_3 , 23 °C, δ): 7.02 (d, J = 7.1 Hz, 1H), 7.00 (d, J = 9.6 Hz, 1H), 3.77 (t, J = 7.2 Hz, 2H), 2.93 (t, J = 7.2 Hz, 2H), 2.65 (s, 4H), 1.54 (s, 18H). ^{13}C NMR (125 MHz, CDCl_3 , 23 °C, δ): 177.0,

158.0 (d, $J = 245$ Hz), 150.8, 150.1, 141.7 (d, $J = 11.0$ Hz), 138.3 (d, $J = 3.6$ Hz), 124.7 (d, $J = 6.4$ Hz), 122.7 (d, $J = 18.3$ Hz), 110.6 (d, $J = 26.4$ Hz), 84.1, 83.8, 37.9, 28.0, 27.5, 27.5, 26.7. ^{19}F NMR (375 MHz, CDCl_3 , 23 °C, δ): -121.3 . HRMS-FIA(m/z) calcd for $\text{C}_{22}\text{H}_{28}\text{FNO}_8$ $[\text{M}+\text{NH}_4]^+$, 471.2137; found, 471.2155.

6-Fluoro-4*H*-chromen-4-one (1.4p)

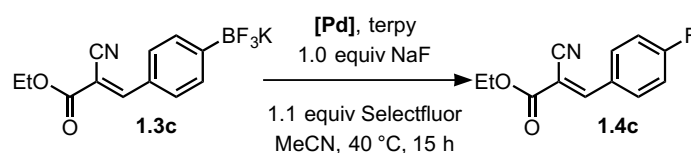


To a mixture of palladium precatalyst **1.1** (5.5 mg, 10 μmol , 0.020 equiv), terpy (4.7 mg, 20 μmol , 0.040 equiv), aryl trifluoroborate **1.3p** (126 mg, 500 μmol , 1.00 equiv), Selectfluor (213 mg, 600 μmol , 1.20 equiv), and sodium fluoride (21.0 mg, 500 μmol , 1.00 equiv) was added acetonitrile (5.0 mL, 0.1 M) at 23 °C. The reaction mixture was stirred for 15 hours at 23 °C and then transferred to a separatory funnel. Pentane (20 mL) was added and the organic layer was washed with water (20 mL). The aqueous layer was extracted with pentane (9×20 mL). The combined organic layers were dried over sodium sulfate, filtered, and concentrated *in vacuo* to afford a yellow solid. The solid was purified by chromatography on silica gel eluting with a solvent mixture of pentane/diethyl ether (7:3 (v/v)) to afford a colorless solid (72.8 mg) containing the title compound (67.9 mg, 413 μmol , 83% yield), dichloromethane, pentane, and water. The remaining solvent was not removed from the sample due to volatility of the product. The solvent content of the residue was determined by integration of the ^1H NMR spectrum of the mixture. Azeotropic evaporation of the trace solvent with CDCl_3 was performed prior to ^1H and ^{13}C NMR characterization.

$R_f = 0.20$ (pentane/diethyl ether 7:3 (v/v)). NMR Spectroscopy: ^1H NMR (600 MHz, CDCl_3 , 23 °C, δ): 7.87 (d, $J = 6.1$ Hz, 1H), 7.85 (dd, $J = 8.2, 3.1$ Hz, 1H), 7.48 (dd, $J = 9.2, 4.2$ Hz,

1H), 7.40 (ddd, $J = 9.2, 7.6, 3.1$ Hz, 1H), 6.34 (d, $J = 6.0$ Hz, 1H). ^{13}C NMR (125 MHz, CDCl_3 , 23 °C, δ): 176.7, 159.4 (d, $J = 245$ Hz), 155.4, 152.7 (d, $J = 1.8$ Hz), 125.9 (d, $J = 7.3$ Hz), 121.9 (d, $J = 25.5$ Hz), 120.3 (d, $J = 7.3$ Hz), 112.1, 110.5 (d, $J = 23.6$ Hz). ^{19}F NMR (375 MHz, CDCl_3 , 23 °C, δ): -117.9. HRMS-FIA(m/z) calcd for $\text{C}_9\text{H}_5\text{FO}_2$ $[\text{M}+\text{H}]^+$, 165.0346; found, 165.0351.

Evaluation of other [Pd] pre-catalysts (Data pertaining to Table 1.2)



General Procedure:

To aryl trifluoroborate **1.3c** (31 mg, 0.10 mmol, 1.0 equiv), Selectfluor (39 mg, 0.11 mmol, 1.1 equiv), NaF (4.2 mg, 0.10 mmol, 1.0 equiv), the [Pd] source (2.0×10^{-3} mmol, 0.020 equiv), and terpy (1.0 mg, 4.0×10^{-3} mmol, 0.040 equiv) in a 4 mL glass vial was added MeCN (1.0 mL). The vial was sealed with a teflon-lined cap, and the reaction mixture was heated at 40 °C with vigorous stirring. After 15 hours, the reaction mixture was cooled to room temperature, and then transferred to a separatory funnel, rinsing the reaction vial with additional MeCN (2×0.5 mL). H_2O (15 mL) was added, and the product was extracted from the aqueous mixture with CH_2Cl_2 (3×4 mL). The combined organic phases were dried over Na_2SO_4 , filtered, and concentrated under vacuum to give an off-white solid. To the solid was added 2 mL of a 10% (v/v) Et_2O /pentane mixture, and the mixture was agitated using an ultrasonic bath. The resulting suspension was filtered over a plug of SiO_2 (~1.5" in a Pasteur pipette), eluting with an additional 15 mL of 10% Et_2O /pentane. The filtrate was concentrated, and the product was further dried under vacuum, affording aryl fluoride **1.4c** as a colorless crystalline solid. Purity of the product was confirmed in each case via ^1H and ^{19}F NMR spectroscopy.

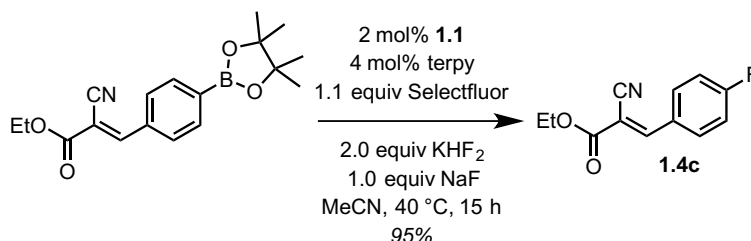
Specific details for each [Pd] source used are given in Table 3.1 below:

Table 3.1. Evaluation of Palladium Pre-Catalysts

<u>[Pd] Source</u>	<u>Commercial Supplier</u>	<u>Additive</u>	<u>Yield ArF 4c</u>
[(terpy) ₂ Pd][BF ₄] ₃ (1.2) (1.7 mg, 2 mol%)	<i>N/A</i>	None	21 mg, 95%
[Pd(MeCN) ₄][BF ₄] ₂ (0.9 mg, 2 mol%)	Strem	None	21 mg, 95%
Pd(OAc) ₂ (1.2 mg, 5 mol%)	Strem	NaBF ₄ (22 mg, 2.0 equiv)	20 mg, 91%
Pd(O ₂ CCF ₃) ₂ (0.7 mg, 2 mol%)	Strem	NaBF ₄ (11 mg, 1.0 equiv)	20 mg, 91%
PdCl ₂ (MeCN) ₂ (1.3 mg, 5 mol%)	Sigma-Aldrich	NaBF ₄ (22 mg, 2.0 equiv)	19 mg, 86% (as a mixture with ~10% ArCl)
PdBr ₂ (1.3 mg, 5 mol%)	Sigma-Aldrich	NaBF ₄ (22 mg, 2.0 equiv)	17 mg, 78% (as a mixture with ~10% ArBr)

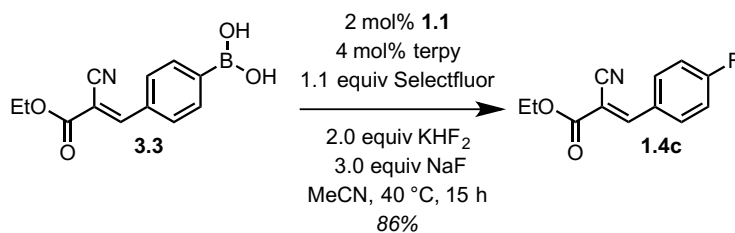
Evaluation of other arylboron reagents (Data pertaining to Scheme 1.2)

Fluorination of [(*E*)-4-(2-cyano-2-ethoxycarbonylvinyl)phenyl]boronic acid pinacol ester



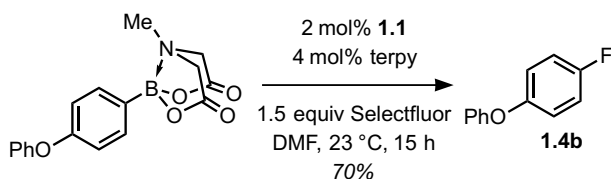
To [(*E*)-4-(2-cyano-2-ethoxycarbonylvinyl)phenyl]boronic acid pinacol ester (33 mg, 0.10 mmol, 1.0 equiv), Selectfluor (39 mg, 0.11 mmol, 1.1 equiv), KHF₂ (16 mg, 0.20 mmol, 2.0 equiv), NaF (4.2 mg, 0.10 mmol, 1.0 equiv), Pd complex **1.1** (1.1 mg, 2.0×10^{-3} mmol, 0.020 equiv), and terpy (1.0 mg, 4.0×10^{-3} mmol, 0.040 equiv) in a 4 mL glass vial was added MeCN (1.0 mL). The vial was sealed with a teflon-lined cap, and the reaction mixture was heated at 40 °C with vigorous stirring. After 15 hours, the reaction mixture was cooled to room temperature, and then transferred to a separatory funnel, rinsing the reaction vial with additional MeCN (2×0.5 mL). H₂O (15 mL) was added, and the product was extracted from the aqueous mixture with CH₂Cl₂ (3×4 mL). The combined organic phases were dried over Na₂SO₄, filtered, and concentrated under vacuum to give an off-white solid. To the solid was added 2 mL of a 10% (v/v) Et₂O/pentane mixture, and the mixture was agitated using an ultrasonic bath. The resulting suspension was filtered over a plug of SiO₂ (~1.5" in a Pasteur pipette), eluting with an additional 15 mL of 10% Et₂O/pentane. The filtrate was concentrated, and the product was further dried under vacuum, affording 21 mg of aryl fluoride **1.4c** as a colorless crystalline solid (95% yield). Purity of the product was confirmed via ¹H and ¹⁹F NMR spectroscopy.

Fluorination of [(*E*)-4-(2-cyano-2-ethoxycarbonylvinyl)phenyl]boronic acid (**3.3**)



To [(*E*)-4-(2-cyano-2-ethoxycarbonylvinyl)phenyl]boronic acid (**3.3**) (25 mg, 0.10 mmol, 1.0 equiv), Selectfluor (39 mg, 0.11 mmol, 1.1 equiv), KHF₂ (16 mg, 0.20 mmol, 2.0 equiv), NaF (13 mg, 0.30 mmol, 3.0 equiv), Pd complex **1.1** (1.1 mg, 2.0×10^{-3} mmol, 0.020 equiv), and terpy (1.0 mg, 4.0×10^{-3} mmol, 0.040 equiv) in a 4 mL glass vial was added MeCN (1.0 mL). The vial was sealed with a teflon-lined cap, and the reaction mixture was heated at 40 °C with vigorous stirring. After 15 hours, the reaction mixture was cooled to room temperature, and then transferred to a separatory funnel, rinsing the reaction vial with additional MeCN (2×0.5 mL). H₂O (15 mL) was added, and the product was extracted from the aqueous mixture with CH₂Cl₂ (3×4 mL). The combined organic phases were dried over Na₂SO₄, filtered, and concentrated under vacuum to give an off-white solid. To the solid was added 2 mL of a 10% (v/v) Et₂O/pentane mixture, and the mixture was agitated using an ultrasonic bath. The resulting suspension was filtered over a plug of SiO₂ (~1.5" in a Pasteur pipette), eluting with an additional 15 mL of 10% Et₂O/pentane. The filtrate was concentrated, and the product was further dried under vacuum, affording 19 mg of aryl fluoride **1.4c** as a colorless crystalline solid (86% yield). Purity of the product was confirmed via ¹H and ¹⁹F NMR spectroscopy.

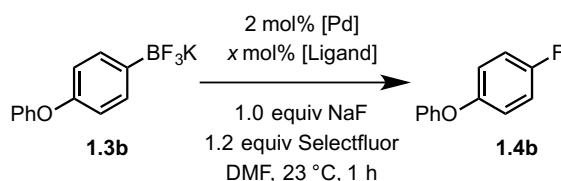
Fluorination of 4-phenoxyphenylboronic acid MIDA ester



To 4-phenoxyphenylboronic acid MIDA ester (65 mg, 0.20 mmol, 1.0 equiv), Selectfluor (110 mg, 0.30 mmol, 1.5 equiv), Pd complex **1.1** (2.2 mg, 4.0×10^{-3} mmol, 0.020 equiv), and terpy (1.9 mg, 8.0×10^{-3} mmol, 0.040 equiv) in a 4 mL glass vial was added DMF (2.0 mL). The vial was sealed with a teflon-lined cap, and the reaction mixture was stirred at 23 °C. After 15 hours, the reaction mixture was transferred to a separatory funnel. Brine (15 mL) was added, and the product was extracted from the resulting aqueous mixture with pentane (5 \times 5 mL). The combined organic phases were dried over Na₂SO₄, and then filtered over a short pad of SiO₂ (~1 cm in a fritted funnel), eluting with an additional 20 mL of pentane. The filtrate was concentrated under vacuum at 0 °C, affording a colorless oil containing 27 mg of aryl fluoride **1.4b** (70% yield), along with water and pentane. The residual solvents were not further removed due to volatility of the product. The yield of **1.4b** was confirmed via ¹⁹F and ¹H NMR spectroscopy using 1-fluoro-3-nitrobenzene (10. μ L, 9.4×10^{-5} mol) as an internal standard.

No formation of aryl fluoride **1.4b** was observed in the reaction between 4-phenoxyphenylboronic acid MIDA ester and Selectfluor in the absence of Pd complex **1.1**.

Evaluation of other nitrogenous ligands



To a mixture of the [Pd] catalyst (14 μ mol, 0.020 equiv) and nitrogenous ligand (see Table

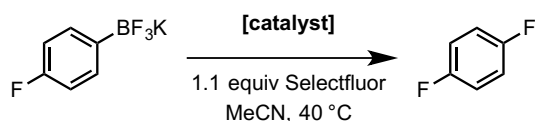
3.2) was added DMF (1 mL, 0.1 M) at 23 °C. This suspension was stirred for approximately 10 minutes, at which point the solution was homogenous. This solution was transferred via syringe to a 4 mL glass vial containing aryl trifluoroborate **1.3b** (28 mg, 100 µmol, 1.0 equiv), Selectfluor (43 mg, 120 µmol, 1.2 equiv), and sodium fluoride (4.2 mg, 100 µmol, 1.0 equiv). The reaction mixture was stirred for 1 hour at 23 °C, at which point the remaining Selectfluor was quenched by the addition of triphenylphosphine (32 mg, 120 µmol, 1.2 equiv), and 1-fluoro-3-nitrobenzene (10. µL, 94 µmol) was added as an internal standard. The yield of the aryl fluoride product was determined via ¹⁹F NMR spectroscopy, integrating against the internal standard peak at –112 ppm.

Table 3.2. Evaluation of other nitrogenous ligands

[Pd] pre-catalyst	Ligand	Yield ArF
1.1	terpy (4 mol%)	48%
1.1	none	<1%
1.1	pyridine (12 mol%)	<1%
Pd(MeCN) ₄ (BF ₄) ₂	2,2'-bipyridine (9 mol%)	7%
Pd(MeCN) ₄ (BF ₄) ₂	1,10-phenanthroline (9 mol%)	28%

The results indicate that while other nitrogenous chelating ligands, such as phenanthroline, are effective in the Pd-catalyzed fluorination reaction, use of terpy provides optimal results.

Evaluation of other single-electron redox catalysts



The proposed mechanism for the Pd-catalyzed fluorination reaction suggests the possibility that other catalysts, capable of single-electron redox chemistry, may also be competent in the fluorination reaction. Therefore, we have performed a preliminary evaluation of other potential catalysts, summarized in Table 3.3 below. The results indicate that other metal complexes are indeed competent to catalyze the fluorination reaction, but that the combination of Pd complex **1.1** and terpyridine is uniquely effective in providing high yields and selectivity.

General Procedure:

To the aryl trifluoroborate (25 mg, 0.11 mmol, 1.0 equiv), Selectfluor (50. mg, 0.14 mmol, 1.1 equiv), and the catalyst (see Table 3.3) in a 4 mL glass vial was added MeCN (1.2 mL). The vial was sealed with a teflon-lined cap, and the reaction mixture was heated at 40 °C with vigorous stirring. After 15 hours, the reaction mixture was cooled to room temperature, and then 1-fluoro-3-nitrobenzene (10. μ L, 9.4×10^{-5} mol) was added as an internal standard. The yield of the aryl fluoride product, as well as unconsumed aryl trifluoroborate and protodeborylated product, was determined via ^{19}F NMR spectroscopy, integrating against the internal standard peak at -112 ppm.

Specific details for each catalyst are given in Table 3.3 below:

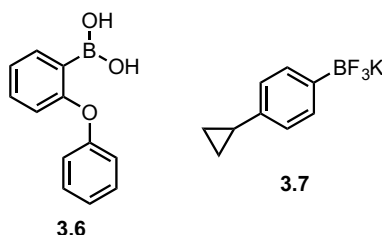
Table 3.3. Evaluation of other single-electron redox catalysts

<u>Catalyst</u>	<u>Additive</u>	<u>Yield ArF</u>	<u>Remaining</u> <u>ArBF₃K</u>	<u>Yield of</u> <u>Protodeborylation</u>
[(terpy) ₂ Ni][OTf] ₂ (2 mol%)	terpy (2 mol%)	19%	35%	22%
[Ni(bpy) ₃][BF ₄] ₂ (2 mol%)	none	17%	51%	<i>not</i> <i>observed</i>
[Ni(phen) ₃][BF ₄] ₂ (2 mol%)	none	13%	56%	< 2%
[(terpy)Pt(MeCN)][BF ₄] ₂ (2 mol%)	terpy (4 mol%)	17%	51%	<i>not</i> <i>observed</i>
Ferrocene (5 mol%)	none	9.5%	28%	42%

Evaluation of radical clock substrates

In order to probe the possibility of radical intermediates, we performed the Pd-catalyzed

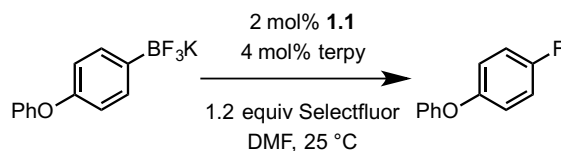
fluorination reaction on substrates **3.6** and **3.7**. Substrate **3.6** probes the intermediacy of an aryl radical formed by homolysis of the C–B bond, and is known to undergo radical cyclization to afford dibenzofuran.¹¹³ Substrate **3.7** can undergo cyclopropane ring opening if a long-lived radical intermediate is formed via SET from the arene π -system. Both **3.6** and **3.7** underwent Pd-catalyzed fluorination to give a single major aryl fluoride product, in 54% and 62% yields, respectively (aryl fluoride yields determined by ^{19}F NMR spectroscopy, using 1-fluoro-3-nitrobenzene as internal standard). In the case of **3.6**, radical cyclization was not observed; in the case of **3.7**, no cyclopropane ring-opening was observed (the crude product mixtures were analyzed by ^1H NMR spectroscopy).



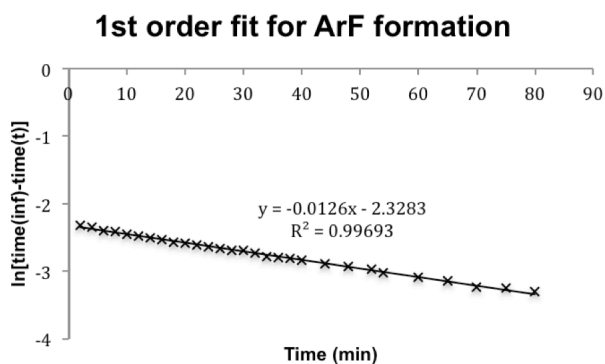
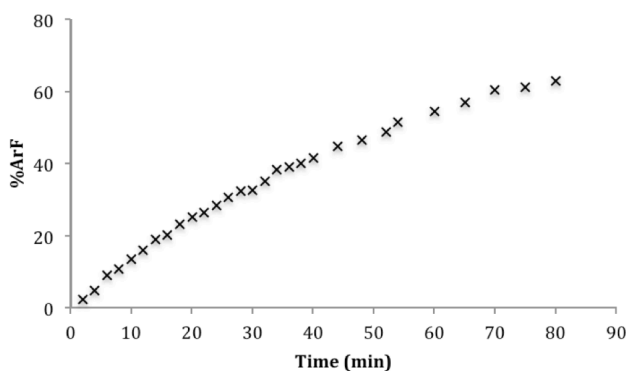
The lack of radical cyclization observed for **3.6** is consistent with our mechanistic hypothesis, in which the C–F bond is formed prior to C–B bond cleavage. We note that the lack of cyclopropane ring opening for **3.7** does not exclude the possibility of a radical mechanism, as the lifetime of the delocalized radical intermediate may be significantly shorter than the timescale of ring opening. In previous mechanistic investigations regarding SET reactivity with Selectfluor, computational evidence suggests that the lifetime of such intermediates are significantly shorter than the ring opening/closing timescale for radical clock substrates.^{90e}

Reaction Kinetics¹¹⁴

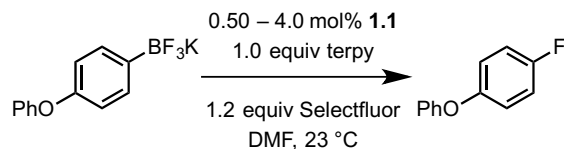
Kinetic Profile of Catalytic Reaction



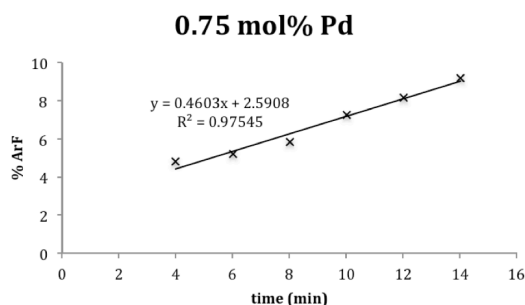
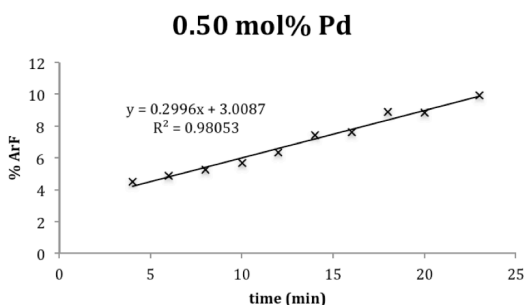
Solution A was prepared containing the aryl trifluoroborate (28 mg, 0.10 mmol, 1.0 equiv), Selectfluor (43 mg, 0.12 mmol, 1.2 equiv), and 1-fluoro-3-nitrobenzene (5.0 μL , 4.7×10^{-5} mol) as internal standard, in 0.80 mL DMF. Solution B was prepared containing Pd(II) complex **1.1** (1.1 mg, 2.0×10^{-3} mmol, 0.020 equiv) and terpy (1.0 mg, 4.0×10^{-3} mmol, 0.040 equiv) in 0.20 mL DMF. Solution A was added to an NMR tube, followed by solution B, and the tube was shaken rapidly to mix the reagents. The reaction was monitored via ^{19}F NMR spectroscopy at 25 $^{\circ}\text{C}$, following evolution of the product signal at -123 ppm and integrating against the internal standard peak at -112 ppm. The reaction was followed to greater than three half-lives, as determined by disappearance of the ^{19}F NMR signal corresponding to the aryl trifluoroborate. Because evolution of product was measured, linear natural log plots were obtained by using an infinite time point set to 100% yield. Data were fitted to a first order regression, shown below.

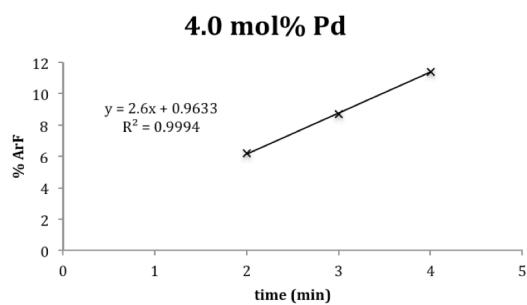
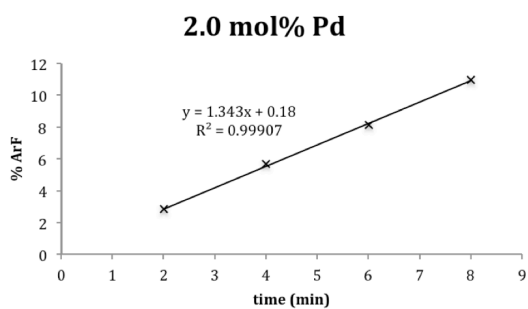
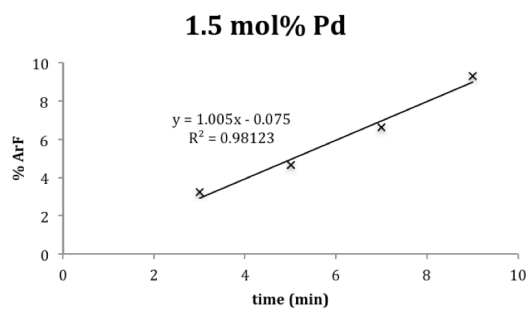
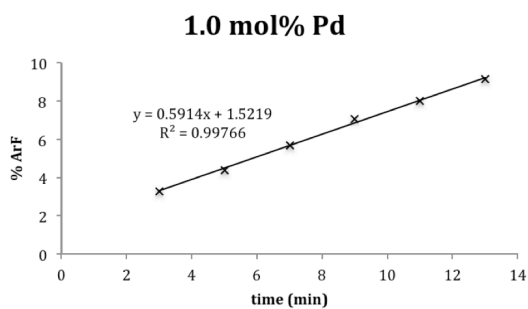


Initial Rate Kinetics of Pd Dependence

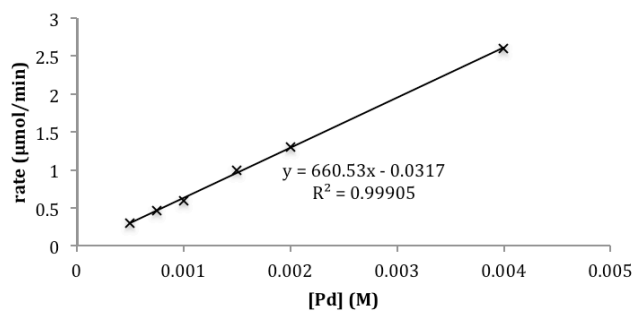


Three stock solutions were prepared: solution A, containing the aryl trifluoroborate (166 mg, 0.601 mmol), Selectfluor (255 mg, 0.720 mmol), and 1-fluoro-3-nitrobenzene (30.0 μL , 2.82×10^{-4} mol) as internal standard, in 3.00 mL DMF; solution B, containing Pd(II) complex **1.1** (5.5 mg, 1.0×10^{-2} mmol) in 0.50 mL DMF; and solution C, containing terpy (116 mg, 0.497 mmol) in 2.00 mL DMF. For each reaction, solution A (0.50 mL) was added to an NMR tube, followed by solution C (0.40 mL), DMF (100 – x μL), and finally solution B (x μL). Pd loadings in the range of 0.50–4.0 mol% were used. The tube was shaken rapidly to mix the reagents, and then the reaction was monitored via ^{19}F NMR spectroscopy at 25 °C, following evolution of the product signal at –123 ppm and integrating against the internal standard peak at –112 ppm. Product formation was monitored up to ~10% yield, and data in the 3–10% yield range was used to determine the initial rates.

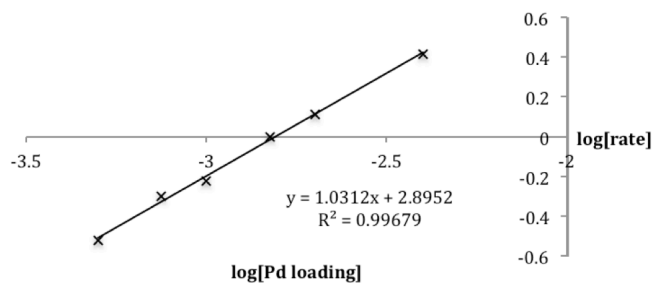




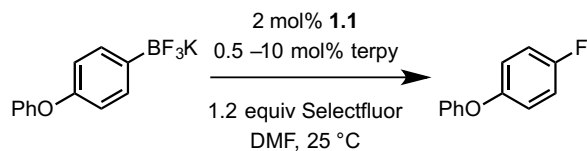
Rate vs. [Pd]



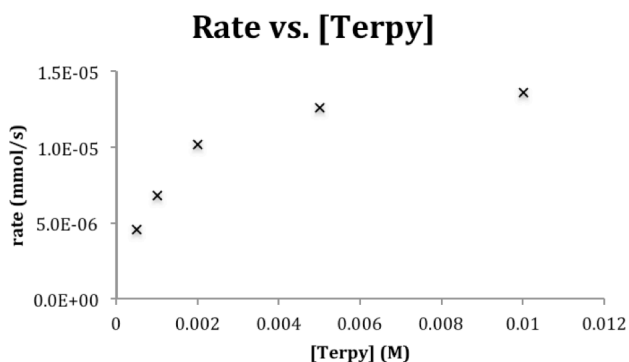
Kinetic order of [Pd]

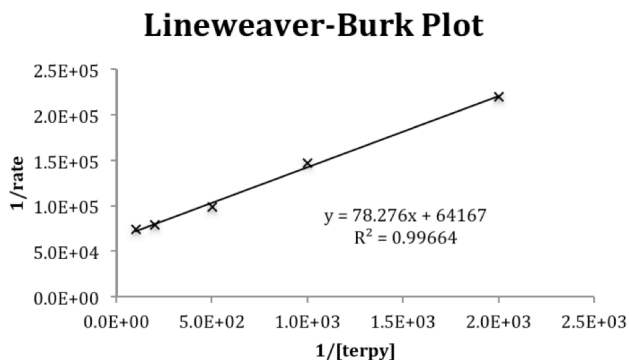


Initial Rate Kinetics of Terpyridine Dependence

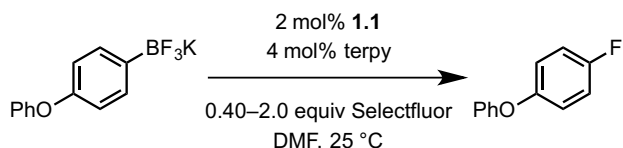


Three stock solutions were prepared: solution A, containing the aryl trifluoroborate (166 mg, 0.601 mmol), Selectfluor (255 mg, 0.720 mmol), and 1-fluoro-3-nitrobenzene (30.0 μL , 2.82×10^{-4} mol) as internal standard, in 3.00 mL DMF; solution B, containing Pd(II) complex **1.1** (3.3 mg, 6.0×10^{-3} mmol) in 0.60 mL DMF; and solution C, containing terpy (9.0 mg, 0.039 mmol) in 0.75 mL DMF. For each reaction, solution A (0.50 mL) was added to an NMR tube, followed by DMF ($400 - x$ μL), solution C (x μL), and finally solution B (100 μL). Terpy loadings in the range of 0.5–10 mol% were used. The tube was shaken rapidly to mix the reagents, and then the reaction was monitored via ^{19}F NMR spectroscopy at 25 °C, following evolution of the product signal at -123 ppm and integrating against the internal standard peak at -112 ppm. Each reaction was monitored to approximately 5% yield, and yield was converted to an initial rate by dividing by the reaction time. The data obtained are presented below, along with a Lineweaver-Burk plot, indicating saturation kinetics with respect to terpyridine.



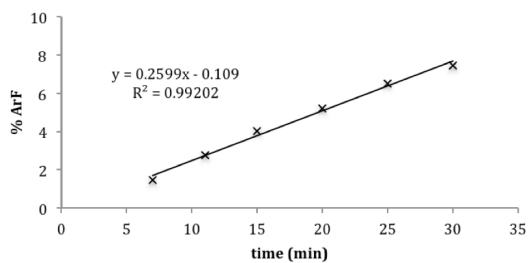


Initial Rate Kinetics of Selectfluor Dependence

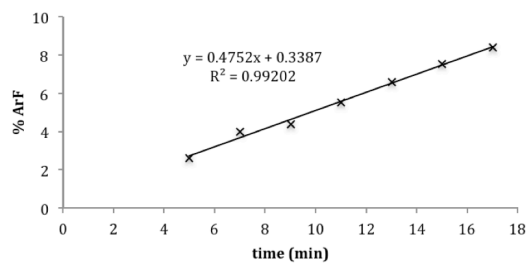


Three stock solutions were prepared: solution A, containing the aryl trifluoroborate (166 mg, 0.601 mmol) and 1-fluoro-3-nitrobenzene (30.0 μL , 2.82×10^{-4} mol) as internal standard, in 2.40 mL DMF; solution B, containing Pd(II) complex **1.1** (6.7 mg, 1.2×10^{-2} mmol) and terpy (5.6 mg, 2.4×10^{-2} mmol) in 1.20 mL DMF; and solution C, containing Selectfluor (176 mg, 0.500 mmol) in 1.00 mL DMF. For each reaction, solution A (0.40 mL) was added to an NMR tube, followed by DMF (400 – x μL), solution C (x μL), and finally solution B (0.20 mL). Selectfluor concentrations in the range of 0.040–0.20 M were used. The tube was shaken rapidly to mix the reagents, and then the reaction was monitored via ^{19}F NMR spectroscopy at 25 $^\circ\text{C}$, following evolution of the product signal at –123 ppm and integrating against the internal standard peak at –112 ppm. Product formation was monitored up to ~10% yield, and data in the 2–10% yield range was used to determine the initial rates. The data obtained are presented below.

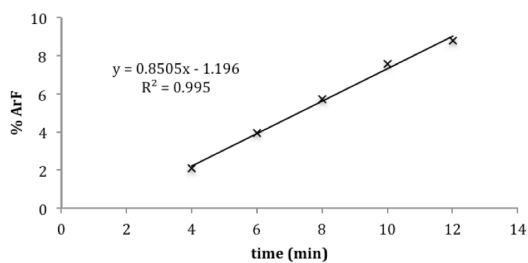
0.040 mmol Selectfluor



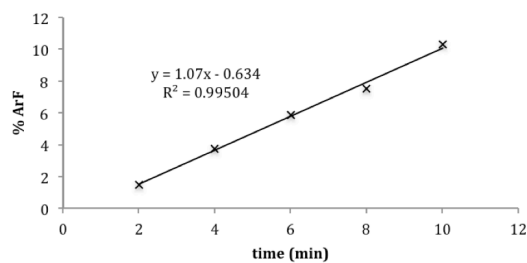
0.060 mmol Selectfluor



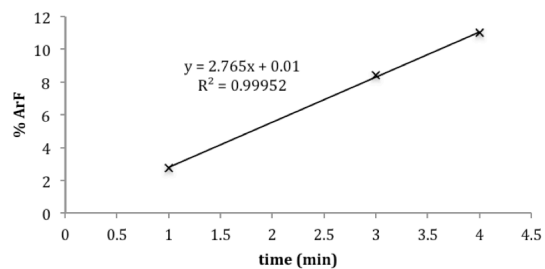
0.080 mmol Selectfluor



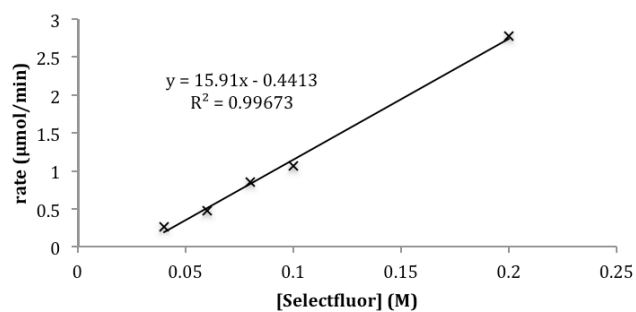
0.10 mmol Selectfluor

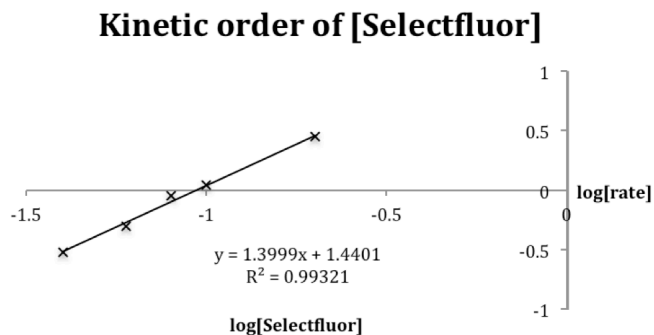


0.20 mmol Selectfluor

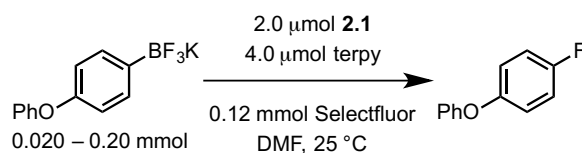


Rate vs. [Selectfluor]

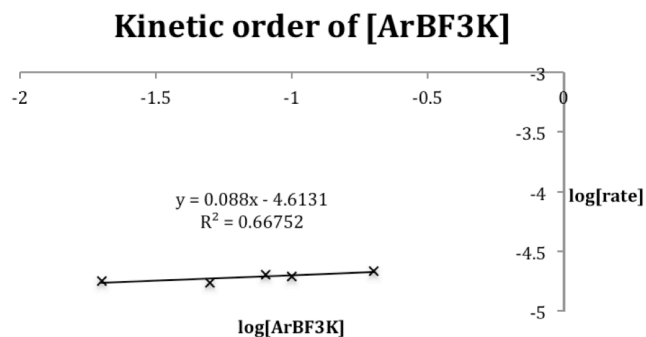
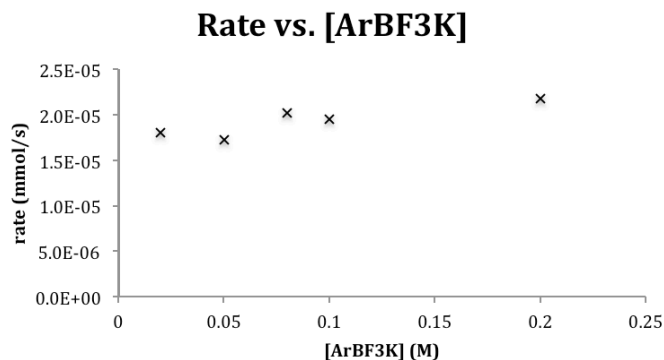




Initial Rate Kinetics of Aryl Trifluoroborate Dependence

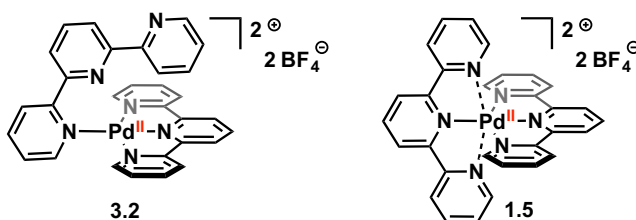


Three stock solutions were prepared: solution A, containing the aryl trifluoroborate (166 mg, 0.601 mmol) in 0.900 mL DMF; solution B, containing Pd(II) complex **1.1** (6.7 mg, 1.2×10^{-2} mmol) and terpy (5.6 mg, 2.4×10^{-2} mmol) in 1.20 mL DMF; and solution C, containing Selectfluor (255 mg, 0.720 mmol) and 1-fluoro-3-nitrobenzene (30.0 μL , 2.82×10^{-4} mol) as internal standard, in 3.00 mL DMF. For each reaction, solution A ($x \mu\text{L}$) was added to an NMR tube, followed by DMF ($300 - x \mu\text{L}$), solution C (500 μL), and finally solution B (200 μL). Aryl trifluoroborate concentrations in the range of 0.020–0.20 M were used. The tube was shaken rapidly to mix the reagents, and then the reaction was monitored via ^{19}F NMR spectroscopy at 25°C , following evolution of the product signal at -123 ppm and integrating against the internal standard peak at -112 ppm. Each reaction was monitored to approximately 6% yield, and yield was converted to an initial rate by dividing by the reaction time. The data obtained are presented below.



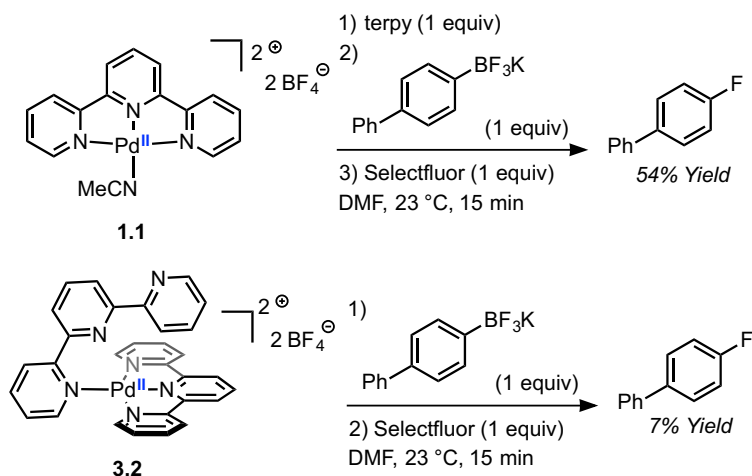
Discussion of the structure of [(terpy)₂Pd][BF₄]₂ (**1.5**)

It is challenging to characterize the structure of the initial adduct formed between Pd(II) complex **1.1** and terpyridine due to rapid equilibria in solution. As described in the Experimental Procedures section, crystallization from a mixture of **1.1** and terpy affords compound **3.2**, the structure of which was determined using X-ray crystallography. However, experimental and theoretical data indicate that **3.2** is not the structure of the initial adduct between **1.1** and terpy, and is not relevant to the Pd-catalyzed fluorination reaction. Data suggest that the relevant structure is likely the pseudo-octahedral Pd(II) complex **1.5**:

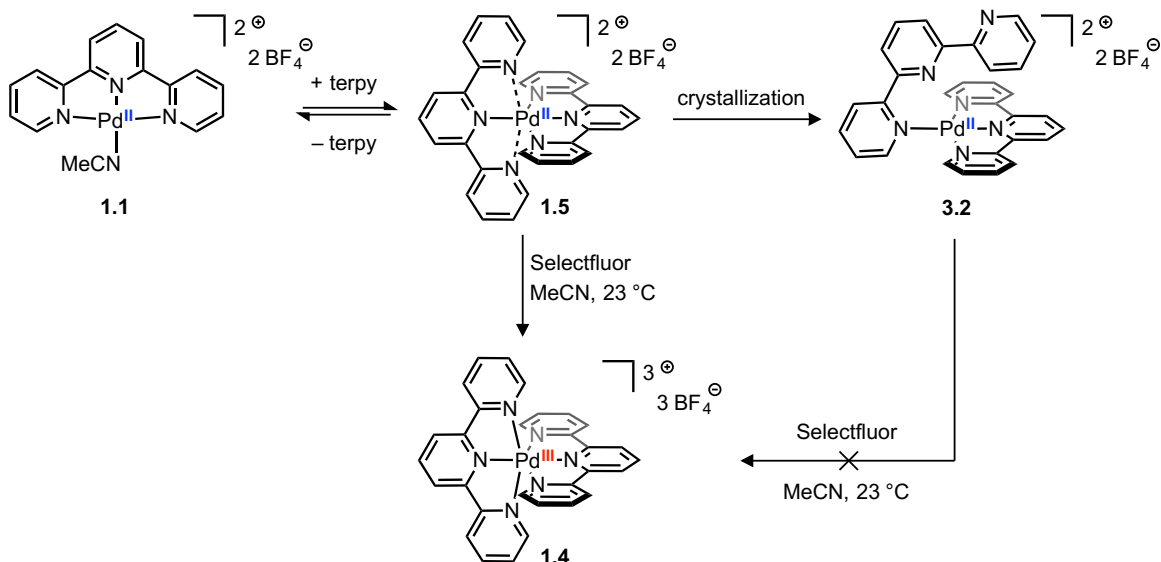


When the reactivity of isolated **3.2** was compared with a freshly prepared solution of **1.1** and terpy, it was found that **3.2** is not chemically competent in the fluorination of aryl

trifluoroborates with Selectfluor (yields determined by ^{19}F NMR spectroscopy vs 1-fluoro-3-nitrobenzene as internal standard):

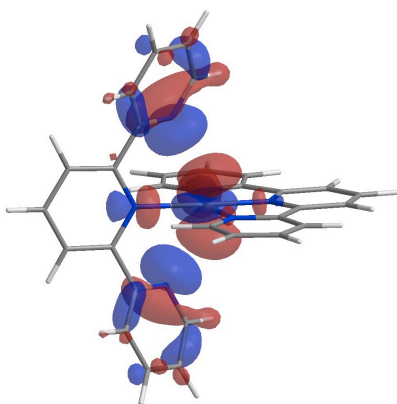


Additionally, **3.2** does not react with Selectfluor to form Pd(III) complex **1.2**. The observed reactivity is summarized in Scheme 3.1, in which **3.2** is a thermodynamically more stable product than **1.5**, but is not relevant in the catalytic fluorination reaction with Selectfluor:

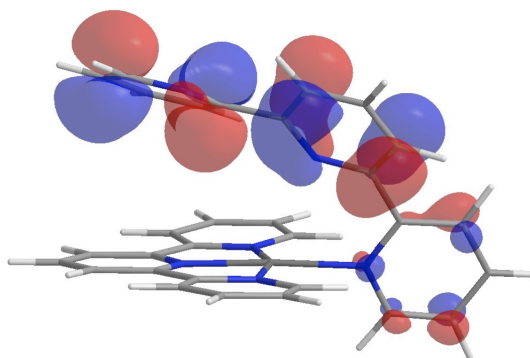


Scheme 3.1. Reactivity of bis-terpyridyl Pd(II) complexes **1.5** and **3.2** with Selectfluor. DFT calculations are consistent with the observed chemical reactivity difference between **1.5** and **3.2** (see DFT Calculations section for details): the optimized structure of **1.5** displays a pseudo-octahedral geometry, in which the apical pyridyl ligands are rotated away from the

z-axis to avoid interaction with the filled d_{z^2} orbital on Pd. The calculated HOMO is primarily of d_{z^2} parentage with respect to Pd, and antibonding with respect to the apical pyridyl ligands. Removal of one electron from this orbital via oxidation would be expected to give a distorted octahedral d^7 Pd(III) complex (e.g. **1.2**), as is indeed observed when **1.1** is treated with terpyridine and Selectfluor. The optimized structure of **3.2** has a calculated HOMO which is primarily based on the π -system of the monodentate terpyridine ligand: this is consistent with the observation that **3.2** is not oxidized to Pd(III) **1.2**. The calculations indicate that **3.2** is thermodynamically favored by 2.3 kcal/mol as compared to **1.5**. Based on the observed reactivity, however, we believe that **3.2** is not kinetically accessible during the Pd-catalyzed fluorination reaction.



Calculated HOMO of **1.5**

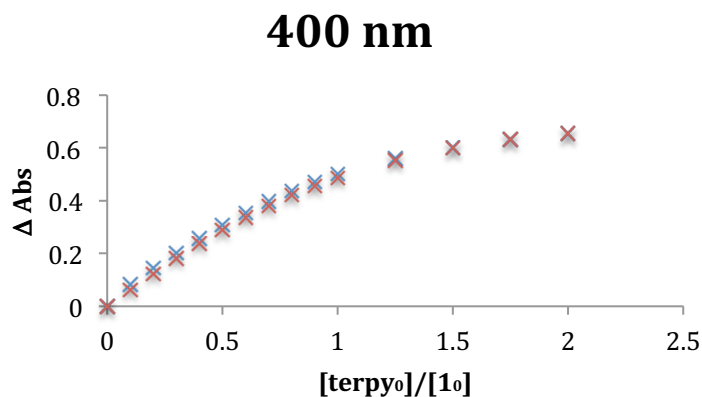


Calculated HOMO of **3.2**

Binding Constant Analysis

The equilibrium between **1.1** and **1.5** was probed experimentally using UV-vis spectroscopy. Exogenous terpy was added to a solution of **1.1** in DMF, and absorbance at 400 nm was measured. 400 nm was chosen based on the fact that neither **1.1** nor terpy display a significant absorption feature at this wavelength (see UV-vis data section), but the absorption value at 400 nm displayed a notable increase when terpy was added to **1.1**. A titration experiment was carried out, and the measured binding isotherm is shown below (the plot

shows overlaid data from two separate experiments):



Fitting of the binding isotherm was performed using a 1:1 binding model between **1.1** and terpyridine,¹¹⁵ which provided satisfactory results. The fitting gave an association constant (K_a) of 3×10^3 ($\pm 19\%$). The output from the fitting program is given below, with K_a and the associated error analysis highlighted in red.

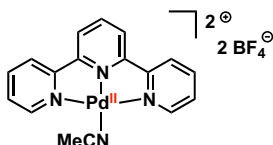
Results from 1:1

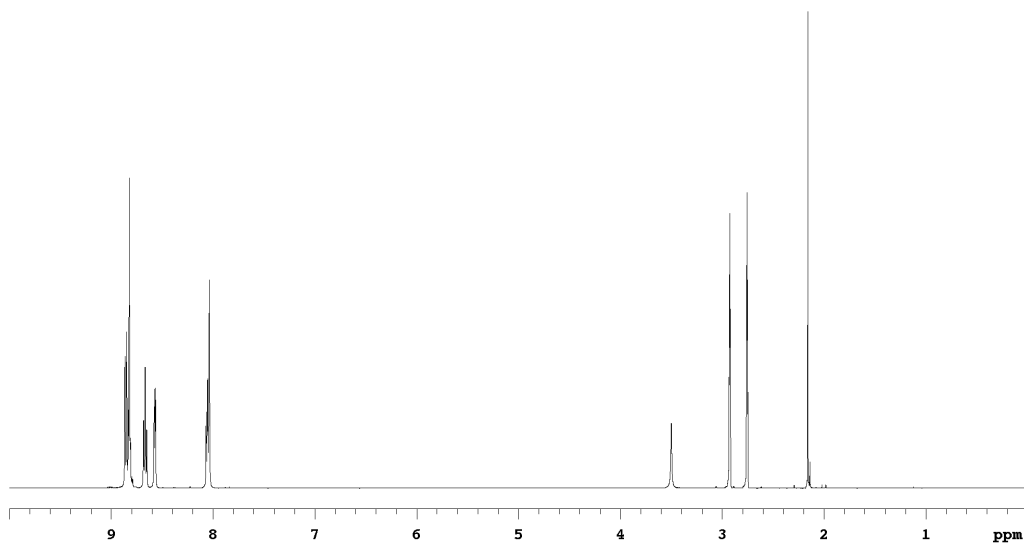
fitting

sum of squares (ss)	Standard error (SEy)	covariance of fit
0.001395689	0.007189728	0.001107889
Results for K_a	Results for other fitted parameters	
2711.11372	441.678802	432.3025342
%confidence interval on parameters (from asymptotic error):		
19.49414486	3.812721295	3.817393058

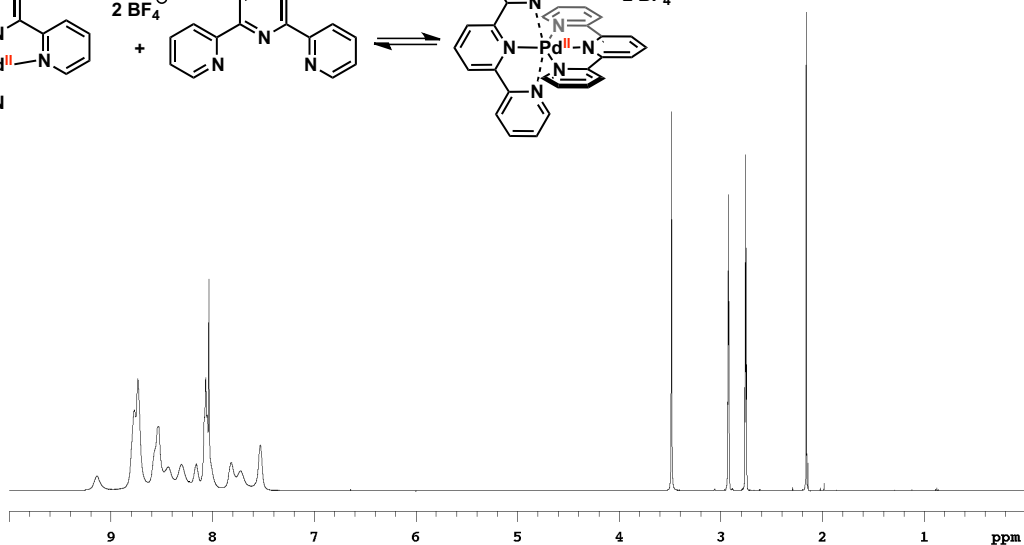
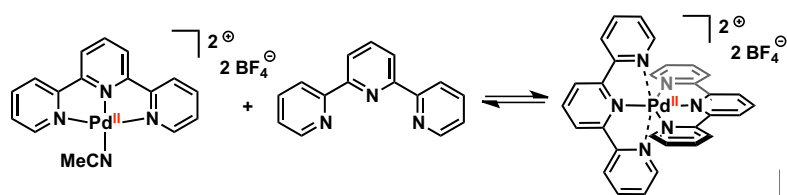
In-Situ ^1H NMR of Pd-Catalyzed Fluorination Reaction

The broad signals for the [Pd] catalyst observed during catalysis are also consistent with the catalyst resting state consisting of a rapid equilibrium involving **1.1** and **1.5**:

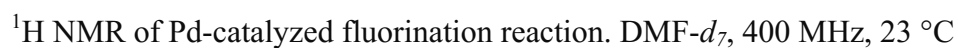




^1H NMR of **1.1**. DMF- d_7 , 500 MHz, 23 °C



^1H NMR of **1.1** with added terpyridine. DMF- d_7 , 500 MHz, 23 °C



The diagram illustrates a catalytic cycle for the fluorination of benzene. The cycle involves the following steps and species:

- Species 1.1:** $[(\text{terpy})\text{Pd}^{\text{II}}(\text{Solv})]^{2+} + \text{terpy}$
- Species 1.5:** $[(\text{terpy})_2\text{Pd}^{\text{II}}]^{2+}$
- Species 1.2:** $[\text{Pd}^{\text{III}}]^{3+} + \text{C}_6\text{H}_5\text{F} + \text{BF}_3\text{K}$
- Species 1.3:** $[\text{Pd}^{\text{III}}]^{3+} + \text{C}_6\text{H}_5\text{F} + \text{BF}_3\text{K}$ (intermediate state)
- Species 1.4:** $[\text{Pd}^{\text{III}}]^{3+} + \text{C}_6\text{H}_5\text{F} + \text{BF}_3\text{K}$ (intermediate state)

The cycle proceeds through the following steps:

- Step 1:** $[(\text{terpy})\text{Pd}^{\text{II}}(\text{Solv})]^{2+} + \text{terpy} \xrightleftharpoons[k_{-1}]{k_1} [(\text{terpy})_2\text{Pd}^{\text{II}}]^{2+}$
- Step 2:** $[(\text{terpy})_2\text{Pd}^{\text{II}}]^{2+} \xrightarrow{\text{turnover-limiting oxidation}} [\text{Pd}^{\text{III}}]^{3+} + \text{C}_6\text{H}_5\text{F} + \text{BF}_3\text{K}$ (rate constant k_2)
- Step 3:** $[\text{Pd}^{\text{III}}]^{3+} + \text{C}_6\text{H}_5\text{F} + \text{BF}_3\text{K} \xrightarrow{\text{F}\cdot \text{ transfer}} [\text{Pd}^{\text{III}}]^{3+} + \text{C}_6\text{H}_5\text{F} + \text{BF}_3\text{K}$
- Step 4:** $[\text{Pd}^{\text{III}}]^{3+} + \text{C}_6\text{H}_5\text{F} + \text{BF}_3\text{K} \xrightarrow{\text{S.E.T.}} [(\text{terpy})\text{Pd}^{\text{II}}(\text{Solv})]^{2+} + \text{terpy}$

A proposed mechanism for the Pd-catalyzed fluorination reaction (as depicted in Scheme 1.3) is shown above. Based on the kinetics data, oxidation of [Pd] by Selectfluor is turnover-limiting during catalysis. The observed saturation kinetics with respect to terpyridine, along with the measurement of a fast equilibrium between **1.5** and [**1.1** + terpy] (*vide supra*: binding constant analysis in Discussion of the Structure of **1.5**), supports a catalyst resting state consisting of an equilibrium between **1.1** and **1.5**. The mechanism shown above would

result in zero-order dependence on the aryl trifluoroborate, first-order dependence on palladium, saturation behavior with respect to terpyridine, and first-order dependence on Selectfluor (rate law derivation given below):

$$\text{rate} = \frac{d[\text{ArF}]}{dt} = k_2[\text{Selectfluor}][\mathbf{1.5}]$$

Applying steady state approximation:

$$\begin{aligned} \frac{d[\mathbf{1.5}]}{dt} = 0 &= k_1[\mathbf{1.1}][\text{terpy}] - k_{-1}[\mathbf{1.5}] - k_2[\text{Selectfluor}][\mathbf{1.5}] \\ &= k_1([\text{Pd}]_0 - [\mathbf{1.5}])([\text{terpy}]) - k_{-1}[\mathbf{1.5}] - k_2[\mathbf{1.5}][\text{Selectfluor}] \\ \left(\begin{array}{l} [\text{Pd}]_0 = \text{total concentration of Pd} \\ = [\mathbf{1.1}] + [\mathbf{1.5}] \end{array} \right) \end{aligned}$$

$$k_1[\text{Pd}]_0[\text{terpy}] = k_1[\mathbf{1.5}][\text{terpy}] + k_{-1}[\mathbf{1.5}] + k_2[\mathbf{1.5}][\text{Selectfluor}]$$

$$k_1[\text{Pd}]_0[\text{terpy}] = [\mathbf{1.5}](k_1[\text{terpy}] + k_{-1} + k_2[\text{Selectfluor}])$$

$$[\mathbf{1.5}] = \frac{k_1[\text{Pd}]_0[\text{terpy}]}{k_{-1} + k_2[\text{Selectfluor}] + k_1[\text{terpy}]}$$

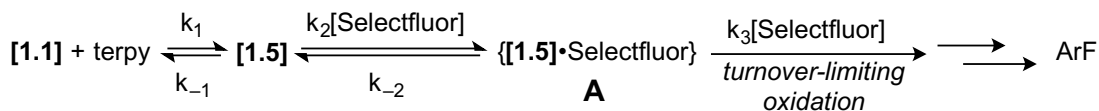
$$\text{rate} = \frac{k_1 k_2 [\text{Pd}]_0 [\text{terpy}] [\text{Selectfluor}]}{k_{-1} + k_2[\text{Selectfluor}] + k_1[\text{terpy}]}$$

if $k_{-1} + k_1[\text{terpy}] \gg k_2[\text{Selectfluor}]$, then

$\text{rate} = \frac{k_1 k_2 [\text{Pd}]_0 [\text{Selectfluor}] [\text{terpy}]}{k_{-1} + k_1[\text{terpy}]}$
--

Due to k_1/k_{-1} being a fast equilibrium, and k_2 being the rate of the turnover-limiting step, assuming $k_{-1} + k_1[\text{terpy}] \gg k_2[\text{Selectfluor}]$ is reasonable, and consistent with the measured data.

The observation of a non-integer kinetic order for Selectfluor (1.4), along with the observation that oxidation of Pd(II) complex **1.5** to Pd(III) **1.2** does not occur via outer-sphere S.E.T. (see Electrochemical data section), suggests the formation of an initial adduct between **1.5** and Selectfluor. If an equilibrium involving such an adduct (**A**) is incorporated into the mechanism proposal outlined above, a rate law can be derived that is consistent with all measured data:



$$\text{rate} = \frac{d[\text{ArF}]}{dt} = k_3[\text{Selectfluor}][\mathbf{A}]$$

Applying steady state approximation for **A**:

$$\frac{d[\mathbf{A}]}{dt} = 0 = k_2[1.5][\text{Selectfluor}] - k_{-2}[\mathbf{A}] - k_3[\text{Selectfluor}][\mathbf{A}]$$

$$[\mathbf{A}] = \frac{k_2[1.5][\text{Selectfluor}]}{k_{-2} + k_3[\text{Selectfluor}]}$$

Applying steady state approximation for **1.5**:

$$\frac{d[1.5]}{dt} = 0 = k_1[1.1][\text{terpy}] - k_{-1}[1.5] - k_2[\text{Selectfluor}][1.5]$$

$$\left(\begin{array}{l} [\text{Pd}]_0 = \text{total concentration of Pd} \\ = [1.1] + [1.5] \end{array} \right)$$

$$[1.5] = \frac{k_1[\text{Pd}]_0[\text{terpy}]}{k_{-1} + k_2[\text{Selectfluor}] + k_1[\text{terpy}]}$$

Incorporating **1.5** into **A**:

$$[\mathbf{A}] = \underbrace{\left(\frac{k_2[\text{Selectfluor}]}{k_{-2} + k_3[\text{Selectfluor}]} \right)}_{\approx k_{-2}} \cdot \left(\frac{k_1[\text{Pd}]_0[\text{terpy}]}{k_{-1} + k_2[\text{Selectfluor}] + k_1[\text{terpy}]} \right)$$

$$[\mathbf{A}] = \frac{k_1 k_2 [\text{Pd}]_0 [\text{terpy}] [\text{Selectfluor}]}{k_{-1} k_{-2} + k_2 k_{-2} [\text{Selectfluor}] + k_1 k_{-2} [\text{terpy}]}$$

$$\text{rate} = \frac{k_1 k_2 k_3 [\text{Pd}]_0 [\text{terpy}] [\text{Selectfluor}]^2}{k_{-1} k_{-2} + k_2 k_{-2} [\text{Selectfluor}] + k_1 k_{-2} [\text{terpy}]}$$

While the nature of the adduct between **1.5** and Selectfluor (**A**) is not known at this point, the data suggest that the interaction between **1.5** and Selectfluor that occurs prior to turnover-limiting oxidation is critical to the success of the Pd-catalyzed fluorination reaction.

Isotopic Labeling Experiment

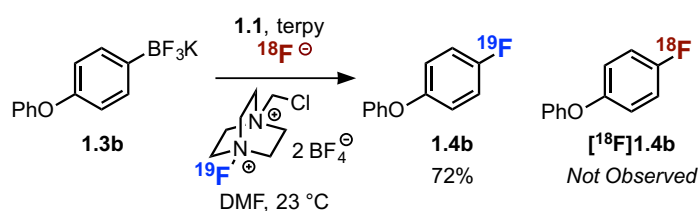
Radiochemistry General Methods and Procedures

No-carrier-added [^{18}F]fluoride was produced from water 97% enriched in ^{18}O (Sigma-Aldrich®) by the nuclear reaction $^{18}\text{O}(\text{p},\text{n})^{18}\text{F}$ using a Siemens Eclipse HP cyclotron and a silver-bodied target at MGH Athinoula A. Martinos Center for Biomedical Imaging. The produced [^{18}F]fluoride in water was transferred from the cyclotron target by helium push. In the analysis of the ^{18}F -labeled compounds, isotopically unmodified reference substances were used for identification. Radioactivity was measured in a Capintec, Inc. CRC-25PET ion chamber. *Solvents and reagents for radiochemical experiments:* Acetonitrile, extra dry, (AcroSeal®) was purchased from Acros® and used as received. *N,N*-dimethylformamide was distilled from 4Å molecular sieves and stored under inert atmosphere. Water was obtained from a Millipore Milli-Q Integral Water Purification System. 18-crown-6 was sublimed. Potassium carbonate ($\geq 99.99\%$) was purchased from Sigma-Aldrich® and used as received.

[^{18}F]Fluoride solution obtained from a cyclotron was loaded onto a Macherey-Nagel SPE Chromafix 30-PS- HCO_3 cartridge that had been previously washed with 2.0 mL of 5.0 mg/mL K_2CO_3 in Millipore Milli-Q water and then 20 mL of Millipore Milli-Q water. After loading, the cartridge was washed with 2 mL of Millipore Milli-Q water. [^{18}F]Fluoride was eluted with 2.0 mL of a 5.0 mg/mL K_2CO_3 in Millipore Milli-Q water solution. The solution was diluted with 8.0 mL of acetonitrile providing 10 mL of 4:1 MeCN: H_2O solution containing 1.0 mg/mL K_2CO_3 . 1.0 mL of this solution was then put in a conical vial that had been washed with acetone and deionized water and dried at 150 °C prior to use. 0.50 mL of a stock solution containing 18-crown-6 (26.2 mg/mL MeCN) was then added. The solution was evaporated at 108 °C with a constant nitrogen gas stream. At dryness, 0.5 mL of acetonitrile was added and evaporated at 108 °C with a constant nitrogen gas stream.

Another 0.5 mL of acetonitrile was added and evaporated at 108 °C with a constant nitrogen gas stream to leave a white precipitate around the bottom and sides of the vial. The vial was purged with nitrogen, and sealed with a cap fitted with a septum. 0.4 mL of *N,N*-dimethylformamide was added and the conical vial was sonicated for 30 seconds before the solution was taken up in a syringe.

Procedure for Labeling Experiment



A 4 mL vial was charged with aryl trifluoroborate **1.3b** (5.0 mg, 0.018 mmol, 1.0 equiv), Selectfluor (6.4 mg, 0.018 mmol, 1.0 equiv), Pd(II) complex **1.1** (2.5 mg, 4.5×10^{-3} mmol, 0.25 equiv) and terpy (2.1 mg, 9.1×10^{-3} mmol, 0.50 equiv), and sealed with a cap fitted with a septum. A DMF solution (0.4 mL) of $[^{18}\text{F}]\text{fluoride}$, prepared and dried as described above, was added to the vial via the septum. The mixture was allowed to stir for 15 minutes at 23 °C, and then a capillary tube was used to spot the solution on a silica gel TLC plate. The TLC plate was eluted with a 10% (v/v) mixture of Et₂O/pentane. The TLC plate was scanned with a Bioscan AR-2000 Radio TLC Imaging Scanner to determine $[^{18}\text{F}]\text{fluoride}$ incorporation into the aryl fluoride product (**1.4b**), using an authentic sample of **1.4b** as a reference. The radio TLC scan is shown in Figure 3.2, and indicates no $[^{18}\text{F}]\text{fluoride}$ incorporation into the organic product:

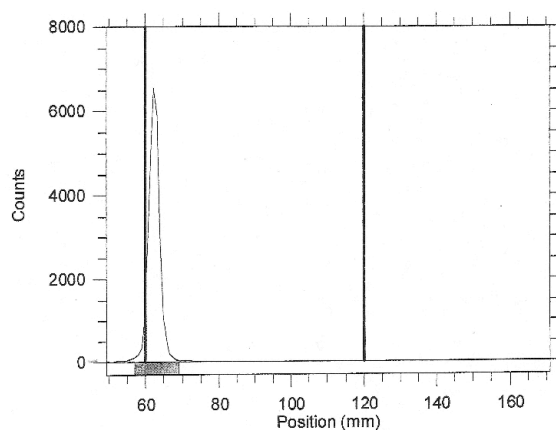


Figure 3.2. Radio TLC scan for the isotopic labeling experiment. The position at 60 mm corresponds to the baseline of the TLC plate, and no [^{18}F] incorporation into aryl fluoride **1.4b** is observed.

The radioactivity was allowed to decay over the course of 3 days, and then 1-fluoro-3-nitrobenzene (5.0 μL , 4.7×10^{-5} mol) was added to the vial as internal standard. The mixture was transferred to an NMR tube, and then the yield of aryl fluoride **1.4b** was determined to be 0.013 mmol (72%) via ^{19}F NMR spectroscopy, integrating against the internal standard peak at -112 ppm.

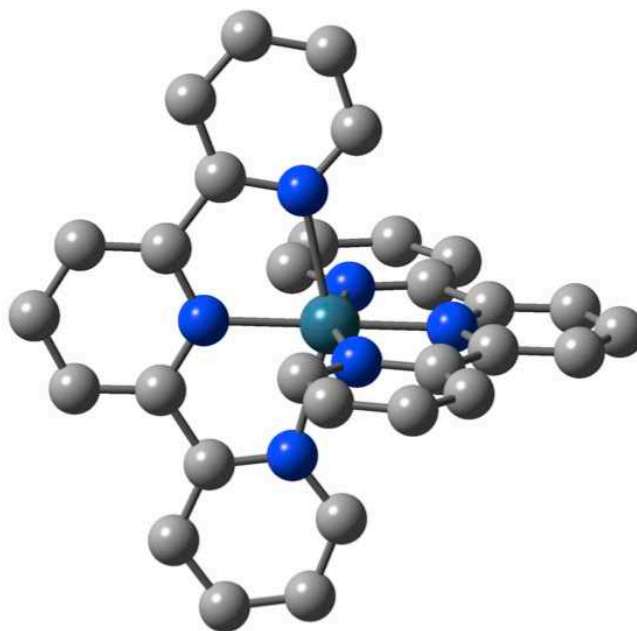
The result of the isotopic labeling experiment suggests that C–F bond formation in the Pd-catalyzed fluorination reaction does not occur via nucleophilic attack by fluoride.

DFT Calculations

Density functional theory (DFT) calculations were performed using Gaussian09¹¹⁶ at the Odyssey cluster at Harvard University. Geometry optimizations were carried out using the atomic coordinates from the crystal structures of **1.2** and **3.2** as starting points. The unrestricted wave function was used for ground state optimizations. BS I includes SDD quasirelativistic pseudopotentials on Pd (MWB28) with basis sets (Pd: (8s7p6d)/[6s5p3d]¹¹⁷) extended by polarization functions (Pd: f, 1.472¹¹⁸) and 6-31G(d,p)¹¹⁹ on H, C, N. All geometry optimizations were performed using the M06 functional with the BS I basis set. Molecular orbitals were generated using an isosurface value of 0.03 with M06/BS I. Atomic contributions to the frontier molecular orbitals (Mulliken contribution) were calculated using Chemissian.¹²⁰ Images were generated using Chem3D or GaussView5.¹²¹

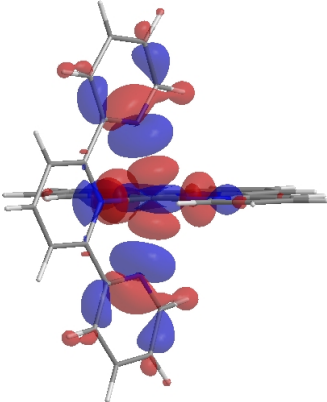
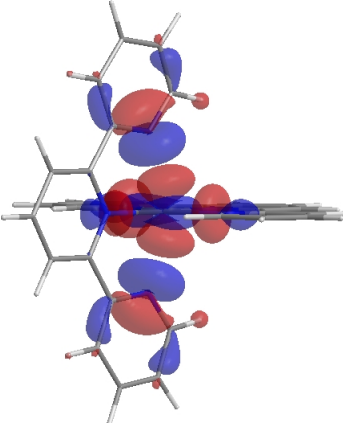
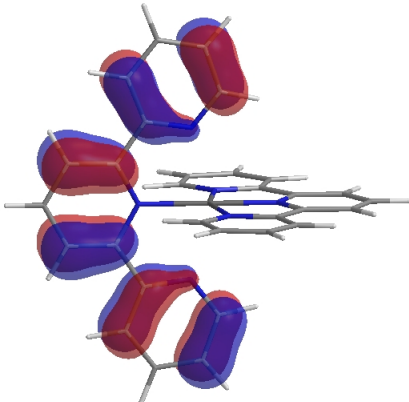
The optimized structure of 1.2 with M06/BS I and Cartesian coordinates (Å)

Atom	X	Y	Z
C	-0.3859153	3.2601299	-0.0029228
C	-0.3857447	-3.2601528	0.0019591
C	0.0749534	4.5719638	-0.0034432
C	2.3121468	-3.6971685	0.0016506
C	0.4476814	0.0021814	3.0558466
C	4.0094389	-1.2029189	0.0003614
C	4.0093664	1.2031441	-0.0008604
C	-2.6877253	-0.0006931	-1.192966
C	0.0689162	-0.0031507	-4.3937792
C	-4.0783461	0.0006164	1.2113523
C	-1.2825659	0.0027586	4.7051837
C	2.617441	1.1889604	-0.000864
C	-4.7661917	-0.0000914	0.0007202
C	-2.6873867	0.0006932	1.1938355
C	-2.2215526	0.0020336	3.6762028
C	1.7840977	-2.4094761	0.0011341
C	4.7035311	0.0001317	-0.0002461
C	0.0701654	0.0028601	4.3938717
C	-1.7896499	-0.0014654	-2.3576439
C	2.3119621	3.6972918	-0.0021118
C	1.7839918	2.4095668	-0.0016692
C	-2.2226056	-0.0022002	-3.6754755
C	-1.7889781	0.0014154	2.3582497
C	-1.2839048	-0.0030426	-4.7047146
C	2.617507	-1.1888313	0.0004109
C	0.075195	-4.5719595	0.0025213
C	1.4467682	-4.7876582	0.0023481
C	-4.0786848	-0.0007564	-1.210108
C	0.4468136	-0.0023419	-3.0558676
C	1.4465141	4.7877305	-0.0029804
N	1.9655339	0.0000444	-0.0001979
N	-0.454182	0.0014689	2.0713335
N	0.4455376	2.2196481	-0.0020462
N	-0.4547851	-0.0015077	-2.0711077
N	-2.0544249	0.0000673	0.0003476
N	0.4456386	-2.219611	0.0012816
Pd	-0.078421	0.0000568	0.00007
H	-1.4519024	3.035544	-0.0032291
H	-1.451744	-3.0356108	0.0020361
H	-0.6289514	5.398267	-0.0041901
H	3.3848868	-3.863958	0.0015167
H	1.4944928	0.0022054	2.7600832

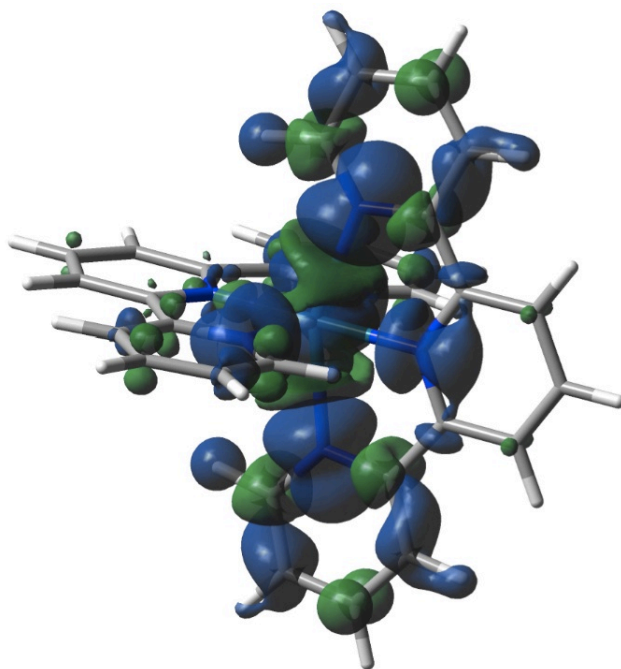


H	4.5528592	-2.1421546	0.0008089
H	4.552729	2.1424121	-0.0013659
H	0.8289274	-0.0038667	-5.1687552
H	-4.6257985	0.0011238	2.1490569
H	-1.6102158	0.0032461	5.7410615
H	-5.8526973	-0.0001385	0.0008748
H	-3.2824799	0.0019567	3.9091442
H	5.789947	0.0001609	-0.0002564
H	0.8303937	0.0034749	5.1686352
H	3.3846921	3.8641521	-0.0017851
H	-3.2835994	-0.0021268	-3.908108
H	-1.6118354	-0.0036112	-5.7405035
H	-0.6286718	-5.3982962	0.0030784
H	1.8463331	-5.7979485	0.0027505
H	-4.6263964	-0.0013346	-2.1476614
H	1.4937014	-0.0023422	-2.7603681
H	1.846039	5.798039	-0.0032914

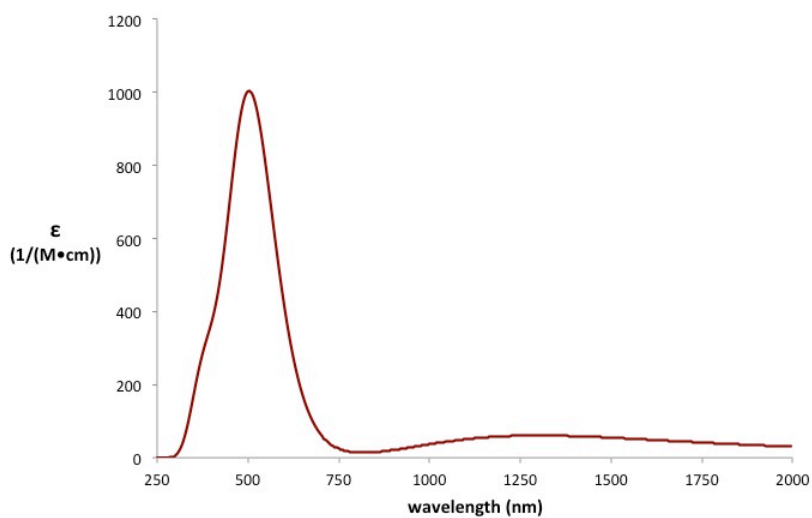
Table 3.4. Selected Frontier MOs for 1.2, with Atomic Contributions

<u>MO #</u> <u>(Energy, eV)</u>	<u>MO</u> <u>(isosurface value 0.03)</u>	<u>Atomic</u> <u>Contributions</u>
α HOMO (130) (-15.003)		Pd: 38% N(axial): 32% N(equatorial): 13%
β LUMO (130) (-12.239)		Pd: 52% N(axial): 26% N(equatorial): 12%
α HOMO-1 (129) (-15.408)		C: 98% N: 2%

Spin Density Plot for 1.2



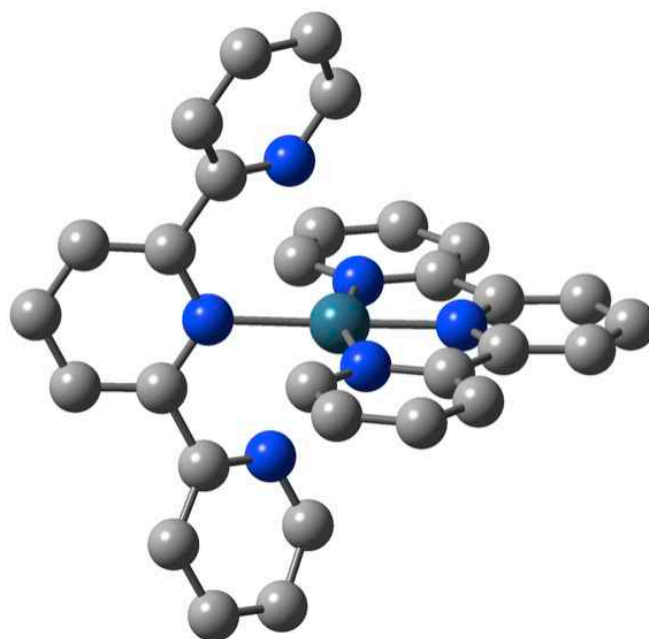
Calculated UV-vis/NIR spectrum for 1.2



The simulated UV-vis/NIR spectrum reproduces the characteristic absorption features observed for **1.2**: the predicted absorbances at 505 nm ($\epsilon = 1.00 \times 10^3 \text{ M}^{-1} \text{ cm}^{-1}$) and 1300 nm ($\epsilon = 60.8 \text{ M}^{-1} \text{ cm}^{-1}$) correspond to the experimental values of 419 nm ($\epsilon = 1.52 \times 10^3 \text{ M}^{-1} \text{ cm}^{-1}$) and 1002 nm ($\epsilon = 95.9 \text{ M}^{-1} \text{ cm}^{-1}$); see UV-vis Data section for the measured spectrum of **1.2**.

The optimized structure of 1.5 with M06/BS I and Cartesian coordinates (Å)

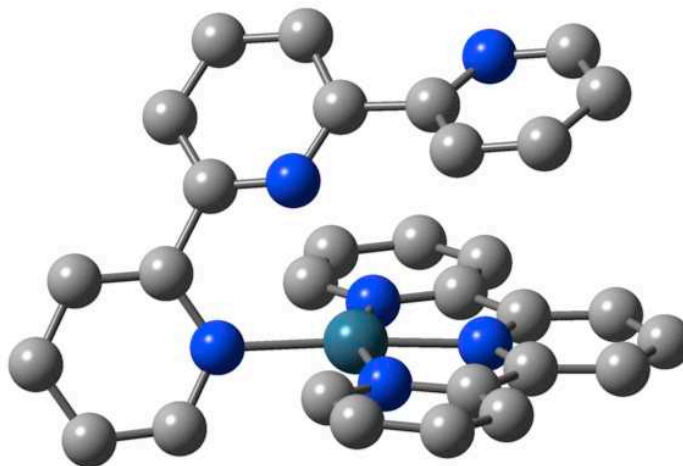
Atom	X	Y	Z
C	0.6367384	3.5915343	-0.5571764
C	-0.4092436	-3.6275313	-0.8690596
C	0.2489311	4.7901551	0.0341997
C	-2.9132926	-3.1896287	0.0994121
C	0.438609	0.0247059	-3.0541408
C	-4.0304378	-0.6201965	-0.8954269
C	-3.6902368	1.7391194	-0.8116021
C	2.3998737	-0.3474722	1.7951073
C	-1.0797925	-0.099027	4.1696253
C	4.3454509	-0.4691316	-0.1732299
C	2.5043847	-0.1402174	-4.2449078
C	-2.3459085	1.5158806	-0.5204391
C	4.7009456	-0.5422825	1.1693875
C	3.0003728	-0.3324553	-0.5031404
C	3.1630231	-0.253179	-3.0241812
C	-2.1396403	-2.1789349	-0.4724075
C	-4.54014	0.6630501	-1.0076797
C	1.1244777	0.0001091	-4.2630157
C	1.2325406	-0.2623459	2.6873673
C	-1.9239596	3.8301277	0.3285001
C	-1.4470976	2.6733698	-0.2897865
C	1.3046114	-0.3290338	4.0706598
C	2.4218969	-0.2240583	-1.8518804
C	0.1360343	-0.2464523	4.8210575
C	-2.6794525	-0.8040779	-0.6067273
C	-1.108897	-4.7021617	-0.3275453
C	-2.3830757	-4.47246	0.172962
C	3.7325778	-0.4805648	2.167514
C	-1.0903819	-0.0352949	2.7821991
C	-1.0565325	4.9041703	0.4914246
N	-1.849639	0.255564	-0.4426617
N	1.0687017	-0.0843372	-1.886924
N	-0.1838288	2.5546103	-0.717257
N	0.0297283	-0.1136408	2.0593275
N	2.0885199	-0.2821511	0.4863751
N	-0.9028404	-2.3920202	-0.9398719
Pd	0.2035015	-0.0495035	0.0056335
H	1.6535658	3.461162	-0.9289463
H	0.5937563	-3.7681855	-1.2720815
H	0.9552576	5.6086616	0.1324626
H	-3.9033526	-2.9790151	0.4953752
H	-0.6415445	0.1346014	-3.0078707



H	-4.6620699	-1.4867707	-1.0644232
H	-4.0519772	2.757396	-0.9140718
H	-2.0129445	-0.0327262	4.7193608
H	5.1068262	-0.515981	-0.9454747
H	3.069808	-0.1614733	-5.1719583
H	5.7469411	-0.6463543	1.4426218
H	4.2428818	-0.3633042	-2.9926673
H	-5.5852825	0.8231095	-1.2569854
H	0.5773716	0.0904912	-5.1956851
H	-2.9455756	3.8894489	0.6942778
H	2.264378	-0.4483654	4.5645762
H	0.1800991	-0.2989152	5.9048353
H	-0.6618357	-5.6911054	-0.3003971
H	-2.9596643	-5.2797221	0.6157613
H	4.0195175	-0.5336568	3.2130481
H	-2.0163403	0.0801182	2.2240089
H	-1.3996492	5.8172747	0.9697538

The optimized structure of 3.2 with M06/BS I and Cartesian coordinates (Å)

Symbol	X	Y	Z
C	-3.0261131	0.1805551	2.4284873
C	-3.8334569	-0.949817	2.4004544
C	-3.2215828	-2.1949354	2.2704261
N	-1.9038685	-2.3572554	2.1689944
C	-1.1329236	-1.2637255	2.1970498
C	0.3259579	-1.502365	2.1077504
C	0.8847812	-2.6918256	2.5880434
C	2.2545495	-2.8709977	2.4863268
C	3.0283277	-1.8862164	1.8771136
C	2.3846471	-0.7471392	1.3987057
C	3.113317	0.2704353	0.6093542
C	4.4474228	0.5886391	0.8588966
C	5.1010645	1.5135713	0.0587764
C	4.411195	2.1084318	-0.9929591
C	3.0872071	1.7606851	-1.1910177
C	1.5288533	-2.1704033	-1.7209617
C	1.4197215	-3.4673626	-2.2058719
C	0.1625667	-3.9545616	-2.5313733
C	-0.948842	-3.1339088	-2.3669356
C	-0.7779646	-1.8465217	-1.8821727
C	-1.8780224	-0.8910173	-1.6836664
C	-3.2269261	-1.0965527	-1.9522849
C	-4.1194287	-0.0547979	-1.7213739
C	-3.6767226	1.1628254	-1.2140184
C	-2.3220023	1.3192866	-0.942645
C	-1.6651572	2.4935901	-0.3484956
C	-2.3400083	3.6362341	0.0538
C	-1.633575	4.6702745	0.6602766
C	-0.2678218	4.5317921	0.8607958
C	0.3548729	3.3654137	0.4341539
C	-1.6486188	0.0284051	2.3210866
N	1.0678012	-0.5500749	1.5345102
N	2.4483416	0.8697158	-0.4083708
N	0.4641694	-1.3797153	-1.5634779
N	-1.4819711	0.3003693	-1.20075
N	-0.3175022	2.379032	-0.1646444
Pd	0.4139481	0.5371455	-0.7719112
H	-3.4646519	1.1676134	2.5629737
H	-4.9122779	-0.877125	2.5018326
H	-3.8220465	-3.1037632	2.2551148
H	0.2353115	-3.4408131	3.0302497
H	2.7206851	-3.7765498	2.8647792
H	4.0984033	-2.0241959	1.7465657
H	4.9563801	0.1257718	1.699472
H	6.1377759	1.7714788	0.2562439
H	4.8850945	2.8290519	-1.6512434
H	2.5031833	2.1946891	-2.0002319
H	2.4921938	-1.7421964	-1.456609
H	2.3113092	-4.0738168	-2.325989
H	0.0429813	-4.9637552	-2.9144523
H	-1.940365	-3.4988595	-2.6170573
H	-3.5808912	-2.0456275	-2.3422987
H	-5.1744823	-0.1943361	-1.9382572
H	-4.3813811	1.9684244	-1.0330696
H	-3.4119013	3.7223836	-0.0979128
H	-2.1509459	5.570996	0.9776006
H	0.3163635	5.30986	1.3409926
H	1.4210479	3.2084031	0.5762145
H	-0.9741022	0.8812221	2.3628366



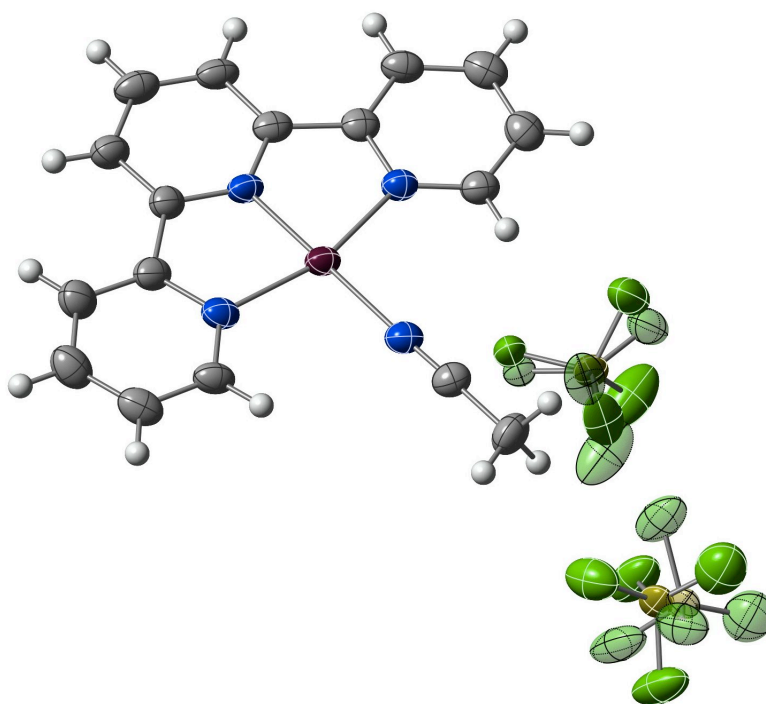
X-ray Crystallographic Analysis

[(terpy)Pd(MeCN)][BF₄]₂ (1.1) (CCDC 935776)

Experimental

Compound **1.1** was crystallized from MeCN/Et₂O as orange prisms. A crystal was mounted on a nylon loop using Paratone-N oil, and transferred to a Bruker APEX II CCD diffractometer (MoK α radiation, $\lambda=0.71073$ Å) equipped with an Oxford Cryosystems nitrogen flow apparatus. The sample was held at 100 K during the experiment. The collection method involved 0.5° scans in ω at 28° in 2θ . Data integration down to 0.82 Å

resolution was carried out using SAINT V7.46 A (Bruker diffractometer, 2009) with reflection spot size optimisation. Absorption corrections were made with the program SADABS (Bruker diffractometer, 2009). The structure was solved by the direct methods procedure and refined by least-squares methods again F^2 using SHELXS-97 and SHELXL-97 (Sheldrick, 2008). Non-hydrogen atoms were refined anisotropically, and hydrogen atoms were allowed to ride on the respective atoms. Restraints on bond lengths and constraints of the atomic displacement parameters on each pair of disorder fragments (SADI and EADP instructions of SHELXL97), as well as the restraints of the atomic displacement parameters (SIMU/DELU instructions of SHELXL97) if necessary, have been applied for the disorder refinement. Crystal data as well as details of data collection and refinement are summarized in Table 3.5. Graphics were produced using the CrystalMaker 8.6 software program (©1994-2012 CrystalMaker Software Ltd.)



X-ray structure of **1.1**. Thermal ellipsoids are drawn at the 50% probability level; the disorder model is depicted using transparent ellipsoids.

Table 3.5. Experimental Details

	Compound 1.1
Crystal data	
Chemical formula	C ₁₇ H ₁₄ B ₂ F ₈ N ₄ Pd
M_r	554.34
Crystal system, space group	Monoclinic, $P2_1/c$
Temperature (K)	100
a, b, c (Å)	13.490 (4), 11.504 (3), 13.834 (4)
β (°)	113.793 (4)
V (Å ³)	1964.4 (10)
Z	4
Radiation type	Mo $K\alpha$
μ (mm ⁻¹)	1.03
Crystal size (mm)	0.30 × 0.25 × 0.20
Data collection	
Diffractometer	CCD area detector diffractometer
Absorption correction	Multi-scan <i>SADABS</i> (Sheldrick, 2009)

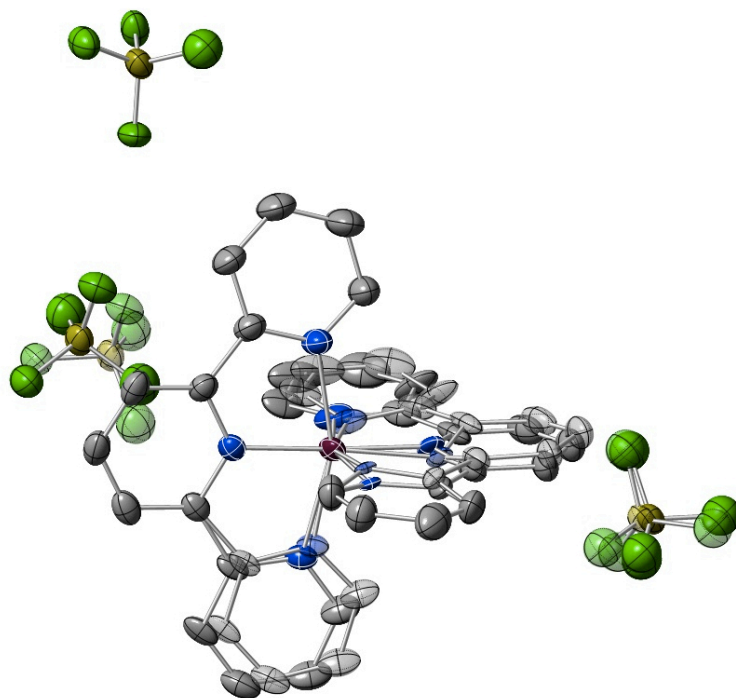
T_{\min}, T_{\max}	0.747, 0.820
No. of measured, independent and observed [$I >$ $2\sigma(I)$] reflections	15857, 3717, 3105
R_{int}	0.039
$(\sin \theta/\lambda)_{\max}$ (\AA^{-1})	0.610
Refinement	
$R[F^2 > 2\sigma(F^2)],$ $wR(F^2), S$	0.050, 0.140, 1.05
No. of reflections	3717
No. of parameters	312
No. of restraints	10
H-atom treatment	H-atom parameters constrained
$\Delta\rho_{\max}, \Delta\rho_{\min}$ (e \AA^{-3})	1.26, -1.03

Computer programs: *APEX2* v2009.3.0 (Bruker-AXS, 2009), *SAINT* 7.46A (Bruker-AXS, 2009), *SHELXS97* (Sheldrick, 2008), *SHELXL97* (Sheldrick, 2008), Bruker *SHELXTL*.

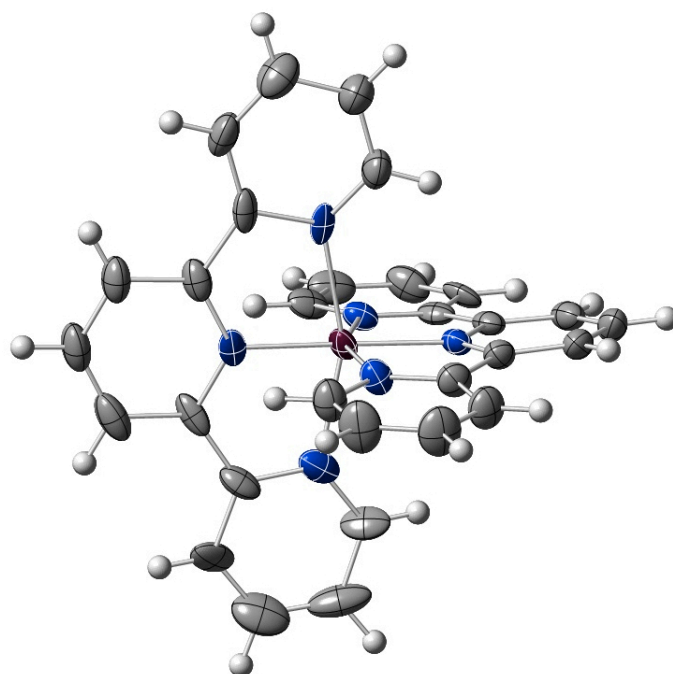
$[(\text{terpy})_2\text{Pd}][\text{BF}_4]_3$ (1.2) (CCDC 935777)

Experimental

Compound **1.2** was crystallized from MeCN/Et₂O as red needles. A crystal was mounted on a nylon loop using Paratone-N oil, and transferred to a Bruker APEX II CCD diffractometer (MoK α radiation, $\lambda=0.71073$ Å) equipped with an Oxford Cryosystems nitrogen flow apparatus. The sample was held at 100 K during the experiment. The collection method involved 0.5° scans in ω at 28° in 2θ . Data integration down to 0.82 Å resolution was carried out using SAINT V7.46 A (Bruker diffractometer, 2009) with reflection spot size optimisation. Absorption corrections were made with the program SADABS (Bruker diffractometer, 2009). The structure was solved by the direct methods procedure and refined by least-squares methods again F^2 using SHELXS-97 and SHELXL-97 (Sheldrick, 2008). Non-hydrogen atoms were refined anisotropically, and hydrogen atoms were allowed to ride on the respective atoms. Restraints on bond lengths and constraints of the atomic displacement parameters on each pair of disorder fragments (SADI and EADP instructions of SHELXL97), as well as the restraints of the atomic displacement parameters (SIMU/DELU instructions of SHELXL97) if necessary, have been applied for the disorder refinement. A solvent mask was implemented in the Olex 2 software due to a non-integer number of highly disordered MeCN solvent molecules. Crystal data as well as details of data collection and refinement are summarized in Table 3.6. Graphics were produced using the CystalMaker 8.6 software program (©1994-2012 CrystalMaker Software Ltd.)



X-ray structure of **1.2**. Thermal ellipsoids are drawn at the 50% probability level; the disorder model is depicted using transparent ellipsoids. H-atoms have been omitted for clarity.



Structure of the Pd(III) cation of **1.2**, with disorder omitted for clarity. Thermal ellipsoids are drawn at the 50% probability level.

Table 3.6. Experimental Details

	Compound 1.2
Crystal data	
Chemical formula	C ₃₀ H ₂₂ B ₃ F ₁₂ N ₆ Pd
M_r	833.37
Crystal system, space group	Monoclinic, $P2_1/n$
Temperature (K)	100
a, b, c (Å)	15.0771 (6), 17.6720 (7), 15.6002 (6)
β (°)	99.830 (1)
V (Å ³)	4095.5 (3)
Z	4
Radiation type	Mo $K\alpha$
μ (mm ⁻¹)	0.54
Crystal size (mm)	1.0 × 0.43 × 0.29
Data collection	
Diffractometer	CCD area detector diffractometer
Absorption correction	Numerical <i>SADABS</i> (Sheldrick, 2009)
T_{\min}, T_{\max}	0.587, 0.862
No. of measured, independent and observed [$I > 2\sigma(I)$] reflections	7791, 7791, 6585
R_{int}	0.0000
$(\sin \theta/\lambda)_{\text{max}}$ (Å ⁻¹)	0.611
Refinement	
$R[F^2 > 2\sigma(F^2)], wR(F^2), S$	0.077, 0.209, 1.04
No. of reflections	7791
No. of parameters	513
No. of restraints	72
H-atom treatment	H-atom parameters constrained
	$w = 1/[\sigma^2(F_o^2) + (0.096P)^2 + 29.5516P]$ where $P = (F_o^2 + 2F_c^2)/3$
$\Delta\rho_{\text{max}}, \Delta\rho_{\text{min}}$ (e Å ⁻³)	3.06, -2.05

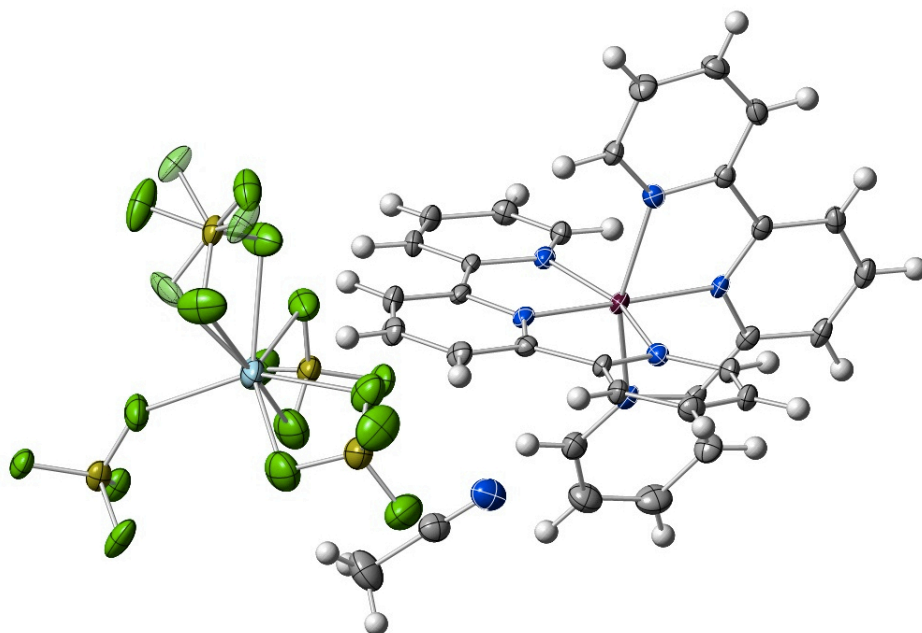
Computer programs: *APEX2* v2009.3.0 (Bruker-AXS, 2009), *SAINT* 7.46A (Bruker-AXS, 2009), *SHELXS97* (Sheldrick, 2008), *SHELXL97* (Sheldrick, 2008), Bruker *SHELXTL*.

[(terpy)₂Pd][BF₄]₃•[NaBF₄] (3.1) (CCDC 935778)

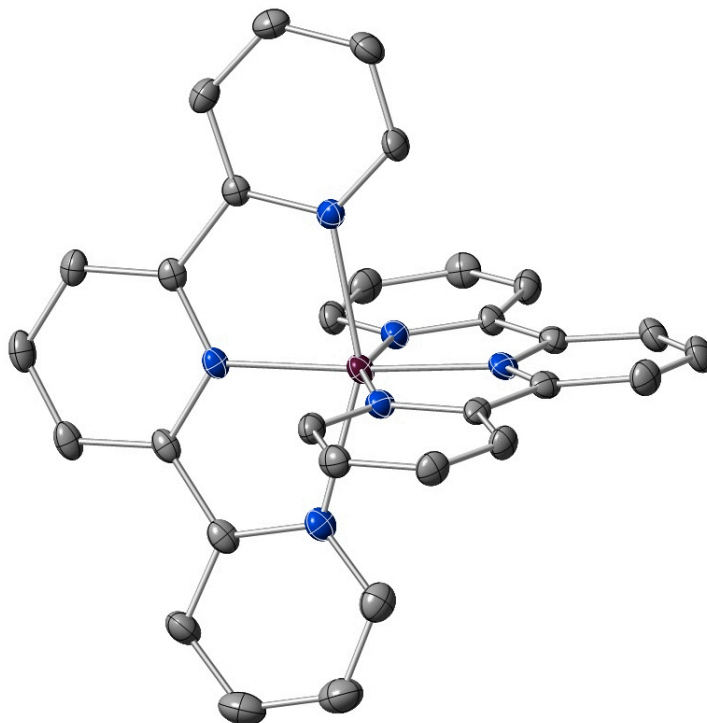
Experimental

Compound **3.1** was crystallized from MeCN/Et₂O as red plates. A crystal was mounted on a

nylon loop using Paratone-N oil, and transferred to a Bruker APEX II CCD diffractometer (MoK α radiation, $\lambda=0.71073$ Å) equipped with an Oxford Cryosystems nitrogen flow apparatus. The sample was held at 100 K during the experiment. The collection method involved 0.5° scans in ω at 28° in 2θ . Data integration down to 0.82 Å resolution was carried out using SAINT V7.46 A (Bruker diffractometer, 2009) with reflection spot size optimisation. Absorption corrections were made with the program SADABS (Bruker diffractometer, 2009). The structure was solved by the direct methods procedure and refined by least-squares methods again F^2 using SHELXS-97 and SHELXL-97 (Sheldrick, 2008). Non-hydrogen atoms were refined anisotropically, and hydrogen atoms were allowed to ride on the respective atoms. Restraints on bond lengths and constraints of the atomic displacement parameters on each pair of disorder fragments (SADI and EADP instructions of SHELXL97), as well as the restraints of the atomic displacement parameters (SIMU/DELU instructions of SHELXL97) if necessary, have been applied for the disorder refinement. Crystal data as well as details of data collection and refinement are summarized in Table 3.7. Graphics were produced using the CrystalMaker 8.6 software program (©1994-2012 CrystalMaker Software Ltd.)



X-ray structure of **3.1**. Thermal ellipsoids are drawn at the 50% probability level; the disorder model is depicted using transparent ellipsoids.



Structure of the Pd(III) cation of **3.1**, with H-atoms omitted for clarity. Thermal ellipsoids are drawn at the 50% probability level.

Table 3.7. Experimental Details

	Compound 3.1
Crystal data	
Chemical formula	C ₃₂ H ₂₅ B ₄ F ₁₆ N ₇ NaPd
M_r	984.22
Crystal system, space group	Triclinic, $P\bar{1}$
Temperature (K)	100
a, b, c (Å)	9.7835 (14), 12.3525 (17), 16.842 (2)
α, β, γ (°)	104.147 (2), 103.269 (2), 100.107 (2)
V (Å ³)	1862.2 (4)
Z	2
Radiation type	Mo $K\alpha$
μ (mm ⁻¹)	0.63
Crystal size (mm)	0.28 × 0.16 × 0.12
Data collection	
Diffractometer	CCD area detector diffractometer
Absorption correction	Numerical <i>SADABS</i> (Sheldrick, 2009)
T_{\min}, T_{\max}	0.844, 0.928
No. of measured, independent and observed [$I > 2\sigma(I)$] reflections	21336, 7078, 6045
R_{int}	0.044
$(\sin \theta/\lambda)_{\text{max}}$ (Å ⁻¹)	0.611
Refinement	
$R[F^2 > 2\sigma(F^2)], wR(F^2), S$	0.046, 0.117, 1.06
No. of reflections	7078
No. of parameters	573
No. of restraints	0
H-atom treatment	H-atom parameters constrained
$\Delta\rho_{\text{max}}, \Delta\rho_{\text{min}}$ (e Å ⁻³)	1.32, -1.37

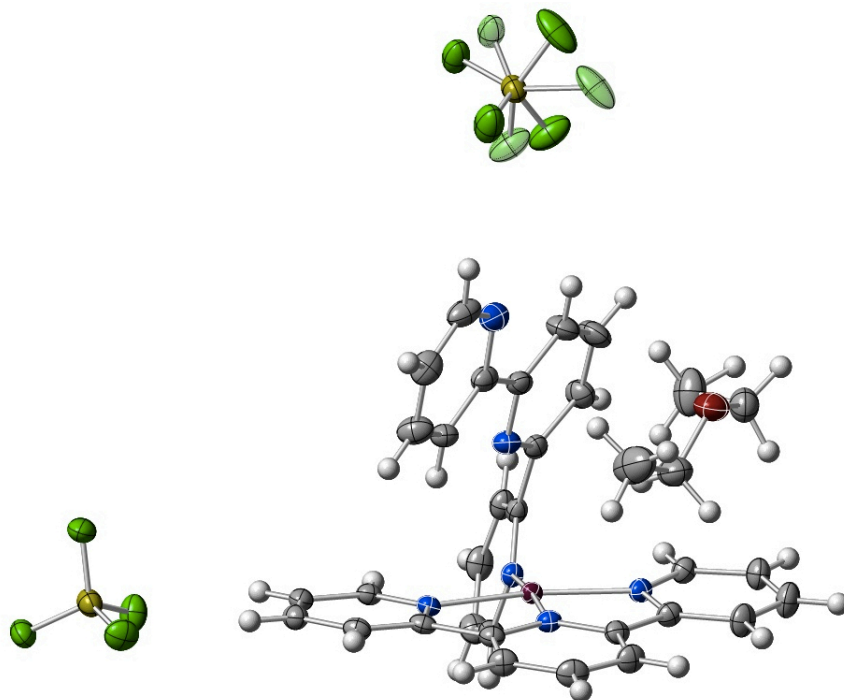
Computer programs: *APEX2* v2009.3.0 (Bruker-AXS, 2009), *SAINT* 7.46A (Bruker-AXS, 2009), *SHELXS97* (Sheldrick, 2008), *SHELXL97* (Sheldrick, 2008), Bruker *SHELXTL*.

[(terpy)₂Pd]/[BF₄]₂ (3.2) (CCDC 935779)

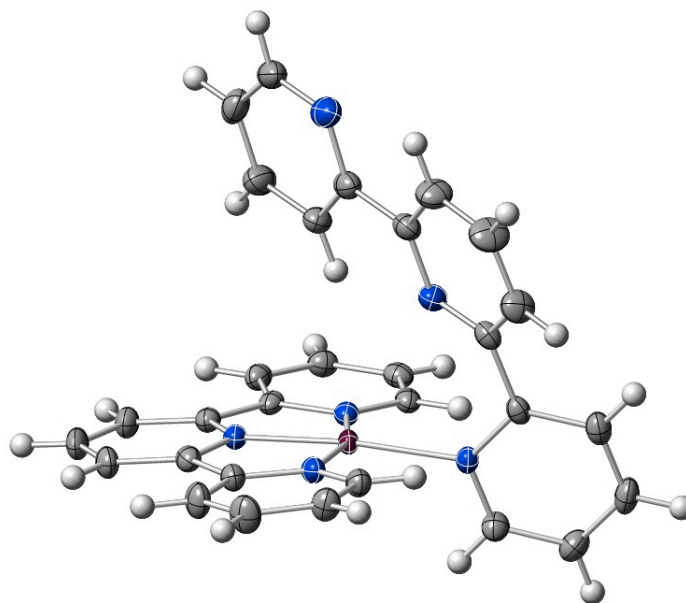
Experimental

Compound **3.2** was crystallized from MeCN/Et₂O as yellow prisms. A crystal was mounted

on a nylon loop using Paratone-N oil, and transferred to a Bruker APEX II CCD diffractometer (MoK α radiation, $\lambda=0.71073$ Å) equipped with an Oxford Cryosystems nitrogen flow apparatus. The sample was held at 100 K during the experiment. The collection method involved 0.5° scans in ω at 28° in 2θ . Data integration down to 0.82 Å resolution was carried out using SAINT V7.46 A (Bruker diffractometer, 2009) with reflection spot size optimisation. Absorption corrections were made with the program SADABS (Bruker diffractometer, 2009). The structure was solved by the direct methods procedure and refined by least-squares methods again *F*² using SHELXS-97 and SHELXL-97 (Sheldrick, 2008). Non-hydrogen atoms were refined anisotropically, and hydrogen atoms were allowed to ride on the respective atoms. The crystal exhibits pseudo-merohedral twinning, but satisfactory refinement was achieved by applying the twin law that was found by using Platon/TwinRotMat. Restraints on bond lengths and constraints of the atomic displacement parameters on each pair of disorder fragments (SADI and EADP instructions of SHELXL97), as well as the restraints of the atomic displacement parameters (SIMU/DELU instructions of SHELXL97) if necessary, have been applied for the disorder refinement. Crystal data as well as details of data collection and refinement are summarized in Table 3.8. Graphics were produced using the CrystalMaker 8.6 software program (©1994-2012 CrystalMaker Software Ltd.)



X-ray structure of **3.2**. Thermal ellipsoids are drawn at the 50% probability level; the disorder model is depicted using transparent ellipsoids.



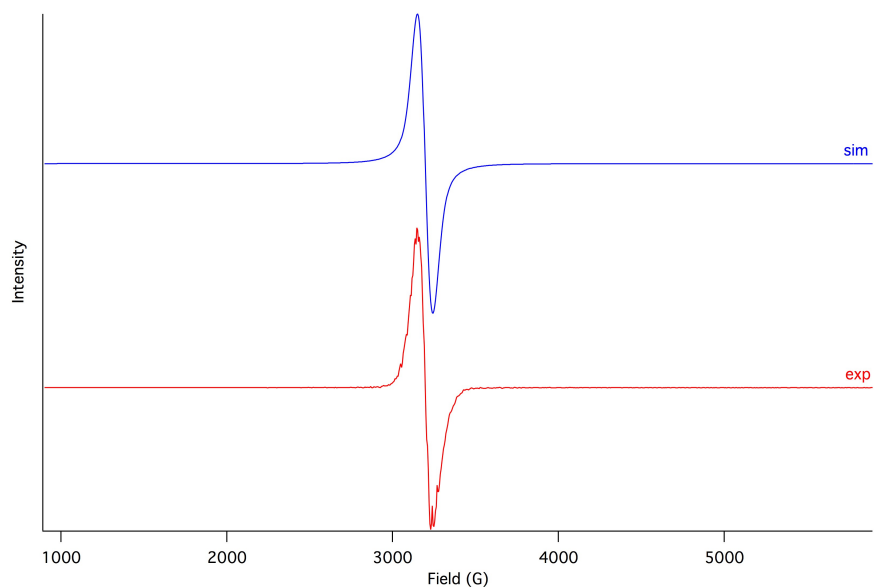
Structure of the Pd(II) cation of **3.2**. Thermal ellipsoids are drawn at the 50% probability level.

Table 3.8. Experimental Details

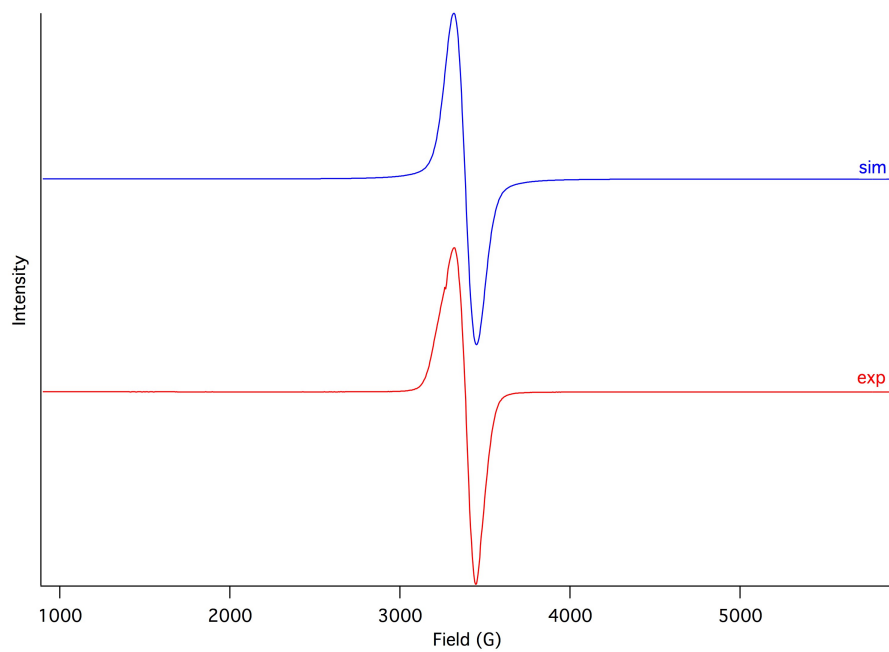
	Compound 3.2
Crystal data	
Chemical formula	C ₃₄ H ₃₂ B ₂ F ₈ N ₆ OPd
M_r	820.68
Crystal system, space group	Monoclinic, $P2_1/n$
Temperature (K)	100
a, b, c (Å)	12.1099 (7), 12.6815 (8), 20.7558 (13)
β (°)	90.080 (1)
V (Å ³)	3187.5 (3)
Z	4
Radiation type	Mo $K\alpha$
μ (mm ⁻¹)	0.67
Crystal size (mm)	0.49 × 0.39 × 0.33
Data collection	
Diffractometer	CCD area detector diffractometer
Absorption correction	Multi-scan <i>SADABS</i> (Sheldrick, 2009)
T_{\min}, T_{\max}	0.735, 0.809
No. of measured, independent and observed [$I >$ $2\sigma(I)$] reflections	49913, 7077, 6487
R_{int}	0.032
$(\sin \theta/\lambda)_{\text{max}}$ (Å ⁻¹)	0.643
Refinement	
$R[F^2 > 2\sigma(F^2)],$ $wR(F^2), S$	0.024, 0.060, 1.03
No. of reflections	7077
No. of parameters	470
No. of restraints	6
H-atom treatment	H-atom parameters constrained
$\Delta\rho_{\text{max}}, \Delta\rho_{\text{min}}$ (e Å ⁻³)	0.52, -0.55

Computer programs: *APEX2* v2009.3.0 (Bruker-AXS, 2009), *SAINT* 7.46A (Bruker-AXS, 2009), *SHELXS97* (Sheldrick, 2008), *SHELXL97* (Sheldrick, 2008), Bruker *SHELXTL*.

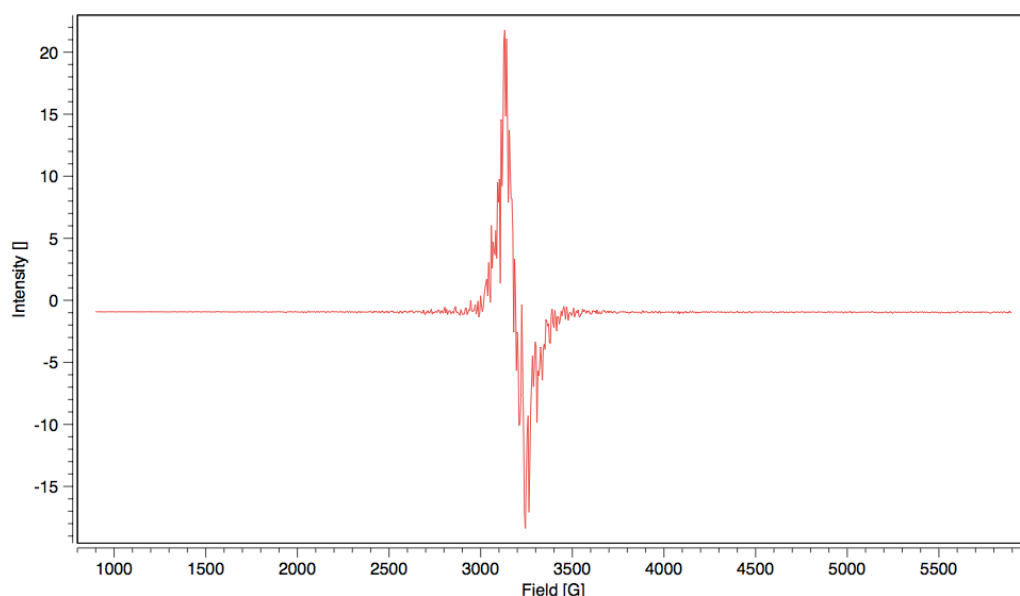
EPR Data



*EPR Spectrum of **1.2** with Simulated Spectrum. Frozen MeCN solution, 77 K*
(*g*-value: 2.089)



*EPR Spectrum of **1.2** with Simulated Spectrum. Single Crystals, 298 K*
(*g*-value: 2.082)



EPR Spectrum of **1.2**. Single Crystals, 77 K

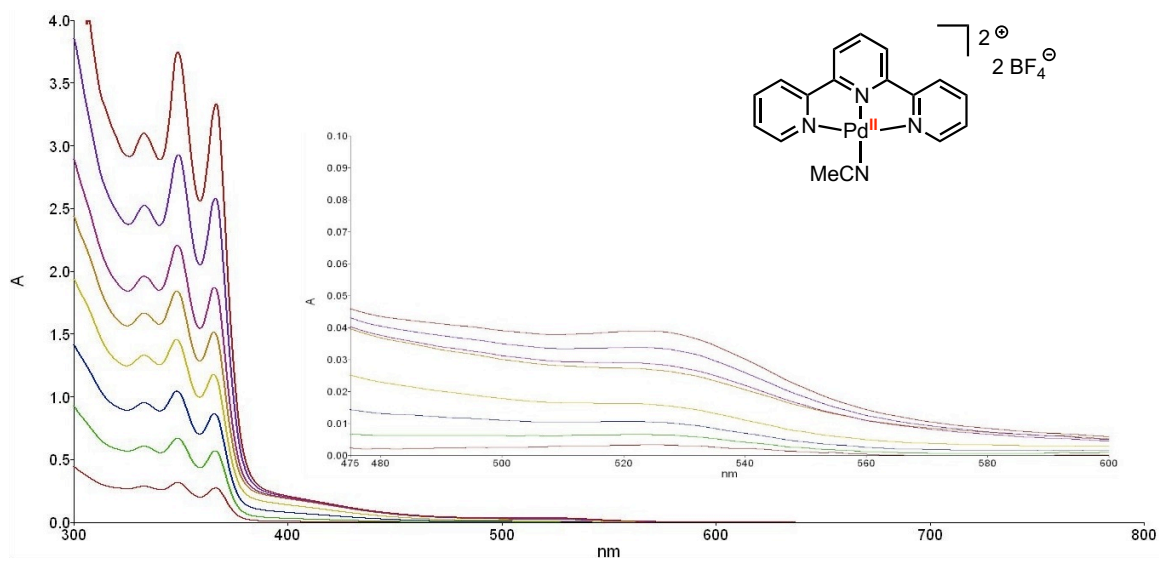
This spectrum is observed to overlay well with the frozen MeCN solution spectrum at 77 K (g -value: 2.089).

Discussion of EPR Data

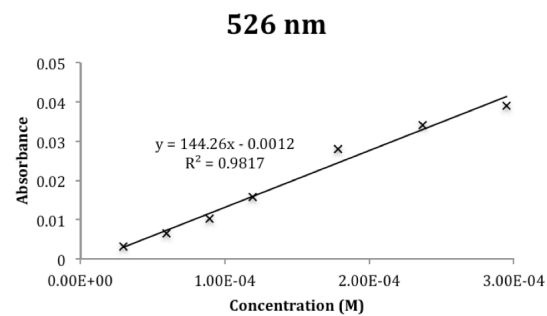
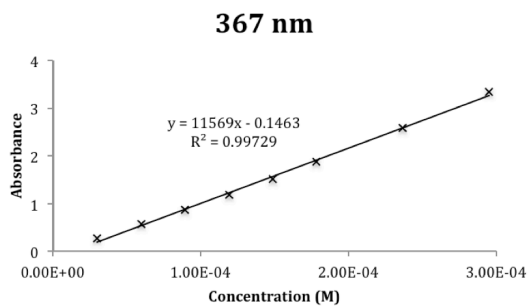
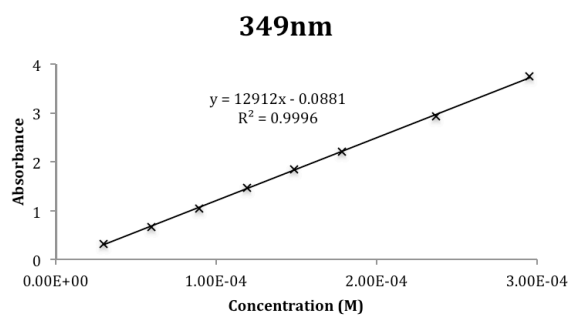
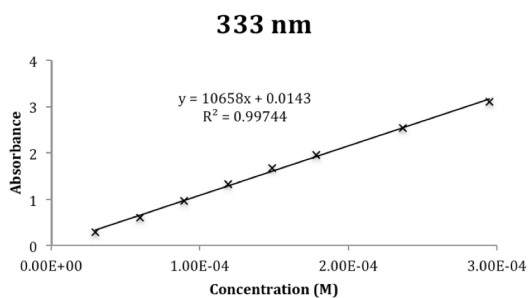
The solid- and solution-state EPR data for Pd(III) complex **1.2** display isotropic spectra at both 298 K and 77 K, with no observable spectral features due to hyperfine coupling or Jahn-Teller distortion (the fine features seen in the spectra at 77 K are due to vibrations caused by liquid nitrogen bubbling in the finger dewar used for data collection, and are not reproducible spectral features). We hypothesize that the lack of features observed in the EPR spectra may be due to a fluxional Jahn-Teller distortion at the temperatures at which the spectra were measured: fluxional Jahn-Teller distortion is well-precedented for cationic bis-terpyridyl transition metal complexes.¹²²

UV-vis/NIR Data

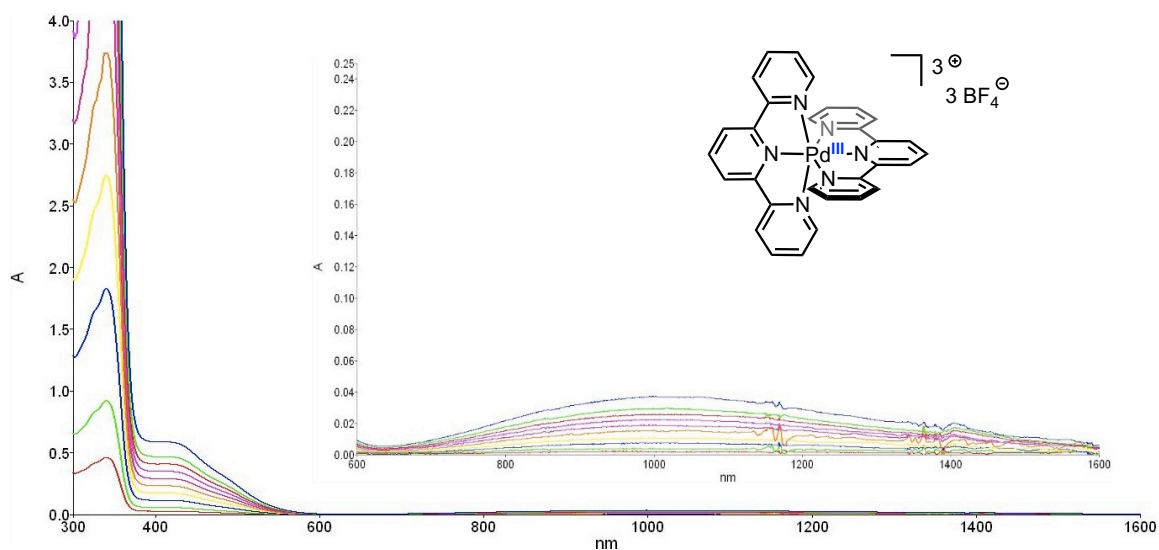
UV-vis Spectrum of 1.1 (DMF, 23 °C)



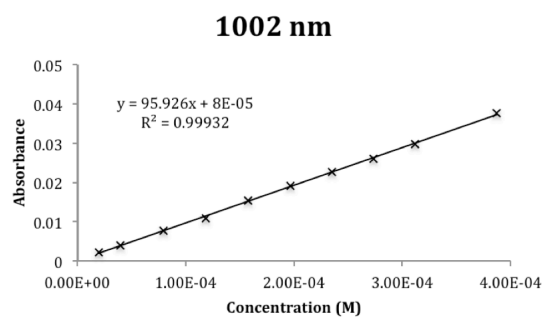
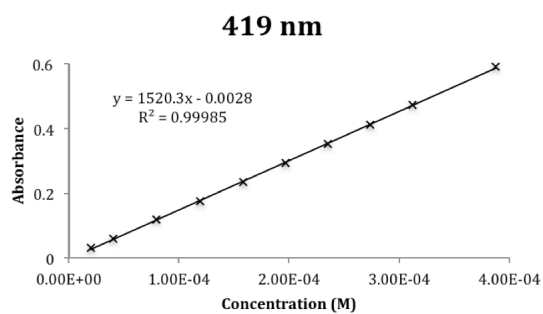
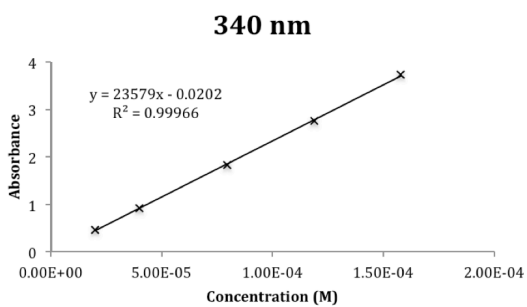
Molar Absorptivity Determinations:



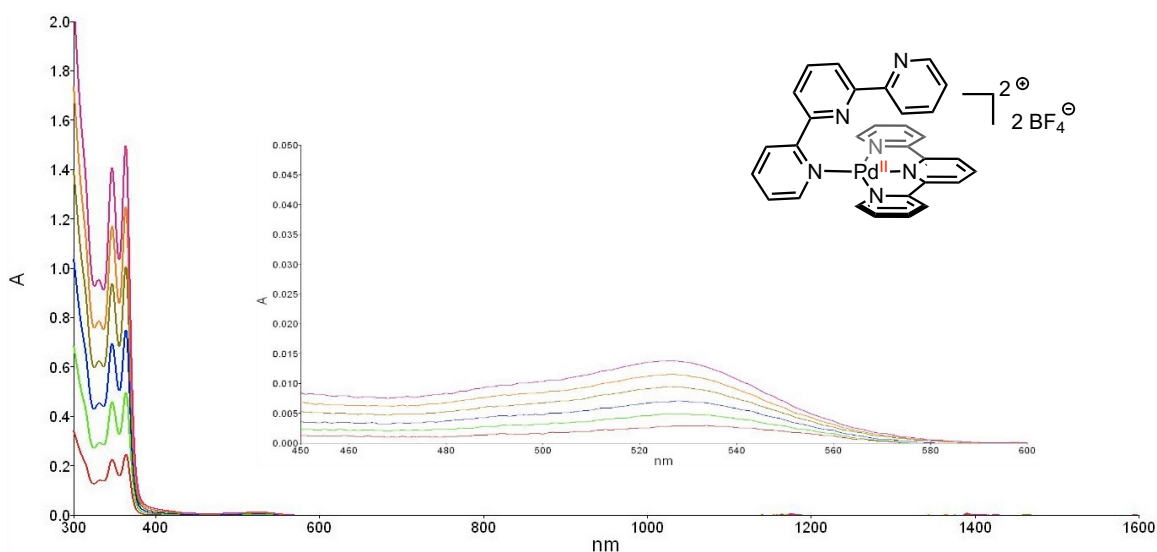
UV-vis/NIR Spectrum of 1.2 (MeCN, 23 °C)



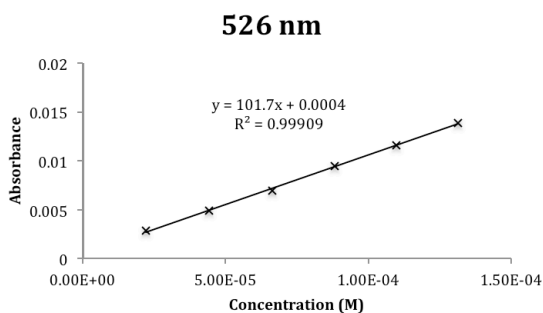
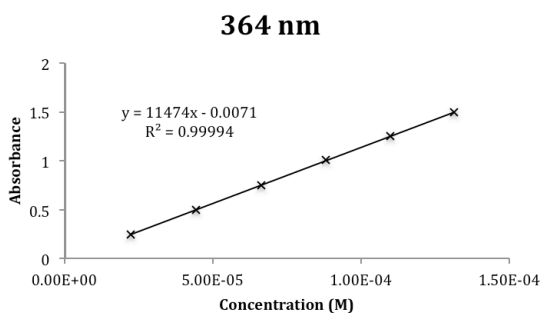
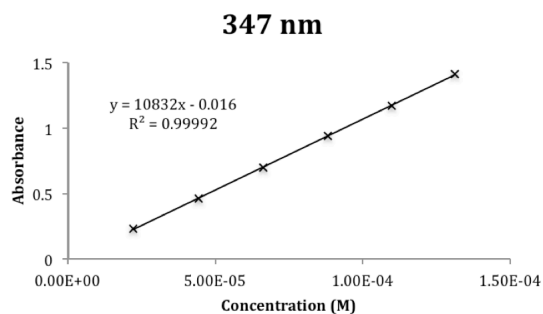
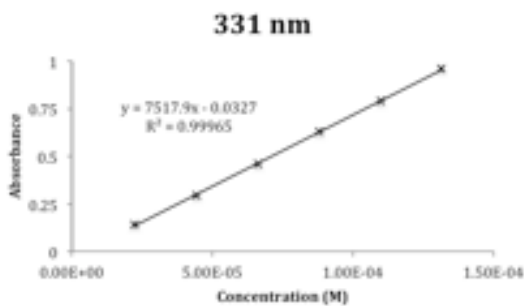
Molar Absorptivity Determinations:



UV-vis/NIR Spectrum of 3.2 (MeCN, 23 °C)



Molar Absorptivity Determinations:



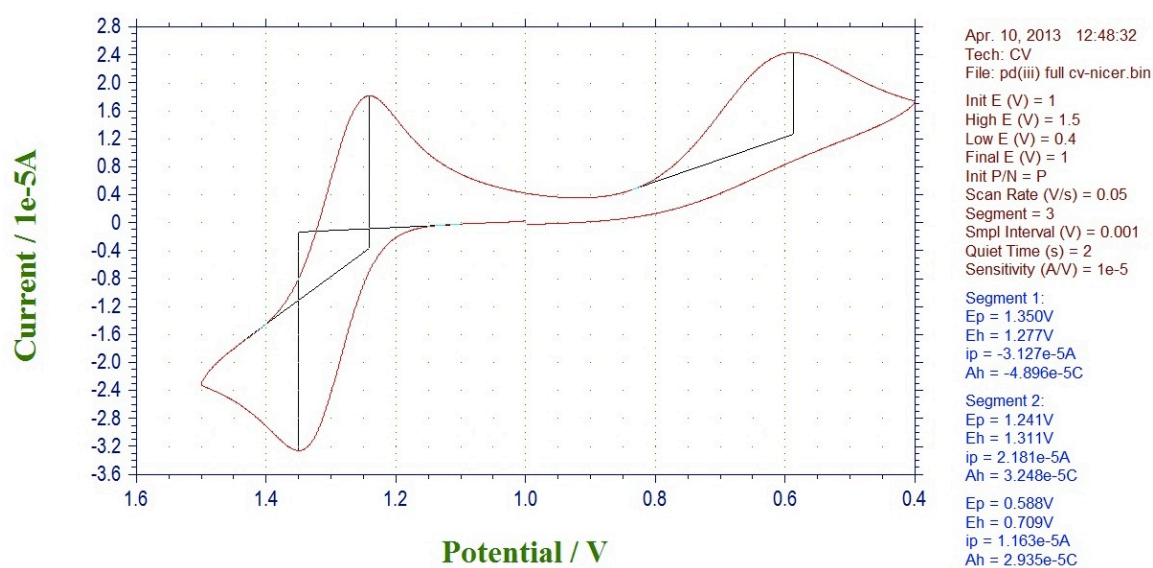
Electrochemical Data

General Methods

Cyclic Voltammetry (CV) was performed using approximately 2 mg/mL solutions of the

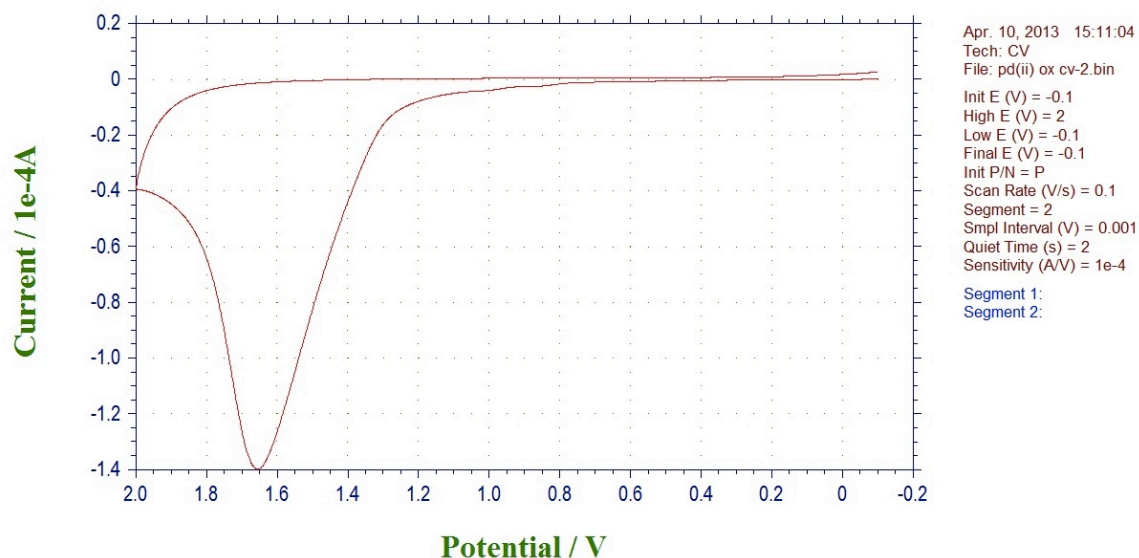
analyte in MeCN, with Bu_4NPF_6 (0.1 M) as the electrolyte. A glassy carbon working electrode was used, along with a Pt wire counter electrode and a non-aqueous Ag/Ag^+ reference electrode. CVs were obtained at a scan rate of 0.1 V/s or 0.05 V/s (indicated for each sample), and ferrocene was used as an external reference. All reported potentials are vs Fc/Fc^+ unless otherwise noted.

CV of $[(\text{terpy})_2\text{Pd}]/[\text{BF}_4]_3$ (1.2)



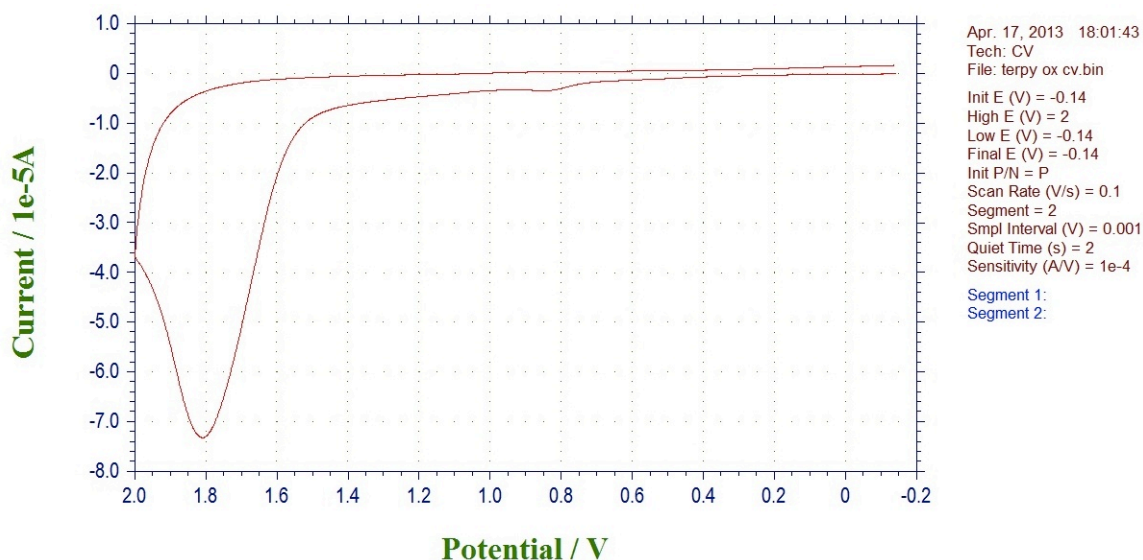
The reversible oxidation at 1.17 V (vs Fc/Fc^+) is assigned as the $\text{Pd(III)}/\text{Pd(IV)}$ redox couple while the irreversible reduction wave at 460 mV (vs. Fc/Fc^+) is assigned as the $\text{Pd(III)}/\text{Pd(II)}$ redox couple.

CV of [(terpy)Pd(MeCN)]/[BF₄]₂ (1.1) with added terpyridine



The only observed feature is an irreversible oxidation wave at 1.5 V (vs. Fc/Fc⁺).

CV of terpyridine



The only observed feature is an irreversible oxidation wave at 1.7 V (vs. Fc/Fc⁺).

Discussion of electrochemical data

The absence of any reversible oxidation waves for the mixture of [(terpy)Pd(MeCN)]²⁺ (**1.1**) and terpyridine, and the observation of an irreversible reduction wave at 460 mV for

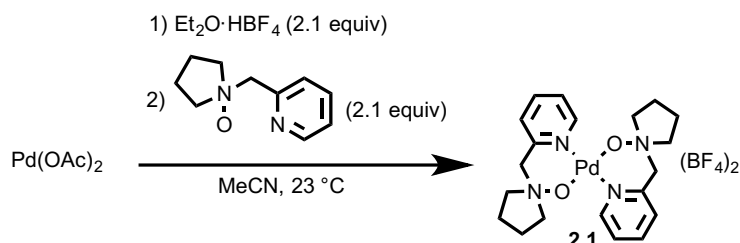
$[(\text{terpy})_2\text{Pd}]^{3+}$ (**1.2**) indicates that the oxidation of **1.1** to **1.2** in the presence of terpyridine and Selectfluor does not occur via an outer-sphere S.E.T. pathway.

Additionally, the Pd(III) complex **1.2** is observed to undergo a reversible one-electron oxidation to the Pd(IV) cation at a potential of 1.17 V. This potential is not accessible under the reaction conditions of the Pd-catalyzed fluorination, and therefore we believe that the intermediacy of Pd(IV) during catalysis is unlikely. It has been notoriously difficult to accurately measure or calculate the reduction potential of Selectfluor:^{90a} the reduction potential of Selectfluor has been measured at -40 mV vs SCE (-199 mV vs Fc/Fc^+),¹²³ which is in agreement with our experimental measurements, but this value is inconsistent with the observed chemical reactivity.^{90e} A better estimate has been provided by chemical means: Gilicinski *et al.* have observed that Selectfluor is capable of oxidizing bromide ion to elemental bromine (690 mV vs Fc/Fc^+), but not of oxidizing chloride ion to elemental chlorine (980 mV Fc/Fc^+).¹¹⁷ The inability to oxidize chloride ion provides an upper limit for the oxidation potential of Selectfluor at 980 mV, well below the observed Pd(III)/Pd(IV) redox couple at 1.17 V.

Experimental Procedures and Compound Characterization for Chapter 2¹²⁴

Synthesis and Characterization of Complex 1

Palladium complex 2.1



A flame-dried, 250 mL 2-neck flask under nitrogen was charged with $\text{Pd}(\text{OAc})_2$ (5.00 g, 22.3 mmol, 1.00 equiv), and the flask was evacuated and refilled with N_2 . Through a septum was

added dry acetonitrile (50 mL, Aldrich Sure/SealTM), followed by Et₂O·HBF₄ (6.4 mL, 47. mmol, 2.1 equiv). The resulting suspension was stirred at 23 °C for 30 min, after which 1-(pyridine-2-ylmethyl)pyrrolidine 1-oxide (8.334 g, 46.77 mmol, 2.10 equiv) was added as a solution in dry acetonitrile (40 mL, Aldrich Sure/SealTM). The resulting mixture was stirred for 1 hr, after which the reaction mixture was diluted with 100 mL acetonitrile to dissolve the precipitated product, and the solution was filtered through celite and then concentrated by rotary evaporation. The resulting brown solid was triturated with dichloromethane (40 mL) with sonication. The product was collected by filtration on a glass frit, then washed with dichloromethane (40 mL) followed by tetrahydrofuran (40 mL), then allowed to dry on the frit with applied suction to yield 10.61 g of a yellow powder (16.66 mmol, 75%).

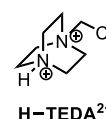
NMR Spectroscopy: ¹H NMR (600 MHz, DMSO, 23 °C, δ): 8.50 (dd, *J* = 5.8, 1.2 Hz, 2H), 8.30 (ddd, *J* = 7.7, 7.7, 1.5 Hz, 2H), 7.86 (ddd, *J* = 7.5, 5.8, 1.4 Hz, 2H), 7.79 (dd, *J* = 7.8, 1.2 Hz, 2H), 5.35 (s, 4H), 3.56–3.46 (m, 4H), 3.45–3.36 (m, 4H), 2.26–2.15 (m, 4H), 2.10–1.99 (m, 4H). ¹³C NMR (125 MHz, DMSO, 23 °C, δ): 149.2, 148.2, 142.0, 128.2, 126.5, 70.1, 67.2, 21.3.

Mass spectrometry: HRMS-FIA(*m/z*) calcd for C₂₀H₂₈N₄O₂Pd [M]²⁺, 231.0622; found, 231.0632.

Anal. Calcd for C₂₀H₂₈B₂F₈N₄O₂Pd: C, 37.74; H, 4.43; N, 8.80. Found: C, 37.83; H, 4.14; N, 9.04.

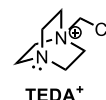
General considerations for aromatic C–H TEDAylation reactions

The Aryl–TEDA products are doubly cationic compounds, and similar cationic compounds are formed as byproducts of the reaction, including H–TEDA²⁺ and TEDA⁺.



Therefore, it is difficult to isolate the Aryl–TEDA products from the reaction mixture.

We have found that performing the reaction with an excess (at least five equivalents) of the arene substrate minimizes formation of H–TEDA²⁺ and TEDA⁺ byproducts. Upon



reaction completion, evaporation of the solvent, followed by trituration of the residue with CH_2Cl_2 /methanol mixtures to remove the excess arene, and the palladium and ruthenium catalysts, results in material that is sufficiently clean for characterization, albeit still contaminated to varying degrees with H-TEDA^{2+} and TEDA^+ . Therefore, we have performed the Ar-TEDA formation reactions twice for each of the Ar-TEDA products **2.2a-g**: once utilizing the arene as limiting reagent (with yield determined by NMR integration relative to an internal standard), and once with excess arene (for characterization purposes). For Ar-TEDA compounds synthesized through the use of excess arene, yields of Ar-TEDA, H-TEDA^{2+} , and TEDA^+ are calculated relative to Selectfluor, and were determined via NMR analysis of a known amount of the mixture by integrating against an internal standard.

The Ar-TEDA products may be isolated from H-TEDA^{2+} , and TEDA^+ by repeated recrystallization. The Ar-TEDA product derived from fluorenone (**2.2f**) was isolated in this way and characterized as a pure compound.

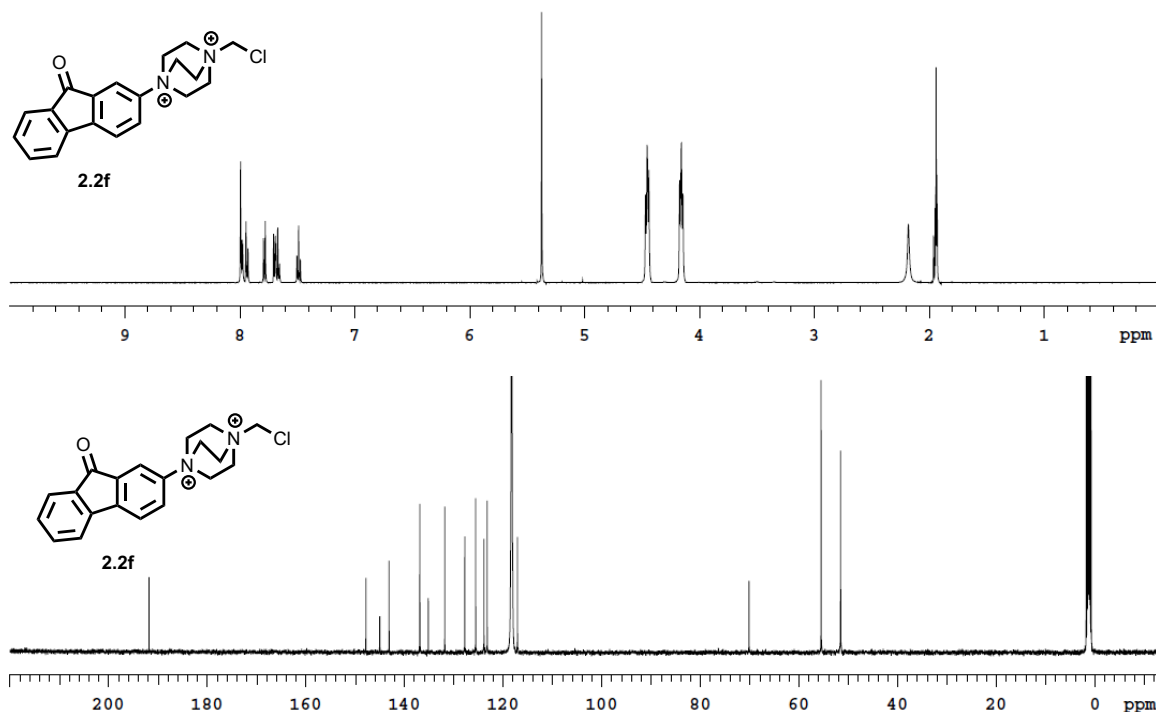
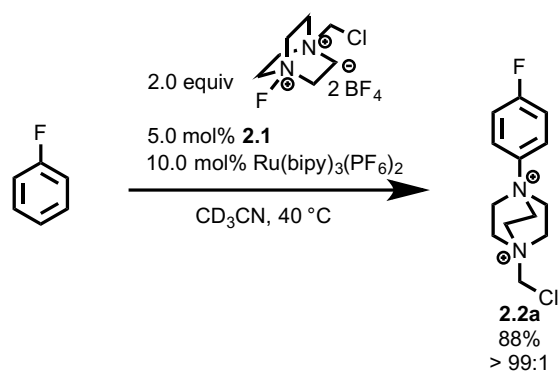


Figure 3.3. ^1H and ^{13}C NMR of pure Ar-TEDA **2.2f** (CD_3CN , 23 °C)

Procedure for aromatic C–H TEDAylation reactions (1 equiv arene)

1-(Chloromethyl)-4-(4-fluorophenyl)-1,4-diazabicyclo[2.2.2]octane²⁺ (2.2a)



A 4 mL vial was charged with Selectfluor (70.9 mg, 0.200 mmol, 2.00 equiv), **2.1** (3.2 mg, 5.0 μmol , 5.0 mol%), and $\text{Ru}(\text{bipy})_3(\text{PF}_6)_2$ (8.6 mg, 10 μmol , 10. mol%), and 0.50 mL CD_3CN , and finally fluorobenzene (9.4 μL , 0.10 mmol, 1.0 equiv). The vial was sealed and the mixture stirred at 40°C for 36 h. The reaction mixture was diluted with 0.25 mL CD_3CN and filtered through a 0.22 μm PVDF syringe filter, and an additional 0.25 mL CD_3CN was washed through the filter to elute any remaining soluble material. The solution was analyzed by ^{19}F NMR:

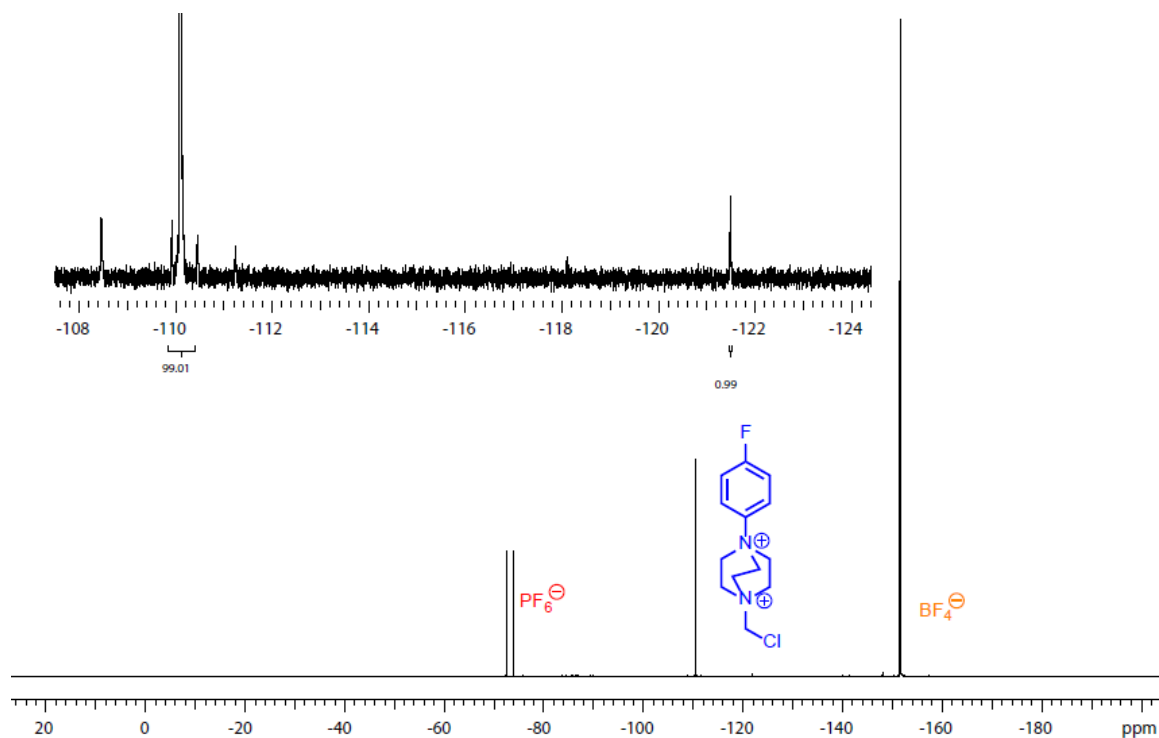


Figure 3.4. ^{19}F NMR evaluation of positional selectivity (CD_3CN , 23 °C)

Only one significant aryl fluoride peak was observed in ^{19}F NMR, corresponding to the title compound. After 24 scans with a relaxation delay of 20 s, another peak in the aromatic region was observed at -121.5 ppm, at a ratio of 0.99:99.1 relative to the peak corresponding to **2.2a**. The ratio between the Ar-F signal and the rms noise over a 100 Hz range was measured to be 1286 (command ‘dsnmax(100)’ in VNMR), implying that any other products have a maximum concentration of 0.08% of the title compound. Given that the next largest peak in the aromatic region had an intensity of below 1% of the signal of **2.2a**, and given the magnitude of the noise level, we conclude that the positional selectivity of the TEDAylation reaction of fluorobenzene is >99:1 in favor of *para* substitution.

The product mixture of the reaction to form **2.2a** was analyzed by ^{19}F NMR in several different solvents in order to rule out coincidental overlap with any peaks corresponding to constitutional isomers of **2.2a**. The analysis was carried out by evaporating the acetonitrile solvent from the reaction mixtures and dissolving the residue in 5:1 $\text{CD}_3\text{CN}:\text{C}_6\text{D}_6$, d_6 -DMSO,

and d_5 -pyridine, respectively. In each of these cases, only one aryl fluoride signal was observed by ^{19}F NMR:

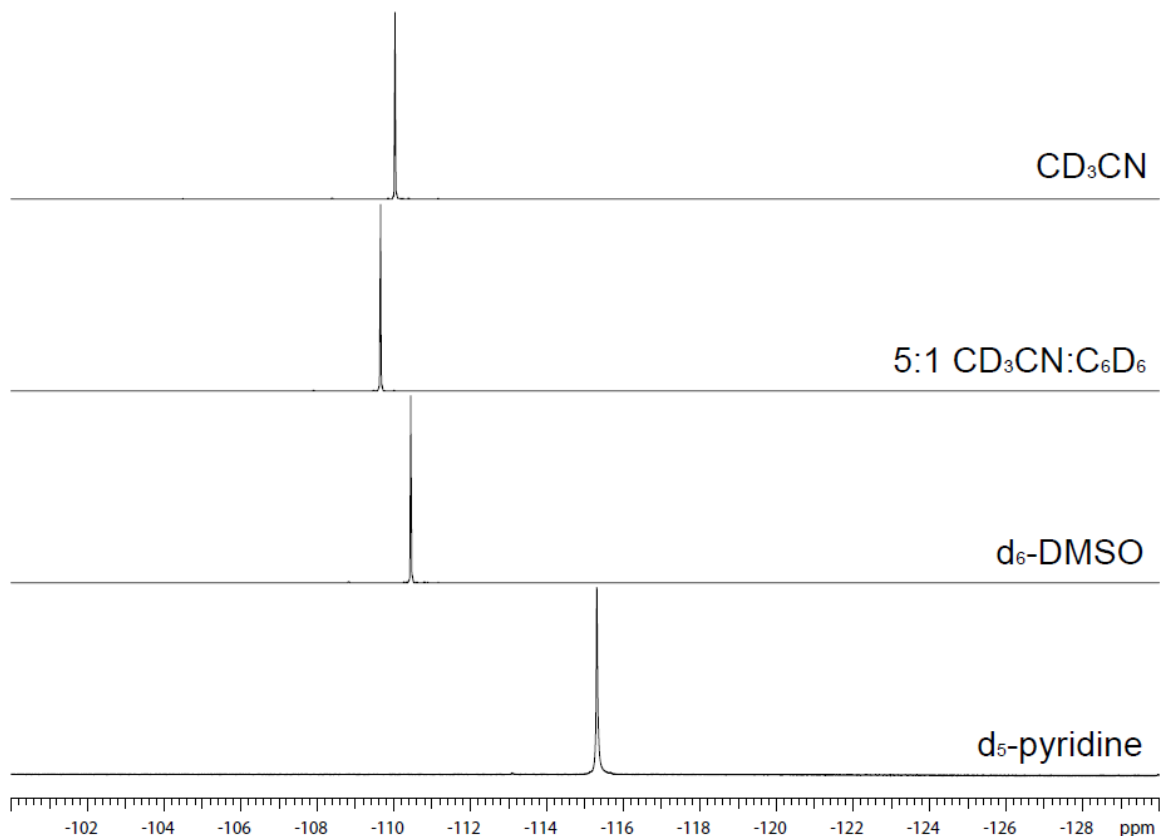
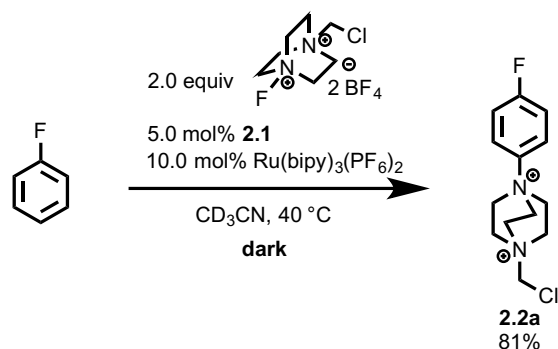


Figure 3.5. ^{19}F NMR evaluation of positional selectivity across solvents (23 °C)

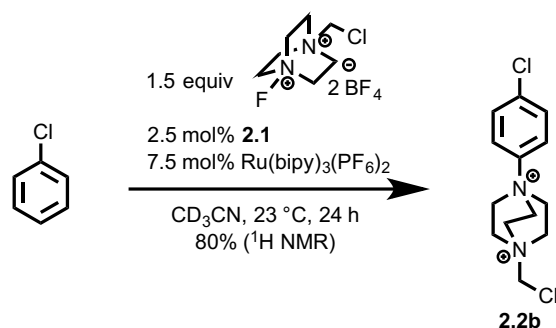
Formation of 2.2a in the absence of light



A 4 mL vial, completely covered with aluminum foil, was charged with Selectfluor (70.9 mg, 0.200 mmol, 2.00 equiv), **2.1** (3.2 mg, 5.0 μmol , 5.0 mol%), and $\text{Ru}(\text{bipy})_3(\text{PF}_6)_2$ (8.6 mg, 10 μmol , 10. mol%), and 0.50 mL CD_3CN , and finally fluorobenzene (9.4 μL , 0.10 mmol, 1.0

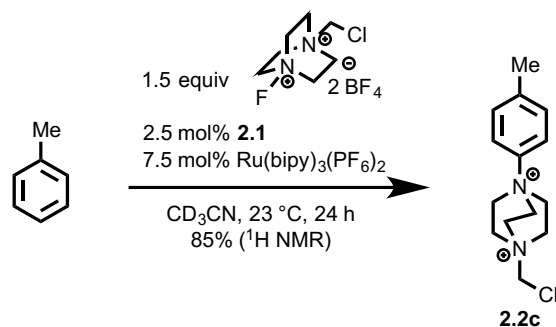
equiv). The vial was sealed and the mixture stirred in the dark at 40 °C for 24 h, after which 2.0 μL of 3-fluoronitrobenzene was added as an internal standard. The reaction mixture was diluted with 0.50 mL CD_3CN , and passed through a 0.22 μm PVDF syringe filter. The resulting solution was analyzed by ^{19}F NMR, and comparison of the Ar–F peak of the product (–110 ppm) with that of the internal standard (–112 ppm) revealed a yield of 81% of **2.2a**.

1-(Chloromethyl)-4-(4-chlorophenyl)-1,4-diazabicyclo[2.2.2]octane²⁺ (**2.2b**)



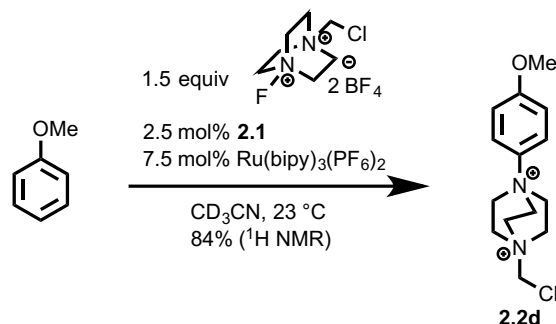
Palladium complex **2.1** (10.3 mg, 16.2 μmol) and $\text{Ru}(\text{bipy})_3(\text{PF}_6)_2$ (41.9 mg, 48.8 μmol) were dissolved in d_3 -acetonitrile (3.25 mL) to afford a stock solution. A 4 mL vial was charged with Selectfluor (52.2 mg, 0.147 mmol, 1.50 equiv). The stock solution (491. μL) containing **2.1** (2.45 μmol , 2.50 mol%) and $\text{Ru}(\text{bipy})_3(\text{PF}_6)_2$ (7.37 μmol , 7.50 mol%) was added, followed by chlorobenzene (10.0 μL 98.2 μmol , 1.00 equiv, $c = 0.20\text{ M}$) via syringe. After stirring at 23 °C for 24 h, the reaction mixture was diluted with d_3 -acetonitrile (3.0 mL). The yield of **2.2b** was determined via ^1H NMR spectroscopy using ethyl acetate (5.0 μL , 51. μmol) as an internal standard. Comparison of the integral of the peak of **2.2b** at 7.78–7.81 ppm (aromatic C–H, 2H) with that of the peak of ethyl acetate at 1.20 ppm (CH_3 , 3H) revealed an 80% yield of **2.2b**.

1-(Chloromethyl)-4-(4-methylphenyl)-1,4-diazabicyclo[2.2.2]octane²⁺ (2.2c)



Palladium complex **2.1** (10.3 mg, 16.2 μ mol) and Ru(bipy)₃(PF₆)₂ (41.9 mg, 48.8 μ mol) were dissolved in *d*₃-acetonitrile (3.25 mL) to afford a stock solution. A 4 mL vial was charged with Selectfluor (49.9 mg, 0.141 mmol, 1.50 equiv). The stock solution (469. μ L) containing **2.1** (2.34 μ mol, 2.50 mol%) and Ru(bipy)₃(PF₆)₂ (7.04 μ mol, 7.50 mol%) was added, followed by toluene (10.0 μ L, 93.9 μ mol, 1.00 equiv, *c* = 0.20 M) via syringe. After stirring at 23 °C for 24 h, the reaction mixture was diluted with *d*₃-acetonitrile (3.0 mL). The yield of **2.2c** was determined via ¹H NMR spectroscopy using ethyl acetate (5.0 μ L, 51. μ mol) as an internal standard. Comparison of the integral of the peak of **2.2c** at 7.67–7.65 ppm (aromatic C–H, 2H) with that of the peak of ethyl acetate at 1.20 ppm (CH₃, 3H) revealed an 85% yield of **2.2c**.

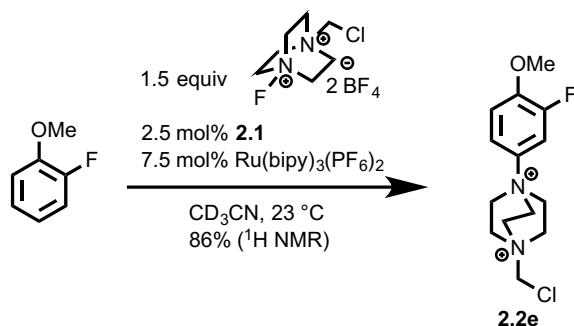
1-(Chloromethyl)-4-(4-methoxyphenyl)-1,4-diazabicyclo[2.2.2]octane²⁺ (2.2d)



Palladium complex **2.1** (10.3 mg, 16.2 μ mol) and Ru(bipy)₃(PF₆)₂ (41.9 mg, 48.8 μ mol) were dissolved in *d*₃-acetonitrile (3.25 mL) to afford a stock solution. A 4 mL vial was charged

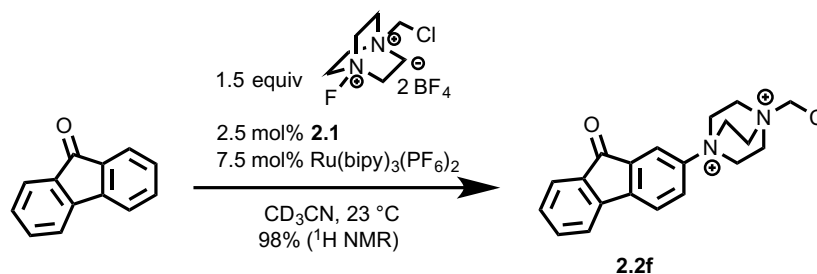
with Selectfluor (48.9 mg, 0.138 mmol, 1.50 equiv). The stock solution (460. μL , $c = 0.200$ M) containing **2.1** (2.34 μmol , 2.50 mol%) and $\text{Ru}(\text{bipy})_3(\text{PF}_6)_2$ (7.04 μmol , 7.50 mol%) was added, followed by anisole (10.0 μL , 92.0 μmol , 1.00 equiv) via syringe. After stirring at 23 $^\circ\text{C}$ for 24 h, the reaction mixture was diluted with d_3 -acetonitrile (3.0 mL). The yield of **2.2d** was determined via ^1H NMR spectroscopy using ethyl acetate (5.0 μL , 51. μmol) as an internal standard. Comparison of the integral of the peak of **2.2d** at 7.72–7.69 ppm (aromatic C–H, 2H) with that of the peak of ethyl acetate at 1.20 ppm (CH_3 , 3H) revealed an 84% yield of **2d**.

1-(Chloromethyl)-4-(3-fluoro-4-methoxyphenyl)-1,4-diazabicyclo[2.2.2]octane²⁺ (2.2e)



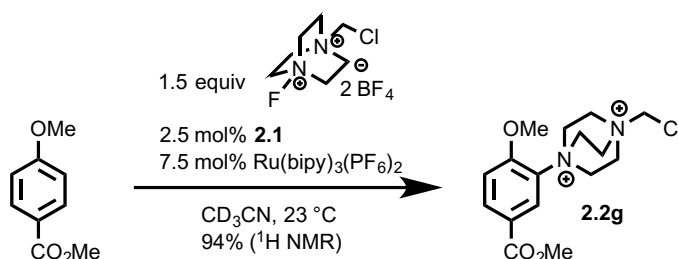
Palladium complex **2.1** (11.3 mg, 17.8 μmol) and $\text{Ru}(\text{bipy})_3(\text{PF}_6)_2$ (45.9 mg, 53.4 μmol) were dissolved in d_3 -acetonitrile (3.56 mL) to afford a stock solution. A 4 mL vial was charged with Selectfluor (47.3 mg, 0.134 mmol, 1.50 equiv). The stock solution (445. μL , $c = 0.200$ M) containing **2.1** (2.23 μmol , 2.50 mol%) and $\text{Ru}(\text{bipy})_3(\text{PF}_6)_2$ (6.68 μmol , 7.50 mol%) was added, followed by 2-fluoroanisole (10.0 μL , 89.0 μmol , 1.00 equiv) via syringe. After stirring at 23 $^\circ\text{C}$ for 24 h, the reaction mixture was diluted with d_3 -acetonitrile (2.5 mL). The yield of **2.2e** was determined via ^1H NMR spectroscopy using ethyl acetate (5.0 μL , 51. μmol) as an internal standard. Comparison of the integral of the peak of **2.2e** at 7.34 ppm (aromatic C–H, 1H) with that of the peak of ethyl acetate at 1.20 ppm (CH_3 , 3H) revealed an 86% yield of **2.2e**.

1-(Chloromethyl)-4-(fluoren-9-yl)-1,4-diazabicyclo[2.2.2]octane²⁺ (2.2f**)**



Palladium complex **2.1** (11.3 mg, 17.8 μmol) and Ru(bipy)₃(PF₆)₂ (45.9 mg, 53.4 μmol) were dissolved in *d*₃-acetonitrile (3.56 mL) to afford a stock solution. A 4 mL vial was charged with Selectfluor (47.3 mg, 0.134 mmol, 1.50 equiv) and fluorenone (16.0 mg, 89.0 μmol, 1.00 equiv). The stock solution (445. μL, *c* = 0.200 M) containing **2.1** (2.23 μmol, 2.50 mol%) and Ru(bipy)₃(PF₆)₂ (6.68 μmol, 7.50 mol%) was added via syringe. After stirring at 23 °C for 24 h, the reaction mixture was diluted with *d*₃-acetonitrile (2.0 mL). The yield of **2.2f** was determined via ¹H NMR spectroscopy using ethyl acetate (5.0 μL, 51. μmol) as an internal standard. Comparison of the integral of the peak of **2.2f** at 7.94–7.93 ppm (aromatic C–H, 1H) with that of the peak of ethyl acetate at 1.20 ppm (CH₃, 3H) revealed an 98% yield of **2.2f**.

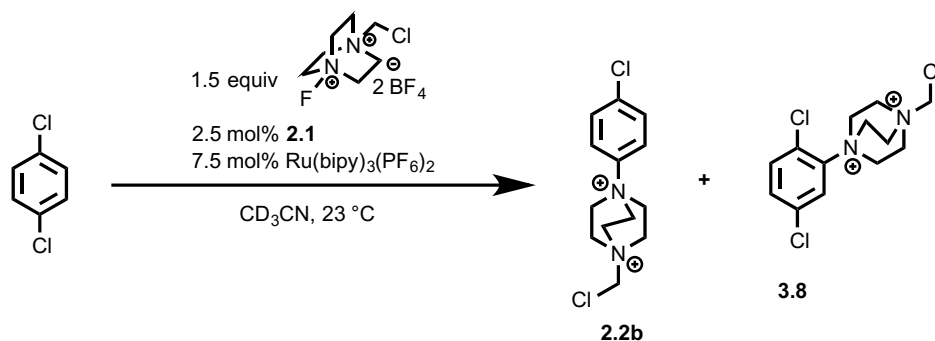
1-(Chloromethyl)-4-(2-methoxy-5-(methoxycarbonyl)phenyl)-1,4-diazabicyclo[2.2.2]octane²⁺ (2.2g**)**



Palladium complex **2.1** (10.3 mg, 16.2 μmol) and Ru(bipy)₃(PF₆)₂ (41.9 mg, 48.8 μmol) were dissolved in *d*₃-acetonitrile (3.25 mL) to afford a stock solution. A 4 mL vial was charged with Selectfluor (53.1 mg, 0.150 mmol, 1.50 equiv) and methyl 4-methoxybenzoate (16.6 mg,

100. μmol , 1.00 equiv). The stock solution (500. μL , $c = 0.200\text{ M}$) containing **2.1** (2.50 μmol , 2.50 mol%) and $\text{Ru}(\text{bipy})_3(\text{PF}_6)_2$ (7.50 μmol , 7.50 mol%) was added via syringe. After stirring at 23 $^\circ\text{C}$ for 24 h, the reaction mixture was diluted with d_3 -acetonitrile (3.0 mL). The yield of **2.2g** was determined via ^1H NMR spectroscopy using ethyl acetate (5.0 μL , 51. μmol) as an internal standard. Comparison of the integral of the peak of **2.2g** at 7.46 ppm (aromatic C–H, 1H) with that of the peak of ethyl acetate at 1.20 ppm (CH_3 , 3H) revealed a 94% yield of **2.2g**.

1-(Chloromethyl)-4-(4-chlorophenyl)-1,4-diazabicyclo[2.2.2]octane²⁺ (**2.2b**) from 1,4-dichlorobenzene



Palladium complex **2.1** (11.3 mg, 17.8 μmol) and $\text{Ru}(\text{bipy})_3(\text{PF}_6)_2$ (45.9 mg, 53.4 μmol) were dissolved in d_3 -acetonitrile (3.56 mL) to afford a stock solution. A 4 mL vial was charged with Selectfluor (47.3 mg, 0.134 mmol, 1.50 equiv) and 1,4-dichlorobenzene (13.1 mg, 89.0 μmol , 1.00 equiv). The stock solution (445 μL , $c = 0.200\text{ M}$) containing **2.1** (2.23 μmol , 2.50 mol%) and $\text{Ru}(\text{bipy})_3(\text{PF}_6)_2$ (6.68 μmol , 7.50 mol%) was added via syringe. After stirring at 23 $^\circ\text{C}$ for 24 h, the reaction mixture was diluted with d_3 -acetonitrile (2.0 mL). The yield of **2.2b** was determined via ^1H NMR spectroscopy using ethyl acetate (5.0 μL , 51. μmol) as an internal standard. Comparison of the integral of the peak of **2.2b** at 7.74–7.72 ppm (aromatic C–H, 2H) with that of the peak of ethyl acetate at 1.20 ppm (CH_3 , 3H) revealed an 48% yield of **2.2b**.

Another compound, consistent with structure **3.8**, was observed in 11% yield:

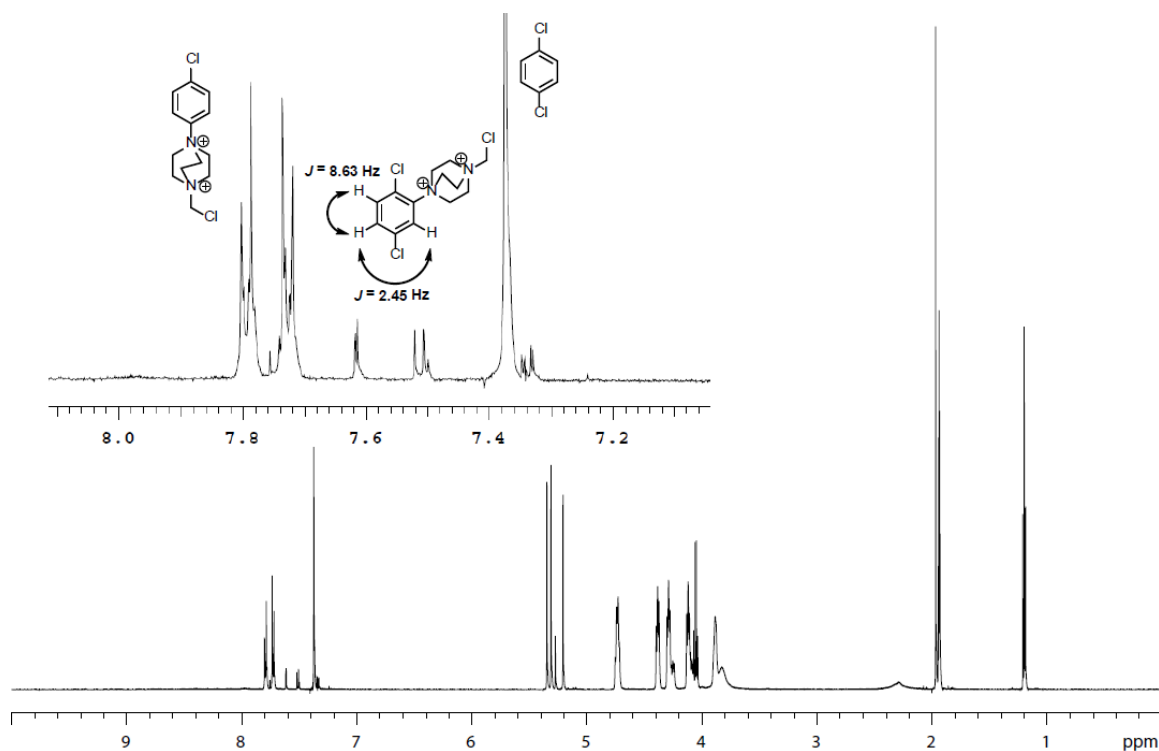
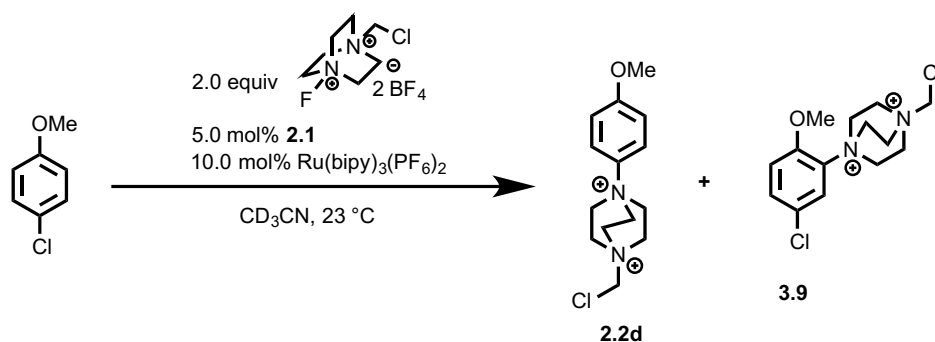


Figure 3.6. ^1H NMR of product mixture of TEDAylation of 1,4-dichlorobenzene (CD_3CN , 23 $^\circ\text{C}$)

1-(Chloromethyl)-4-(4-methoxyphenyl)-1,4-diazabicyclo[2.2.2]octane $^{2+}$ (**2.2d**) from 4-chloroanisole

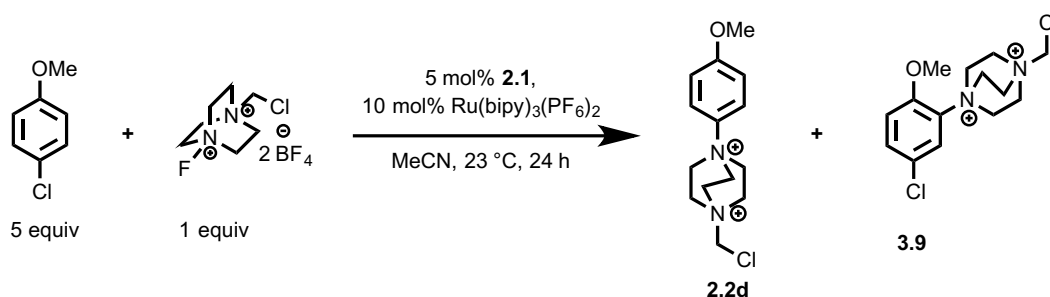


A stock solution was prepared, containing **2.1** (11.4 mg, 15.0 μmol) and $\text{Ru}(\text{bipy})_3(\text{PF}_6)_2$ (25.8 mg, 30.0 μmol) were dissolved in d_3 -acetonitrile (1.50 mL) to afford a stock solution. A 4 mL vial was charged with Selectfluor (35.4 mg, 0.100 mmol, 2.0 equiv) and 4-chloroanisole (6.1 μL , 0.050 mmol, 1.0 equiv). The stock solution (250 μL , $c = 0.20$ M)

containing **2.1** (2.5 μmol , 5.0 mol%) and $\text{Ru}(\text{bipy})_3(\text{PF}_6)_2$ (5.00 μmol , 10.0 mol%) was added via syringe. After stirring at 23 °C for 48 h, the reaction mixture was diluted with d_3 -acetonitrile (0.50 mL).

The yield of **2.2d** was determined via ^1H NMR spectroscopy using ethyl acetate (5.0 μL , 51. μmol) as an internal standard. Comparison of the integral of the peak of **2.2d** at 7.21–7.17 ppm (aromatic C–H, 2H) with that of the peak of ethyl acetate at 1.20 ppm (CH_3 , 3H) revealed an 26% yield of **2.2d**.

The above reaction was repeated with 5 equivalents of 4-chloroanisole in order to isolate the Ar–TEDA products from other products.



To a 20 mL vial were weighed **2.1** (31.8 mg, 50.0 μmol , 5.00 mol%), $\text{Ru}(\text{bipy})_3(\text{PF}_6)_2$ (86.0 mg, 0.100 mmol, 10.0 mol%), and Selectfluor (354. mg, 1.00 mmol, 1.00 equiv).

Acetonitrile was added (5.0 mL, $c = 0.20\text{ M}$), followed by 4-chloroanisole (612. μL , 5.00 mmol, 5.00 equiv). The mixture was stirred for 24 hours at room temperature, after which the mixture was diluted with 10 mL acetonitrile, then filtered through celite. The filtrate was concentrated, and the residue was triturated with 20 mL of 9:1 dichloromethane:methanol. The solid was collected by filtration, then washed with 10 mL 9:1 dichloromethane:methanol, then dichloromethane ($3 \times 10\text{ mL}$). The solid was dried in vacuo to yield 316. mg of a tan solid. ^1H NMR analysis revealed **2.2d** as the dominant Ar–TEDA product, along with ca. 29% of **3.9**:

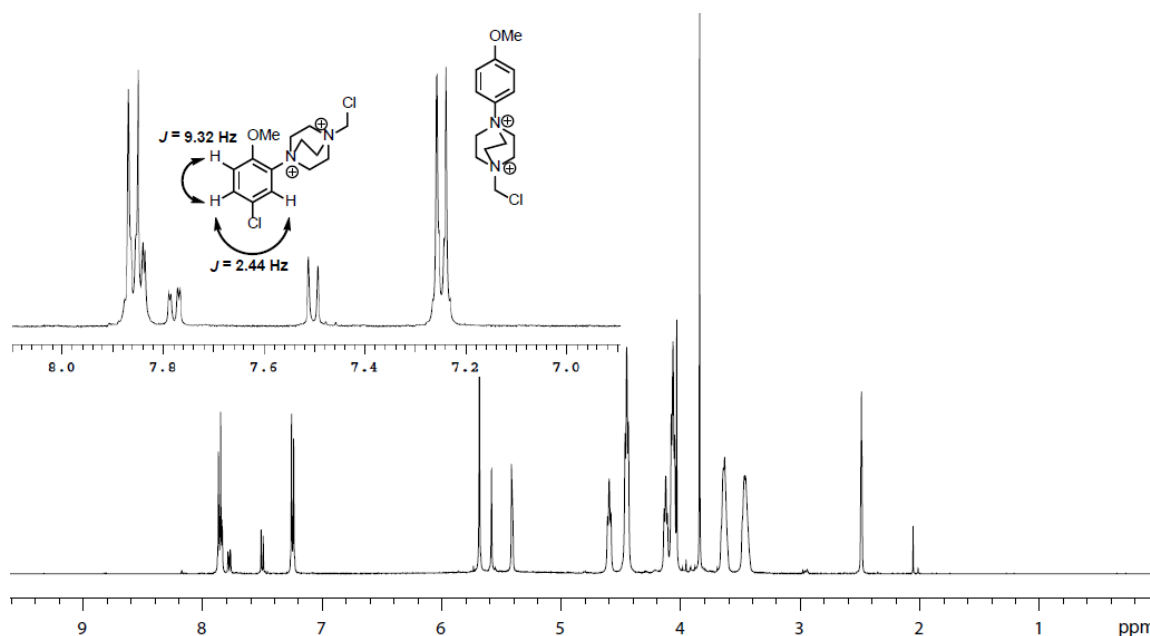
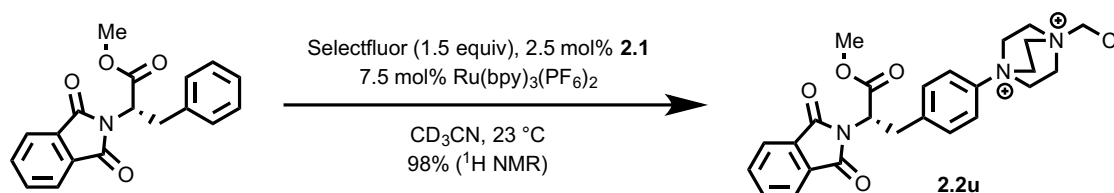


Figure 3.7. ^1H NMR spectrum of TEDAylation reaction mixture of 4-chloroanisole (CD_3CN , 23 $^\circ\text{C}$)

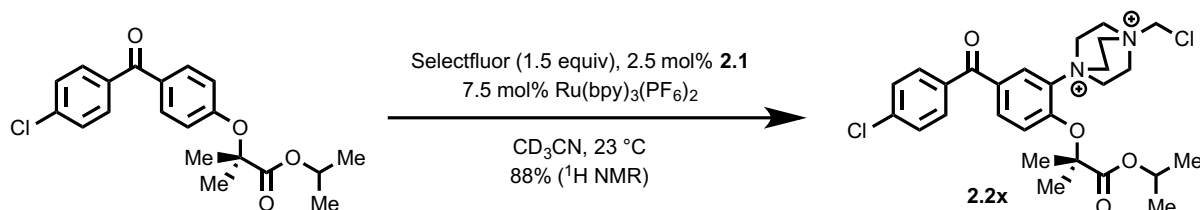
(*S*)-1-(Chloromethyl)-4-(4-(2-(1,3-dioxoisindolin-2-yl)-3-methoxy-3-oxopropyl)phenyl)-1,4-diazabicyclo[2.2.2]octane-1,4-diium (2.2u**)¹²⁵**



Palladium complex **2.1** (3.5 mg, 5.5 μmol) and $\text{Ru}(\text{bipy})_3(\text{PF}_6)_2$ (14.2 mg, 16.5 μmol) were dissolved in d_3 -acetonitrile (1.10 mL) to afford a stock solution. A 4 mL vial was charged with Selectfluor (53.1 mg, 0.150 mmol, 1.50 equiv) and methyl (*S*)-2-(1,3-dioxoisindolin-2-yl)-3-phenylpropanoate (30.9 mg, 0.100 mmol, 1.00 equiv). The stock solution (1.0 mL, $c = 0.20$ M) containing **2.1** (2.5 μmol , 2.5 mol%) and $\text{Ru}(\text{bipy})_3(\text{PF}_6)_2$ (7.50 μmol , 7.50 mol%) was added via syringe. After stirring at 23 $^\circ\text{C}$ for 24 h, the reaction mixture was diluted with d_3 -acetonitrile (2.0 mL). The yield of **2.2u** was determined via ^1H NMR spectroscopy using *N,N*-dimethylformamide (5.0 μL , 64. μmol) as an internal standard. Comparison of the integral of the peak of **2.2u** at 4.28–4.30 ppm (alkyl C–H, 6H) with that of the peak of *N,N*-

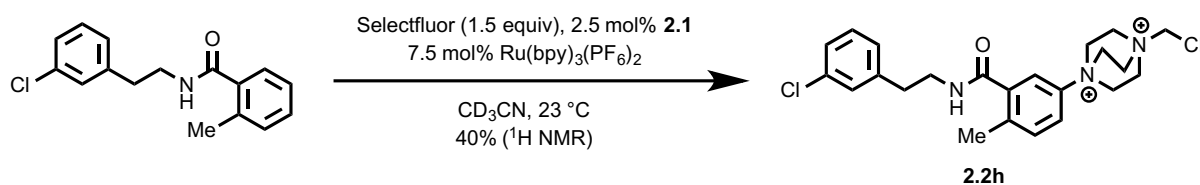
dimethylformamide at 2.89 ppm (CH₃, 3H) revealed an 98% yield of **2.2u**.

1-(5-(4-Chlorobenzoyl)-2-((1-isopropoxy-2-methyl-1-oxopropan-2-yl)oxy)phenyl)-4-(chloromethyl)-1,4-diazabicyclo[2.2.2]octane-1,4-diium (2.2x)



Palladium complex **2.1** (3.5 mg, 5.5 μmol) and Ru(bipy)₃(PF₆)₂ (14.2 mg, 16.5 μmol) were dissolved in *d*₃-acetonitrile (1.10 mL) to afford a stock solution. A 4 mL vial was charged with Selectfluor (53.1 mg, 0.150 mmol, 1.50 equiv) and fenofibrate (36.1 mg, 0.100 mmol, 1.00 equiv). The stock solution (1.0 mL, *c* = 0.20 M) containing **2.1** (2.5 μmol, 2.5 mol%) and Ru(bipy)₃(PF₆)₂ (7.50 μmol, 7.50 mol%) was added via syringe. After stirring at 23 °C for 24 h, the reaction mixture was diluted with *d*₃-acetonitrile (2.0 mL). The yield of **2.2x** was determined via ¹H NMR spectroscopy using *N,N*-dimethylformamide (5.0 μL, 64. μmol) as an internal standard. Comparison of the integral of the peak of **2.2x** at 4.61–4.64 ppm (alkyl C–H, 6H) with that of the peak of *N,N*-dimethylformamide at 2.89 ppm (CH₃, 3H) revealed an 88% yield of **2.2x**.

1-(Chloromethyl)-4-(3-((3-chlorophenethyl)carbamoyl)-4-methylphenyl)-1,4-diazabicyclo[2.2.2]octane-1,4-diium (2.2h)

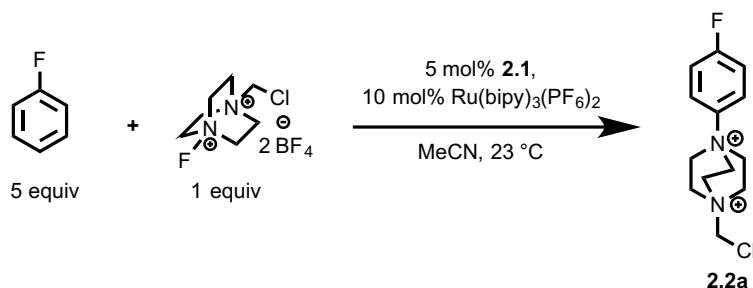


Palladium complex **2.1** (7.2 mg, 11. μmol) and Ru(bipy)₃(PF₆)₂ (29.0 mg, 33.8 μmol) were

dissolved in d_3 -acetonitrile (2.25 mL) to afford a stock solution. A 4 mL vial was charged with Selectfluor (26.6 mg, 75.0 μmol , 1.50 equiv) and *N*-(3-chlorophenethyl)-2-methylbenzamide (13.7 mg, 50.0 μmol , 1.00 equiv). The stock solution (0.25 mL, $c = 0.20$ M) containing **2.1** (1.2 μmol , 2.5 mol%) and $\text{Ru}(\text{bipy})_3(\text{PF}_6)_2$ (3.75 μmol , 7.50 mol%) was added via syringe. After stirring at 23 °C for 24 h, the reaction mixture was diluted with d_3 -acetonitrile (2.0 mL). The yield of **2.2h** was determined via ^1H NMR spectroscopy using *N,N*-dimethylformamide (2.0 μL , 26. μmol) as an internal standard. Comparison of the integral of the peak of **2.2h** at 7.66 ppm (aromatic C–H, 1H) with that of the peak of *N,N*-dimethylformamide at 2.89 ppm (CH, 1H) revealed an 40% yield of **2.2h**.

Procedure for aromatic C–H TEDAylation reactions (excess arene)

1-(Chloromethyl)-4-(4-fluorophenyl)-1,4-diazabicyclo[2.2.2]octane²⁺ (2.2a)



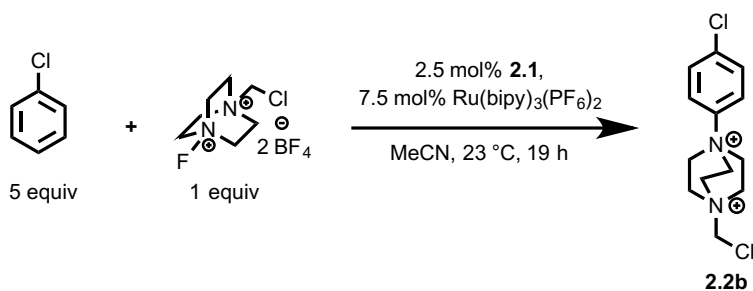
To a 20 mL vial were added palladium complex **2.1** (31.8 mg, 50.0 μmol , 5.00 mol%), $\text{Ru}(\text{bipy})_3(\text{PF}_6)_2$ (86.0 mg, 100. μmol , 10.0 mol%), Selectfluor (354. mg, 1.00 mmol, 1.00 equiv), and fluorobenzene (0.530 mL, 5.00 mmol, 5.00 equiv), and acetonitrile (2.5 mL, $c = 0.20$ M). The reaction mixture was stirred at 40 °C for 48 h. The reaction mixture was diluted with acetonitrile, filtered through celite, and the filtrate was concentrated *in vacuo*. The residue was triturated with 20 mL methanol:dichloromethane. The solid was collected by filtration on a glass frit, washed with 10 mL 1:9 methanol:dichloromethane, followed by 3 \times 10 mL dichloromethane, then dried *in vacuo* to afford 341. mg of a tan powder. For yield determination, an NMR sample in d_3 -acetonitrile was prepared containing 10.0 mg of the

product mixture and 5.0 μL of ethyl acetate (51. μmol) as internal standard. Comparison of the integral of the peak of **2.2a** at 4.45–4.37 ppm ($3 \times \text{CH}_2$, 6H) with that of the peak of ethyl acetate at 1.20 ppm (CH_3 , 3H) revealed the bulk mixture to contain 0.60 mmol of Ar–TEDA (60% yield). Also present was 0.18 mmol H–TEDA²⁺ (18%), measured by integration of the peak at 3.85–3.81 ppm ($3 \times \text{CH}_2$, 6H).

NMR Spectroscopy: ¹H NMR (500 MHz, CD₃CN, 23 °C, δ): 7.91–7.84 (m, 2H), 7.49–7.42 (m, 2H), 5.36 (s, 2H), 4.45–4.37 (m, 6H), 4.18–4.11 (m, 6H). ¹³C NMR (125 MHz, CD₃CN, 23 °C, δ): 163.4 (d, $J = 252.4$ Hz), 140.7 (s), 123.8 (d, $J = 9.6$ Hz), 118.9 (d, $J = 24.0$ Hz), 70.1 (s), 55.6 (s), 51.6 (s). ¹⁹F NMR (470 MHz, CD₃CN, 23 °C, δ): –110.0.

Mass spectrometry: HRMS-FIA(m/z) calcd for C₁₃H₁₇ClFN₂ [M–H]⁺, 255.1059; found, 255.1061.

1-(Chloromethyl)-4-(4-chlorophenyl)-1,4-diazabicyclo[2.2.2]octane²⁺ (**2.2b**)



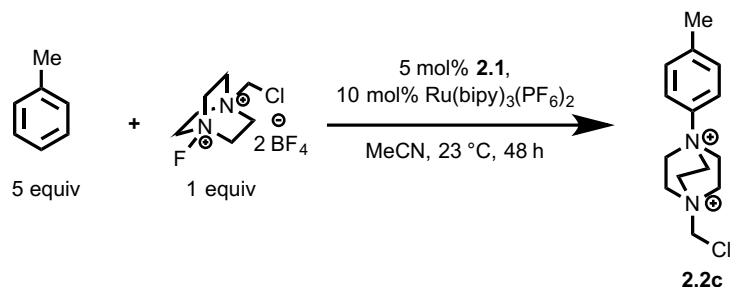
A 50 mL round-bottom flask was charged with palladium complex **2.1** (31.8 mg, 50.0 μmol , 5.00 mol%), Ru(bipy)₃(PF₆)₂ (86.0 mg, 0.100 mmol, 10.0 mol%), and Selectfluor (354. mg, 1.00 mmol, 1.00 equiv). Acetonitrile (5.0 mL, $c = 0.20$ M) was added, followed by chlorobenzene (509 μL , 5.00 mmol, 5.00 equiv) via syringe. After stirring at 23 °C for 19 h, the reaction mixture was filtered through celite and concentrated *in vacuo*. The residue was triturated with a solvent mixture of dichloromethane/methanol (9/1 (v/v), 10 mL) and dichloromethane (5×10 mL) at 23 °C to afford 463 mg of the title compound as a light yellow solid. For yield determination, an NMR sample in *d*₃-acetonitrile was prepared

containing 20.0 mg of the product mixture and 3.0 μL of ethyl acetate (31. μmol) as internal standard. Comparison of the integral of the peak of **2.2b** at 7.79–7.77 ppm (aromatic C–H, 2H) with that of the peak of ethyl acetate at 1.20 ppm (CH_3 , 3H) revealed the bulk mixture to contain 0.80 mmol of Ar–TEDA (80% yield). Also present was 0.14 mmol H–TEDA^{2+} (14%), measured by integration of the peak at 3.85–3.81 ppm ($3 \times \text{CH}_2$, 6H).

NMR Spectroscopy: ^1H NMR (600 MHz, CD_3CN , 23 $^\circ\text{C}$, δ): 7.79–7.82 (m, 2H), 7.70–7.73 (m, 2H), 5.36 (s, 2H), 4.40–4.43 (m, 6H), 4.13–4.15 (m, 6H). ^{13}C NMR (125 MHz, CD_3CN , 23 $^\circ\text{C}$, δ): 142.9, 137.9, 131.6, 122.9, 69.7, 55.1, 51.2.

Mass Spectrometry: HRMS-FIA(m/z) calcd for $\text{C}_{13}\text{H}_{18}\text{Cl}_2\text{N}_2^{2+}$ $[\text{M}]^{2+}$, 136.0418; found, 136.0419.

1-(Chloromethyl)-4-(4-methyl-phenyl)-1,4-diazabicyclo[2.2.2]octane $^{2+}$ (**2.2c**)



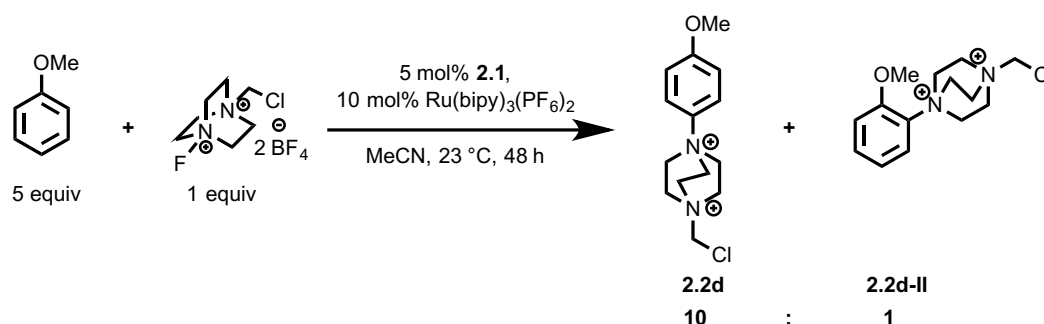
To a 20 mL vial were added palladium complex **2.1** (31.8 mg, 50.0 μmol , 5.00 mol%), $\text{Ru}(\text{bipy})_3(\text{PF}_6)_2$ (86.0 mg, 100. μmol , 10.0 mol%), Selectfluor (354. mg, 1.00 mmol, 1.0 equiv), and toluene (0.530 mL, 5.00 mmol, 5.00 equiv), and acetonitrile (2.5 mL, $c = 0.20$ M). The reaction mixture was stirred at 23 $^\circ\text{C}$ for 48 h. The reaction mixture was concentrated *in vacuo*, then triturated with CH_2Cl_2 to afford 324 mg of a tan powder. For yield determination, an NMR sample in d_3 -acetonitrile was prepared containing 10.0 mg of the product mixture and 5.0 μL of ethyl acetate (51. μmol) as internal standard. Comparison of the integral of the peak of **2.2c** at 4.37–4.32 ppm ($3 \times \text{CH}_2$, 6H) with that of the peak of ethyl acetate at 1.20 ppm (CH_3 , 3H) revealed the bulk mixture to contain 0.59 mmol of Ar–TEDA

(59% yield). Also present was 0.18 mmol H–TEDA²⁺ (18%), measured by integration of the peak at 3.85–3.81 ppm (3 × CH₂, 6H).

NMR Spectroscopy: ¹H NMR (600 MHz, CD₃CN, 23 °C, δ): 7.67–7.63 (m, 2H), 7.54–7.00 (m, 2H), 5.33 (s, 2H), 4.37–4.32 (m, 6H), 4.11–4.07 (m, 6H), 2.44 (s, 3H). ¹³C NMR (125 MHz, DMSO, 23 °C, δ): 142.1, 141.4, 131.0, 120.3, 68.2, 53.94, 50.4, 20.3.

Mass spectrometry: HRMS-FIA(m/z) calcd for C₁₄H₂₀ClN₂⁺ [M–H]⁺, 251.1310; found, 251.1312.

1-(Chloromethyl)-4-(4-methyl-phenyl)-1,4-diazabicyclo[2.2.2]octane²⁺ (**2.2d**)



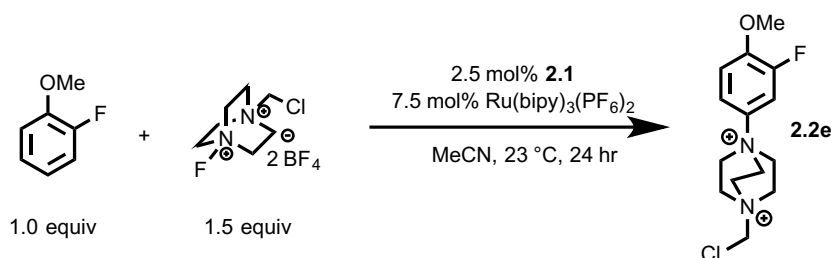
To a 20 mL vial were added palladium complex **2.1** (31.8 mg, 50.0 μmol, 5.00 mol%), Ru(bipy)₃(PF₆)₂ (86.0 mg, 100. μmol, 10.0 mol%), Selectfluor (354. mg, 1.00 mmol, 1.0 equiv), and anisole (0.544 mL, 5.00 mmol, 5.0 equiv), and acetonitrile (2.5 mL, c = 0.20 M). The reaction mixture was stirred at 23 °C for 48 h. The reaction mixture was concentrated *in vacuo*, then triturated with CH₂Cl₂ to afford 324. mg of a tan powder. For yield determination, an NMR sample in *d*₃-acetonitrile was prepared containing 10.0 mg of the product mixture and 5.0 μL of ethyl acetate (51. μmol) as internal standard. Comparison of the integral of the peak of **2.2d** at 4.36–4.31 ppm (3 × CH₂, 6H) with that of the peak of ethyl acetate at 1.20 ppm (CH₃, 3H) revealed the bulk mixture to contain 0.43 mmol of **2.2d** (43% yield). An additional compound was observed in 4.3% yield, assignable to **2.2d-II**; (upon reduction, *N*-(2-methoxyphenyl)piperazine (**2.3e-II**) is observed in small amounts). Also present was 0.31 mmol H–TEDA²⁺ (31%), measured by integration of the peak at 3.85–3.81

ppm ($3 \times \text{CH}_2$, 6H).

NMR Spectroscopy: ^1H NMR (600 MHz, CD_3CN , 23 °C, δ): 7.72–7.67 (m, 2H), 7.21–7.17 (m, 2H), 5.33 (s, 2H), 4.36–4.31 (m, 6H), 4.20–4.15 (m, 6H), 3.88 (s, 3H). ^{13}C NMR (125 MHz, DMSO, 23 °C, δ): 160.5, 137.0, 122.1, 115.5, 68.2, 54.1, 50.4, 43.4.

Mass spectrometry: HRMS-FIA(m/z) calcd for $\text{C}_{14}\text{H}_{20}\text{ClN}_2\text{O}^+$ $[\text{M}-\text{H}]^+$, 267.1259; found, 267.1263.

1-(Chloromethyl)-4-(3-fluoro-4-methoxyphenyl)-1,4-diazabicyclo[2.2.2]octane²⁺ (2.2e)



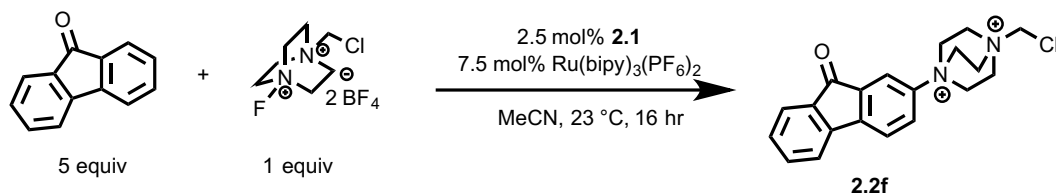
A 50 mL round-bottom flask was charged with palladium complex **2.1** (31.8 mg, 50.0 μmol , 5.00 mol%), $\text{Ru}(\text{bipy})_3(\text{PF}_6)_2$ (86.0 mg, 0.100 mmol, 10.0 mol%), and Selectfluor (531. mg, 1.50 mmol, 1.50 equiv). Acetonitrile (5.0 mL, $c = 0.20 \text{ M}$) was added, followed by 2-fluoroanisole (112 μL , 1.00 mmol, 1.00 equiv) via syringe. After stirring at 23 °C for 24 h, the reaction mixture was filtered through celite and concentrated *in vacuo*. The residue was triturated with a solvent mixture of dichloromethane/methanol (9/1 (v/v), 10 mL) and dichloromethane ($5 \times 10 \text{ mL}$) at 23 °C to afford 573 mg of a orange solid. The solid was triturated with a solvent mixture of dichloromethane/methanol (9/1 (v/v), 10 mL) and dichloromethane ($5 \times 10 \text{ mL}$) at 23 °C to afford 562 mg of the title compound as a light orange solid. For yield determination, an NMR sample in *d*3-acetonitrile was prepared containing 20.0 mg of the product mixture and 3.0 μL of ethyl acetate ($3.1 \times 10^{-5} \text{ mol}$) as internal standard. Comparison of the integral of the peak of **2.2e** at 7.34 ppm (aromatic C–H, 1H) with that of the peak of ethyl acetate at 1.20 ppm (CH_3 , 3H) revealed the bulk mixture to contain 0.76 mmol of Ar–TEDA (76% yield). Also present was 0.42 mmol H–TEDA²⁺

(42%) measured by integration of the peak at 3.85–3.81 ppm ($3 \times \text{CH}_2$, 6H).

NMR Spectroscopy: ^1H NMR (600 MHz, CD_3CN , 23 °C, δ): 7.67 (dd, $J = 12.2$, 3.3 Hz, 1H), 7.59 (ddd, $J = 9.3$, 3.3, 1.6 Hz, 1H), 7.34 (dd, $J = 9.3$, 9.3 Hz, 1H), 5.36 (s, 2H), 4.36–4.38 (m, 6H), 4.11–4.13 (m, 6H), 3.96 (s, 3H). ^{13}C NMR (125 MHz, CD_3CN , 23 °C, δ): 152.0 (d, $J = 249.4$ Hz), 150.3 (d, $J = 9.7$ Hz), 135.9 (d, $J = 7.8$ Hz), 117.5 (d, $J = 3.8$ Hz), 114.9 (d, $J = 2.8$ Hz), 110.0 (d, $J = 25.0$ Hz), 69.5, 55.1, 51.0, 50.4. ^{19}F NMR (475 MHz, CD_3CN , 23 °C, δ): –130.2.

Mass Spectrometry: HRMS-FIA(m/z) calcd for $\text{C}_{14}\text{H}_{20}\text{ClFN}_2\text{O}^{2+}$ $[\text{M}]^{2+}$, 143.0619; found, 143.0626.

1-(Chloromethyl)-4-(fluoren-9-yl)-1,4-diazabicyclo[2.2.2]octane²⁺ (2.2f)



A 50 mL round-bottom flask was charged with palladium complex **2.1** (31.8 mg, 50.0 μmol , 5.00 mol%), $\text{Ru}(\text{bipy})_3(\text{PF}_6)_2$ (86.0 mg, 0.100 mmol, 10.0 mol%), Selectfluor (354. mg, 1.00 mmol, 1.00 equiv), and 9H-fluoren-9-one (901 mg, 5.00 mmol, 5.00 equiv). Acetonitrile (5.0 mL, $c = 0.20$ M) was added via syringe. After stirring at 23 °C for 16 h, the reaction mixture was filtered through celite and concentrated *in vacuo*. The residue was triturated with a solvent mixture of dichloromethane/methanol (9/1 (v/v), 10 mL) and dichloromethane (5×10 mL) at 23 °C to afford 559. mg of a yellow solid. The solid was triturated with a solvent mixture of dichloromethane/methanol (9/1 (v/v), 10 mL) and dichloromethane (5×10 mL) at 23 °C to afford 468. mg of a bright yellow solid. The solid was triturated with a solvent mixture of dichloromethane/methanol (9/1 (v/v), 10 mL) and dichloromethane (5×10 mL) at 23 °C to afford 453. mg of the title compound as a bright yellow solid. For yield

determination, an NMR sample in d_3 -acetonitrile was prepared containing 20.0 mg of the product mixture and 3.0 μL of ethyl acetate (3.1×10^{-5} mol) as internal standard.

Comparison of the integral of the peak of **2.2f** at 5.36 ppm (CH_2Cl , 2H) with that of the peak of ethyl acetate at 1.20 ppm (CH_3 , 3H) revealed the bulk mixture to contain 0.77 mmol of Ar-TEDA (77% yield). Also present was 0.069 mmol H-TEDA²⁺ (7%), measured by integration of the peak at 3.85–3.81 ppm ($3 \times \text{CH}_2$, 6H).

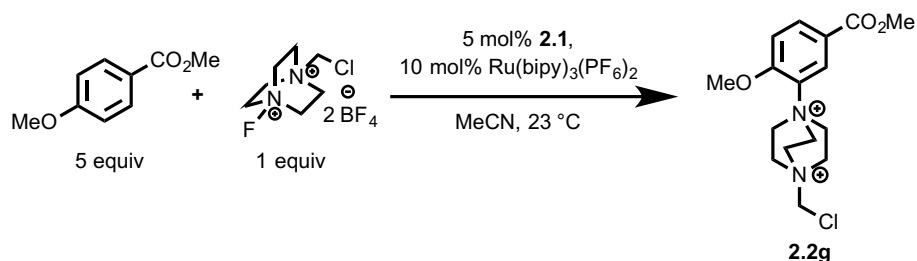
The product mixture of **2.2f** obtained above (50 mg) was further purified through repeated recrystallization by vapor diffusion of diethyl ether into an acetonitrile solution. Pure product **2.2f** (15 mg) was obtained as yellow crystals and characterized.

Note: Compound **2.2f** exhibits concentration-dependent chemical shifts. The chemical shifts listed below were recorded from a sample of 12 mg **2.2f** in 7.5 mL CD_3CN .

NMR Spectroscopy: ^1H NMR (600 MHz, CD_3CN , 23 °C, δ): 8.00–7.97 (m, 2H), 7.95–7.92 (m, 1H), 7.80–7.77 (m, 1H), 7.71–7.65 (m, 2H), 7.51–7.47 (m, 1H), 5.38 (s, 2H), 4.45–4.47 (m, 6H), 4.15–4.18 (m, 6H). ^{13}C NMR (125 MHz, CD_3CN , 23 °C, δ): 191.7, 147.7, 145.0, 143.0, 136.8, 136.7, 135.0, 131.7, 127.7, 125.4, 123.8, 123.1, 116.9, 70.0, 55.4, 51.5.

Mass Spectrometry: HRMS-FIA(m/z) calcd for $\text{C}_{20}\text{H}_{21}\text{ClN}_2\text{O}^{2+}$ [M]²⁺, 170.0666; found, 170.0672.

1-(Chloromethyl)-4-(5-methoxy-2-(methoxycarbonyl)phenyl)²⁺ (**2.2g**)



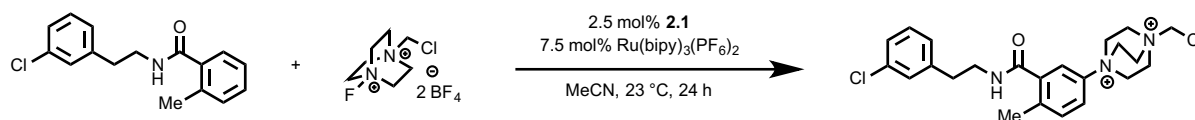
To a 20 mL vial were added palladium complex **2.1** (19.0 mg, 25.0 μmol , 5.00 mol%), $\text{Ru}(\text{bipy})_3(\text{PF}_6)_2$ (43.0 mg, 5.00 μmol , 10.0 mol%), Selectfluor (177. mg, 0.500 mmol, 1.00

equiv), and methyl 4-methoxybenzoate (416 mg, 2.50 mmol, 5.00 equiv), and acetonitrile (2.5 mL, c = 0.20 M). The reaction mixture was stirred at 23 °C for 48 h. The reaction mixture was concentrated *in vacuo*, then triturated with CH₂Cl₂ to afford 191. mg of a tan powder. ¹H NMR shows ca. 35% contamination by H–TEDA²⁺.

NMR Spectroscopy: ¹H NMR (500 MHz, CD₃CN, 23 °C, δ): 8.27 (dd, *J* = 8.9, 1.8 Hz, 1H), 8.21 (d, *J* = 1.8 Hz, 1H), 7.46 (d, *J* = 8.9 Hz, 1H), 5.33 (s, 2H), 4.62–4.54 (m, 6H), 4.15–4.09 (m, 6H), 4.14 (s, 3H), 3.92 (s, 3H). ¹³C NMR (125 MHz, CD₃CN, 23 °C, δ): 165., 156.51, 135.4, 130.8, 124.7, 124.3, 116.6, 70.4, 58.4, 53.7, 51.6, 45.1.

Mass spectrometry: HRMS-FIA(m/z) calcd for C₁₆H₂₂ClN₂O₃⁺ [M–H]⁺, 325.1313; found, 325.1315.

1-(Chloromethyl)-4-(3-((3-chlorophenethyl)carbamoyl)-4-methylphenyl)-1,4-diazabicyclo[2.2.2]octane-1,4-diium (2.2h)



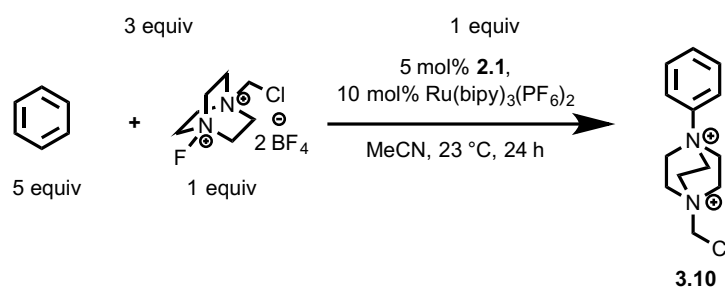
A 4 mL vial was charged with palladium complex **2.1** (3.2 mg, 5.0 μmol, 2.5 mol%), Ru(bpy)₃(PF₆)₂ (12.9 mg, 15.0 μmol, 7.50 mol%), Selectfluor (70.9 mg, 0.200 mmol, 1.00 equiv), and *N*-(3-chlorophenethyl)-2-methylbenzamide (164. mg, 0.600 mmol, 3.00 equiv). Acetonitrile (1.0 mL, c = 0.20 M) was added via syringe, and the reaction mixture was stirred at 23 °C for 24 h. The reaction mixture was concentrated *in vacuo* to afford a red heterogeneous solid mixture. The solid was triturated with dichloromethane to afford 62 mg of the title compound as a light yellow solid (20% yield). Also present was ca. 49% contamination by H–TEDA²⁺, measured by integration of the peak at 3.85–3.81 ppm (3 × CH₂, 6H).

NMR Spectroscopy: ¹H NMR (600 MHz, CD₃CN, 23 °C, δ): 7.71 (dd, *J* = 8.8, 2.9 Hz, 1H),

7.67 (d, $J = 2.9$ Hz, 1H), 7.53 (d, $J = 8.8$ Hz, 1H), 7.30–7.33 (m, 2H), 7.23–7.25 (m, 2H), 6.99 (bs, 1H), 5.36 (s, 2H), 4.38–4.40 (m, 6H), 4.12–4.15 (m, 6H), 3.61–3.64 (m, 2H), 2.91 (t, $J = 6.9$ Hz, 2H), 2.34 (s, 3H). ^{13}C NMR (125 MHz, CD_3CN , 23 °C, δ): 168.2, 142.9, 142.0, 141.3, 140.1, 134.6, 134.1, 131.0, 129.9, 128.6, 127.3, 121.9, 120.0, 70.1, 55.4, 51.6, 41.4, 35.8, 19.3.

Mass Spectrometry: HRMS-FIA(m/z) calcd for $\text{C}_{23}\text{H}_{29}\text{Cl}_2\text{N}_3\text{O}^{2+}$ $[\text{M}]^{2+}$, 216.5838; found, 216.5846.

1-(Chloromethyl)-4-phenyl-1,4-diazabicyclo[2.2.2]octane $^{2+}$ (**3.10**)



To a 20 mL vial were added palladium complex **2.1** (31.8 mg, 50.0 μmol , 5.00 mol%), $\text{Ru}(\text{bipy})_3(\text{PF}_6)_2$ (86.0 mg, 100. μmol , 10.0 mol%), Selectfluor (354. mg, 1.00 mmol, 1.00 equiv), and benzene (0.446 mL, 5.00 mmol, 5.0 equiv), and acetonitrile (2.5 mL, $c = 0.20$ M). The reaction mixture was stirred at 23 °C for 48 h. The reaction mixture was concentrated *in vacuo*, then triturated with CH_2Cl_2 to afford 360 mg of a tan powder. For yield determination, an NMR sample in d_3 -acetonitrile was prepared containing 10.0 mg of the product mixture and 5.0 μL of ethyl acetate (51. μmol) as internal standard. Comparison of the integral of the peak of **3.10** at 4.41–4.36 ppm ($3 \times \text{CH}_2$, 6H) with that of the peak of ethyl acetate at 1.20 ppm (CH_3 , 3H) revealed the bulk mixture to contain 0.67 mmol of Ar–TEDA (67% yield). Also present was 0.15 mmol H–TEDA $^{2+}$ (15%), measured by integration of the peak at 3.85–3.81 ppm ($3 \times \text{CH}_2$, 6H).

NMR Spectroscopy: ^1H NMR (600 MHz, CD_3CN , 23 °C, δ): 7.82–7.77 (m, 2H); 7.75–7.69

(m, 3H), 5.35 (s, 2H), 4.41–4.36 (m, 6H), 4.41–4.09 (m, 6H). ^{13}C NMR (125 MHz, CD_3CN , 23 $^\circ\text{C}$, δ): 144.4, 131.3, 130.8, 120.7, 68.2, 53.9, 50.4

Mass spectrometry: HRMS-FIA(m/z) calcd for $\text{C}_{13}\text{H}_{18}\text{ClN}_2^+$ $[\text{M}-\text{H}]^+$, 237.1153; found, 237.1154.

Fluoro- N,N,N -trimethylanilinium cations

We have synthesized *ortho*-, *meta*-, and *para*-fluoro- N,N,N -trimethylanilinium iodide to ascertain the likelihood of the ^{19}F NMR signal overlap of the different constitutional isomers of fluoroaryl trialkylammonium salts. We found the ^{19}F chemical shifts in CD_3CN of the *para*, *meta*, and *ortho* isomers to be -112.4 ppm, -110.2 ppm, and -113.3 ppm, respectively:

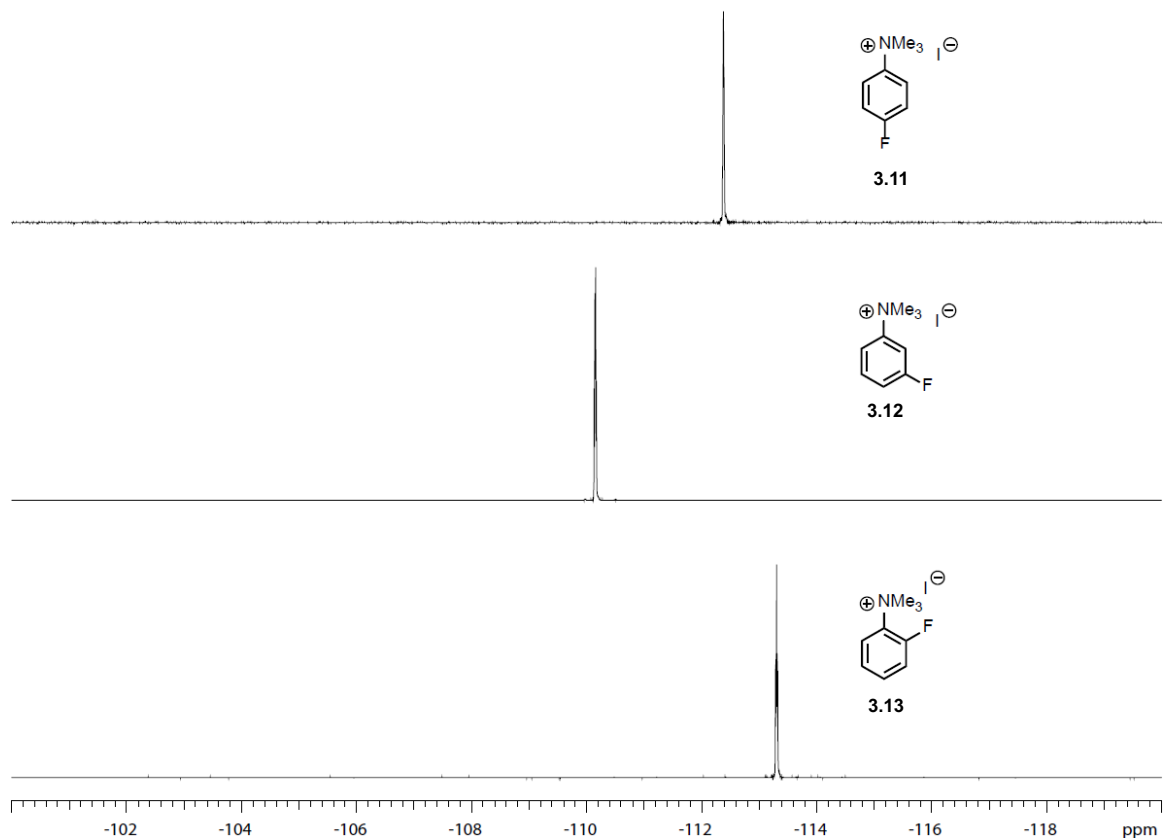
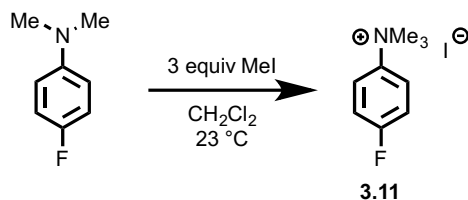


Figure 3.8. ^{19}F NMR chemical shifts of **3.11**, **3.12**, and **3.13** (CD_3CN , 23 $^\circ\text{C}$)

4-Fluoro-*N,N,N*-trimethylanilinium iodide (3.11)

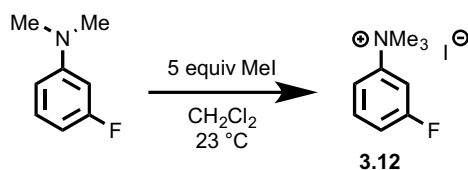


In a 20 mL vial, *N,N*-dimethylaniline (696. mg, 5.00 mmol, 1.00 equiv) was dissolved in CH_2Cl_2 (5.0 mL), and iodomethane (0.93 mL, 15. mmol, 3.0 equiv) was added dropwise via syringe. The mixture was stirred at room temperature for 4 hours, over which time a white precipitate formed. The precipitate was collected by filtration, then washed with dichloromethane (3×5 mL) to afford 767. mg of 4-fluoro-*N,N,N*-trimethylanilinium iodide as a white powder (2.73 mmol, 55%).

NMR Spectroscopy: ^1H NMR (500 MHz, CD_3CN , 23 $^{\circ}\text{C}$, δ): 7.89–7.84 (m, 2H), 7.39–7.34 (m, 2H), 3.58 (s, 9H). ^{13}C NMR (125 MHz, DMSO, 23 $^{\circ}\text{C}$, δ): 161.8 (d, $J = 248.6$ Hz), 143.3 (d, $J = 3.1$ Hz), 123.3 (d, $J = 9.3$ Hz), 116.6 (d, $J = 23.5$ Hz), 56.7 (s). ^{19}F NMR (470 MHz, CD_3CN , 23 $^{\circ}\text{C}$, δ): –112.4.

Mass spectrometry: HRMS-FIA(m/z) calcd for $\text{C}_9\text{H}_{13}\text{NF} [\text{M}]^+$, 154.1027; found, 154.1023.

3-Fluoro-*N,N,N*-trimethylanilinium iodide (3.12)



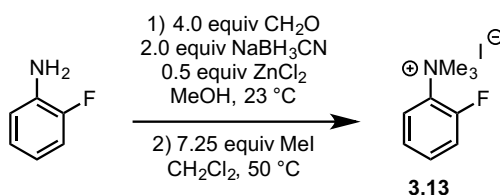
In a 20 mL vial, *N,N*-dimethylaniline (500 mg, 3.59 mmol, 1.0 equiv) was dissolved in CH_2Cl_2 (5.0 mL), and iodomethane (1.12 mL, 18.0 mmol, 5.0 equiv) was added dropwise via syringe. The mixture was stirred at room temperature for 48 hours, over which time a white precipitate formed. The precipitate was collected by filtration, then washed with dichloromethane (3×5 mL) to afford 754 mg of 4-fluoro-*N,N,N*-trimethylanilinium iodide as

a white powder (2.68 mmol, 75%).

NMR Spectroscopy: ^1H NMR (500 MHz, CD_3CN , 23 °C, δ): 7.80–7.73 (m, 2H), 7.68–7.63 (ddd, J = 6.47 Hz, 8.50 Hz, 14.7 Hz, 1H), 7.39–7.34 (ddd, J = 0.83 Hz, 2.33 Hz, 7.86 Hz, 1H), 3.67 (s, 9H). ^{13}C NMR (125 MHz, CD_3CN , 23 °C, δ): 161.8 (d, J = 246.4 Hz), 148.3 (d, J = 9.1 Hz), 131.8 (d, J = 9.0 Hz), 117.1 (d, J = 21.0 Hz), 116.9 (d, J = 3.8 Hz), 109.2 (d, J = 27.4 Hz), 56.5 (s). ^{19}F NMR (470 MHz, CD_3CN , 23 °C, δ): –110.2.

Mass spectrometry: HRMS-FIA(m/z) calcd for $\text{C}_9\text{H}_{13}\text{NF} [\text{M}]^+$, 154.1027; found, 154.1020.

2-Fluoro-*N,N,N*-trimethylanilinium iodide (3.13)



In a round bottom flask were added 3-fluoroaniline (1.50 mL, 15.6 mmol, 1.00 equiv), methanol (50 mL), and 37% aqueous formaldehyde (5.0 mL, 62 mmol, 4.0 equiv). To this mixture was added a solution of sodium cyanoborohydride (2.010 g, 32.01 mmol, 2.00 equiv) and zinc chloride (1.090 g, 8.00 mmol, 0.500 equiv) in 50 mL methanol. The mixture was stirred for 12 hours at room temperature, after which time 50 mL 0.16 M NaOH was added, and the methanol was removed by rotary evaporation. The aqueous mixture was then extracted with dichloromethane (4×20 mL). The combined organic layers were dried over MgSO_4 and concentrated to give a brown oil. The residue was redissolved in 15 mL dichloromethane and added to a pressure vessel, along with 7.00 mL of iodomethane (112. mmol, 7.25 equiv). The vessel was sealed and heated to 50 °C for 12 hours, over which time a white precipitate formed. The precipitate was collected by filtration, washed with dichloromethane (5×20 mL), and dried in vacuo to afford 2.27 g of 2-fluoro-*N,N,N*-trimethylanilinium iodide as a white powder (8.08 mmol, 52%).

NMR Spectroscopy: ^1H NMR (500 MHz, CD_3CN , 23 °C, δ): 7.85–7.79 (dd, J = 8.6, 1.4 Hz, 1H), 7.69–7.64 (dddd, J = 8.3, 7.5, 4.7, 1.5 Hz, 1H), 7.50–7.55 (ddd, J = 14.3, 8.3, 1.5 Hz, 1H), 7.45–7.41 (ddd, J = 7.5, 1.4, 0.80 Hz, 1H), 3.68 (s, 9H). ^{13}C NMR (125 MHz, DMSO, 23 °C, δ): 154.1 (d, J = 251.2 Hz), 132.9 (d, J = 6.4), 132.9 (d, J = 9.6 Hz), 125.8 (d, 3.6 Hz), 122.9 (s), 118.8 (d, J = 22.3), 56.1 (d, J = 5.5 Hz). ^{19}F NMR (470 MHz, CD_3CN , 23 °C, δ): –113.3.

Mass spectrometry: HRMS-FIA(m/z) calcd for $\text{C}_9\text{H}_{13}\text{NF}$ $[\text{M}]^+$, 154.1027; found, 154.1027.

Aromatic TEDAylation trials with 1.05 equivalents of Selectfluor

For the aromatic TEDAylation reaction, we have generally used 1.5–2.0 equivalents of Selectfluor, as we have found that the excess is required to push most substrates to completion. To probe the tolerance of the reaction to a reduction in the loading of Selectfluor, we have attempted the TEDAylation of toluene and anisole with 1.05 equivalents of Selectfluor, and compared the results to the standard conditions with 1.5 equivalents of Selectfluor. We have found only minor diminution of yield for these substrates with the reduced loading of Selectfluor:

Substrate	Selectfluor	Yield
	Loading	
anisole	1.05 equivalents	85%
	1.50 equivalents	89%
toluene	1.05 equivalents	83%
	1.50 equivalents	92%

Toluene substrate, 1.05 equivalents Selectfluor

Palladium complex **2.1** (13.4 mg, 21.1 μmol) and $\text{Ru}(\text{bipy})_3(\text{PF}_6)_2$ (36.1 mg, 42.0 μmol) were dissolved in d_3 -acetonitrile (2.1 mL) to afford a stock solution. A 4 mL vial was charged

with Selectfluor (37.2 mg, 0.105 mmol, 1.05 equiv), followed by 0.50 mL of the stock solution containing **2.1** (5.0 μ mol, 5.0 mol%) and Ru(bipy)₃(PF₆)₂ (10. μ mol, 10. mol%). Finally, 10.7 μ L toluene (0.10 mmol, 1.0 equiv) was added, and the solution was stirred at 23 °C for 48 h. The reaction mixture was diluted with *d*₃-acetonitrile (0.25 mL), passed through a 0.2 μ m PVDF syringe filter, and analyzed by ¹H NMR.

The yield of **2.2c** was determined via ¹H NMR spectroscopy using ethyl acetate (5.0 μ L, 51. μ mol) as an internal standard. Comparison of the integral of the peak of **2.2c** at 7.67–7.65 ppm (aromatic C–H, 2H) with that of the peak of ethyl acetate at 1.20 ppm (CH₃, 3H) revealed an 85% yield of **2.2c**.

Toluene substrate, 1.50 equivalents Selectfluor

Palladium complex **2.1** (13.4 mg, 21.1 μ mol) and Ru(bipy)₃(PF₆)₂ (36.1 mg, 42.0 μ mol) were dissolved in *d*₃-acetonitrile (2.1 mL) to afford a stock solution. A 4 mL vial was charged with Selectfluor (53.1 mg, 0.150 mmol, 1.50 equiv), followed by 0.50 mL of the stock solution containing **2.1** (5.0 μ mol, 5.0 mol%) and Ru(bipy)₃(PF₆)₂ (10. μ mol, 10. mol%). Finally, 10.7 μ L toluene (0.10 mmol, 1.0 equiv) was added, and the solution was stirred at 23 °C for 48 h. The reaction mixture was diluted with *d*₃-acetonitrile (0.25 mL), passed through a 0.2 μ m PVDF syringe filter, and analyzed by ¹H NMR.

The yield of **2.2c** was determined via ¹H NMR spectroscopy using ethyl acetate (5.0 μ L, 51. μ mol) as an internal standard. Comparison of the integral of the peak of **2.2c** at 7.67–7.65 ppm (aromatic C–H, 2H) with that of the peak of ethyl acetate at 1.20 ppm (CH₃, 3H) revealed an 89% yield of **2.2c**.

Anisole substrate, 1.05 equivalents Selectfluor

Palladium complex **2.1** (13.4 mg, 21.1 μ mol) and Ru(bipy)₃(PF₆)₂ (36.1 mg, 42.0 μ mol) were dissolved in *d*₃-acetonitrile (2.1 mL) to afford a stock solution. A 4 mL vial was charged

with Selectfluor (37.2 mg, 0.105 mmol, 1.05 equiv), followed by 0.50 mL of the stock solution containing **2.1** (5.0 μ mol, 5.0 mol%) and Ru(bipy)₃(PF₆)₂ (10. μ mol, 10. mol%). Finally, 10.9 μ L anisole (0.10 mmol, 1.0 equiv) was added, and the solution was stirred at 23 °C for 48 h. The reaction mixture was diluted with *d*₃-acetonitrile (0.25 mL), passed through a 0.2 μ m PVDF syringe filter, and analyzed by ¹H NMR.

The yield of **2.2d** was determined via ¹H NMR spectroscopy using ethyl acetate (5.0 μ L, 51. μ mol) as an internal standard. Comparison of the integral of the peak of **2.2d** at 7.72–7.69 ppm (aromatic C–H, 2H) with that of the peak of ethyl acetate at 1.20 ppm (CH₃, 3H) revealed an 83% yield of **2.2d**.

Anisole substrate, 1.50 equivalents Selectfluor

Palladium complex **2.1** (13.4 mg, 21.1 μ mol) and Ru(bipy)₃(PF₆)₂ (36.1 mg, 42.0 μ mol) were dissolved in *d*₃-acetonitrile (2.1 mL) to afford a stock solution. A 4 mL vial was charged with Selectfluor (53.1 mg, 0.150 mmol, 1.50 equiv), followed by 0.50 mL of the stock solution containing **2.1** (5.0 μ mol, 5.0 mol%) and Ru(bipy)₃(PF₆)₂ (10. μ mol, 10. mol%). Finally, 10.9 μ L anisole (0.10 mmol, 1.0 equiv) was added, and the solution was stirred at 23 °C for 48 h. The reaction mixture was diluted with *d*₃-acetonitrile (0.25 mL), passed through a 0.2 μ m PVDF syringe filter, and analyzed by ¹H NMR.

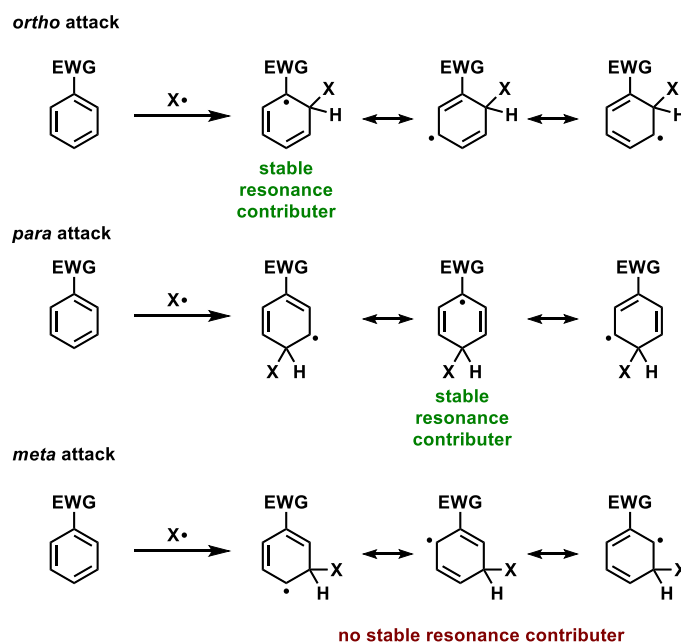
The yield of **2.2d** was determined via ¹H NMR spectroscopy using ethyl acetate (5.0 μ L, 51. μ mol) as an internal standard. Comparison of the integral of the peak of **2.2d** at 7.72–7.69 ppm (aromatic C–H, 2H) with that of the peak of ethyl acetate at 1.20 ppm (CH₃, 3H) revealed an 92% yield of **2.2d**.

Selectivity of TEDAylation with Resonance Electron-withdrawing Substituents

Radicals are stabilized both by electron-donating and electron-withdrawing substituents.

Therefore, in radical aromatic substitution of arenes bearing electron-withdrawing groups,

intermediates resulting from radical attack at the *ortho* and *para* positions are more stable than the one arising from attack at the *meta* position, because the *ortho* and *para* addition isomers provide opportunity for resonance stabilization of the radical. Therefore, by Hammond's postulate, the rate of attack in the *ortho* and *para* position is more rapid. This stands in contrast to electrophilic aromatic substitution, in which resonance electron-withdrawing substituents direct electrophilic attack to the *meta* position.



We have found that upon reaction with TEDA^{2+} , benzonitrile yields the *para* substituted Ar-TEDA isomer in ca. 10% conversion. No other isomer is observable. This result can be understood by considering the resonance stabilization effect described above. For arenes substituted with electron-donating groups, attack at the *ortho* and *para* positions are favored by resonance considerations, while attack at the *para* position is further favored by charge transfer in the transition state of addition. In the case of arenes bearing resonance electron-withdrawing groups, we rationalize that attack is constrained to the *ortho* and *para* positions by resonance stabilization considerations. Thus, attack occurs at the *para* position, even though the *meta* position may be capable of greater charge-transfer stabilization.

TEDAylation of benzonitrile

In a 4 mL vial, palladium complex **2.1** (3.2 mg, 5.0 μmol , 5.0 mol%), $\text{Ru}(\text{bipy})_3(\text{PF}_6)_2$ (8.6 mg, 10. μmol , 10.0 mol%), and Selectfluor (70.9 mg, 0.200 mmol, 2.00 equiv) were dissolved in d_3 -acetonitrile (0.50 mL). Finally, 10.2 μL benzonitrile (0.100 mmol, 1.00 equiv) was added, and the solution was stirred at 40 $^\circ\text{C}$ for 48 h. The reaction mixture was diluted with d_3 -acetonitrile (0.25 mL), passed through a 0.2 μm PVDF syringe filter, and analyzed by ^1H NMR:

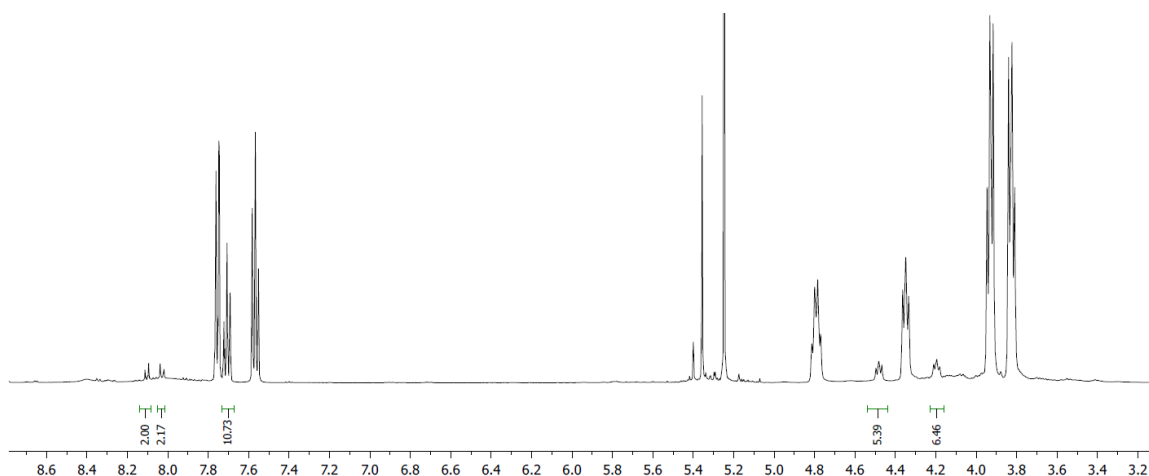


Figure 3.9. ^1H NMR of reaction mixture of TEDAylation of benzonitrile (CD_3CN , 23 $^\circ\text{C}$)

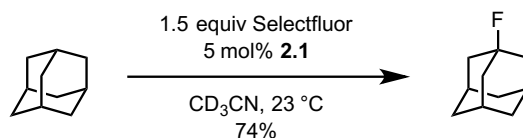
Evidence for TEDA^{2+} radical dication as the C–N bond forming species

Lectka has reported that treatment of adamantane with Selectfluor in the presence of various radical initiators leads to C–H fluorination.^{56, 100a} It was proposed that such reactions proceed through the intermediacy of TEDA^{2+} , which abstracts a hydrogen atom from the substrate.

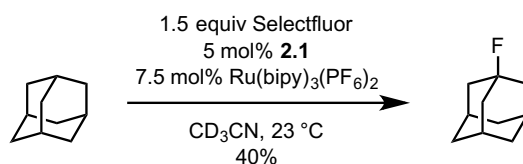
We have observed aliphatic C–H fluorination in the presence of Selectfluor and **2.1**, which is consistent with the formation of TEDA^{2+} through the action of **2.1** on Selectfluor. We propose that the yield is diminished in the presence of $\text{Ru}(\text{bipy})_3(\text{PF}_6)_2$ due to oxidation by Ru^{III} of the alkyl radical generated upon hydrogen atom abstraction, leading to non-fluorinated products.

We have furthermore observed the formation of **2.2a** from fluorobenzene via copper catalysis, under conditions similar to those reported by Baran.^{100b} This finding indicates that neither **2.1** or Ru(bipy)₃(PF₆)₂ is uniquely effective catalyst for Ar–TEDA formation, and is consistent with the free TEDA²⁺ radical as the C–N bond forming species.

Observation of aliphatic C–H fluorination under TEDAylation conditions

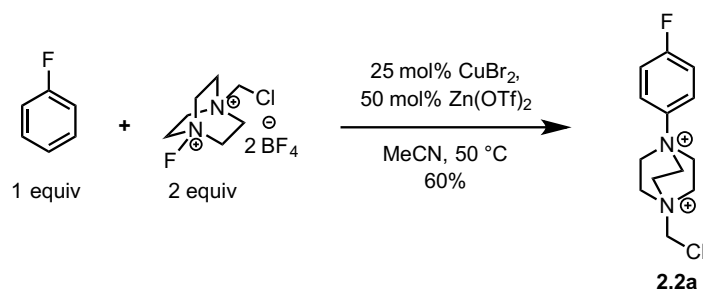


To a 4 mL vial were added adamantane (13.6 mg, 0.100 mmol, 1.00 equiv), Selectfluor (53.2 mg, 0.150 mmol, 1.50 equiv), **2.1** (3.2 mg, 5.0 μmol, 5.0 mol%), and CD₃CN (0.70 mL). The reaction was stirred for 16 hours at room temperature, after which 2.0 μL of 3-fluoronitrobenzene was added as an internal standard, and the solution was analyzed by ¹⁹F NMR. 1-Fluoroadamantane was observed in 74% yield.



To a 4 mL vial were added adamantane (13.6 mg, 0.100 mmol, 1.00 equiv), Selectfluor (53.2 mg, 0.150 mmol, 1.50 equiv), **2.1** (3.2 mg, 5.0 μmol, 5.0 mol%), Ru(bipy)₃(PF₆)₂ (6.4 mg, 7.5 μmol, 7.5 mol%) and CD₃CN (0.70 mL). The reaction was stirred for 16 hours at room temperature, after which 2.0 μL of 3-fluoronitrobenzene was added as an internal standard, and the solution was analyzed by ¹⁹F NMR. 1-Fluoroadamantane was observed in 40% yield.

Observation of Aryl–TEDA formation under copper catalysis



To a 4 mL vial were added cupric bromide (7.3 mg, 33. μ mol, 25 mol%), zinc triflate (23.6 mg, 64.9 μ mol, 50.0 mol%), and Selectfluor-PF₆ (135. mg, 0.286 mmol, 2.00 equiv). Acetonitrile-*d*₃ (1.0 mL) was then added, followed by fluorobenzene (12.0 μ L, 0.128 mmol, 1.00 equiv). The reaction mixture was stirred for 16 hours at 50 °C. The mixture was allowed to cool to room temperature, 2.0 μ L of 3-fluoronitrobenzene was added as internal standard. The mixture was filtered through a PVDF syringe filter to remove insoluble materials, and the filtrate was analyzed by ¹H and ¹⁹F NMR. Compound **2.2a** was observed in 60% yield, along with ca. 32% of 4-fluorobromobenzene.

The NMR sample was concentrated by rotary evaporation, and the residue was triturated with dichloromethane (3 \times 1 mL), then tetrahydrofuran (2 \times 2 mL) to yield a tan powder.

Analysis by ¹H and ¹⁹F NMR shows **2.2a** is the only Ar–TEDA product formed in significant amounts:

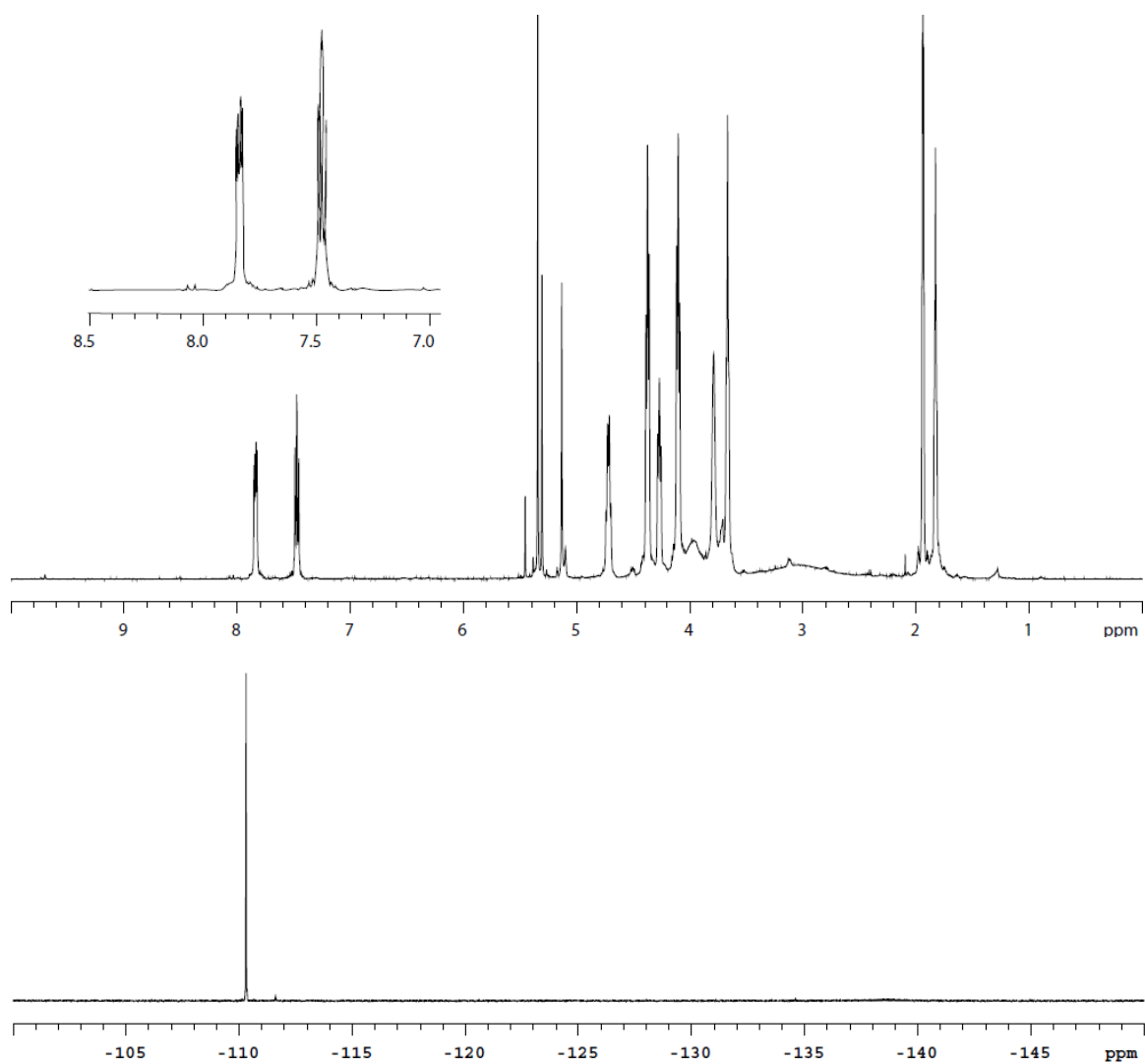
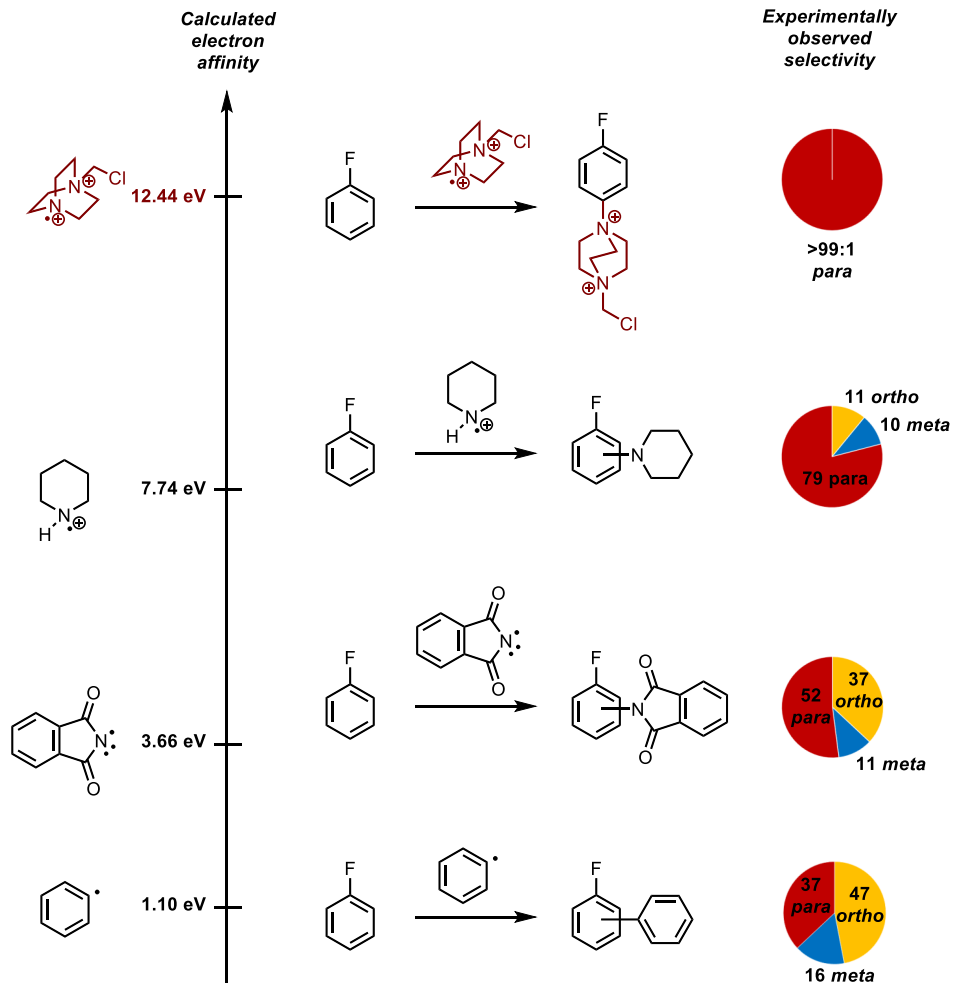


Figure 3.10. ^1H and ^{19}F NMR of **2.2a** synthesized via Cu catalysis (CD_3CN , 23°C)

Positional Selectivity as a Function of Electron Affinity: A Discussion



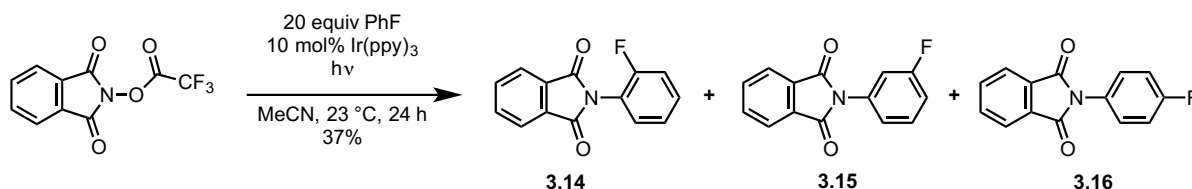
We argue in this work that the electron affinity of a radical has a strong effect on the positional selectivity exhibited by the radical in aromatic substitution, with higher electron affinity leading to higher selectivity for the *para* position of monosubstituted arenes. To illustrate this trend, we compare the selectivity of several radicals across a range of electron affinities in their aromatic substitution with fluorobenzene. It should be noted that electron affinity is not the only factor influencing positional selectivity. Different radicals with similar electron affinities may yield differing positional selectivity due to the influence of other factors, such as differing degrees of steric hinderance. Furthermore, the same radical may exhibit somewhat differing positional selectivities with the same substrate under varying experimental conditions.^{103c} Thus, to illustrate the general trend, we have chosen four radicals

with widely varying electron affinities, so that the influence of confounding factors is minimized:

- Phenyl radical: data taken from the work of Li *et al*¹⁰²
- Phthalimidyl radical: aromatic substitution carried out based on conditions reported by Sanford *et al*^{103a}
- Piperidine aminium radical: aromatic substitution carried out based on conditions reported by Minsci *et al*^{103b, 103c, 104}
- TEDA²⁺: the subject of this work

Full experimental procedures and characterization of products for the reactions of phthalimidyl radical and piperidine aminium radical are found in the sections below.

Aromatic substitution of fluorobenzene by phthalimidyl radical



In an N₂-filled glovebox, into a 4 mL vial were weighed N-trifluoroacetoxy phthalimide (13.0 mg, 50.2 μmol, 1.00 equiv) and tris(2-phenylpyridyl)iridium(III) (3.3 mg, 5.0 μmol, 10. mol%). Acetonitrile (1.0 mL) was then added, followed by fluorobenzene (94. μL, 1.0 mmol, 20 equiv). The vial was sealed, removed from the glovebox, and stirred magnetically for 24 hours at room temperature under irradiation by a 60 W desk lamp. The volatile components were removed by rotary evaporation. The residue was taken up in CD₃CN, and 2.0 μL (18.8 μmol) of 3-fluoronitrobenzene was added as internal standard. The mixture was filtered through a PVDF syringe filter to remove all insoluble materials, and the filtrate was analyzed by ¹⁹F NMR. The following amounts of **3.14**, **3.15**, and **3.16** were observed:

N-(2-fluorophenyl)phthalimide 7.1 μmol
(**3.14**)

N-(3-fluorophenyl)phthalimide 1.9 μmol

(3.15)

N-(4-fluorophenyl)phthalimide 9.7 μmol

(3.16)

The total yield is thus 18.7 μmol (37%), and the *ortho:meta:para* ratio is 37:11:52.

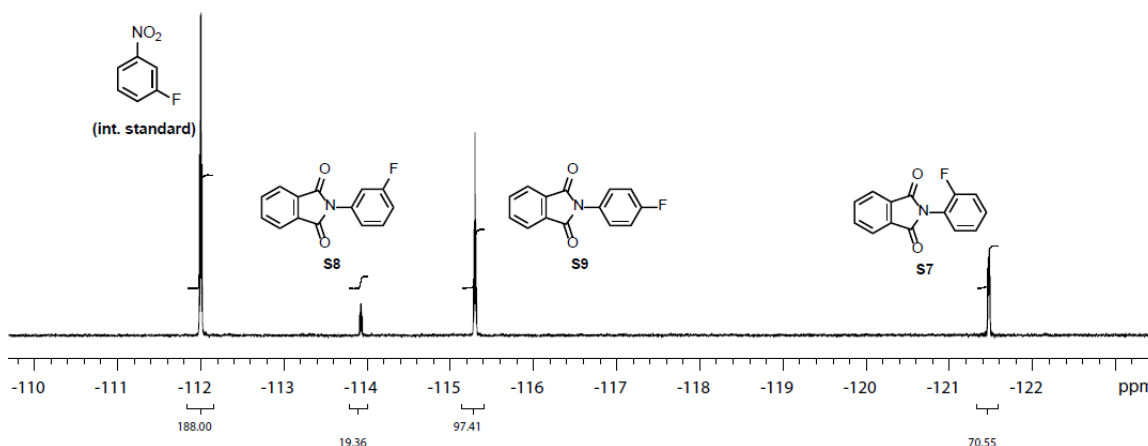
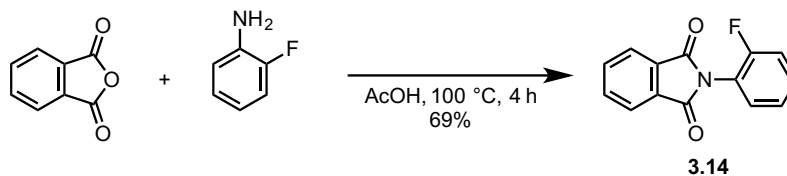


Figure 3.11. ^{19}F NMR analysis of product mixture of phthalimidyl radical substitution (CD_3CN , 23 °C)

Synthesis of authentic samples of 3.14, 3.15, and 3.16

N-(2-Fluorophenyl)-phthalimide (3.14)

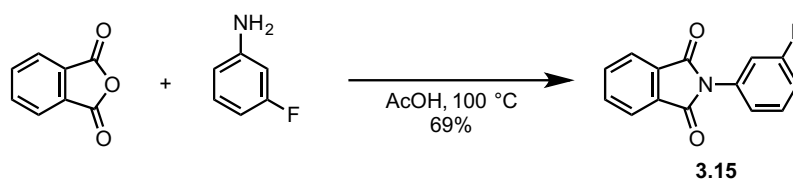


To a 20 mL vial were added phthalic anhydride (296. mg, 2.00 mmol, 1.00 equiv), acetic acid (5.0 mL), and 2-fluoroaniline (193. μL , 2.00 mmol, 1.00 equiv). The vial was sealed and magnetically stirred for 4 hr at 100 °C. The reaction mixture was allowed to come to room temperature, and 10 mL water was added to precipitate the product. The precipitate was collected by filtration, washed with water (4×10 mL), and dried *in vacuo* to yield 334. mg (1.38 mmol, 69%) of the title compound as a colorless powder.

NMR Spectroscopy: ^1H NMR (500 MHz, CD_3CN , 23 °C, δ): 7.97–7.93 (m, 2H), 7.90–7.86 (m, 2H), 7.57–7.51 (m, 1H), 7.49–7.44 (m, 1H), 7.39–7.32 (m, 2H). ^{13}C NMR (125 MHz, CDCl_3 , 23 °C, δ): 166.4 (s), 157.8 (d, $J = 252.7$ Hz), 134.4 (s), 131.8 (s), 130.7 (d, $J = 8.0$ Hz), 129.8 (d, $J = 0.9$ Hz), 124.6 (d, $J = 4.0$ Hz), 123.8 (s), 119.3 (d, $J = 13.2$ Hz), 116.7 (d, $J = 19.5$ Hz). ^{19}F NMR (470 MHz, CD_3CN , 23 °C, δ): –113.9.

Mass spectrometry: HRMS-FIA(m/z) calcd for $\text{C}_{14}\text{H}_9\text{FNO}_2$ $[\text{M}+\text{H}]^+$, 242.0612; found, 242.0613.

***N*-(3-Fluorophenyl)-phthalimide (3.15)**

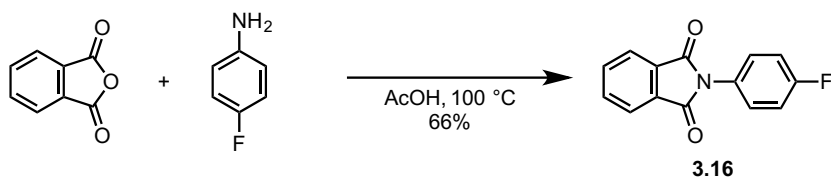


To a 20 mL vial were added phthalic anhydride (296. mg, 2.00 mmol, 1.00 equiv), acetic acid (5.0 mL), and 3-fluoroaniline (192. μL , 2.00 mmol, 1.00 equiv). The vial was sealed and magnetically stirred for 2 hr at 100 °C. The reaction mixture was allowed to come to room temperature, and 10 mL water was added to precipitate the product. The precipitate was collected by filtration, washed with water (4×10 mL), and dried *in vacuo* to yield 334. mg (1.38 mmol, 69%) of the title compound as a colorless powder.

NMR Spectroscopy: ^1H NMR (500 MHz, CD_3CN , 23 °C, δ): 7.96–7.92 (m, 2H), 7.89–7.85 (m, 2H), 7.55 (ddd, $J = 14.7, 8.3, 6.4$ Hz, 1H), 7.32 (ddd, $J = 8.0, 1.9, 0.9$ Hz, 1H), 7.28–7.24 (m, 1H), 7.21 (ddd, $J = 8.7, 2.6, 0.9$ Hz, 1H). ^{13}C NMR (125 MHz, CDCl_3 , 23 °C, δ): 166.8 (s), 162.6 (d, $J = 246.7$ Hz), 134.6 (s), 133.0 (d, $J = 10.3$ Hz), 131.5 (s), 130.2 (d, $J = 9.0$ Hz), 123.9 (s), 122.0 (d, $J = 3.5$ Hz), 115.0 (d, $J = 21.1$ Hz), 113.9 (d, $J = 24.7$ Hz). ^{19}F NMR (470 MHz, CD_3CN , 23 °C, δ): –121.5.

Mass spectrometry: HRMS-FIA(m/z) calcd for $\text{C}_{14}\text{H}_9\text{FNO}_2$ $[\text{M}+\text{H}]^+$, 242.0612; found, 242.0611.

***N*-(4-Fluorophenyl)-phthalimide (3.16)**

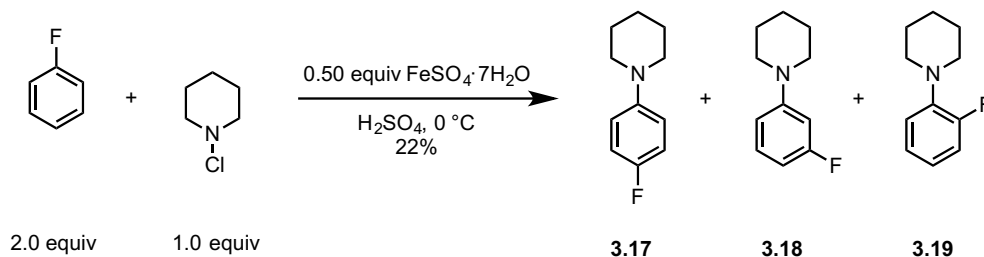


To a 20 mL vial were added phthalic anhydride (296. mg, 2.00 mmol, 1.00 equiv), acetic acid (5.0 mL), and 4-fluoroaniline (190. μ L, 2.00 mmol, 1.00 equiv). The vial was sealed and magnetically stirred for 2 hr at 100 °C. The reaction mixture was allowed to come to room temperature, and 10 mL water was added to precipitate the product. The precipitate was collected by filtration, washed with water (4×10 mL), and dried *in vacuo* to yield 319. mg (1.32 mmol, 66%) of the title compound as a tan powder.

NMR Spectroscopy: ^1H NMR (500 MHz, CD_3CN , 23 °C, δ): 7.94–7.90 (m, 2H), 7.88–7.84 (m, 2H), 7.48–7.43 (m, 2H), 7.30–7.25 (m, 2H). ^{13}C NMR (125 MHz, CDCl_3 , 23 °C, δ): 167.1 (s), 161.8 (d, $J = 247.6$ Hz), 134.4 (s), 131.5 (s), 128.3 (d, $J = 8.7$ Hz), 127.5 (d, $J = 3.2$ Hz), 123.7 (s), 116.1 (d, $J = 22.5$ Hz). ^{19}F NMR (470 MHz, CD_3CN , 23 °C, δ): –115.3.

Mass spectrometry: HRMS-FIA(m/z) calcd for $\text{C}_{14}\text{H}_9\text{FNO}_2$ $[\text{M}+\text{H}]^+$, 242.0612; found, 242.0615.

Aromatic substitution of fluorobenzene by piperidine aminium radical



To 2.00 g of concentrated sulfuric acid in a 20 mL vial at 0 °C were added 188. μ L of fluorobenzene (2.00 mmol, 2.00 equiv), 120. mg of *N*-chloropiperidine (1.00 mmol, 1.00 equiv), and finally 139. mg of pulverized ferrous sulfate heptahydrate (0.500 mmol, 0.500

equiv). The mixture rapidly turned brown upon addition of ferrous sulfate heptahydrate, and was stirred at 0 °C for 2 hours, after which significant beige precipitate was observed. The reaction mixture was poured onto ice and filtered through a glass frit. The acidic filtrate was extracted with diethyl ether (2 × 10 mL), then brought to pH 14 with 6 M NaOH. The basic mixture was extracted with dichloromethane (5 × 20 mL), until no more UV-active compound was observed in the organic extract. The combined organic layers were dried over Na₂SO₄ and concentrated to yield 39.1 mg of a brown oil (0.218 mmol, 22%). ¹⁹F NMR analysis revealed an *o*:*m*:*p* ratio of 11:10:79.

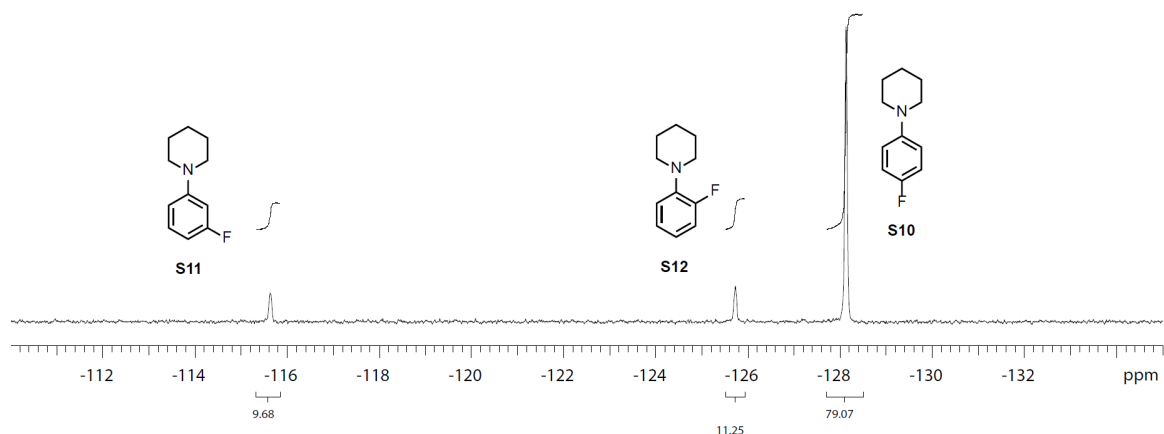
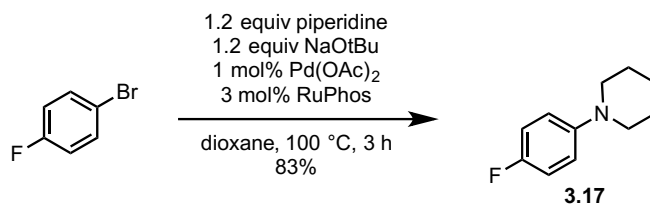


Figure 3.12. ¹⁹F NMR analysis of product mixture of piperidine aminium radical substitution (CDCl₃, 23 °C)

Synthesis of authentic samples of 3.17, 3.18, and 3.19

1-(4-Fluorophenyl)piperidine (3.17)



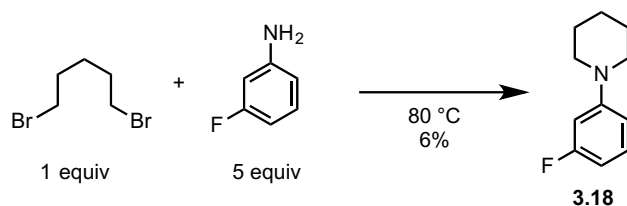
To a flame-dried 50 mL Schlenk flask were added 22.5 mg palladium acetate (22.5 mg, 0.100 mmol, 1.00 mol%), 140. mg RuPhos (0.300 mmol, 3.00 mol%), and 1.153 g of sodium tert-

butoxide (12.00 mmol, 1.20 equiv). The flask was sealed with a septum, then evacuated and refilled with N₂ three times. Anhydrous dioxane (10.0 mL) was added via syringe through the septum, followed by 1.75 g 4-fluorobromobenzene (10.0 mmol, 1.00 equiv) and 1.19 mL piperidine (12.0 mmol, 1.20 equiv). The mixture was degassed via N₂ sparge for 10 minutes, then heated at 100 °C for 3 hours. The reaction mixture was diluted with ethyl acetate to 50 mL, and filtered through celite to remove the precipitated palladium metal. The filtrate was washed with water (3 × 50 mL) and brine (2 × 50 mL), dried over NaSO₄, and concentrated. The residue was purified by flash chromatography on silica gel (hexanes → 19:1 hexanes:EtOAc) to yield 1.48 g of the title compound as a brown oil (8.28 mmol, 83%).

NMR Spectroscopy: ¹H NMR (500 MHz, CDCl₃, 23 °C, δ): 7.94–7.90 (m, 2H), 7.88–7.84 (m, 2H), 7.48–7.43 (m, 2H), 7.30–7.25 (m, 2H). ¹³C NMR (125 MHz, CDCl₃, 23 °C, δ): 167.1 (s), 161.8 (d, *J* = 247.6 Hz), 134.4 (s), 131.5 (s), 128.3 (d, *J* = 8.7 Hz), 127.5 (d, *J* = 3.2 Hz), 123.7 (s), 116.1 (d, *J* = 22.5 Hz). ¹⁹F NMR (470 MHz, CDCl₃, 23 °C, δ): –128.1.

Mass spectrometry: HRMS-FIA(*m/z*) calcd for C₁₁H₁₅FN [M+H]⁺, 180.1183; found, 180.1182.

1-(3-Fluorophenyl)piperidine (3.18)



To a 20 mL vial were added 0.55 mL 1,5-dibromopentane (4.0 mmol, 1.0 equiv) and 1.92 mL 3-fluoroaniline (20.0 mmol, 5.0 equiv). The vial was sealed, and the mixture was heated with stirring at 80 °C for 4 hours, after which the mixture was allowed to come to room temperature, and 10 mL of 6 M NaOH was added. The mixture was then extracted with diethyl ether (3 × 10 mL), and the combined organic layers were concentrated. To the

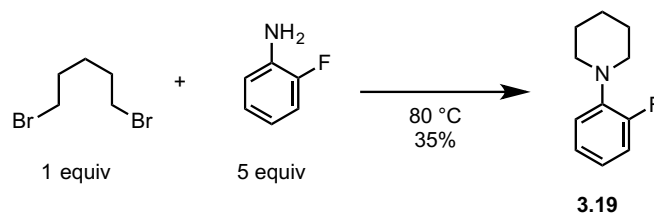
residue was added 10 mL Ac₂O, and the mixture was stirred for 30 minutes at room temperature. To the mixture was added 20 mL of 1 M HCl and 10 mL water. The mixture was extracted with dichloromethane (2 × 20 mL), then basified to pH 14 with 6 M NaOH. The basic mixture was extracted with dichloromethane (3 × 20 mL). The combined organic layers were dried over Na₂SO₄, and concentrated to give a brown oil. The brown oil was distilled with a Hickmann still to give 126. mg of a colorless oil.

To remove the remaining 3-fluoroacetanilide impurity, the oil was dissolved in 20 mL diethyl ether, and extracted with (3 × 10 mL) 0.1 M HCl. The combined acidic aqueous layers were basified to pH 14 with 6 M NaOH, then extracted with dichloromethane (3 × 10 mL). The combined organic layers were dried over Na₂SO₄ and concentrated to yield 40.0 mg of the title compound as a colorless liquid (0.223 mmol, 6%).

NMR Spectroscopy: ¹H NMR (500 MHz, CDCl₃, 23 °C, δ): 7.20–7.14 (m, 1H), 6.71–6.68 (m, 1H), 6.64–6.59 (m, 1H), 6.52–6.47 (m, 1H), 3.20–3.16 (m, 4H), 1.74–1.68 (m, 4H), 1.63–1.58 (m, 2H). ¹³C NMR (125 MHz, CDCl₃, 23 °C, δ): 163.9 (d, *J* = 242.6 Hz), 153.6 (d, 10.9 Hz), 129.9 (d, *J* = 10.1 Hz), 111.4 (d, *J* = 2.2 Hz), 105.1 (d, *J* = 21.6 Hz), 102.8 (d, *J* = 24.8 Hz), 50.0 (s), 25.5 (s), 24.2 (s). ¹⁹F NMR (470 MHz, CDCl₃, 23 °C, δ): –115.6.

Mass spectrometry: HRMS-FIA(*m/z*) calcd for C₁₁H₁₅FN [M+H]⁺, 180.1183; found, 180.1183.

1-(2-Fluorophenyl)piperidine (3.19)



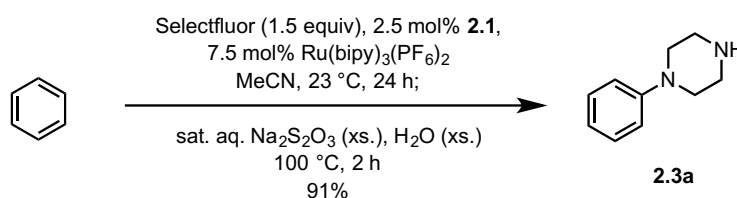
To a 20 mL vial were added 2.20 mL 1,5-dibromopentane (16.2 mmol, 1.00 equiv) and 7.80 mL 3-fluoroaniline (80.8 mmol, 5.00 equiv). The vial was sealed, and the mixture was

heated with stirring at 80 °C for 24 hours, after which the mixture was allowed to come to room temperature, and 20 mL of 1 M NaOH was added. The mixture was then extracted with dichloromethane (3 × 20 mL), and the combined organic layers were dried over Na₂SO₄, then concentrated. To the residue was added 50 mL Ac₂O, and the mixture was stirred for 2 hours at room temperature. To the solution was added 50 mL of 1 M HCl and ice. The mixture was extracted with dichloromethane (5 × 25 mL), then basified to pH 14 with 6 M NaOH. The basic mixture was extracted with dichloromethane (5 × 25 mL). The combined organic layers were dried over Na₂SO₄, and concentrated to give 994. mg of the title compound as a yellow oil (5.55 mmol, 35%).

NMR Spectroscopy: ¹H NMR (500 MHz, CDCl₃, 23 °C, δ): 7.09–6.97 (m, 3H), 6.95–6.90 (m, 1H), 3.07–3.04 (m, 4H), 1.81–1.76 (m, 4H), 1.64–1.58 (m, 2H). ¹³C NMR (125 MHz, CDCl₃, 23 °C, δ): 155.8 (d, *J* = 245.6 Hz), 141.3 (d, *J* = 8.4 Hz), 124.2 (d, *J* = 3.6 Hz), 121.9 (d, *J* = 7.9 Hz), 119.1 (d, *J* = 3.2 Hz), 115.8 (d, *J* = 21.1 Hz), 52.0 (s), 26.1 (s), 24.2 (s). ¹⁹F NMR (470 MHz, CDCl₃, 23 °C, δ): –125.7.

*Procedures for the preparation of aryl piperazines*¹²⁶

1-Phenylpiperazine (2.3a)



A 100 mL pressure tube was charged with palladium complex **2.1** (17.8 mg, 28.0 μmol, 2.50 mol%), Ru(bipy)₃(PF₆)₂ (72.1 mg, 83.9 μmol, 7.50 mol%), and Selectfluor (595. mg, 1.68 mmol, 1.50 equiv). Acetonitrile (5.6 mL, *c* = 0.20 M) was added, followed by benzene (100. μL, 1.12 mmol, 1.00 equiv) via syringe. The reaction mixture was stirred at 23 °C for 24 h. Saturated aqueous sodium thiosulfate (11 mL) and water (11 mL) were added, the pressure

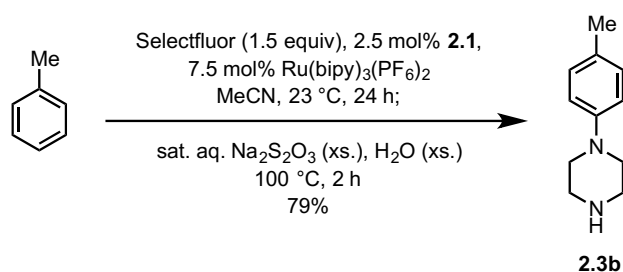
tube was sealed, and the reaction mixture was stirred at 100 °C for 2 h. After cooling to 23 °C, the reaction mixture was transferred to a separatory funnel. Dichloromethane (20 mL) and ethylenediamine (1.5 mL) were added and the organic layer was washed with 6 M aqueous sodium hydroxide (5 mL). The aqueous layer was extracted with dichloromethane (2 × 10 mL). The combined organic layers were extracted with 1 M aqueous hydrochloric acid (2 × 10 mL). Ethylenediamine (6.5 mL) was added to the combined acidic aqueous layers, followed by basification with 6 M aqueous sodium hydroxide (5 mL). The basic aqueous layer was extracted with dichloromethane (3 × 10 mL). The combined organic layers were dried over sodium sulfate, filtered, and concentrated *in vacuo* to afford a red oil (190. mg). The residue was purified by chromatography on silica gel eluting with a solvent mixture of dichloromethane/methanol/28% aqueous ammonium hydroxide (95.5/4.0/0.5 (v/v/v)) to afford 163. mg of the title compound as a yellow oil (91% yield).

R_f = 0.32 (dichloromethane/methanol/28% aqueous ammonium hydroxide 90.5:9.0:0.5 (v/v/v)).

NMR Spectroscopy: ^1H NMR (600 MHz, CDCl_3 , 23 °C, δ): 7.27 (dd, J = 9.0, 7.8 Hz, 2H), 6.94 (d, J = 7.8 Hz, 2H), 6.86 (t, J = 7.8 Hz, 1H), 3.14–3.16 (m, 4H), 3.03–3.05 (m, 4H), 1.65 (s, 1H). ^{13}C NMR (125 MHz, CDCl_3 , 23 °C, δ): 151.9, 129.2, 119.9, 116.3, 50.5, 46.3.

Mass Spectrometry: HRMS-FIA(m/z) calcd for $\text{C}_{10}\text{H}_{15}\text{N}_2$ $[\text{M}+\text{H}]^+$, 163.1230; found, 163.1238.

1-(*p*-Tolyl)piperazine (2.3b)



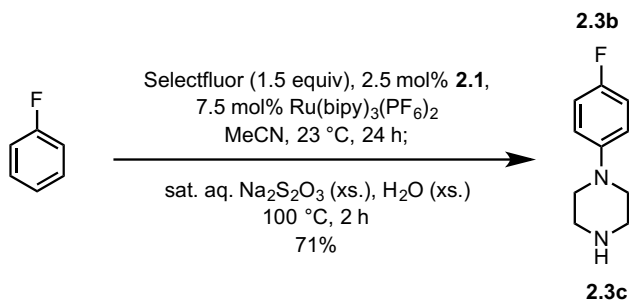
A 100 mL pressure tube was charged with palladium complex **2.1** (13.6 mg, 21.4 μ mol, 2.50 mol%), Ru(bipy)₃(PF₆)₂ (55.2 mg, 64.2 μ mol, 7.50 mol%), and Selectfluor (455. mg, 1.28 mmol, 1.50 equiv). Acetonitrile (4.3 mL, c = 0.20 M) was added, followed by toluene (91.1 μ L, 0.856 mmol, 1.00 equiv) via syringe. The reaction mixture was stirred at 23 °C for 24 h. Saturated aqueous sodium thiosulfate (8.6 mL) and water (8.6 mL) were added, the pressure tube was sealed, and the reaction mixture was stirred at 100 °C for 2 h. After cooling to 23 °C, the reaction mixture was transferred to a separatory funnel. Dichloromethane (20 mL) and ethylenediamine (1.5 mL) were added and the organic layer was washed with 6 M aqueous sodium hydroxide (5 mL). The aqueous layer was extracted with dichloromethane (2 \times 10 mL). The combined organic layers were extracted with 1 M aqueous hydrochloric acid (2 \times 15 mL). Ethylenediamine (5.0 mL) was added to the combined acidic aqueous layers, followed by basification with 6 M aqueous sodium hydroxide (8 mL). The basic aqueous layer was extracted with dichloromethane (3 \times 15 mL). The combined organic layers were dried over sodium sulfate, filtered, and concentrated *in vacuo* to afford a red oil (143. mg). The residue was purified by chromatography on silica gel eluting with a solvent mixture of dichloromethane/methanol/28% aqueous ammonium hydroxide (97.5/2.0/0.5 (v/v/v)) to afford 119. mg of the title compound as a yellow oil (79% yield).

R_f = 0.35 (dichloromethane/methanol/28% aqueous ammonium hydroxide 90.5:9.0:0.5 (v/v/v)).

NMR Spectroscopy: ¹H NMR (500 MHz, CDCl₃, 23 °C, δ): 7.07–7.09 (m, 2H), 6.84–6.86 (m, 2H), 3.07–3.10 (m, 4H), 3.01–3.04 (m, 4H), 2.28 (s, 3H), 1.68 (s, 1H). ¹³C NMR (125 MHz, CDCl₃, 23 °C, δ): 149.7, 129.7, 129.3, 116.5, 50.9, 46.1, 20.5.

Mass Spectrometry: HRMS-FIA(m/z) calcd for C₁₁H₁₇N₂ [M+H]⁺, 177.1386; found, 177.1387.

1-(4-Fluorophenyl)piperazine (2.3c)



A 100 mL pressure tube was charged with palladium complex **2.1** (17.0 mg, 26.6 μ mol, 2.50 mol%), Ru(bipy)₃(PF₆)₂ (68.7 mg, 80.0 μ mol, 7.50 mol%), and Selectfluor (566. mg, 1.60 mmol, 1.50 equiv). Acetonitrile (11 mL, c = 0.10 M) was added, followed by fluorobenzene (100. μ L, 1.06 mmol, 1.00 equiv) via syringe. The reaction mixture was stirred at 23 °C for 24 h. Saturated aqueous sodium thiosulfate (21 mL) and water (21 mL) were added, the pressure tube was sealed, and the reaction mixture was stirred at 100 °C for 2 h. After cooling to 23 °C, the reaction mixture was transferred to a separatory funnel.

Dichloromethane (30 mL) and ethylenediamine (1.5 mL) were added and the organic layer was washed with 6 M aqueous sodium hydroxide (5 mL). The aqueous layer was extracted with dichloromethane (2 \times 15 mL). The combined organic layers were extracted with 1 M aqueous hydrochloric acid (2 \times 15 mL). Ethylenediamine (6.5 mL) was added to the combined acidic aqueous layers, followed by basification with 6 M aqueous sodium hydroxide (5 mL). The basic aqueous layer was extracted with dichloromethane (3 \times 15 mL). The combined organic layers were dried over sodium sulfate, filtered, and concentrated *in vacuo* to afford a red oil (160. mg). The residue was purified by chromatography on silica gel eluting with a solvent mixture of dichloromethane/methanol/28% aqueous ammonium hydroxide (91.5/8.0/0.5 (v/v/v)) to afford 136. mg of the title compound as a yellow oil (71% yield).

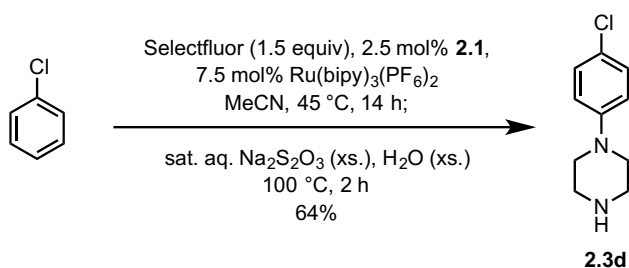
R_f = 0.14 (dichloromethane/methanol/28% aqueous ammonium hydroxide 91.5:8.0:0.5)

(v/v/v)).

NMR Spectroscopy: ^1H NMR (600 MHz, CDCl_3 , 23 °C, δ): 6.94–6.96 (m, 2H), 6.85–6.87 (m, 2H), 3.03–3.07 (m, 8H), 2.45 (s, 1H). ^{13}C NMR (125 MHz, CDCl_3 , 23 °C, δ): 157.3 (d, J = 238.8 Hz), 148.5 (d, J = 2.8 Hz), 118.0 (d, J = 7.7 Hz), 115.6 (d, J = 22.0 Hz), 51.4 (s), 46.1 (s). ^{19}F NMR (500 MHz, CDCl_3 , 23 °C, δ): –127.4.

Mass Spectrometry: HRMS-FIA(m/z) calcd for $\text{C}_{10}\text{H}_{14}\text{FN}_2$ [$\text{M}+\text{H}$] $^+$, 181.1136; found, 181.1128.

1-(4-Chlorophenyl)piperazine (2.3d)



A 100 mL pressure tube was charged with palladium complex **2.1** (15.6 mg, 24.6 μmol , 2.50 mol%), $\text{Ru}(\text{bipy})_3(\text{PF}_6)_2$ (63.3 mg, 73.7 μmol , 7.50 mol%), and Selectfluor (522 mg, 1.47 mmol, 1.50 equiv). Acetonitrile (4.9 mL, c = 0.20 M) was added, followed by chlorobenzene (100. μL , 0.982 mmol, 1.00 equiv) via syringe. The reaction mixture was stirred at 45 °C for 14 h. Saturated aqueous sodium thiosulfate (9.8 mL) and water (9.8 mL) were added, the pressure tube was sealed, and the reaction mixture was stirred at 100 °C for 2 h. After cooling to 23 °C, the reaction mixture was transferred to a separatory funnel.

Dichloromethane (20 mL), ethylenediamine (0.5 mL), and 6 M aqueous sodium hydroxide (5 mL) were added and the organic layer was separated. The aqueous layer was extracted with dichloromethane (2×15 mL). The combined organic layers were extracted with 1 M aqueous hydrochloric acid (3×10 mL). Ethylenediamine (5.0 mL) was added to the combined acidic aqueous layers, followed by basification with 6 M aqueous sodium

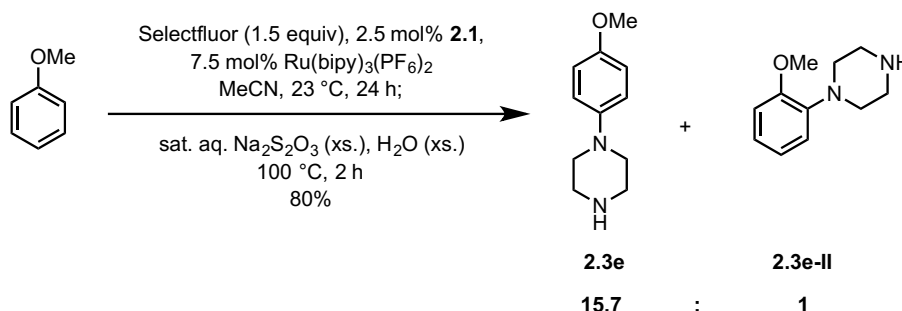
hydroxide (5 mL). The basic aqueous layer was extracted with dichloromethane (4×15 mL). The combined organic layers were dried over sodium sulfate, filtered, and concentrated *in vacuo* to afford a red solid (180. mg). The residue was purified by chromatography on silica gel eluting with a solvent mixture of dichloromethane/methanol/28% aqueous ammonium hydroxide (94.5/5.0/0.5 (v/v/v)) to afford a yellow solid (171. mg). The residue was further purified by preparatory HPLC with a solvent mixture of water/acetonitrile/trifluoroacetic acid (89.9/10.0/0.1 to 49.9/50.0/0.1 (v/v/v)) to afford 125. mg of the title compound as a bright yellow solid (64% yield).

R_f = 0.26 (dichloromethane/methanol/28% aqueous ammonium hydroxide 90.5:9.0:0.5 (v/v/v)).

NMR Spectroscopy: ^1H NMR (500 MHz, CDCl_3 , 23 °C, δ): 7.18–7.21 (m, 2H), 6.81–6.84 (m, 2H), 3.08–3.10 (m, 4H), 3.00–3.02 (m, 4H), 1.62 (s, 1H). ^{13}C NMR (500 MHz, CDCl_3 , 23 °C, δ): 150.6, 129.0, 124.6, 117.4, 50.5, 46.2.

Mass Spectrometry: HRMS-FIA(m/z) calcd for $\text{C}_{10}\text{H}_{14}\text{ClN}_2$ $[\text{M}+\text{H}]^+$, 197.0846; found, 197.0846.

1-(4-Methoxyphenyl)piperazine (2.3e)



A 100 mL pressure tube was charged with palladium complex **2.1** (14.6 mg, 23.0 μmol , 2.50 mol%), $\text{Ru}(\text{bipy})_3(\text{PF}_6)_2$ (59.3 mg, 69.0 μmol , 7.50 mol%), and Selectfluor (489. mg, 1.38 mmol, 1.50 equiv). Acetonitrile (4.6 mL, $c = 0.20$ M) was added, followed by anisole (100. μL , 0.920 mmol, 1.00 equiv) via syringe. The reaction mixture was stirred at 23 °C for 24 h.

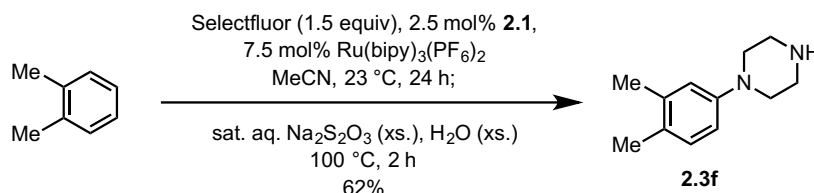
Saturated aqueous sodium thiosulfate (9.2 mL) and water (9.2 mL) were added, the pressure tube was sealed, and the reaction mixture was stirred at 100 °C for 2 h. After cooling to 23 °C, the reaction mixture was transferred to a separatory funnel. Dichloromethane (25 mL) and ethylenediamine (3.0 mL) were added and the organic layer was washed with 6 M aqueous sodium hydroxide (5 mL). The aqueous layer was extracted with dichloromethane (2 × 15 mL). The combined organic layers were extracted with 1 M aqueous hydrochloric acid (2 × 15 mL). Ethylenediamine (6.5 mL) was added to the combined acidic aqueous layers, followed by basification with 6 M aqueous sodium hydroxide (5 mL). The basic aqueous layer was extracted with dichloromethane (3 × 20 mL). The combined organic layers were dried over sodium sulfate, filtered, and concentrated *in vacuo* to afford a red oil (170. mg). The residue was purified by chromatography on silica gel eluting with a solvent mixture of dichloromethane/methanol/28% aqueous ammonium hydroxide (93.0/6.5/0.5 (v/v/v)) to afford 152. mg of the title compound as a light yellow solid (80% yield), containing 1-(2-methoxyphenyl)piperazine (6%). For characterization, 35. mg of the mixture was further purified by preparatory HPLC with a solvent mixture of water/acetonitrile/trifluoroacetic acid (89.9/10.0/0.1 to 69.9/30.0/0.1 (v/v/v)) to afford 23. mg of the title compound as an off-white solid.

R_f = 0.46 (dichloromethane/methanol/28% aqueous ammonium hydroxide 90.5:9.0:0.5 (v/v/v)).

NMR Spectroscopy: ^1H NMR (500 MHz, CDCl_3 , 23 °C, δ): 6.86–6.89 (m, 2H), 6.81–6.84 (m, 2H), 3.74 (s, 3H), 3.03 (s, 8H), 2.74 (s, 1H). ^{13}C NMR (125 MHz, CDCl_3 , 23 °C, δ): 153.9, 146.1, 118.4, 114.5, 55.6, 51.7, 46.1.

Mass Spectrometry: HRMS-FIA(m/z) calcd for $\text{C}_{11}\text{H}_{17}\text{N}_2\text{O}$ $[\text{M}+\text{H}]^+$, 193.1335; found, 193.1332.

1-(3,4-Dimethylphenyl)piperazine (2.3f)



A 100 mL pressure tube was charged with palladium complex **2.1** (13.2 mg, 20.7 μ mol, 2.50 mol%), Ru(bipy)₃(PF₆)₂ (53.4 mg, 62.1 μ mol, 7.50 mol%), and Selectfluor (440. mg, 1.24 mmol, 1.50 equiv). Acetonitrile (5.0 mL, c = 0.20 M) was added, followed by *o*-xylene (100. μ L, 1.00 mmol, 1.00 equiv) via syringe. The reaction mixture was stirred at 23 °C for 24 h. Saturated aqueous sodium thiosulfate (8.3 mL) and water (8.3 mL) were added, the pressure tube was sealed, and the reaction mixture was stirred at 100 °C for 2 h. After cooling to 23 °C, ethylenediamine (5.0 mL) and water (15 mL) were added, and the mixture was stirred for 1 h further. The reaction mixture was transferred to a separatory funnel.

Dichloromethane (20 mL) was added and the organic layer was separated. The aqueous layer was extracted with dichloromethane (2 \times 15 mL). The combined organic layers were extracted with 1 M aqueous hydrochloric acid (3 \times 10 mL). Ethylenediamine (2.0 mL) was added to the combined acidic aqueous layers, followed by basification with 6 M aqueous sodium hydroxide (6 mL). The basic aqueous layer was extracted with dichloromethane (3 \times 10 mL). The combined organic layers were dried over sodium sulfate, filtered, and concentrated *in vacuo* to afford a red solid (117. mg). The residue was purified by chromatography on silica gel eluting with a solvent mixture of dichloromethane/methanol/28% aqueous ammonium hydroxide (97.5/2.0/0.5 (v/v/v)) to afford 97.0 mg of the title compound as a yellow solid (62% yield).

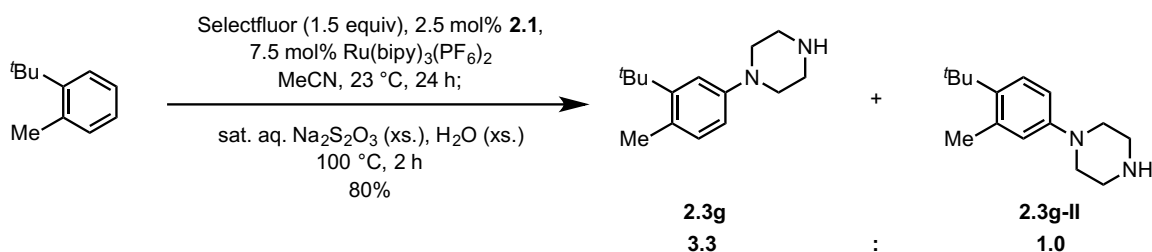
R_f = 0.32 (dichloromethane/methanol/28% aqueous ammonium hydroxide 90.5:9.0:0.5 (v/v/v)).

NMR Spectroscopy: ¹H NMR (600 MHz, CDCl₃, 23 °C, δ): 7.03 (d, J = 8.2 Hz, 1H), 6.76 (d,

$J = 2.6$ Hz, 1H), 6.69 (dd, $J = 8.2, 2.6$ Hz, 1H), 3.09 (m, 4H), 3.03 (m, 4H), 2.24 (s, 3H), 2.19 (s, 3H), 1.72 (s, 1H). ^{13}C NMR (125 MHz, CDCl_3 , 23 °C, δ): 150.3, 137.2, 130.2, 128.2, 118.2, 114.0, 51.2, 46.4, 20.3, 18.9.

Mass Spectrometry: HRMS-FIA(m/z) calcd for $\text{C}_{12}\text{H}_{19}\text{N}_2$ $[\text{M}+\text{H}]^+$, 191.1543; found, 191.1538.

1-(3-(*tert*-Butyl)-4-methylphenyl)piperazine (3g), 1-(4-(*tert*-Butyl)-3-methylphenyl)piperazine (2.3g-II)



A 100 mL pressure tube was charged with palladium complex **2.1** (7.16 mg, 11.2 μmol , 2.50 mol%), $\text{Ru}(\text{bipy})_3(\text{PF}_6)_2$ (29.0 mg, 33.8 μmol , 7.50 mol%), and Selectfluor (239. mg, 0.675 mmol, 1.50 equiv). Acetonitrile (2.2 mL, $c = 0.20$ M) was added, followed by 1-(*tert*-butyl)-2-methylbenzene (75.0 μL , 0.450 mmol, 1.00 equiv) via syringe. The reaction mixture was stirred at 23 °C for 24 h. Saturated aqueous sodium thiosulfate (4.5 mL) and water (4.5 mL) were added, the pressure tube was sealed, and the reaction mixture was stirred at 100 °C for 2 h. After cooling to 23 °C, the reaction mixture was transferred to a separatory funnel.

Dichloromethane (20 mL), ethylenediamine (0.5 mL), water (5 mL) and 6 M aqueous sodium hydroxide (0.5 mL) were added and the organic layer was separated. The aqueous layer was extracted with dichloromethane (2×15 mL). The combined organic layers were extracted with 1 M aqueous hydrochloric acid (3×10 mL). Ethylenediamine (2.0 mL) was added to the combined acidic aqueous layers, followed by basification with 6 M aqueous sodium hydroxide (5 mL). The basic aqueous layer was extracted with dichloromethane (3×15 mL). The combined organic layers were dried over sodium sulfate, filtered, and concentrated *in*

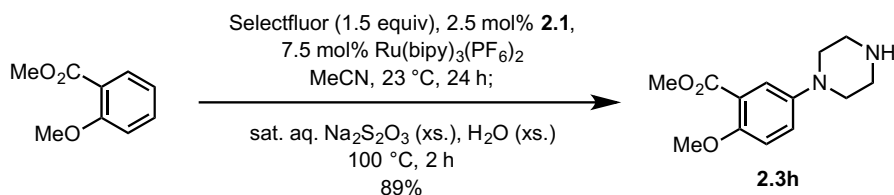
vacuo to afford a red oil (91.4 mg). The residue was purified by chromatography on silica gel eluting with a solvent mixture of dichloromethane/methanol/28% aqueous ammonium hydroxide (96.5/3.0/0.5 (v/v/v)) to afford 83.5 mg of the title compounds (**2.3g**:**2.3g-II** = 3.3 : 1.0) as a yellow oil (80% yield).

R_f = 0.25 (dichloromethane/methanol/28% aqueous ammonium hydroxide 90.5:9.0:0.5 (v/v/v)).

NMR Spectroscopy: ^1H NMR (600 MHz, CDCl_3 , 23 °C, δ): **2.3g** 7.01–7.03 (m, 2H), 6.68 (dd, J = 8.3, 2.6 Hz, 1H), 3.09–3.13 (m, 4H), 3.01–3.06 (m, 4H), 2.46 (s, 3H), 1.88 (s, 1H), 1.40 (s, 9H). **2.3g-II** 7.26 (d, J = 8.7 Hz, 1H), 6.67–6.72 (m, 2H), 3.09–3.13 (m, 4H), 3.01–3.06 (m, 4H), 2.51 (s, 3H), 1.38 (s, 9H). ^{13}C NMR (125 MHz, CDCl_3 , 23 °C, δ): 150.0, 149.6, 148.6, 139.5, 137.1, 133.4, 128.0, 126.9, 120.6, 115.6, 113.6, 113.0, 51.3, 50.4, 46.4, 46.3, 36.2, 35.2, 31.2, 30.8, 23.6, 22.5.

Mass Spectrometry: HRMS-FIA(m/z) calcd for $\text{C}_{15}\text{H}_{25}\text{N}_2$ $[\text{M}+\text{H}]^+$, 233.2012; found, 233.2022.

Methyl 2-methoxy-5-(piperazin-1-yl)benzoate (**2.3h**)



A 100 mL pressure tube was charged with palladium complex **2.1** (11.1 mg, 17.4 μmol , 2.50 mol%), $\text{Ru}(\text{bipy})_3(\text{PF}_6)_2$ (44.9 mg, 52.2 μmol , 7.50 mol%), and Selectfluor (370. mg, 1.04 mmol, 1.50 equiv). Acetonitrile (3.5 mL, c = 0.20 M) was added, followed by methyl 2-methoxybenzoate (100. μL , 0.700 mmol, 1.00 equiv) via syringe. The reaction mixture was stirred at 23 °C for 24 h. Saturated aqueous sodium thiosulfate (7.0 mL) and water (7.0 mL) were added, the pressure tube was sealed, and the reaction mixture was stirred at 100 °C for 2

h. After cooling to 23 °C, the reaction mixture was transferred to a separatory funnel.

Dichloromethane (20 mL) and ethylenediamine (0.3 mL) were added and the organic layer

was separated. The aqueous layer was extracted with dichloromethane (2 × 15 mL). The

combined organic layers were extracted with 10% aqueous glacial acetic acid (2 × 15 mL).

The combined acidic aqueous layers were basified with ethylenediamine (4.0 mL). The basic

aqueous layer was extracted with dichloromethane (3 × 15 mL). The combined organic

layers were dried over sodium sulfate, filtered, and concentrated *in vacuo* to afford a red oil

(175. mg). The residue was purified by chromatography on silica gel eluting with a solvent

mixture of dichloromethane/methanol/28% aqueous ammonium hydroxide (96.5/3.0/0.5

(v/v/v)) to afford 155. mg of the title compound as a yellow oil (89% yield).

R_f = 0.16 (dichloromethane/methanol/28% aqueous ammonium hydroxide 90.5:9.0:0.5

(v/v/v)).

NMR Spectroscopy: ^1H NMR (125 MHz, CDCl_3 , 23 °C, δ): 7.35 (d, J = 3.0 Hz, 1H), 7.03

(dd, J = 9.0, 3.0 Hz, 1H), 6.88 (d, J = 9.0 Hz, 1H), 3.85 (s, 3H), 3.82 (s, 3H), 2.98–3.03 (m,

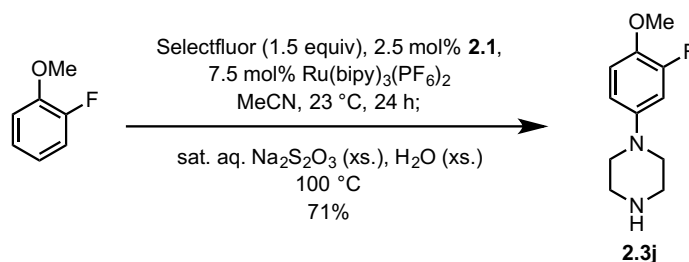
8H), 1.67 (s, 1H). ^{13}C NMR (500 MHz, CDCl_3 , 23 °C, δ): 166.9, 153.2, 145.6, 122.1, 120.3,

119.8, 113.5, 56.6, 52.1, 51.5, 46.2.

Mass Spectrometry: HRMS-FIA(m/z) calcd for $\text{C}_{13}\text{H}_{18}\text{N}_2\text{O}_3\text{Na}$ [$\text{M}+\text{Na}$] $^+$, 273.1210; found,

273.1207.

1-(3-Fluoro-4-methoxyphenyl)piperazine (2.3j)



A 100 mL pressure tube was charged with palladium complex **2.1** (15.9 mg, 25.0 μmol , 2.50

mol%), Ru(bipy)₃(PF₆)₂ (64.5 mg, 75.0 μmol, 7.50 mol%), Selectfluor (531.5 mg, 1.500 mmol, 1.50 equiv), and 2-fluoroanisole (112 μL, 1.00 mmol, 1.00 equiv). Acetonitrile (5.0 mL, c = 0.20 M) was added via syringe. The reaction mixture was stirred at 23 °C for 24 h. Saturated aqueous sodium thiosulfate (10 mL) and water (10 mL) were added, the pressure tube was sealed, and the reaction mixture was stirred at 100 °C for 1 h. After cooling to 23 °C, the reaction mixture was filtered through celite, and the filter cake was extracted with 5 × 15 mL acetonitrile and 2 × 15 mL water. The acetonitrile was removed from the filtrate by rotary evaporation. To the remaining aqueous mixture 0.50 mL ethylene diamine was added, and the aqueous mixture was basified to pH 14 with 6 M NaOH, then transferred to a separatory funnel. The aqueous layer was extracted with dichloromethane (5 × 15 mL). The combined organic layers were extracted with 1 M HCl (5 × 15 mL). To the combined acidic aqueous layers was added ethylene diamine (0.5 mL), and the mixture was basified to pH 14 with 6 M NaOH. The basic aqueous layer was extracted with dichloromethane (5 × 15 mL). The combined organic layers were dried over sodium sulfate, filtered, and concentrated *in vacuo* to afford a red oil. The residue was purified by chromatography on silica gel eluting with dichloromethane/methanol 9:1 (v/v) to afford 150. mg of the title compound as a brown oil (71% yield).

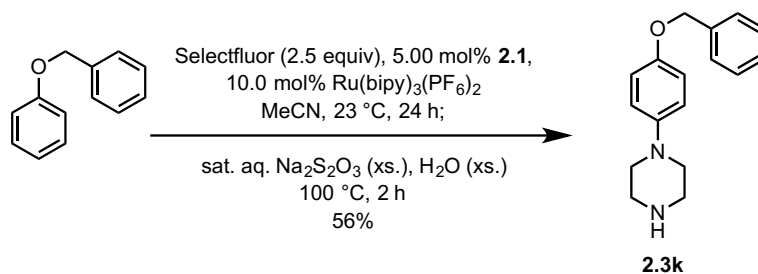
R_f = 0.28 (dichloromethane/methanol 9:1 (v/v)).

NMR Spectroscopy: ¹H NMR (500 MHz, CDCl₃, 23 °C, δ): 6.86 (dd, *J* = 9.1, 9.1 Hz, 1H), 6.69 (dd, *J* = 14.0, 2.8 Hz, 1H), 6.59 (m, 1H), 3.81 (s, 4H), 3.63 (br, 1H), 3.05 (s, 4H). ¹³C

NMR (125 MHz, CDCl₃, 23 °C, δ): 152.8 (d, *J* = 243.7 Hz), 146.3 (d, *J* = 7.8 Hz), 141.3 (d, *J* = 10.6 Hz), 114.6 (d, *J* = 2.9 Hz), 111.6 (d, *J* = 3.5 Hz), 105.7 (d, *J* = 21.1 Hz), 56.9 (s), 50.5 (s), 45.5 (s).

Mass Spectrometry: HRMS-FIA(*m/z*) calcd for C₁₁H₁₆FN₂O [M+H]⁺, 211.1247; found, 211.1245.

1-(4-(Benzyloxy)phenyl)piperazine (**2.3k**)



A 100 mL pressure tube was charged with palladium complex **2.1** (31.8 mg, 50.0 μ mol, 5.00 mol%), Ru(bipy)₃(PF₆)₂ (86.0 mg, 100. μ mol, 10.0 mol%), Selectfluor (886. mg, 2.50 mmol, 2.50 equiv), and benzyl phenyl ether (184. mg, 1.00 mmol, 1.00 equiv). Acetonitrile (5.0 mL, *c* = 0.20 M) was added via syringe. The reaction mixture was stirred at 23 °C for 24 h.

Saturated aqueous sodium thiosulfate (10 mL) and water (10 mL) were added, the pressure tube was sealed, and the reaction mixture was stirred at 100 °C for 2 h. After cooling to 23 °C, 0.5 mL ethylene diamine was added and the reaction mixture was basified to pH 14 with 6 M NaOH, then filtered through celite. The filter cake was extracted with acetonitrile (5 \times 15 mL). The acetonitrile was removed from the filtrate by rotary evaporation. The remaining aqueous mixture was transferred to a separatory funnel and extracted with dichloromethane (5 \times 15 mL). The combined organic layers were extracted with 1 M HCl (5 \times 15 mL). To the combined acidic aqueous layers was added ethylene diamine (0.5 mL), and the mixture was basified to pH 14 with 6 M NaOH. The basic aqueous layer was extracted with dichloromethane (5 \times 15 mL). The combined organic layers were dried over sodium sulfate, filtered, and concentrated *in vacuo* to afford a red oil. The residue was purified by chromatography on silica gel eluting with dichloromethane/methanol 19:1 \rightarrow 9:1 (v/v) to afford 151. mg of the title compound as an off-white powder (56% yield).

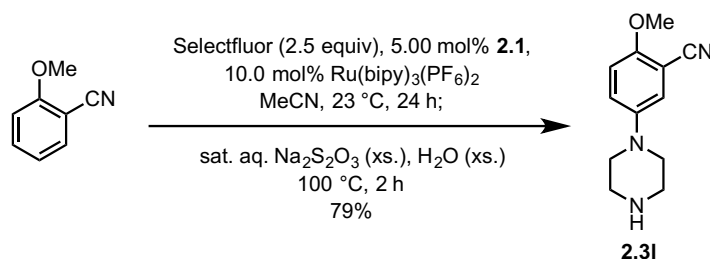
*R*_f = 0.35 (dichloromethane/methanol 9:1 (v/v)).

NMR Spectroscopy: ¹H NMR (600 MHz, CDCl₃, 23 °C, δ): 7.44–7.41 (m, 2H), 7.40–7.33 (m, 2H), 7.34–7.30 (m, 1H), 6.94–6.88 (m, 4H), 5.02 (s, 2H), 3.07 (s, 8H). ¹³C NMR (125 MHz,

CDCl₃, 23 °C, δ): 153.1, 146.2, 137.3, 128.5, 127.8, 127.5, 118.3, 115.6, 70.5, 51.4, 46.0.

Mass Spectrometry: HRMS-FIA(m/z) calcd for C₁₇H₂₁N₂O [M+H]⁺, 269.1648; found, 269.1635.

2-Methoxy-5-(piperazin-1-yl)benzonitrile (2.3I)



A 100 mL pressure tube was charged with palladium complex **1** (31.8 mg, 50.0 μmol, 5.00 mol%), Ru(bipy)₃(PF₆)₂ (86.0 mg, 100. μmol, 10.0 mol%), Selectfluor (886. mg, 2.50 mmol, 2.50 equiv), and 2-methoxybenzonitrile (122. μL, 1.00 mmol, 1.00 equiv). Acetonitrile (5.0 mL, c = 0.20 M) was added via syringe. The reaction mixture was stirred at 23 °C for 24 h. Saturated aqueous sodium thiosulfate (10 mL) and water (10 mL) were added, the pressure tube was sealed, and the reaction mixture was stirred at 100 °C for 2 h. After cooling to 23 °C, 0.5 mL ethylene diamine was added and the reaction mixture was basified to pH 14 with 6 M NaOH, then filtered through celite. The filter cake was extracted with acetonitrile (5 × 15 mL). The acetonitrile was removed from the filtrate by rotary evaporation. The remaining aqueous mixture was transferred to a separatory funnel and extracted with dichloromethane (5 × 15 mL), then 9:1 dichloromethane/methanol (v/v) (3 × 15 mL). The combined organic layers were extracted with 1 M HCl (5 × 15 mL). To the combined acidic aqueous layers was added ethylene diamine (0.5 mL), and the mixture was basified to pH 14 with 6 M NaOH. The basic aqueous layer was extracted with 9:1 dichloromethane/methanol (v/v) (6 × 15 mL). The combined organic layers were dried over sodium sulfate, filtered, and concentrated *in vacuo* to afford a red oil. The residue was purified by chromatography on

silica gel eluting with dichloromethane/methanol 9:1 (v/v) to afford 190. mg of the title compound as a brown oil (79% yield).

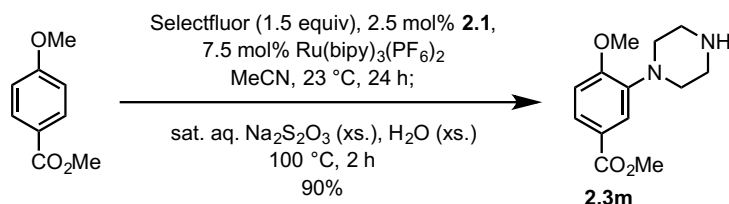
R_f = 0.31 (dichloromethane/methanol 9:1 (v/v)).

NMR Spectroscopy: ^1H NMR (500 MHz, CDCl_3 , 23 °C, δ): 7.12 (dd, J = 9.1, 3.1 Hz, 1H), 7.07 (d, J = 3.1 Hz, 1H), 6.88 (d, J = 9.1 Hz, 1H), 3.86 (s, 4H), 3.04 (s, 4H), 2.56 (br, 1H).

^{13}C NMR (125 MHz, CDCl_3 , 23 °C, δ): 155.2, 145.8, 123.2, 121.1, 116.7, 112.3, 101.7, 56.2, 50.9, 40.8.

Mass Spectrometry: HRMS-FIA(m/z) calcd for $\text{C}_{12}\text{H}_{16}\text{N}_3\text{O}$ $[\text{M}+\text{H}]^+$, 218.1293; found, 218.1300.

Methyl 4-methoxy-3-(piperazin-1-yl)benzoate (2.3m)



A 100 mL pressure tube was charged with palladium complex **2.1** (15.9 mg, 25.0 μmol , 2.50 mol%), $\text{Ru}(\text{bipy})_3(\text{PF}_6)_2$ (64.5 mg, 75.0 μmol , 7.50 mol%), Selectfluor (531. mg, 1.50 mmol, 1.50 equiv), and methyl 4-methoxybenzoate (166. mg, 1.00 mmol, 1.00 equiv). Acetonitrile (5.0 mL, c = 0.20 M) was added via syringe. The reaction mixture was stirred at 23 °C for 24 h. Saturated aqueous sodium thiosulfate (10 mL) and water (10 mL) were added, the pressure tube was sealed, and the reaction mixture was stirred at 100 °C for 2 h. After cooling to 23 °C, ethylenediamine (1.5 mL) and water (15 mL) were added, and the mixture was stirred for 1 h further. The reaction mixture was transferred to a separatory funnel. Dichloromethane (20 mL) was added and the organic layer was separated. The aqueous layer was extracted with dichloromethane (2×15 mL). The combined organic layers were extracted with 10% aqueous glacial acetic acid (2×15 mL). The combined acidic aqueous

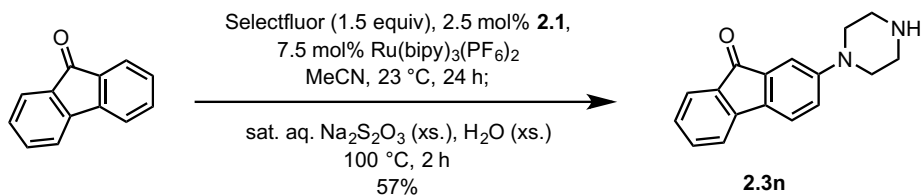
layers were basified with ethylenediamine (4.5 mL). The basic aqueous layer was extracted with dichloromethane (3 × 15 mL). The combined organic layers were dried over sodium sulfate, filtered, and concentrated *in vacuo* to afford a red oil (252. mg). The residue was purified by chromatography on silica gel eluting with a solvent mixture of dichloromethane/methanol/28% aqueous ammonium hydroxide (91.5/8.0/0.5 (v/v/v)) to afford 226. mg of the title compound as a yellow solid (90% yield).

R_f = 0.16 (dichloromethane/methanol/28% aqueous ammonium hydroxide 90.5:9.0:0.5 (v/v/v)).

NMR Spectroscopy: ^1H NMR (600 MHz, CDCl_3 , 23 °C, δ): 7.74 (dd, J = 8.1, 2.1 Hz, 1H), 7.61 (d, J = 2.4 Hz, 1H), 6.88 (d, J = 8.4 Hz, 1H), 3.92 (s, 3H), 3.88 (s, 3H), 3.09–3.11 (m, 8H), 1.67 (s, 1H). ^{13}C NMR (125 MHz, CDCl_3 , 23 °C, δ): 167.1, 156.2, 141.3, 125.6, 122.9, 119.7, 110.5, 55.8, 52.0, 51.6, 46.0.

Mass Spectrometry: HRMS-FIA (m/z) calcd for $\text{C}_{13}\text{H}_{18}\text{N}_2\text{O}_3\text{Na}$ $[\text{M}+\text{Na}]^+$, 273.1210; found, 273.1215.

2-(Piperazin-1-yl)-9H-fluoren-9-one (2.3n)



A 100 mL pressure tube was charged with palladium complex **2.1** (8.83 mg, 13.9 μmol , 2.50 mol%), $\text{Ru}(\text{bipy})_3(\text{PF}_6)_2$ (35.8 mg, 41.6 μmol , 7.50 mol%), Selectfluor (295. mg, 0.832 mmol, 1.50 equiv), and fluorenone (100. mg, 0.555 mmol, 1.00 equiv). Acetonitrile (2.8 mL, c = 0.20 M) was added via syringe. The reaction mixture was stirred at 23 °C for 24 h. Saturated aqueous sodium thiosulfate (5.5 mL) and water (5.5 mL) were added, the pressure tube was sealed, and the reaction mixture was stirred at 100 °C for 2 h. After cooling to 23 °C, the

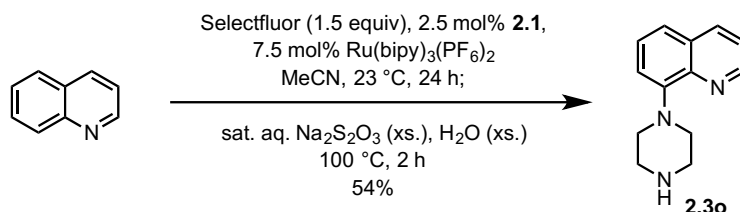
reaction mixture was transferred to a separatory funnel. Dichloromethane (20 mL) and ethylenediamine (0.3 mL) were added and the organic layer was separated. The aqueous layer was extracted with dichloromethane (3×15 mL). The combined organic layers were extracted with 10% aqueous glacial acetic acid (3×15 mL). Ethylenediamine (3.0 mL) was added to the combined acidic aqueous layers, followed by basification with saturated aqueous sodium carbonate (5 mL). The basic aqueous layer was extracted with dichloromethane (4×15 mL). The combined organic layers were dried over sodium sulfate, filtered, and concentrated *in vacuo* to afford a red solid (102. mg). The residue was purified by chromatography on silica gel eluting with a solvent mixture of dichloromethane/methanol/28% aqueous ammonium hydroxide (96.0/3.5/0.5 (v/v/v)) to afford 83.1 mg of the title compound as a yellow solid (57% yield).

$R_f = 0.34$ (dichloromethane/methanol/28% aqueous ammonium hydroxide 90.5:9.0:0.5 (v/v/v)).

NMR Spectroscopy: ^1H NMR (600 MHz, CDCl_3 , 23 °C, δ): 7.57 (d, $J = 7.3$ Hz, 1H), 7.40 (td, $J = 7.4$, 1.1 Hz, 1H), 7.34–7.36 (m, 2H), 7.23 (d, $J = 2.4$ Hz, 1H), 7.15 (td, $J = 7.4$, 1.1 Hz, 1H), 6.93 (dd, $J = 8.2$, 2.4 Hz, 1H), 3.19–3.21 (m, 4H), 3.02–3.04 (m, 4H), 1.74 (s, 1H). ^{13}C NMR (125 MHz, CDCl_3 , 23 °C, δ): 194.6, 152.9, 145.4, 135.7, 135.1, 134.9, 134.4, 127.6, 124.3, 121.2, 120.5, 119.5, 111.9, 50.1, 46.1.

Mass Spectrometry: HRMS-FIA(m/z) calcd for $\text{C}_{17}\text{H}_{17}\text{N}_2\text{O}$ $[\text{M}+\text{H}]^+$, 265.1335; found, 265.1341.

8-(Piperazin-1-yl)quinoline (2.3o)



A 100 mL pressure tube was charged with palladium complex **2.1** (13.5 mg, 21.2 μmol , 2.50 mol%), $\text{Ru}(\text{bipy})_3(\text{PF}_6)_2$ (54.6 mg, 63.5 μmol , 7.50 mol%), and Selectfluor (450. mg, 1.27 mmol, 1.50 equiv). Acetonitrile (4.2 mL, $c = 0.20 \text{ M}$) was added, followed by quinoline (100. μL , 84.6 mmol, 1.00 equiv) via syringe. The reaction mixture was stirred at 23 $^\circ\text{C}$ for 24 h. Saturated aqueous sodium thiosulfate (8.5 mL) and water (8.5 mL) were added, the pressure tube was sealed, and the reaction mixture was stirred at 100 $^\circ\text{C}$ for 2 h. After cooling to 23 $^\circ\text{C}$, the reaction mixture was transferred to a separatory funnel. Dichloromethane (20 mL) and ethylenediamine (2.5 mL) were added and the organic layer was washed with 6 M aqueous sodium hydroxide (5 mL). The aqueous layer was extracted with dichloromethane ($2 \times 15 \text{ mL}$). The combined organic layers were extracted with 1 M aqueous hydrochloric acid ($2 \times 15 \text{ mL}$). Ethylenediamine (5.0 mL) was added to the combined acidic aqueous layers, followed by basification with 6 M aqueous sodium hydroxide (5 mL). The basic aqueous layer was extracted with dichloromethane ($3 \times 15 \text{ mL}$). The combined organic layers were dried over sodium sulfate, filtered, and concentrated *in vacuo* to afford a red oil (137. mg). The residue was purified by chromatography on silica gel eluting with a solvent mixture of dichloromethane/methanol/28% aqueous ammonium hydroxide (91.5/8.0/0.5 (v/v/v)) to afford 98.2 mg of the title compound as a yellow oil (54% yield).

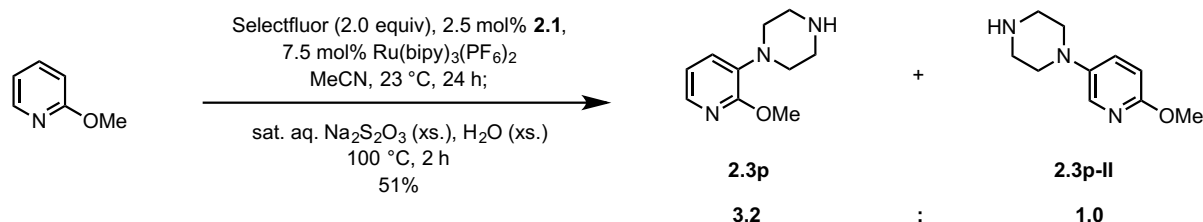
$R_f = 0.18$ (dichloromethane/methanol/28% aqueous ammonium hydroxide 90.5:9.0:0.5 (v/v/v)).

NMR Spectroscopy: ^1H NMR (600 MHz, CDCl_3 , 23 $^\circ\text{C}$, δ): 8.86 (dd, $J = 4.1, 1.8 \text{ Hz}$, 1H), 8.08 (dd, $J = 8.2, 1.8 \text{ Hz}$, 1H), 7.42–7.44 (m, 2H), 7.34 (dd, $J = 8.2, 4.1 \text{ Hz}$, 1H), 7.12 (dd, $J = 6.5, 2.4 \text{ Hz}$, 1H). ^{13}C NMR (125 MHz, CDCl_3 , 23 $^\circ\text{C}$, δ): 149.8, 148.3, 142.8, 136.6, 129.7, 126.8, 121.8, 120.9, 116.1, 53.2, 46.2.

Mass Spectrometry: HRMS-FIA(m/z) calcd for $\text{C}_{13}\text{H}_{16}\text{N}_3$ $[\text{M}+\text{H}]^+$, 214.1339; found, 214.1328.

1-(2-Methoxypyridin-3-yl)piperazine (2.3p), 1-(6-methoxypyridin-3-yl)piperazine (2.3p-II)

II)



A 100 mL pressure tube was charged with palladium complex **2.1** (15.1 mg, 23.8 μmol , 2.50 mol%), $\text{Ru}(\text{bipy})_3(\text{PF}_6)_2$ (61.3 mg, 71.3 μmol , 7.50 mol%), and Selectfluor (674. mg, 1.90 mmol, 2.00 equiv). Acetonitrile (4.8 mL, $c = 0.20 \text{ M}$) was added, followed by 2-methoxypyridine (100. μL , 0.951 mmol, 1.00 equiv) via syringe. The reaction mixture was stirred at 23 °C for 24 h. Saturated aqueous sodium thiosulfate (9.5 mL) and water (9.5 mL) were added, the pressure tube was sealed, and the reaction mixture was stirred at 100 °C for 2 h. After cooling to 23 °C, the reaction mixture was transferred to a separatory funnel. Dichloromethane (15 mL) and ethylenediamine (2.5 mL) were added and the organic layer was washed with 6 M aqueous sodium hydroxide (5 mL). Volume of the aqueous layer was reduced by half and then the aqueous layer was extracted with dichloromethane ($2 \times 15 \text{ mL}$) and then mixture of dichloromethane/methanol (9.0/1.0 (v/v), $3 \times 15 \text{ mL}$). The combined organic layers were extracted with 1 M aqueous hydrochloric acid ($3 \times 15 \text{ mL}$). Ethylenediamine (5.0 mL) was added to the combined acidic aqueous layers, followed by basification with 6 M aqueous sodium hydroxide (5 mL). The basic aqueous layer was extracted with dichloromethane ($2 \times 15 \text{ mL}$) and then mixture of dichloromethane/methanol (9.0/1.0 (v/v), $3 \times 15 \text{ mL}$). The combined organic layers were dried over sodium sulfate, filtered, and concentrated *in vacuo* to afford a red oil (120. mg). The residue was purified by chromatography on silica gel eluting with a solvent mixture of dichloromethane/methanol/28% aqueous ammonium hydroxide (96.0/3.5/0.5 (v/v/v)) to

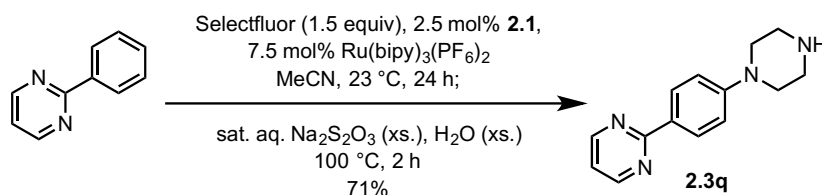
afford 94.5 mg of the title compounds (**2.3p**:**2.3p-II** = 3.2:1.0) as a yellow oil (51% yield).

R_f = 0.16 (dichloromethane/methanol/28% aqueous ammonium hydroxide 90.5:9.0:0.5 (v/v/v)).

NMR Spectroscopy: ^1H NMR (600 MHz, CDCl_3 , 23 °C, δ): **2.3p** 7.76 (dd, J = 4.9, 1.7 Hz, 1H), 7.05 (dd, J = 7.7, 1.7 Hz, 1H), 6.80 (dd, J = 7.7, 4.9 Hz, 1H), 3.95 (s, 3H), 2.98–3.02 (m, 8H), 2.19 (s, 1H). **2.3p-II** 7.74 (d, J = 3.0 Hz, 1H), 7.24 (dd, J = 8.9, 3.0 Hz, 1H), 6.64 (d, J = 8.9 Hz, 1H), 3.84 (s, 3H), 2.98–3.02 (m, 8H), 2.19 (s, 1H). ^{13}C NMR (500 MHz, CDCl_3 , 23 °C, δ): **2.3p** 156.9, 139.0, 136.6, 124.7, 117.1, 53.4, 51.3, 46.1. **2.3p-II** 158.9, 142.9, 134.6, 129.8, 110.7, 53.4, 51.6, 46.1.

Mass Spectrometry: HRMS-FIA(m/z) calcd for $\text{C}_{10}\text{H}_{16}\text{N}_3\text{O}$ $[\text{M}+\text{H}]^+$, 194.1293; found, 194.1295.

2-(4-(Piperazin-1-yl)phenyl)pyrimidine (**2.3q**)



A 100 mL pressure tube was charged with palladium complex **2.1** (15.9 mg, 25.0 μmol , 2.50 mol%), $\text{Ru}(\text{bipy})_3(\text{PF}_6)_2$ (64.5 mg, 75.0 μmol , 7.50 mol%), Selectfluor (531. mg, 1.50 mmol, 1.50 equiv), and 2-phenylpyrimidine (156. mg, 1.00 mmol, 1.00 equiv). Acetonitrile (5.0 mL, c = 0.20 M) was added via syringe. The reaction mixture was stirred at 23 °C for 24 h. Saturated aqueous sodium thiosulfate (10 mL) and water (10 mL) were added, the pressure tube was sealed, and the reaction mixture was stirred at 100 °C for 2 h. After cooling to 23 °C, the reaction mixture was basified with aqueous 6 M sodium hydroxide solution (10 mL) and ethylenediamine (0.5 mL), filtered through celite rinsing with acetonitrile (5×15 mL), and acetonitrile removed *in vacuo* to afford a brown aqueous solution. The aqueous

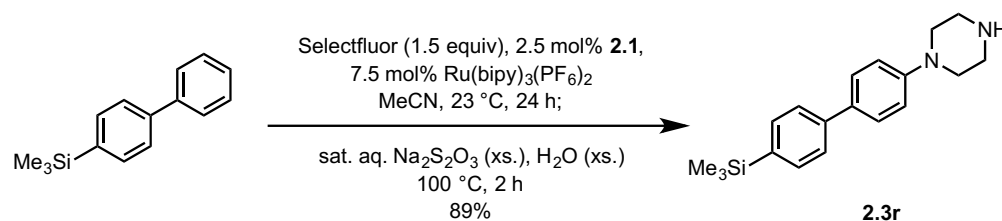
layer was transferred to a separatory funnel and extracted with a solvent mixture of methanol/dichloromethane (1/9 (v/v), 5 × 15 mL). The combined organic layers were extracted with aqueous 1M hydrochloric acid solution (3 × 15 mL). The combined acidic aqueous layers were basified to pH 14 with aqueous 6M sodium hydroxide solution and ethylenediamine (0.5 mL). The basic aqueous layer was extracted with a solvent mixture of methanol/dichloromethane (1/9 (v/v), 5 × 15 mL). The organic layers were dried over sodium sulfate, filtered, and concentrated *in vacuo* to afford a red oil. The residue was purified by chromatography on silica gel eluting with a solvent mixture of dichloromethane/methanol (9/1 (v/v)) to afford 171. mg of the title compound as an off-white solid (71% yield).

R_f = 0.08 (dichloromethane/methanol/28% aqueous ammonium hydroxide 90.5:9.0:0.5 (v/v/v)).

NMR Spectroscopy: ^1H NMR (500 MHz, DMSO- d_6 , 23 °C, δ): 8.77 (d, J = 5.0 Hz, 2H), 8.23 (d, J = 9.5 Hz, 2H), 7.27 (t, J = 4.5 Hz, 1H), 7.00 (d, J = 8.5 Hz, 2H), 3.21 (t, J = 5.0 Hz, 4H), 2.86 (t, J = 5.0 Hz, 4H). ^{13}C NMR (125 MHz, DMSO- d_6 , 23 °C, δ): 163.5, 157.4, 153.0, 128.8, 126.7, 118.4, 114.1, 47.9, 45.2.

Mass Spectrometry: HRMS-FIA(m/z) calcd for $\text{C}_{14}\text{H}_{17}\text{N}_4$ $[\text{M}+\text{H}]^+$, 241.1448; found, 241.1457.

1-(4'-(Trimethylsilyl)-[1,1'-biphenyl]-4-yl)piperazine (2.3r)



A 100 mL pressure tube was charged with palladium complex **2.1** (7.03 mg, 11.0 μmol , 2.50 mol%), $\text{Ru}(\text{bipy})_3(\text{PF}_6)_2$ (28.5 mg, 33.1 μmol , 7.50 mol%), Selectfluor (235. mg, 0.662 mmol,

1.50 equiv), and [1,1'-biphenyl]-4-yltrimethylsilane (100. mg, 0.442 mmol, 1.00 equiv). Acetonitrile (2.2 mL, $c = 0.20$ M) was added via syringe. The reaction mixture was stirred at 23 °C for 24 h. Saturated aqueous sodium thiosulfate (10 mL) and water (10 mL) were added, the pressure tube was sealed, and the reaction mixture was stirred at 100 °C for 2 h. After cooling to 23 °C, ethylenediamine (2.5 mL) and water (20 mL) were added, and the mixture was stirred for 1 h further. The reaction mixture was transferred to a separatory funnel. Dichloromethane (20 mL) was added and the organic layer was separated. The aqueous layer was extracted with dichloromethane (3×15 mL). The combined organic layers were dried over sodium sulfate, filtered, and concentrated *in vacuo* to afford a red oil (220. mg). The residue was purified by chromatography on silica gel eluting with a solvent mixture of dichloromethane/methanol/28% aqueous ammonium hydroxide (97.5/2.0/0.5 (v/v/v)) to afford 122. mg of the title compound as a yellow solid (89% yield).

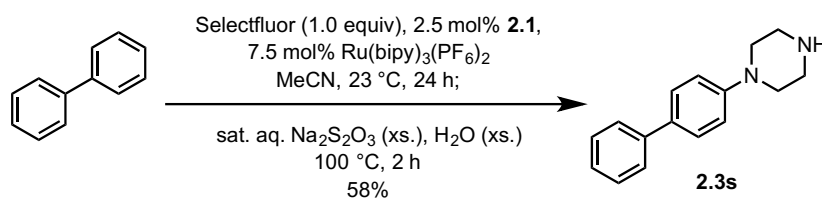
$R_f = 0.31$ (dichloromethane/methanol/28% aqueous ammonium hydroxide 90.5:9.0:0.5 (v/v/v)).

NMR Spectroscopy: ^1H NMR (600 MHz, CDCl_3 , 23 °C, δ): 7.56–7.60 (m, 4H), 7.53–7.55 (m, 2H), 6.99–7.02 (m, 2H), 3.21–3.23 (m, 4H), 3.06–3.08 (m, 4H), 2.16 (s, 1H), 0.31 (s, 9H).

^{13}C NMR (125 MHz, CDCl_3 , 23 °C, δ): 151.2, 141.4, 138.2, 133.9, 132.3, 127.8, 125.9, 116.2, 50.2, 46.2, -0.9.

Mass Spectrometry: HRMS-FIA(m/z) calcd for $\text{C}_{19}\text{H}_{27}\text{N}_2\text{Si}$ $[\text{M}+\text{H}]^+$, 311.1938; found, 311.1950.

1-([1,1'-Biphenyl]-4-yl)piperazine (2.3s)



A 100 mL pressure tube was charged with palladium complex **2.1** (15.9 mg, 25.0 μmol , 2.50 mol%), $\text{Ru}(\text{bipy})_3(\text{PF}_6)_2$ (64.5 mg, 75.0 μmol , 7.50 mol%), Selectfluor (531. mg, 1.00 mmol, 1.00 equiv), and 1,1'-biphenyl (154. mg, 1.00 mmol, 1.00 equiv). Acetonitrile (5.0 mL, $c = 0.20 \text{ M}$) was added via syringe. The reaction mixture was stirred at 23 °C for 24 h. An aliquot was removed, concentrated, redissolved in CD_3CN , and analyzed by ^1H NMR, which showed a 9:1 mixture of biphenyl–TEDA:biphenyl, with no significant double TEDAylation product:

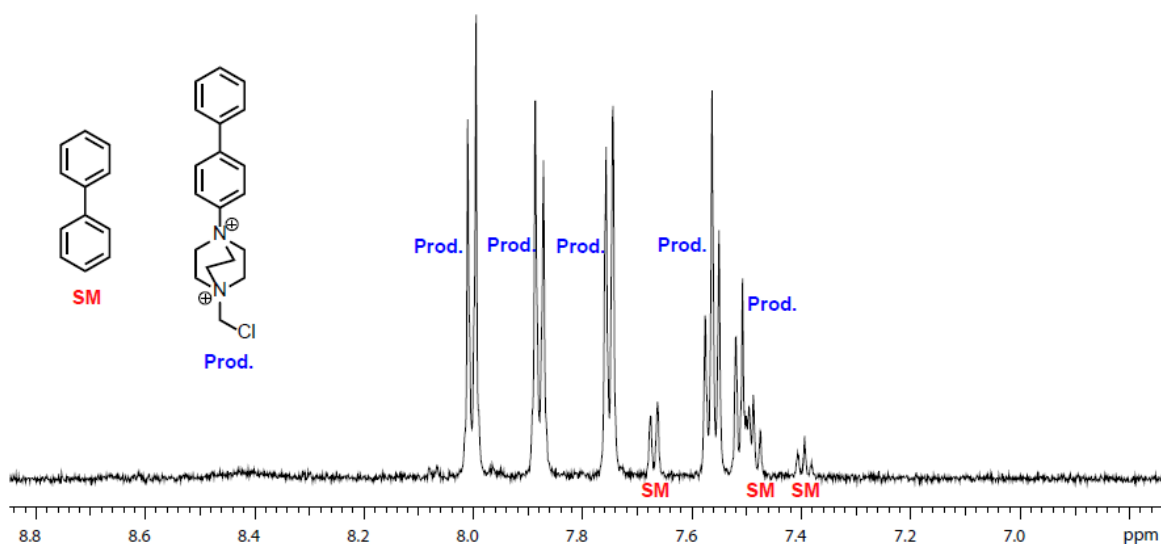


Figure 3.13. ^1H NMR of biphenyl TEDAylation reaction (CD_3CN , 23 °C)

Saturated aqueous sodium thiosulfate (10 mL) and water (10 mL) were added, the pressure tube was sealed, and the reaction mixture was stirred at 100 °C for 2 h. After cooling to 23 °C, the reaction mixture was basified with aqueous 6 M sodium hydroxide solution (10 mL) and ethylenediamine (0.5 mL), filtered through celite rinsing with acetonitrile ($5 \times 15 \text{ mL}$), and acetonitrile removed *in vacuo* to afford a brown aqueous solution. The aqueous layer was transferred to a separatory funnel and extracted with a solvent mixture of methanol/dichloromethane (1/9 (v/v), $5 \times 15 \text{ mL}$). The combined organic layers were extracted with aqueous 1M hydrochloric acid solution ($3 \times 15 \text{ mL}$). The combined acidic aqueous layers were basified to pH 14 with aqueous 6M sodium hydroxide solution and

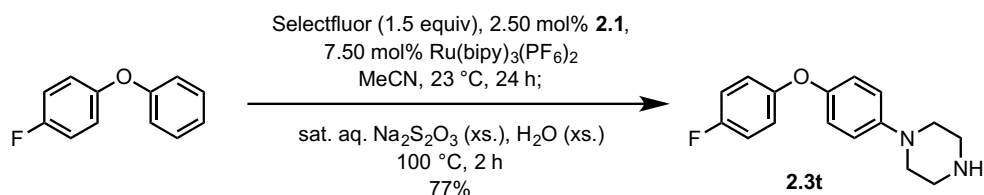
ethylenediamine (0.5 mL). The basic aqueous layer was extracted with a solvent mixture of methanol/dichloromethane (1/9 (v/v), 5 × 15 mL). The organic layers were dried over sodium sulfate, filtered, and concentrated *in vacuo* to afford a red oil. The residue was purified by chromatography on silica gel eluting with a solvent mixture of dichloromethane/methanol (9/1 (v/v)) to afford 138. mg of the title compound as an off-white solid (58% yield).

R_f = 0.10 (dichloromethane/methanol/28% aqueous ammonium hydroxide 90.5:9.0:0.5 (v/v/v)).

NMR Spectroscopy: ^1H NMR (600 MHz, $\text{F}_3\text{CO}_2\text{D}$, 23 °C, δ): 7.83 (m, 2H), 7.65 (m, 2H), 7.53 (m, 2H), 7.41 (m, 2H), 7.36 (m, 1H), 4.31 (s, 4H), 4.15 (s, 4H). ^{13}C NMR (125 MHz, $\text{F}_3\text{CO}_2\text{D}$, 23 °C, δ): 149.6, 141.4, 133.0, 132.2, 132.0, 130.1, 123.6, 55.9, 45.8.

Mass Spectrometry: HRMS-FIA(m/z) calcd for $\text{C}_{16}\text{H}_{19}\text{N}_2$ $[\text{M}+\text{H}]^+$, 239.1543; found, 239.1545.

1-(3-Fluoro-4-methoxyphenyl)piperazine (2.3t)



A 100 mL pressure tube was charged with palladium complex **2.1** (15.9 mg, 25.0 μmol , 2.50 mol%), $\text{Ru}(\text{bipy})_3(\text{PF}_6)_2$ (64.5 mg, 75.0 μmol , 7.50 mol%), Selectfluor (532. mg, 1.50 mmol, 1.50 equiv), and phenyl 4-fluorophenyl ether (188. mg, 1.00 mmol, 1.00 equiv). Acetonitrile (5.0 mL, c = 0.20 M) was added via syringe. The reaction mixture was stirred at 23 °C for 24 h. Saturated aqueous sodium thiosulfate (10 mL) and water (10 mL) were added, the pressure tube was sealed, and the reaction mixture was stirred at 100 °C for 2 h. After cooling to 23 °C, the reaction mixture was filtered through celite, and the filter cake was

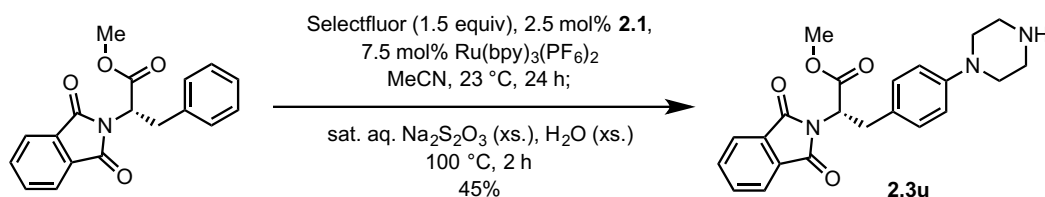
extracted with 5×15 mL acetonitrile and 2×15 mL water. The acetonitrile was removed from the filtrate by rotary evaporation. To the remaining aqueous mixture 0.50 mL ethylene diamine was added, and the aqueous mixture was basified to pH 14 with 6 M NaOH, then transferred to a separatory funnel. The aqueous layer was extracted with dichloromethane (7×30 mL). The combined organic layers were extracted with 1 M HCl (5×30 mL). To the combined acidic aqueous layers was added ethylene diamine (0.5 mL), and the mixture was basified to pH 14 with 6 M NaOH. The basic aqueous layer was extracted with dichloromethane (5×30 mL). The combined organic layers were dried over sodium sulfate, filtered, and concentrated *in vacuo* to afford a red oil (220. mg). The residue was purified by chromatography on silica gel eluting with dichloromethane/methanol 19:1 \rightarrow 9:1 (v/v) to afford 190. mg of the title compound as an off-white powder (77% yield).

R_f = 0.35 (dichloromethane/methanol 9:1 (v/v)).

NMR Spectroscopy: ^1H NMR (600 MHz, CDCl_3 , 23 $^\circ\text{C}$, δ): 7.00–6.95 (m, 2H), 6.94–6.88 (m, 6H), 3.74 (br, 1H), 3.19–3.12 (m, 4H), 3.12–3.06 (m, 4H). ^{13}C NMR (125 MHz, CDCl_3 , 23 $^\circ\text{C}$, δ): 158.3 (d, J = 240.4 Hz), 154.1 (d, J = 2.5 Hz), 156.6 (s), 147.9 (s), 119.8 (s), 119.2 (d, J = 8.1 Hz), 117.9 (s), 116.0 (d, J = 23.2 Hz), 50.6 (s), 45.7 (s).

Mass Spectrometry: HRMS-FIA(m/z) calcd for $\text{C}_{16}\text{H}_{18}\text{FN}_2\text{O}$ $[\text{M}+\text{H}]^+$, 273.1398; found, 273.1397.

Methyl (*S*)-2-(1,3-dioxoisindolin-2-yl)-3-(4-(piperazin-1-yl)phenyl)propanoate (**2.3u**)



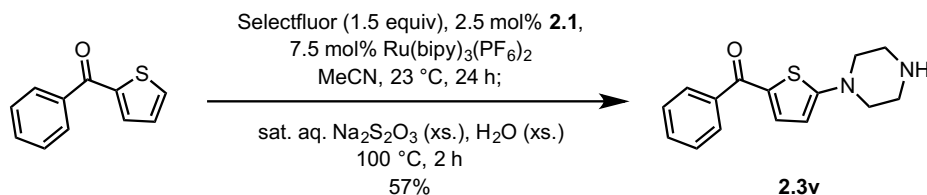
A 100 mL pressure tube was charged with palladium complex **2.1** (5.9 mg, 9.3 μmol , 2.5 mol%), $\text{Ru}(\text{bpy})_3(\text{PF}_6)_2$ (24.0 mg, 27.9 μmol , 7.50 mol%), and Selectfluor (198 mg, 0.558

mmol, 1.50 equiv). Solution of methyl (*S*)-2-(1,3-dioxoisindolin-2-yl)-3-phenylpropanoate (115 mg, 0.372 mmol, 1.00 equiv) in dry acetonitrile (1.9 mL, *c* = 0.20 M) was added via syringe. The reaction mixture was stirred at 23 °C for 24 h. Saturated aqueous sodium thiosulfate (3.8 mL) and water (3.8 mL) were added, the pressure tube was sealed, and the reaction mixture was stirred at 100 °C for 2 h. After cooling to 23 °C, water (5 mL) and saturated aqueous sodium carbonate (1 mL) were added, and the mixture was filtered over a glass frit with a filter paper. The filtrate was transferred to a separatory funnel.

Dichloromethane (30 mL) was added and the organic layer was separated. The aqueous layer was extracted with dichloromethane (2 × 20 mL). The combined organic layers were dried over sodium sulfate, filtered, and concentrated *in vacuo* to afford a red solid (123 mg). The residue was purified by chromatography on silica gel eluting with a solvent mixture of dichloromethane/methanol/28% aqueous ammonium hydroxide (93.7/6.0/0.3 (v/v/v)) to afford 66.3 mg of the title compound as a yellow solid (45% yield).

R_f = 0.76 (dichloromethane/methanol/28% aqueous ammonium hydroxide 93.7:6.0:0.3 (v/v/v)). NMR Spectroscopy: ^1H NMR (600 MHz, CDCl_3 , 23 °C, δ): 7.76–7.79 (m, 2H), 7.68–7.70 (m, 2H), 7.04–7.07 (m, 2H), 6.72–6.75 (m, 2H), 5.12 (dd, J = 11.0, 5.7 Hz, 1H), 3.77 (s, 3H), 3.46–3.53 (m, 2H), 3.08–3.11 (m, 4H), 3.04–3.06 (m, 4H). ^{13}C NMR (125 MHz, CDCl_3 , 23 °C, δ): 169.6, 167.6, 150.1, 134.2, 131.8, 129.7, 128.4, 123.6, 116.7, 53.5, 53.0, 49.4, 45.5, 33.8. Mass Spectrometry: HRMS-FIA(m/z) calcd for $\text{C}_{22}\text{H}_{23}\text{N}_3\text{O}_4$ [$\text{M}+\text{H}$] $^+$, 394.1761; found, 394.1760.

Phenyl(5-(piperazin-1-yl)thiophen-2-yl)methanone (2.3v)



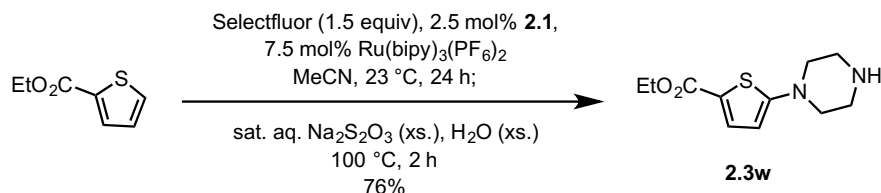
A 100 mL pressure tube was charged with palladium complex **2.1** (8.5 mg, 13. μ mol, 2.5 mol%), Ru(bipy)₃(PF₆)₂ (34.2 mg, 40.0 μ mol, 7.50 mol%), Selectfluor (282. mg, 0.800 mmol, 1.50 equiv), and phenyl(thiophen-2-yl)methanone (100. mg, 0.530 mmol, 1.00 equiv). Acetonitrile (2.6 mL, c = 0.20 M) was added via syringe. The reaction mixture was stirred at 23 °C for 24 h. Saturated aqueous sodium thiosulfate (5.3 mL) and water (5.3 mL) were added, the pressure tube was sealed, and the reaction mixture was stirred at 100 °C for 2 h. After cooling to 23 °C, the reaction mixture was transferred to a separatory funnel. Dichloromethane (20 mL), ethylenediamine (0.5 mL) and saturated aqueous sodium carbonate (5 mL) were added and the organic layer was separated. The aqueous layer was extracted with dichloromethane (3 \times 15 mL). The combined organic layers were extracted with 1 M aqueous hydrochloric acid (3 \times 10 mL). Ethylenediamine (6.0 mL) was added to the combined acidic aqueous layers, followed by basification with 3 M aqueous sodium hydroxide (6 mL). The basic aqueous layer was extracted with dichloromethane (4 \times 15 mL). The combined organic layers were dried over sodium sulfate, filtered, and concentrated *in vacuo* to afford a red solid (126. mg). The residue was purified by chromatography on silica gel eluting with a solvent mixture of dichloromethane/methanol/28% aqueous ammonium hydroxide (95.5/4.0/0.5 (v/v/v)) to afford 82. mg of the title compound as a yellow solid (57% yield).

R_f = 0.38 (dichloromethane/methanol/28% aqueous ammonium hydroxide 90.5:9.0:0.5 (v/v/v)).

NMR Spectroscopy: ¹H NMR (600 MHz, CDCl₃, 23 °C, δ): 7.73 (d, *J* = 7.5 Hz, 2H), 7.49 (t, *J* = 7.5 Hz, 1H), 7.42 (t, *J* = 7.5 Hz, 2H), 7.36 (d, *J* = 4.3 Hz, 1H), 6.03 (d, *J* = 4.3 Hz, 1H), 3.30 (t, *J* = 4.9 Hz, 4H), 2.99 (t, *J* = 4.9 Hz, 4H), 2.00 (s, 1H). ¹³C NMR (125 MHz, CDCl₃, 23 °C, δ): 186.7, 167.8, 139.0, 138.3, 131.1, 128.7, 128.3, 127.5, 104.4, 50.6, 45.2. Mass Spectrometry: HRMS-FIA(*m/z*) calcd for C₁₅H₁₆N₂OS [M+H]⁺, 273.1056; found, 273.1046.

Mass spectrometry: HRMS-FIA(m/z) calcd for C₁₅H₁₇N₂OS [M+H]⁺, 273.1056; found, 273.1044.

Ethyl 5-(piperazin-1-yl)thiophene-2-carboxylate (**2.3w**)

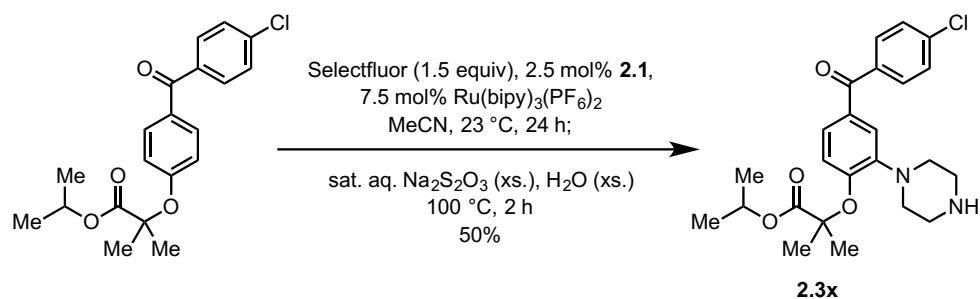


A 100 mL pressure tube was charged with palladium complex **2.1** (11.8 mg, 18.6 μmol, 2.50 mol%), Ru(bipy)₃(PF₆)₂ (47.9 mg, 55.7 μmol, 7.50 mol%), and Selectfluor (395. mg, 1.11 mmol, 1.50 equiv). Acetonitrile (3.7 mL, c = 0.20 M) was added, followed by ethyl thiophene-2-carboxylate (100. μL, 0.743 mmol, 1.00 equiv) via syringe. The reaction mixture was stirred at 23 °C for 24 h. Saturated aqueous sodium thiosulfate (7.4 mL) and water (7.4 mL) were added, the pressure tube was sealed, and the reaction mixture was stirred at 100 °C for 2 h. After cooling to 23 °C, the reaction mixture was transferred to a separatory funnel. Dichloromethane (20 mL) and ethylenediamine (0.5 mL) were added and the organic layer was separated. The aqueous layer was extracted with dichloromethane (2 × 15 mL). The combined organic layers were extracted with 10% aqueous glacial acetic acid (3 × 10 mL). The combined acidic aqueous layers were basified with ethylenediamine (4.5 mL). The basic aqueous layer was extracted with dichloromethane (3 × 15 mL). The combined organic layers were dried over sodium sulfate, filtered, and concentrated *in vacuo* to afford a red solid (156. mg). The residue was purified by chromatography on silica gel eluting with a solvent mixture of dichloromethane/methanol/28% aqueous ammonium hydroxide (95.5/4.0/0.5 (v/v/v)) to afford 135. mg of the title compound as a yellow solid (76% yield). R_f = 0.52 (dichloromethane/methanol/28% aqueous ammonium hydroxide 90.5:9.0:0.5 (v/v/v)).

NMR Spectroscopy: ^1H NMR (500 MHz, CDCl_3 , 23 °C, δ): 7.52 (d, J = 4.3 Hz, 1H), 6.00 (d, J = 4.3 Hz, 1H), 4.25 (q, J = 7.1 Hz, 2H), 3.19–3.20 (m, 4H), 2.98–2.99 (m, 4H), 2.17 (s, 1H), 1.30 (t, J = 7.1 Hz, 3H). ^{13}C NMR (125 MHz, CDCl_3 , 23 °C, δ): 165.2, 162.9, 134.9, 116.9, 104.1, 60.5, 50.8, 45.2, 14.5.

Mass Spectrometry: HRMS-FIA(m/z) calcd for $\text{C}_{11}\text{H}_{17}\text{N}_2\text{O}_2\text{S}$ $[\text{M}+\text{H}]^+$, 241.1005; found, 241.0995.

Isopropyl 2-(4-(4-chlorobenzoyl)-2-(piperazin-1-yl)phenoxy)-2-methylpropanoate (**2.3x**)



A 100 mL pressure tube was charged with palladium complex **2.1** (4.4 mg, 6.9 μmol , 2.5 mol%), $\text{Ru}(\text{bpy})_3(\text{PF}_6)_2$ (17.9 mg, 20.8 μmol , 7.50 mol%), Selectfluor (147 mg, 0.416 mmol, 1.50 equiv), and fenofibrate (100 mg, 0.277 mmol, 1.00 equiv). Acetonitrile (1.4 mL, c = 0.20 M) was added via syringe, and the reaction mixture was stirred at 23 °C for 24 h. Saturated aqueous sodium thiosulfate (2.8 mL) and water (2.8 mL) were added, the pressure tube was sealed, and the reaction mixture was stirred at 100 °C for 2 h. After cooling to 23 °C, water (10 mL), saturated aqueous sodium carbonate (0.25 mL), and ethylenediamine (70 μL) were added, and the mixture was filtered over a glass frit with a filter paper. The filtrate was transferred to a separatory funnel. Dichloromethane (40 mL) was added and the organic layer was separated. The aqueous layer was extracted with dichloromethane (3×20 mL). The combined organic layers were dried over sodium sulfate, filtered, and concentrated *in vacuo* to afford a red solid (146 mg). The residue was purified by chromatography on silica gel eluting with a solvent mixture of dichloromethane/methanol/28% aqueous

ammonium hydroxide (96.5/3.0/0.5 to 94.5/5.0/0.5 (v/v/v)) to afford 62 mg of the title compound as a yellow solid (50% yield).

$R_f = 0.11$ (dichloromethane/methanol/28% aqueous ammonium hydroxide 95.5:4.0:0.5 (v/v/v)). NMR Spectroscopy: ^1H NMR (600 MHz, CD_3CN , 23 °C, δ): 7.69–7.71 (m, 2H), 7.51–7.53 (m, 2H), 7.37 (d, $J = 2.2$ Hz, 1H), 7.31 (dd, $J = 8.4, 2.2$ Hz, 1H), 6.73 (d, $J = 8.4$ Hz, 1H), 5.02 (hept, $J = 6.2$ Hz, 1H), 3.01–3.06 (m, 8H), 2.68 (bs, 1H), 1.65 (s, 6H), 1.18 (d, $J = 6.2$ Hz, 6H). ^{13}C NMR (125 MHz, CD_3CN , 23 °C, δ): 195.0, 173.7, 153.4, 144.4, 138.6, 137.8, 132.2, 131.4, 129.4, 126.4, 121.1, 116.7, 80.8, 70.2, 51.7, 46.5, 25.6, 21.7. Mass Spectrometry: HRMS-FIA(m/z) calcd for $\text{C}_{24}\text{H}_{29}\text{ClN}_2\text{O}_4$ $[\text{M}+\text{H}]^+$, 445.1889; found, 445.1888.

Positively Charged Oxyl Radicals

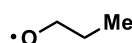
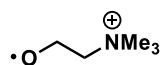
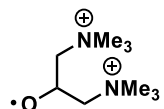
	<i>Calculated electron affinity</i>
	1.04 eV
	5.55 eV
	10.28 eV

Figure 3.14. Positive charge increases electron affinity for alkoxyl radicals

To address the question of whether other radicals can be found with electron affinities comparable to TEDA²⁺, we have calculated electron affinities for a series of alkoxyl radicals bearing 0, 1, and 2 proximal positive charges. We have found that electron affinities increase significantly with each additional positive charge. It is noteworthy that this trend holds despite the lack of a positive formal charge centered on the open-shell atom.

We rationalize these results in terms of electrostatic effects. When an electron is absorbed by

TEDA²⁺, the Coulombic repulsion between the two proximal positive charges is alleviated, which leads to a large energetic benefit. For the oxyl radicals, Coulombic attraction is created instead, which is worth the same amount of energy, but with opposite sign.

Therefore, in principle, radicals centered on any atom could be made to have electron affinity comparable to TEDA²⁺ through incorporation of proximal positive charges.

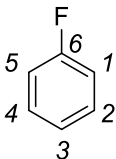
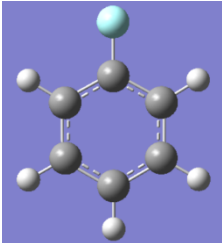
DFT Calculations

Density functional theory (DFT) calculations were performed using Gaussian09¹¹⁶ on the Odyssey cluster at Harvard University. BS I includes 6-311G(d) on H and 6-31G(d,p) on all other nuclei.¹¹⁹ All geometry optimizations were performed using the B3PW91 functional with the BS I basis set. Geometry optimization was carried out using the atomic coordinates from MM2 optimization in Chem3D as a starting point. Images were generated using Chem3D.

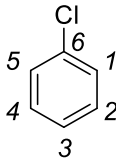
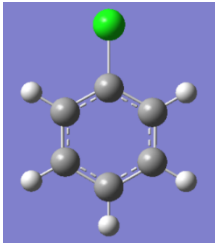
Calculation and visualization of Fukui indices

Fukui indices were calculated in the following way: The neutral arene (with N electrons) was subjected to a geometry optimization, and total local atomic electron populations were determined by NBO analysis. NBO electron populations of the corresponding cationic arene ($N-1$ electrons) were calculated without geometry reoptimization. Fukui nucleophilicity indices were calculated for each atom by subtracting the atomic electron population in the cationic arene from the population in the neutral arene. A color gradient for the set of Fukui values was generated using the conditional formatting tool in Microsoft Excel 2013, with the maximum value assigned a shade of red (RGB code 255:00:00) and the smallest value assigned a shade of blue (RGB 0:112:192).

Fluorobenzene

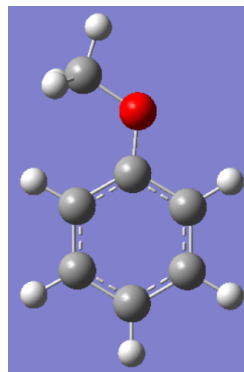
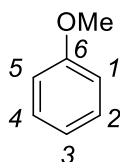
Atom	No.	X	Y	Z	neutral pop.	cation pop.	f-	RGB color
C	1	0.259886	1.216343	0.000001	6.3189	6.2378	0.0811	36:96:165
C	2	-1.134888	1.20758	0.000002	6.22836	6.17806	0.0503	0:112:192
C	3	-1.83353	0	-0.000003	6.26548	6.00175	0.26373	255:00:00
C	4	-1.134888	-1.20758	-0.000001	6.22836	6.17806	0.0503	0:112:192
C	5	0.259886	-1.216343	0.000004	6.3189	6.2378	0.0811	36:96:165
C	6	0.926134	0	0.000001	5.57659	5.38877	0.18782	164:40:69
H	7	2.284414	0	-0.000003				
H	8	0.823179	2.140225	0				
H	9	-1.672798	2.147473	0.000007				
H	10	-2.916086	0	-0.000008				
H	11	-1.672798	-2.147473	-0.000004				
H	12	0.823179	-2.140225	0.000011				
								

Chlorobenzene

Atom	No.	X	Y	Z	neutral pop.	cation pop.	f-	RGB color
C	1	0.179285	-1.21559	0.000165	6.27732	6.2134	0.06392	30:99:170
C	2	1.573669	-1.2065	0.000139	6.22736	6.1853	0.04206	0:112:192
C	3	2.27212	0	-0.000004	6.24852	6.02219	0.22633	10:625
C	4	1.573669	1.2065	0.000105	6.22736	6.1853	0.04206	0:112:192
C	5	0.179285	1.21559	0.000197	6.27732	6.2134	0.06392	30:99:170
C	6	-0.496734	0	0.000085	6.01645	5.87299	0.14346	140:51:87
Cl	7	-2.266123	0	-0.000282				
H	8	-0.368529	-2.148194	0.000212				
H	9	2.109408	-2.147525	0.000224				
H	10	3.354575	0	-0.000209				
H	11	2.109408	2.147525	0.000097				
H	12	-0.368529	2.148194	0.000342				
								

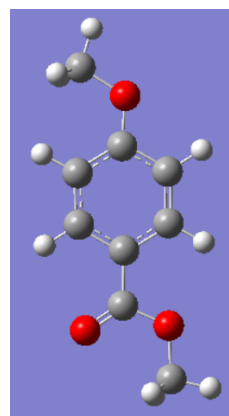
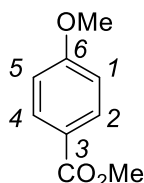
Anisole

Atom	No.	X	Y	Z	neutral pop.	cation pop.	f-	RGB code
C	1	-0.033836	1.060164	0.000014	6.33899	6.24884	0.09015	100:68:117
C	2	1.332708	1.351578	0.000002	6.22761	6.18489	0.04272	41:94:161
C	3	2.282523	0.334411	-0.000005	6.28458	6.07066	0.21392	255:00:00
C	4	1.854924	-0.996328	-0.00001	6.23365	6.22391	0.00974	0:112:192
C	5	0.499813	-1.302165	-0.000013	6.29766	6.18131	0.11635	133:54:92
C	6	-0.453266	-0.274134	0.000006	5.671	5.56534	0.10566	119:60:102
O	7	-1.757597	-0.674453	0.000051				
C	8	-2.775555	0.326026	-0.000034				
H	9	-0.75023	1.869366	0.000028				
H	10	1.648206	2.388251	0.000004				
H	11	3.339052	0.570766	-0.000001				
H	12	2.580826	-1.80078	-0.000015				
H	13	0.156078	-2.329145	-0.000018				
H	14	-3.721506	-0.212468	-0.000184				
H	15	-2.717873	0.956111	0.892796				
H	16	-2.717645	0.956213	-0.892776				



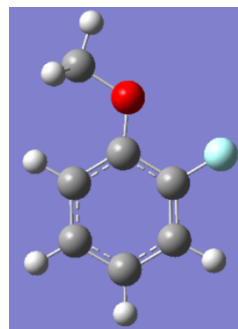
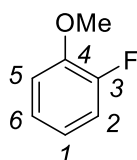
Methyl 4-methoxybenzoate

Atom	No.	X	Y	Z	neutral pop	cation pop.	f-	RGB code
C	1	-1.601873	0.989296	-0.002515	6.33589	6.24271	0.09318	116:61:105
C	2	-0.227542	1.197998	-0.003572	6.17724	6.1546	0.02264	30:99:170
C	3	0.668545	0.125151	-0.003953	6.19724	5.99103	0.20621	255:00:00
C	4	0.157707	-1.183531	-0.004934	6.19285	6.195	-0.00215	0:112:192
C	5	-1.20764	-1.404584	-0.004408	6.29373	6.17326	0.12047	150:47:80
C	6	-2.100704	-0.320323	-0.002287	5.64165	5.55312	0.08853	110:64:109
O	7	-3.416329	-0.641362	0.000343				
C	8	2.122181	0.416199	-0.00178				
O	9	2.873255	-0.703082	0.001834				
O	10	2.603652	1.531646	-0.002239				
C	11	4.301648	-0.5117	0.007744				
C	12	-4.383654	0.413925	0.008411				
H	13	-2.267946	1.839732	-0.001523				
H	14	0.162764	2.20751	-0.003306				
H	15	0.837023	-2.024738	-0.005716				
H	16	-1.611431	-2.408873	-0.004859				
H	17	4.727268	-1.512171	0.010726				
H	18	4.619059	0.034312	-0.881153				
H	19	4.61118	0.036185	0.898343				
H	20	-5.354109	-0.0776	0.011292				
H	21	-4.285845	1.033512	0.903987				
H	22	-4.294588	1.039928	-0.88353				



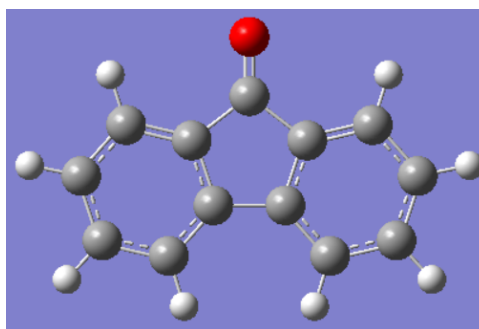
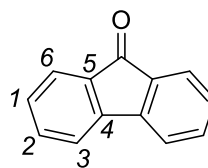
2-Fluoroanisole

Atom	No.	X	Y	Z	neutral pop.	cation pop.	f-	RGB code
C	1	2.262553	-0.684283	0.00009	6.2645	6.07427	0.19023	255:00:00
C	2	1.860767	0.654606	0.000099	6.30621	6.30142	0.00479	0:112:192
C	3	0.51384	0.954606	-0.000018	5.61834	5.50098	0.11736	154:45:83
C	4	-0.476755	-0.039137	-0.000116	5.73459	5.62397	0.11062	145:49:83
C	5	-0.061865	-1.373036	-0.000126	6.32203	6.26755	0.05448	68:82:141
C	6	1.300232	-1.687381	-0.000036	6.24341	6.16008	0.08333	108:65:111
O	7	-1.763375	0.39429	-0.000224				
C	8	-2.800369	-0.589598	0.000232				
F	9	0.116766	2.251437	-0.000008				
H	10	3.316139	-0.930699	0.000182				
H	11	2.57862	1.464685	0.000207				
H	12	-0.792961	-2.168943	-0.000239				
H	13	1.599854	-2.727755	-0.000069				
H	14	-3.734618	-0.031988	-0.000278				
H	15	-2.750507	-1.219218	-0.892868				
H	16	-2.750829	-1.217995	0.894177				

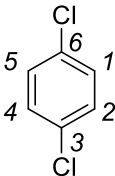
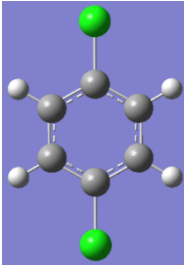


Fluorenone

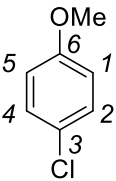
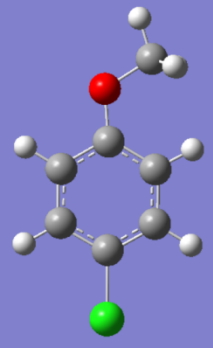
Atom	No.	X	Y	Z	neutral pop	cation pop	f-	RGB color
C	1	-3.464482	-0.066685	0.00001	6.24593	6.10276	0.14317	255:00:00
C	2	-3.02693	-1.392015	0.000004	6.20893	6.17721	0.03172	48:91:156
C	3	-1.660952	-1.708684	-0.000006	6.23588	6.18207	0.05381	89:73:125
C	4	-0.741884	-0.668882	-0.000007	6.01765	5.94323	0.07442	127:57:97
C	5	-1.188548	0.666481	-0.000003	6.12856	6.05053	0.07803	134:54:92
C	6	-2.537913	0.98222	0.000004	6.19665	6.19085	0.0058	0:112:192
C	7	0.741884	-0.668882	-0.000007				
C	8	1.188548	0.666481	-0.000003				
C	9	0	1.576164	-0.000006				
C	10	1.660952	-1.708684	-0.000007				
C	11	3.02693	-1.392015	0.000004				
C	12	3.464482	-0.066685	0.000011				
C	13	2.537913	0.982221	0.000005				
O	14	0	2.792501	-0.000007				
H	15	-4.525551	0.148606	0.000021				
H	16	-3.756128	-2.193077	0.000009				
H	17	-1.343091	-2.743965	-0.000011				
H	18	-2.863832	2.015329	0.000009				
H	19	1.343091	-2.743965	-0.000012				
H	20	3.756128	-2.193077	0.000008				
H	21	4.525551	0.148606	0.000022				
H	22	2.863832	2.015329	0.00001				



1,4-Dichlorobenzene

Atom	No.	X	Y	Z	neutral pop.	cation pop.	f-	RGB code
C	1	-0.696474	-1.213336	-0.000036	6.25498	6.20651	0.04847	0:112:192
C	2	0.696474	-1.213336	0	6.25498	6.20651	0.04847	0:112:192
C	3	1.37651	0	0.000038	6.02094	5.89246	0.12848	255:00:00
C	4	0.696474	1.213336	0.000047	6.25498	6.20651	0.04847	0:112:192
C	5	-0.696474	1.213336	0.000014	6.25498	6.20651	0.04847	0:112:192
C	6	-1.37651	0	-0.000031	6.02094	5.89246	0.12848	255:00:00
Cl	7	-3.13958	0	-0.000085				
Cl	8	3.13958	0	0.000071				
H	9	-1.239177	-2.148648	-0.000069				
H	10	1.239177	-2.148648	-0.000002				
H	11	1.239177	2.148648	0.000079				
H	12	-1.239177	2.148648	0.000022				
								

4-Chloroanisole

Atom	No	X	Y	Z	neutral pop.	cation pop.	total f-	RGB color
C	1	0.797679	-0.99734	-0.00153	6.31747	6.23401	0.08346	138:52:88
C	2	-0.59062	-1.14466	-0.00118	6.25568	6.21406	0.04162	50:91:155
C	3	-1.40103	-0.01937	-0.00024	6.04578	5.90732	0.13846	255:00:00
C	4	-0.85138	1.261271	0.000005	6.26128	6.2433	0.01798	0:112:192
C	5	0.528284	1.406969	-0.00049	6.2745	6.17893	0.09557	164:40:69
C	6	1.364223	0.281188	-0.00106	5.66925	5.56888	0.10037	174:36:61
O	7	2.700233	0.535292	-0.00096				
Cl	8	-3.16102	-0.20975	0.000878				
C	9	3.603996	-0.57207	0.002255				
H	10	1.414708	-1.88405	-0.0022				
H	11	-1.0265	-2.13458	-0.00156				
H	12	-1.49132	2.133269	0.000755				
H	13	0.977672	2.391617	-0.00017				
H	14	4.601996	-0.13856	0.002292				
H	15	3.47503	-1.18804	0.897014				
H	16	3.476992	-1.19211	-0.88994				
								

Electron affinity calculations

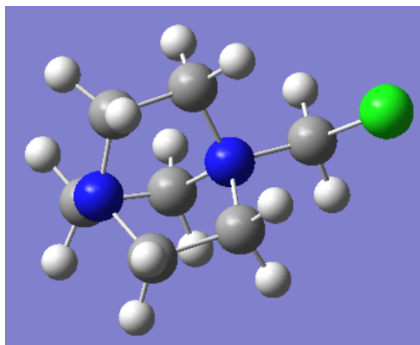
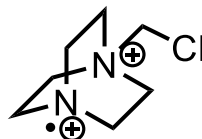
Adiabatic gas-phase electron affinities were calculated by performing independent geometry optimizations on the neutral amine (N electrons) and the corresponding aminium radical cation (N–1 electrons). The energy of the optimal geometry of the neutral species was subtracted from that of the cation to obtain the electron affinity. The computational methodology was validated by comparing computed and experimental electron affinities of amines for which experimental data is available: computed electron affinities of the dimethylamine radical cation and the piperazine radical cation were both within experimental error of the values measured by photoelectron spectroscopy.

TEDA²⁺ aminium radical electron affinity

	B3LYP Energy (Hartrees)	EA (Hartrees)	EA (eV)
TEDA-radical	-844.269588	0.45723623	12.44186
TEDA-amine	-844.7268242		

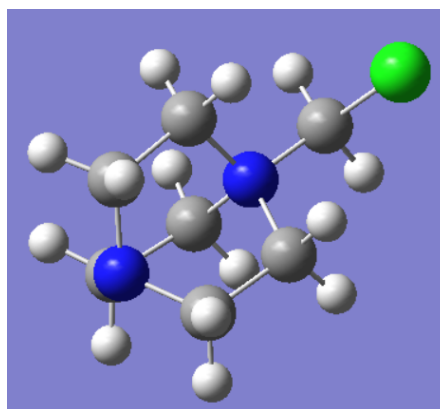
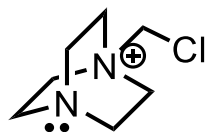
Aminium radical coordinates:

Atom	No.	X	Y	Z
C	1	-1.502796	-1.053089	1.17534
N	2	-2.081089	-0.422573	0.001872
C	3	-2.224674	1.020409	0.092382
C	4	-0.018599	-0.552881	-1.192487
C	5	-0.074436	-0.385706	1.291968
N	6	0.213142	0.373179	-0.000623
C	7	-0.749673	1.55458	-0.100918
C	8	-1.560298	-0.902954	-1.265036
C	9	1.655183	0.933436	-0.002893
Cl	10	2.870297	-0.338254	0.000836
H	11	-2.100747	-0.8362	2.061814
H	12	-1.436613	-2.129349	1.023332
H	13	-2.631327	1.293433	1.06508
H	14	-2.875104	1.3901	-0.70155
H	15	0.58468	-1.44623	-1.048307
H	16	0.3007	-0.039896	-2.09928
H	17	-0.034077	0.329972	2.11247
H	18	0.691474	-1.147074	1.429798
H	19	-0.503325	2.276454	0.677428
H	20	-0.617851	2.012672	-1.08054
H	21	-2.054477	-0.390531	-2.089246
H	22	-1.704096	-1.980554	-1.353857
H	23	1.756835	1.543483	0.89278
H	24	1.756278	1.53703	-0.903006



Amine coordinates:

Atom	No.	X	Y	Z
C	1	-1.52039	-0.97889	1.177463
N	2	-2.20498	-0.44473	0.001019
C	3	-2.19114	1.01465	0.039047
C	4	-0.03551	-0.51737	-1.21788
C	5	-0.06416	-0.42926	1.27014
N	6	0.22812	0.364061	-6.1E-05
C	7	-0.72967	1.554396	-0.0538
C	8	-1.54381	-0.91583	-1.21508
C	9	1.633869	0.914167	-0.00103
Cl	10	2.889936	-0.34304	0.000453
H	11	-2.07823	-0.705	2.073361
H	12	-1.51093	-2.06716	1.112894
H	13	-2.65914	1.348855	0.965326
H	14	-2.78159	1.403113	-0.79108
H	15	0.626516	-1.37658	-1.13689
H	16	0.250636	0.062813	-2.09572
H	17	0.074763	0.260884	2.103103
H	18	0.682059	-1.21783	1.339754
H	19	-0.47067	2.21366	0.774959
H	20	-0.53251	2.072774	-0.99243
H	21	-2.05201	-0.48833	-2.07993
H	22	-1.64019	-1.99987	-1.27725
H	23	1.752754	1.520072	0.893925
H	24	1.752484	1.517753	-0.8976



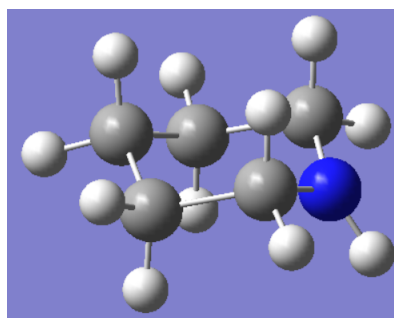
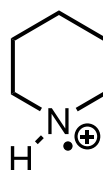
Piperidine aminium radical electron affinity

	B3LYP Energy (Hartrees)	EA (Hartrees)	EA (eV)
piperidine- radical	- 251.6866948	0.28432455	7.736755
piperidine-amine	- 251.9710194		

The gas-phase adiabatic electron affinity of the piperazine aminium radical was measured by photoelectron spectroscopy to be 7.78 ± 0.1 eV.¹²⁷ Therefore, the computed electron affinity is within experimental error.

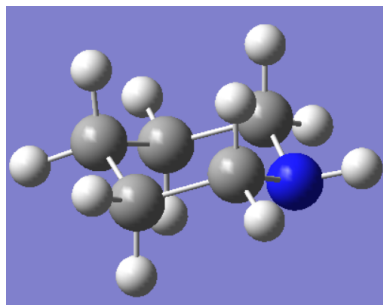
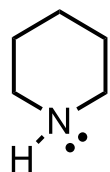
Aminium radical coordinates

Atom	No.	X	Y	Z
C	1	-1.2674	0.722618	-0.23782
C	2	-1.23889	-0.78513	0.236564
N	3	0.00005	-1.35192	-0.20833
C	4	1.23901	-0.78503	0.236397
C	5	1.26733	0.722812	-0.23765
C	6	-0.00012	1.439559	0.224229
H	7	-2.17206	1.160151	0.188847
H	8	-1.36391	0.742646	-1.32591
H	9	-2.07727	-1.34799	-0.16937
H	10	-1.26126	-0.79989	1.330253
H	11	0.000001	-1.93408	-1.04411
H	12	2.077366	-1.34771	-0.16985
H	13	1.261626	-0.80008	1.330083
H	14	2.171829	1.16041	0.189278
H	15	1.364063	0.743055	-1.32572
H	16	-0.00022	1.543908	1.31352
H	17	-0.00016	2.454033	-0.18903



Amine coordinates:

Atom	No.	X	Y	Z
C	1	-1.30906	0.629959	-0.22682
C	2	-1.16377	-0.83228	0.206876
N	3	0.092106	-1.37689	-0.315
C	4	1.264356	-0.66972	0.20663
C	5	1.213439	0.798713	-0.22658
C	6	-0.09743	1.454954	0.232918
H	7	-2.23538	1.047365	0.178815
H	8	-1.38159	0.662432	-1.31864
H	9	-1.99119	-1.42774	-0.18922
H	10	-1.22068	-0.88329	1.310862
H	11	0.158196	-2.36509	-0.09977
H	12	2.163568	-1.14972	-0.18989
H	13	1.327906	-0.71324	1.310598
H	14	2.075799	1.335918	0.17951
H	15	1.281378	0.841131	-1.31833
H	16	-0.102	1.521478	1.327989
H	17	-0.16598	2.479185	-0.14513



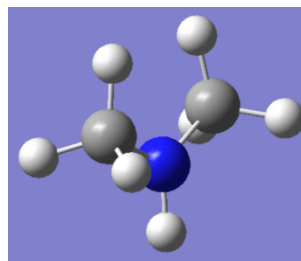
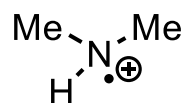
Dimethylamine radical cation electron affinity

	B3LYP Energy (Hartrees)	EA (Hartrees)	EA (eV)
dimethylamine- radical	- 134.9054068	0.29774864	8.102038
dimethylamine- amine	- 135.2031554		

The gas-phase adiabatic electron affinity of the piperazine aminium radical was measured by photoelectron spectroscopy to be 8.08 ± 0.1 eV.¹²⁷ Therefore, the computed electron affinity is within experimental error.

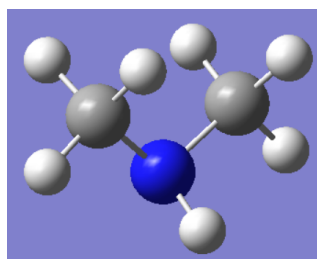
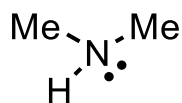
Aminium radical coordinates:

Atom	No.	X	Y	Z
C	1	1.279205	0.207143	-0.0037
N	2	0.000034	-0.444643	-0.00405
C	3	-1.278752	0.20804	0.002496
H	4	1.166922	1.278438	-0.150269
H	5	1.91543	-0.240072	-0.777665
H	6	1.776845	0.007374	0.959843
H	7	-0.000709	-1.466021	0.007209
H	8	-1.832183	-0.084906	-0.903177
H	9	-1.867394	-0.161104	0.854054
H	10	-1.161861	1.287694	0.045576



Amine coordinates:

Atom	No.	X	Y	Z
C	1	1.215605	-0.222816	0.020462
N	2	0	0.563444	-0.147187
C	3	-1.215605	-0.222816	0.020462
H	4	1.280145	-0.965613	-0.780483
H	5	1.27918	-0.76513	0.980323
H	6	2.088595	0.428644	-0.063204
H	7	0	1.333879	0.511497
H	8	-1.279179	-0.765131	0.980323
H	9	-2.088595	0.428644	-0.063203
H	10	-1.280146	-0.965612	-0.780484

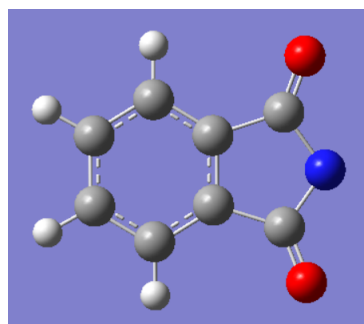
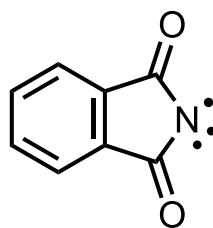


Phthalimide radical electron affinity

	B3LYP Energy (Hartrees)	EA (Hartrees)	EA (eV)
phthalimide- radical	- 512.5232453	0.13462626	3.663315
phthalimide-anion	- 512.6578715		

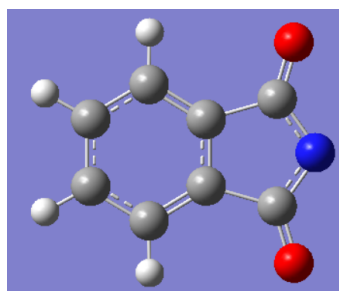
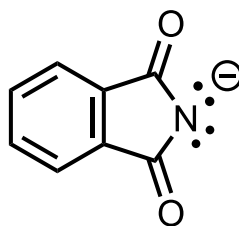
Radical coordinates

Atom	No.	X	Y	Z
C	1	2.519142	0.702378	0.000171
C	2	2.519141	-0.70238	0.000186
C	3	1.326846	-1.42438	0.009011
C	4	0.142758	-0.69785	0.012201
C	5	0.142758	0.697852	0.012195
C	6	1.326847	1.424379	0.008988
C	7	-1.27998	-1.15123	0.01175
N	8	-2.09713	0.000001	0.229165
C	9	-1.27998	1.151234	0.011756
O	10	-1.71191	2.269465	-0.12492
O	11	-1.71192	-2.26946	-0.12494
H	12	3.465318	1.2294	-0.01006
H	13	3.465317	-1.2294	-0.01003
H	14	1.317325	-2.50664	0.008664
H	15	1.317326	2.506639	0.008622



Anion coordinates

Atom	No.	X	Y	Z
C	1	-2.53043	0.698872	-0.000052
C	2	-2.53041	-0.69904	0.000581
C	3	-1.32437	-1.41527	0.000104
C	4	-0.14256	-0.69334	-0.000595
C	5	-0.14259	0.693361	-0.00063
C	6	-1.32443	1.415172	-0.000413
C	7	1.326985	-1.11371	-0.000106
N	8	2.115615	-4.7E-05	0.000547
C	9	1.32692	1.113913	-0.000157
O	10	1.675405	2.293616	0.00047
O	11	1.675676	-2.29351	-0.000191
H	12	-3.47668	1.231066	-0.000013
H	13	-3.47664	-1.23125	0.001487
H	14	-1.30962	-2.49976	0.000585
H	15	-1.30973	2.499652	-0.000515

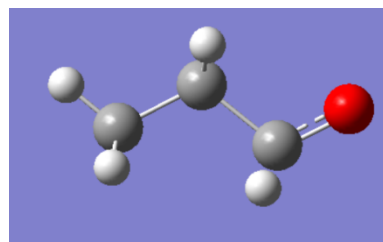
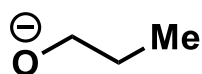


Propyloxyl radical electron affinity

	B3LYP Energy (Hartrees)	EA (Hartrees)	EA (eV)
oxyl-radical	- 193.7386246	0.03826599	1.041255854
oxyl-adiab	- 193.7768906		

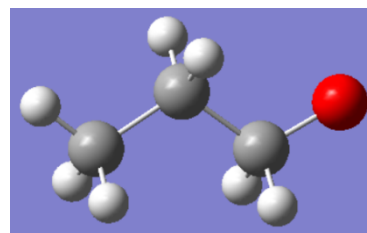
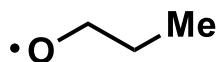
Oxide coordinates

Atom	No.	X	Y	Z
C	1	0.763732	-0.43796	-0.00011
C	2	-0.47058	0.544986	-0.0001
O	3	1.937513	0.150841	0.000133
C	4	-1.83673	-0.15272	0.00009
H	5	0.534858	-1.13448	0.889117
H	6	0.535038	-1.13425	-0.88954
H	7	-0.37396	1.193723	-0.88044
H	8	-0.37382	1.193933	0.880077
H	9	-2.68559	0.543467	-0.0005
H	10	-1.93777	-0.79695	0.881912
H	11	-1.93743	-0.79803	-0.88099



Radical coordinates

Atom	No.	X	Y	Z
C	1	0.705869	-0.42319	0.001047
C	2	-0.47505	0.550545	0.000715
O	3	1.947649	0.143382	-0.00068
C	4	-1.82722	-0.1683	-0.00062
H	5	0.653282	-1.11833	0.864516
H	6	0.654521	-1.11517	-0.86529
H	7	-0.3879	1.198174	-0.87669
H	8	-0.38937	1.197086	0.879089
H	9	-2.65307	0.545654	-0.00146
H	10	-1.94108	-0.80444	0.88226
H	11	-1.93921	-0.80437	-0.88381

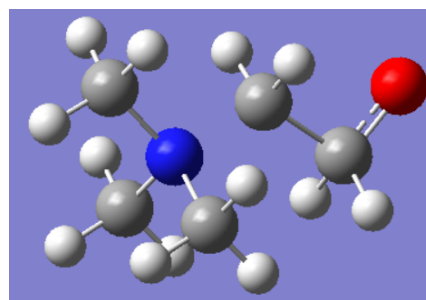
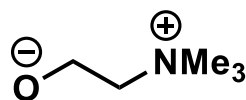


2-(trimethylammonium)ethyl-oxyl radical electron affinity

	B3LYP Energy (Hartrees)	EA (Hartrees)	EA (eV)
oxyl-ium-radical	- 328.0938967	0.20405086	5.552427951
oxyl-ium-adiab	- 328.2979475		

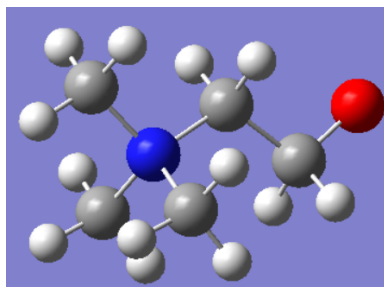
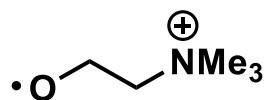
Oxide coordinates

Atom	No.	X	Y	Z
C	1	-1.86801	-0.435	0.000092
C	2	-0.65391	0.552462	-0.00081
O	3	-2.88665	0.390796	-0.00031
N	4	0.878361	0.023995	-3.5E-05
C	5	1.814541	1.18381	-0.00172
C	6	1.097568	-0.80077	1.224285
C	7	1.097998	-0.80456	-1.2217
H	8	-1.7524	-1.12517	-0.89084
H	9	-1.75215	-1.12366	0.892317
H	10	-0.72042	1.171774	0.893078
H	11	-0.72017	1.170197	-0.8958
H	12	2.850333	0.834773	0.006975
H	13	1.633037	1.779764	-0.89469
H	14	1.62184	1.790948	0.881286
H	15	2.121396	-1.18021	1.235152
H	16	0.382097	-1.61954	1.227742
H	17	0.923361	-0.17734	2.099921
H	18	0.913328	-0.18672	-2.09913
H	19	2.125133	-1.17488	-1.23652
H	20	0.390134	-1.62991	-1.21771



Radical coordinates

Atom	No.	X	Y	Z
C	1	-1.76307	-0.36881	-6.9E-05
C	2	-0.57413	0.615749	-0.00826
O	3	-2.93211	0.32905	0.000177
N	4	0.830879	0.019991	-2.4E-05
C	5	1.820594	1.161259	-0.02513
C	6	1.061778	-0.79366	1.248917
C	7	1.055773	-0.84322	-1.21627
H	8	-1.77203	-1.0454	-0.87245
H	9	-1.76672	-1.03902	0.87736
H	10	-0.64592	1.25885	0.869294
H	11	-0.64331	1.240845	-0.89896
H	12	2.829461	0.752275	-0.01506
H	13	1.664044	1.74477	-0.93036
H	14	1.662635	1.785398	0.852353
H	15	2.095226	-1.13588	1.257254
H	16	0.396794	-1.65407	1.25459
H	17	0.872429	-0.16701	2.118828
H	18	0.85082	-0.25572	-2.10966
H	19	2.092315	-1.17604	-1.22201
H	20	0.399284	-1.70926	-1.17759

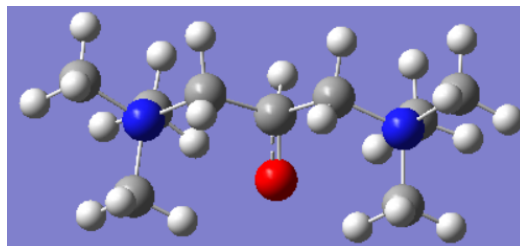
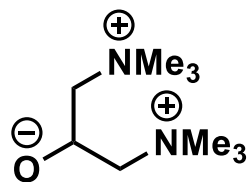


2-(trimethylammonium)-1-(trimethylammoniummethyl)ethyl-oxyl radical electron affinity

	B3LYP Energy (Hartrees)	EA (Hartrees)	EA (eV)
oxyl-dium- radical	-541.0113122	0.37791639	10.28348289
oxyl-dium- adiab	-541.3892286		

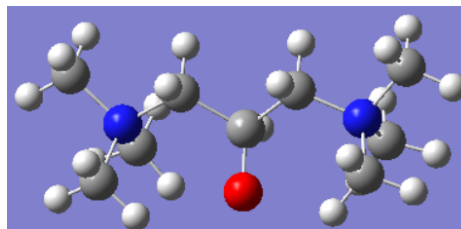
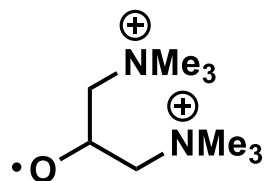
Oxide coordinates

Atom	No.	X	Y	Z
C	1	0.003972	0.082421	0.33451
O	2	0.001594	-1.17519	-0.06517
C	3	1.258936	0.88764	-0.17453
N	4	2.535536	0.107476	-0.02127
C	5	3.714939	1.054572	-0.11223
C	6	2.593767	-0.6241	1.299861
C	7	2.641502	-0.90692	-1.13822
C	8	-1.25427	0.898854	-0.15155
N	9	-2.55073	0.111279	-0.0254
C	10	-3.70511	1.051243	-0.11679
C	11	-2.6426	-0.90787	-1.14078
C	12	-2.60063	-0.62004	1.302508
H	13	-0.00151	0.227491	1.424172
H	14	1.184025	1.150219	-1.22523
H	15	1.383749	1.83829	0.414384
H	16	4.635672	0.47366	-0.09962
H	17	3.643194	1.610744	-1.04393
H	18	3.688909	1.733993	0.733137
H	19	3.569584	-1.1009	1.389718
H	20	1.792942	-1.34699	1.292212
H	21	2.468739	0.106017	2.108177
H	22	2.736597	-0.37066	-2.08172
H	23	3.529742	-1.51996	-0.97034
H	24	1.718505	-1.48611	-1.10079
H	25	-1.38436	1.824445	0.406385
H	26	-1.18069	1.153561	-1.23884
H	27	-4.63524	0.469773	-0.10575
H	28	-3.69079	1.731341	0.730114
H	29	-3.64083	1.610057	-1.04619
H	30	-3.52584	-1.52244	-0.96826
H	31	-1.7115	-1.49518	-1.09734
H	32	-2.73266	-0.377	-2.07892
H	33	-2.46751	0.109132	2.105681
H	34	-3.56259	-1.09468	1.388782
H	35	-1.78767	-1.3494	1.295525



Radical coordinates

Atom	No.	X	Y	Z
C	1	-0.0057	-0.03555	0.177828
O	2	-0.00119	-1.36205	-0.09346
C	3	1.26408	0.748281	-0.31241
N	4	2.627074	0.12118	-0.01488
C	5	3.681719	1.185113	-0.25827
C	6	2.727635	-0.34261	1.435245
C	7	2.921764	-1.06837	-0.93445
C	8	-1.27162	0.744921	-0.31466
N	9	-2.61992	0.122391	-0.00592
C	10	-3.67365	1.179757	-0.26033
C	11	-2.91034	-1.05432	-0.92768
C	12	-2.72158	-0.34284	1.426886
H	13	-0.00362	-0.01253	1.288262
H	14	1.222717	0.86727	-1.38614
H	15	1.262237	1.729523	0.148307
H	16	4.631522	0.741642	-0.12027
H	17	3.56892	1.542206	-1.26471
H	18	3.528728	1.99126	0.448004
H	19	3.740306	-0.63678	1.620674
H	20	2.060791	-1.1876	1.597292
H	21	2.462091	0.495955	2.094908
H	22	2.882601	-0.70528	-1.94496
H	23	3.88048	-1.42501	-0.69407
H	24	2.164008	-1.82908	-0.77142
H	25	-1.27056	1.725545	0.143449
H	26	-1.22763	0.864193	-1.38953
H	27	-4.65455	0.731339	-0.12331
H	28	-3.53634	1.990987	0.444053
H	29	-3.57467	1.540283	-1.28085
H	30	-3.90544	-1.44012	-0.69204
H	31	-2.1616	-1.83909	-0.76828
H	32	-2.88715	-0.71096	-1.95797
H	33	-2.46918	0.499853	2.091176
H	34	-3.76013	-0.6421	1.622159
H	35	-2.06798	-1.18634	1.595646



REFERENCES

1. (a) Jeschke, P., The Unique Role of Fluorine in the Design of Active Ingredients for Modern Crop Protection. *ChemBioChem* **2004**, 5 (5), 570-589; (b) Maienfisch, P.; Hall, R. G., The importance of fluorine in the life science industry. *Chimia* **2004**, 58 (3), 93-99.
2. (a) Böhm, H.-J.; Banner, D.; Bendels, S.; Kansy, M.; Kuhn, B.; Müller, K.; Obst-Sander, U.; Stahl, M., Fluorine in Medicinal Chemistry. *ChemBioChem* **2004**, 5 (5), 637-643; (b) Kirk, K. L., The use of selective fluorination in drug design and development. *Current Topics in Medicinal Chemistry* **2006**, 6 (14), 1445-1445; (c) Kirk, K. L., Selective fluorination in drug design and development: An overview of biochemical rationales. *Current Topics in Medicinal Chemistry* **2006**, 6 (14), 1447-1456; (d) Begue, J.-P.; Bonnet-Delpon, D., Recent advances (1995-2005) in fluorinated pharmaceuticals based on natural products. *Journal of Fluorine Chemistry* **2006**, 127 (8), 992-1012; (e) Isanbor, C.; O'Hagan, D., Fluorine in medicinal chemistry: A review of anticancer agents. *J. Fluorine Chem.* **2006**, 127 (3), 303-319; (f) Muller, K.; Faeh, C.; Diederich, F., Fluorine in Pharmaceuticals: Looking Beyond Intuition. *Science* **2007**, 317 (5846), 1881-1886; (g) Hagmann, W. K., The many roles for fluorine in medicinal chemistry. *Journal of Medicinal Chemistry* **2008**, 51 (15), 4359-4369; (h) O'Hagan, D., Understanding organofluorine chemistry. An introduction to the C-F bond. *Chemical Society Reviews* **2008**, 37 (2), 308-319; (i) Purser, S.; Moore, P. R.; Swallow, S.; Gouverneur, V., Fluorine in medicinal chemistry. *Chemical Society Reviews* **2008**, 37 (2), 320-330; (j) Ismail, F. M. D., Important fluorinated drugs in experimental and clinical use. *Journal of Fluorine Chemistry* **2002**, 118 (1-2), 27-33.
3. (a) Guittard, F.; de Givenchy, E. T.; Geribaldi, S.; Cambon, A., Highly fluorinated thermotropic liquid crystals: an update. *Journal of Fluorine Chemistry* **1999**, 100 (1-2), 85-96; (b) Babudri, F.; Farinola, G. M.; Naso, F.; Ragni, R., Fluorinated organic materials for electronic and optoelectronic applications: the role of the fluorine atom. *Chemical Communications* **2007**, (10), 1003-1022; (c) Cametti, M.; Crousse, B.; Metrangolo, P.; Milani, R.; Resnati, G., The fluorous effect in biomolecular applications. *Chemical Society Reviews* **2012**, 41 (1), 31-42; (d) Berger, R.; Resnati, G.; Metrangolo, P.; Weber, E.; Hulliger, J., Organic fluorine compounds: a great opportunity for enhanced materials properties. *Chemical Society Reviews* **2011**, 40 (7), 3496-3508.
4. (a) Kassis, C. M.; Steehler, J. K.; Betts, D. E.; Guan, Z. B.; Romack, T. J.; DeSimone, J. M.; Linton, R. W., XPS studies of fluorinated acrylate polymers and block copolymers with polystyrene. *Macromolecules* **1996**, 29 (9), 3247-3254; (b) Dhara, M. G.; Banerjee, S., Fluorinated high-performance polymers: Poly(arylene ether)s and aromatic polyimides containing trifluoromethyl groups. *Progress in Polymer Science* **2010**, 35 (8), 1022-1077; (c) Schloegl, S.; Kramer, R.; Lenko, D.; Schroettner, H.; Schaller, R.; Holzner, A.; Kern, W., Fluorination of elastomer materials. *European Polymer Journal* **2011**, 47 (12), 2321-2330; (d) Anton, D., Surface-fluorinated coatings. *Advanced Materials* **1998**, 10 (15), 1197-1205.
5. (a) Phelps, M. E., Positron emission tomography provides molecular imaging of biological processes. *Proceedings of the National Academy of Sciences of the United States of America* **2000**, 97 (16), 9226-9233; (b) Bolton, R., Radiohalogen incorporation into organic systems. *Journal of Labelled Compounds & Radiopharmaceuticals* **2002**, 45 (6), 485-528; (c) Ametamey, S. M.; Honer, M.; Schubiger, P. A., Molecular Imaging with PET. *Chemical Reviews* **2008**, 108, 1501-1516; (d) Cai, L.; Lu, S.; Pike, V. W., Chemistry with F-18 fluoride ion. *European Journal of Organic Chemistry* **2008**, (17), 2853-2873; (e) Miller,

- P. W.; Long, N. J.; Vilar, R.; Gee, A. D., Synthesis of C-11, F-18, O-15, and N-13 Radiolabels for Positron Emission Tomography. *Angewandte Chemie-International Edition* **2008**, 47 (47), 8998-9033; (f) Littich, R.; Scott, P. J. H., Novel Strategies for Fluorine-18 Radiochemistry. *Angewandte Chemie-International Edition* **2012**, 51 (5), 1106-1109.
6. Böhm, H. J.; Banner, D.; Bendels, S.; Kansy, M.; Kuhn, B.; Müller, K.; Obst-Sander, U.; Stahl, M., *Chembiochem* **2004**, 5, 637.
 7. Müller, K.; Faeh, C.; Diederich, F., Fluorine in Pharmaceuticals: Looking Beyond Intuition. *Science* **2007**, 317 (5846), 1881-1886.
 8. Isanbor, C.; O'Hagan, D., Fluorine in medicinal chemistry: A review of anti-cancer agents. *Journal of Fluorine Chemistry* **2006**, 127 (3), 303-319.
 9. Langlois, B.; Gilbert, L.; Forat, G., Fluorination of aromatic compounds by halogen exchange with fluoride anions ("halex" reaction). In *Industrial Chemistry Library*, Jean-Roger, D.; Serge, R., Eds. Elsevier: 1996; Vol. Volume 8, pp 244-292.
 10. (a) Liang, T.; Neumann, C. N.; Ritter, T., Introduction of Fluorine and Fluorine-Containing Functional Groups. *Angewandte Chemie International Edition* **2013**, 52 (32), 8214-8264; (b) Petrone, D. A.; Ye, J.; Lautens, M., Modern Transition-Metal-Catalyzed Carbon-Halogen Bond Formation. *Chemical Reviews* **2016**.
 11. Danielson, P. B., The Cytochrome P450 Superfamily: Biochemistry, Evolution and Drug Metabolism in Humans. *Current Drug Metabolism* **2002**, 3 (6), 561-597.
 12. (a) Van Heek, M.; France, C. F.; Compton, D. S.; McLeod, R. L.; Yumibe, N. P.; Alton, K. B.; Sybertz, E. J.; Davis, H. R., In Vivo Metabolism-Based Discovery of a Potent Cholesterol Absorption Inhibitor, SCH58235, in the Rat and Rhesus Monkey through the Identification of the Active Metabolites of SCH48461. *Journal of Pharmacology and Experimental Therapeutics* **1997**, 283 (1), 157-163; (b) Clader, J. W., The Discovery of Ezetimibe: A View from Outside the Receptor. *Journal of Medicinal Chemistry* **2004**, 47 (1), 1-9; (c) Penning, T. D.; Talley, J. J.; Bertenshaw, S. R.; Carter, J. S.; Collins, P. W.; Docter, S.; Graneto, M. J.; Lee, L. F.; Malecha, J. W.; Miyashiro, J. M.; Rogers, R. S.; Rogier, D. J.; Yu, S. S.; Anderson, G. D.; Burton, E. G.; Cogburn, J. N.; Gregory, S. A.; Koboldt, C. M.; Perkins, W. E.; Seibert, K.; Veenhuizen, A. W.; Zhang, Y. Y.; Isakson, P. C., Synthesis and biological evaluation of the 1,5-diarylpyrazole class of cyclooxygenase-2 inhibitors: Identification of 4- 5-(4-methylphenyl)-3-(trifluoromethyl)-1H-pyrazol-1-yl benzenesulfonamide (SC-58635, Celecoxib). *Journal of Medicinal Chemistry* **1997**, 40 (9), 1347-1365.
 13. Martinez, C. R.; Iverson, B. L., Rethinking the term "pi-stacking". *Chemical Science* **2012**, 3 (7), 2191-2201.
 14. (a) Abbate, F.; Casini, A.; Scozzafava, A.; Supuran, C. T., Carbonic anhydrase inhibitors: X-ray crystallographic structure of the adduct of human isozyme II with the perfluorobenzoyl analogue of methazolamide. Implications for the drug design of fluorinated inhibitors. *Journal of Enzyme Inhibition and Medicinal Chemistry* **2003**, 18 (4), 303-308; (b) Doyon, J. B.; Jain, A., The pattern of fluorine substitution affects binding affinity in a small library of fluoroaromatic inhibitors for carbonic anhydrase. *Organic Letters* **1999**, 1 (2), 183-185; (c) Kim, C. Y.; Chang, J. S.; Doyon, J. B.; Baird, T. T.; Fierke, C. A.; Jain, A.; Christianson, D. W., Contribution of fluorine to protein-ligand affinity in the binding of

fluoroaromatic inhibitors to carbonic anhydrase II. *Journal of the American Chemical Society* **2000**, *122* (49), 12125-12134; (d) Kim, C. Y.; Chandra, P. P.; Jain, A.; Christianson, D. W., Fluoroaromatic-fluoroaromatic interactions between inhibitors bound in the crystal lattice of human carbonic anhydrase II. *Journal of the American Chemical Society* **2001**, *123* (39), 9620-9627.

15. Smart, B. E., Fluorine substituent effects (on bioactivity). *Journal of Fluorine Chemistry* **2001**, *109* (1), 3-11.

16. Fallingborg, J., Intraluminal pH of the human gastrointestinal tract. (0907-8916 (Print)).

17. (a) van Niel, M. B.; Collins, I.; Beer, M. S.; Broughton, H. B.; Cheng, S. K. F.; Goodacre, S. C.; Heald, A.; Locker, K. L.; MacLeod, A. M.; Morrison, D.; Moyes, C. R.; O'Connor, D.; Pike, A.; Rowley, M.; Russell, M. G. N.; Sohal, B.; Stanton, J. A.; Thomas, S.; Verrier, H.; Watt, A. P.; Castro, J. L., Fluorination of 3-(3-(Piperidin-1-yl)propyl)indoles and 3-(3-(Piperazin-1-yl)propyl)indoles Gives Selective Human 5-HT_{1D} Receptor Ligands with Improved Pharmacokinetic Profiles. *Journal of Medicinal Chemistry* **1999**, *42* (12), 2087-2104; (b) Morgenthaler, M.; Schweizer, E.; Hoffmann-Roeder, A.; Benini, F.; Martin, R. E.; Jaeschke, G.; Wagner, B.; Fischer, H.; Bendels, S.; Zimmerli, D.; Schneider, J.; Diederich, F.; Kansy, M.; Mueller, K., Predicting properties and tuning physicochemical in lead optimization: Amine basicities. *ChemMedChem* **2007**, *2* (8), 1100-1115.

18. van der Plas, H. C.; Katritzky, A. R., *Advances in Heterocyclic Chemistry*. Elsevier Science: 1999.

19. (a) Leo, A.; Hansch, C.; Elkins, D., PARTITION COEFFICIENTS AND THEIR USES. *Chemical Reviews* **1971**, *71* (6), 525-616; (b) Hansch, C.; Leo, A.; Unger, S. H.; Kim, K. H.; Nikaitan, D.; Lien, E. J., AROMATIC SUBSTITUENT CONSTANTS FOR STRUCTURE-ACTIVITY CORRELATIONS. *Journal of Medicinal Chemistry* **1973**, *16* (11), 1207-1216; (c) Hansch, C.; Rockwell, S. D.; Jow, P. Y. C.; Leo, A.; Steller, E. E., SUBSTITUENT CONSTANTS FOR CORRELATION ANALYSIS. *Journal of Medicinal Chemistry* **1977**, *20* (2), 304-306; (d) Hansch, C.; Leo, A.; Taft, R. W., A survey of Hammett substituent constants and resonance and field parameters. *Chem. Rev.* **1991**, *91*, 165.

20. (a) Fujita, T.; Iwasa, J.; Hansch, C., A New Substituent Constant, π , Derived from Partition Coefficients. *Journal of the American Chemical Society* **1964**, *86* (23), 5175-5180; (b) Sun, S.; Adejare, A., Fluorinated molecules as drugs and Imaging agents in the CNS. *Current Topics in Medicinal Chemistry* **2006**, *6* (14), 1457-1464.

21. (a) Balz, G.; Schiemann, G., On aromatic fluoric compounds, I A new method for its representation. *Berichte Der Deutschen Chemischen Gesellschaft* **1927**, *60*, 1186-1190; (b) Rutherford, K. G.; Redmond, W.; Rigamonti, J., The Use of Hexafluorophosphoric Acid in the Schiemann Reaction1. *The Journal of Organic Chemistry* **1961**, *26* (12), 5149-5152; (c) Sellers, C.; Suschitzky, H., The use of arenediazonium hexafluoro-antimonates and -arsenates in the preparation of aryl fluorides. *Journal of the Chemical Society C: Organic* **1968**, (0), 2317-2319.

22. Gottlieb, H. B., The Replacement of Chlorine by Fluorine in Organic Compounds. *Journal of the American Chemical Society* **1936**, *58* (3), 532-533.

23. Finger, G. C.; Kruse, C. W., AROMATIC FLUORINE COMPOUNDS .7. REPLACEMENT OF AROMATIC -CL AND -NO₂ GROUPS BY -F. *Journal of the American Chemical Society* **1956**, 78 (23), 6034-6037.
24. Sun, H.; DiMagno, S. G., Room-Temperature Nucleophilic Aromatic Fluorination: Experimental and Theoretical Studies. *Angewandte Chemie International Edition* **2006**, 45 (17), 2720-2725.
25. Tang, P.; Wang, W.; Ritter, T., Deoxyfluorination of Phenols. *Journal of the American Chemical Society* **2011**, 133 (30), 11482-11484.
26. Fujimoto, T.; Ritter, T., PhenoFluorMix: Practical Chemoselective Deoxyfluorination of Phenols. *Organic Letters* **2015**, 17 (3), 544-547.
27. Neumann, C. N.; Hooker, J. M.; Ritter, T., Concerted nucleophilic aromatic substitution with ¹⁹F⁻ and ¹⁸F⁻. *Nature* **2016**, advance online publication.
28. Terrier, F., *Modern Nucleophilic Aromatic Substitution*. Wiley: 2013.
29. Watson, D. A.; Su, M.; Teverovskiy, G.; Zhang, Y.; Garcia-Fortanet, J.; Kinzel, T.; Buchwald, S. L., Formation of ArF from LPdAr(F): Catalytic Conversion of Aryl Triflates to Aryl Fluorides. *Science* **2009**, 325 (5948), 1661-1664.
30. (a) Lee, H. G.; Milner, P. J.; Buchwald, S. L., Pd-Catalyzed Nucleophilic Fluorination of Aryl Bromides. *Journal of the American Chemical Society* **2014**, 136 (10), 3792-3795; (b) Milner, P. J.; Kinzel, T.; Zhang, Y.; Buchwald, S. L., Studying Regioisomer Formation in the Pd-Catalyzed Fluorination of Aryl Triflates by Deuterium Labeling. *Journal of the American Chemical Society* **2014**, 136 (44), 15757-15766.
31. Sather, A. C.; Lee, H. G.; De La Rosa, V. Y.; Yang, Y.; Müller, P.; Buchwald, S. L., A Fluorinated Ligand Enables Room-Temperature and Regioselective Pd-Catalyzed Fluorination of Aryl Triflates and Bromides. *Journal of the American Chemical Society* **2015**, 137 (41), 13433-13438.
32. Subramanian, M. A.; Manzer, L. E., A "greener" synthetic route for fluoroaromatics via copper (II) fluoride. *Science* **2002**, 297 (5587), 1665-1665.
33. (a) Chambers, R. D.; Skinner, C. J.; Hutchinson, J.; Thomson, J., Elemental fluorine. Part 1. Synthesis of fluoroaromatic compounds. *Journal of the Chemical Society, Perkin Transactions 1* **1996**, (7), 605-609; (b) Chambers, R. D.; Hutchinson, J.; Sparrowhawk, M. E.; Sandford, G.; Moilliet, J. S.; Thomson, J., Elemental fluorine Part 12. Fluorination of 1,4-disubstituted aromatic compounds. *Journal of Fluorine Chemistry* **2000**, 102 (1-2), 169-173; (c) L. Coe, P.; M. Stuart, A.; J. Moody, D., Trifluoromethanesulfonic acid: a novel solvent for the electrophilic fluorination of fluoroaromatics. *Journal of the Chemical Society, Perkin Transactions 1* **1998**, (11), 1807-1812; (d) Chambers, R. D.; Fox, M. A.; Sandford, G.; Trmcić, J.; Goeta, A., Elemental fluorine: Part 20. Direct fluorination of deactivated aromatic systems using microreactor techniques. *Journal of Fluorine Chemistry* **2007**, 128 (1), 29-33; (e) Alric, J. P.; Marquet, B.; Billard, T.; Langlois, B. R., Electrophilic aromatic fluorination with fluorine: meta-Directed fluorination of anilines. *Journal of Fluorine Chemistry* **2005**, 126 (4), 659-665.
34. (a) Barton, D. H. R.; Ganguly, A. K.; Hesse, R. H.; Loo, S. N.; Pechet, M. M.,

ORGANIC REACTIONS OF FLUOROXY-COMPOUNDS - ELECTROPHILIC FLUORINATION OF AROMATIC RINGS. *Chemical Communications* **1968**, (14), 806-808; (b) Sheppard, W. A., Mechanism of fluorination by perchloryl fluoride. *Tetrahedron Letters* **1969**, 10 (2), 83-84; (c) Barton, D. H. R.; Westcott, N. D.; Toh, H. T.; Tarzia, G.; Hesse, R. H.; Pechet, M. M., GENERALIZED ELECTROPHILIC FLUORINATION BY FLUOROXY-COMPOUNDS. *Journal of the Chemical Society-Chemical Communications* **1972**, (3), 122-123; (d) Airey, J.; Barton, D. H. R.; Ganguly, A. K.; Hesse, R. H.; Pechet, M. M., ELECTROPHILIC FLUORINATION OF AROMATIC SUBSTRATES BY FLUOROXYTRIFLUOROMETHANE. *Anales De Quimica* **1974**, 70 (12), 871-875.

35. Differding, E.; Ofner, H., N-FLUOROBENZENESULFONIMIDE - A PRACTICAL REAGENT FOR ELECTROPHILIC FLUORINATIONS. *Synlett* **1991**, (3), 187-189.

36. (a) Umemoto, T.; Kawada, K.; Tomita, K., N-FLUOROPYRIDINIUM TRIFLATE AND ITS DERIVATIVES - USEFUL FLUORINATING AGENTS. *Tetrahedron Letters* **1986**, 27 (37), 4465-4468; (b) Umemoto, T.; Tomita, K., N-FLUOROPYRIDINIUM TRIFLATE AND ITS ANALOGS, THE 1ST STABLE 1-1 SALTS OF PYRIDINE NUCLEUS AND HALOGEN ATOM. *Tetrahedron Letters* **1986**, 27 (28), 3271-3274; (c) Tomita, K.; Kawada, K.; Umemoto, T., USE AND APPLICATION OF NEW FLUORINATING AGENTS, N-FLUOROPYRIDINIUM TRIFLATE AND ITS DERIVATIVES. *Journal of Fluorine Chemistry* **1987**, 35 (1), 52-52; (d) Umemoto, T.; Tomita, K., N-FLUOROPYRIDINIUM TRIFLATE AND ITS DERIVATIVES - USEFUL FLUORINATING AGENTS. *Journal of Fluorine Chemistry* **1987**, 35 (1), 14-14; (e) Umemoto, T.; Tomizawa, G., BASE-INITIATED REACTIONS OF N-FLUOROPYRIDINIUM SALTS - A NOVEL CYCLIC CARBENE PROPOSED AS A REACTIVE SPECIES. *Tetrahedron Letters* **1987**, 28 (24), 2705-2708; (f) Umemoto, T.; Fukami, S.; Tomizawa, G.; Harasawa, K.; Kawada, K.; Tomita, K., POWER AND STRUCTURE-VARIABLE FLUORINATING AGENTS - THE N-FLUOROPYRIDINIUM SALT SYSTEM. *Journal of the American Chemical Society* **1990**, 112 (23), 8563-8575; (g) Umemoto, T.; Harasawa, K.; Tomizawa, G.; Kawada, K.; Tomita, K., SYNTHESSES AND PROPERTIES OF N-FLUOROPYRIDINIUM SALTS. *Bulletin of the Chemical Society of Japan* **1991**, 64 (4), 1081-1092; (h) Umemoto, T.; Tomizawa, G., HIGHLY SELECTIVE FLUORINATING AGENTS - A COUNTERANION-BOUND N-FLUOROPYRIDINIUM SALT SYSTEM. *Journal of Organic Chemistry* **1995**, 60 (20), 6563-6570; (i) Umemoto, T.; Nagayoshi, M.; Adachi, K.; Tomizawa, G., Synthesis, properties, and reactivity of N,N'-difluorobipyridinium and related salts and their applications as reactive and easy-to-handle electrophilic fluorinating agents with high effective fluorine content. *Journal of Organic Chemistry* **1998**, 63 (10), 3379-3385.

37. Banks, R. E.; Mohialdinkhaffaf, S. N.; Lal, G. S.; Sharif, I.; Syvret, R. G., 1-ALKYL-4-FLUORO-1,4-DIAZONIABICYCLO 2.2.2 OCTANE SALTS - A NOVEL FAMILY OF ELECTROPHILIC FLUORINATING AGENTS. *Journal of the Chemical Society-Chemical Communications* **1992**, (8), 595-596.

38. (a) DeYoung, J.; Kawa, H.; Lagow, R. J., Selective direct fluorination of organolithium and organomagnesium compounds. *J. Chem. Soc., Chem. Commun.* **1992**, (Copyright (C) 2012 American Chemical Society (ACS). All Rights Reserved.), 811-12; (b) Anbarasan, P.; Neumann, H.; Beller, M., Efficient Synthesis of Aryl Fluorides. *Angewandte Chemie* **2010**, 122 (12), 2265-2268; (c) Anbarasan, P.; Neumann, H.; Beller, M., Efficient Synthesis of Aryl Fluorides. *Angewandte Chemie-International Edition* **2010**, 49 (12), 2219-2222; (d) Yamada, S.; Gavryushin, A.; Knochel, P., Convenient Electrophilic Fluorination of

Functionalized Aryl and Heteroaryl Magnesium Reagents. *Angewandte Chemie-International Edition* **2010**, 49 (12), 2215-2218; (e) Anbarasan, P.; Neumann, H.; Beller, M., A New and Practical Grignard-Coupling-Fluorination Sequence: Synthesis of 2-Aryl Fluoroarenes. *Chem. Asian J.* **2010**, 5 (8), 1775-1778.

39. (a) Snieckus, V.; Beaulieu, F.; Mohri, K.; Han, W.; Murphy, C. K.; Davis, F. A., DIRECTED ORTHO-METALATION - MEDIATED F⁺ INTRODUCTION - REGIOSPECIFIC SYNTHESIS OF FLUORINATED AROMATICS. *Tetrahedron Letters* **1994**, 35 (21), 3465-3468; (b) Slocum, D. W.; Shelton, P.; Moran, K. M., Processing aryllithium and hetaryllithium intermediates: Formation of halogen and chalcogen derivatives. *Synthesis* **2005**, (Copyright (C) 2012 American Chemical Society (ACS). All Rights Reserved.), 3477-3498.

40. Hull, K. L.; Anani, W. Q.; Sanford, M. S., Palladium-catalyzed fluorination of carbon-hydrogen bonds. *Journal of the American Chemical Society* **2006**, 128 (22), 7134-7135.

41. Wang, X.; Mei, T. S.; Yu, J.-Q., Versatile Pd(OTf)₂·2H₂O-Catalyzed ortho-Fluorination Using NMP as a Promoter. *Journal of the American Chemical Society* **2009**, 131 (22), 7520-7521.

42. (a) Desai, L. V.; Stowers, K. J.; Sanford, M. S., Insights into directing group ability in palladium-catalyzed C-H bond functionalization. *Journal of the American Chemical Society* **2008**, 130 (40), 13285-13293; (b) Stowers, K. J.; Sanford, M. S., Mechanistic Comparison between Pd-Catalyzed Ligand-Directed C-H Chlorination and C-H Acetoxylation. *Organic Letters* **2009**, 11 (20), 4584-4587.

43. (a) Powers, D. C.; Ritter, T., Bimetallic Pd(III) complexes in palladium-catalysed carbon-heteroatom bond formation. *Nature Chemistry* **2009**, 1 (4), 302-309; (b) Powers, D. C.; Ritter, T., Bimetallic Redox Synergy in Oxidative Palladium Catalysis. *Accounts of Chemical Research* **2012**, 45 (6), 840-850.

44. Chan, K. S. L.; Wasa, M.; Wang, X.; Yu, J.-Q., Palladium(II)-Catalyzed Selective Monofluorination of Benzoic Acids Using a Practical Auxiliary: A Weak-Coordination Approach. *Angewandte Chemie International Edition* **2011**, 50 (39), 9081-9084.

45. (a) Lou, S.-J.; Xu, D.-Q.; Xia, A.-B.; Wang, Y.-F.; Liu, Y.-K.; Du, X.-H.; Xu, Z.-Y., Pd(OAc)₂-catalyzed regioselective aromatic C-H bond fluorination. *Chemical Communications* **2013**, 49 (55), 6218; (b) Ding, Q.; Ye, C.; Pu, S.; Cao, B., Pd(PPh₃)₄-catalyzed direct ortho-fluorination of 2-arylbenzothiazoles with an electrophilic fluoride N-fluorobenzenesulfonimide (NFSI). *Tetrahedron* **2014**, 70 (2), 409-416; (c) Lou, S.-J.; Xu, D.-Q.; Xu, Z.-Y., Mild and versatile nitrate-promoted C-H bond fluorination. *Angewandte Chemie (International ed. in English)* **2014**, 53 (39), 10330-10335.

46. Tang, P.; Furuya, T.; Ritter, T., Silver-Catalyzed Late-Stage Fluorination. *Journal of the American Chemical Society* **2010**, 132 (34), 12150-12154.

47. (a) Tius, M. A.; Kawakami, J. K., VINYL FLUORIDES FROM VINYL STANNANES. *Synthetic Communications* **1992**, 22 (10), 1461-1471; (b) Tius, M. A.; Kawakami, J. K., Rapid Fluorination of Alkenyl Stannanes with Silver Triflate and Xenon Difluoride. *Synlett* **1993**, 1993 (03), 207-208; (c) Tius, M. A.; Kawakami, J. K., The reaction

of XeF₂ with trialkylvinylstannanes: Scope and some mechanistic observations. *Tetrahedron* **1995**, *51* (14), 3997-4010.

48. Furuya, T.; Strom, A. E.; Ritter, T., Silver-Mediated Fluorination of Functionalized Aryl Stannanes. *Journal of the American Chemical Society* **2009**, *131* (5), 1662-1663.

49. Powers, D. C.; Benitez, D.; Tkatchouk, E.; Goddard, W. A.; Ritter, T., Bimetallic Reductive Elimination from Dinuclear Pd(III) Complexes. *Journal of the American Chemical Society* **2010**, *132* (40), 14092-14103.

50. Fier, P. S.; Hartwig, J. F., Selective C-H Fluorination of Pyridines and Diazines Inspired by a Classic Amination Reaction. *Science* **2013**, *342* (6161), 956-960.

51. Furuya, T.; Kaiser, H. M.; Ritter, T., Palladium-mediated fluorination of arylboronic acids. *Angewandte Chemie-International Edition* **2008**, *47* (32), 5993-5996.

52. Furuya, T.; Ritter, T., Carbon-Fluorine Reductive Elimination from a High-Valent Palladium Fluoride. *Journal of the American Chemical Society* **2008**, *130* (31), 10060-10061.

53. Furuya, T.; Benitez, D.; Tkatchouk, E.; Strom, A. E.; Tang, P.; Goddard, W. A., III; Ritter, T., Mechanism of C-F Reductive Elimination from Palladium(IV) Fluorides. *Journal of the American Chemical Society* **2010**, *132* (11), 3793-3807.

54. (a) Yin, F.; Wang, Z.; Li, Z.; Li, C., Silver-Catalyzed Decarboxylative Fluorination of Aliphatic Carboxylic Acids in Aqueous Solution. *Journal of the American Chemical Society* **2012**, 10401-10404; (b) Rueda-Becerril, M.; Chatalova Sazepin, C.; Leung, J. C. T.; Okbinoglu, T.; Kennepohl, P.; Paquin, J.-F.; Sammis, G. M., Fluorine Transfer to Alkyl Radicals. *Journal of the American Chemical Society* **2012**, *134* (9), 4026-4029; (c) Leung, J. C. T.; Chatalova-Sazepin, C.; West, J. G.; Rueda-Becerril, M.; Paquin, J.-F.; Sammis, G. M., Photo-fluorodecarboxylation of 2-Aryloxy and 2-Aryl Carboxylic Acids. *Angewandte Chemie International Edition* **2012**, *51* (43), 10804-10807.

55. Liu, W.; Huang, X.; Cheng, M. J.; Nielsen, R. J.; Goddard, W. A.; Groves, J. T., Oxidative Aliphatic C-H Fluorination with Fluoride Ion Catalyzed by a Manganese Porphyrin. *Science* **2012**, *337* (6100), 1322-1325.

56. Bloom, S.; Pitts, C. R.; Miller, D. C.; Haselton, N.; Holl, M. G.; Urheim, E.; Lectka, T., A Polycomponent Metal-Catalyzed Aliphatic, Allylic, and Benzylic Fluorination. *Angewandte Chemie International Edition* **2012**, *51* (42), 10580-10583.

57. (a) Amaoka, Y.; Nagatomo, M.; Inoue, M., Metal-Free Fluorination of C(sp³)-H Bonds Using a Catalytic N-Oxyl Radical. *Organic Letters* **2013**, *15* (9), 2160-2163; (b) Bloom, S.; Knippel, J. L.; Lectka, T., A photocatalyzed aliphatic fluorination. *Chemical Science* **2014**, *5* (3), 1175-1178; (c) Kee, C. W.; Chin, K. F.; Wong, M. W.; Tan, C.-H., Selective fluorination of alkyl C-H bonds via photocatalysis. *Chemical Communications* **2014**, *50* (60), 8211-8214; (d) Xia, J.-B.; Ma, Y.; Chen, C., Vanadium-catalyzed C(sp³)-H fluorination reactions. *Organic Chemistry Frontiers* **2014**, *1* (5), 468-472.

58. Godula, K.; Sames, D., C-H Bond Functionalization in Complex Organic Synthesis. *Science* **2006**, *312* (5770), 67-72.

59. Wencel-Delord, J.; Glorius, F., C-H bond activation enables the rapid construction

and late-stage diversification of functional molecules. *Nat Chem* **2013**, 5 (5), 369-375.

60. (a) Dai, H.-X.; Stepan, A. F.; Plummer, M. S.; Zhang, Y.-H.; Yu, J.-Q., Divergent C–H Functionalizations Directed by Sulfonamide Pharmacophores: Late-Stage Diversification as a Tool for Drug Discovery. *Journal of the American Chemical Society* **2011**, 133 (18), 7222-7228; (b) Pham, M. V.; Ye, B.; Cramer, N., Access to Sultams by Rhodium(III)-Catalyzed Directed C–H Activation. *Angewandte Chemie International Edition* **2012**, 51 (42), 10610-10614; (c) Meyer, C.; Neue, B.; Schepmann, D.; Yanagisawa, S.; Yamaguchi, J.; Wurthwein, E.-U.; Itami, K.; Wunsch, B., Exploitation of an additional hydrophobic pocket of σ_1 receptors: Late-stage diverse modifications of spirocyclic thiophenes by C–H bond functionalization. *Organic & Biomolecular Chemistry* **2011**, 9 (23), 8016-8029; (d) Meyer, C.; Schepmann, D.; Yanagisawa, S.; Yamaguchi, J.; Itami, K.; Wünsch, B., Late-Stage C–H Bond Arylation of Spirocyclic σ_1 Ligands for Analysis of Complementary σ_1 Receptor Surface. *European Journal of Organic Chemistry* **2012**, 2012 (30), 5972-5979.
61. (a) Dick, A. R.; Sanford, M. S., Transition metal catalyzed oxidative functionalization of carbon-hydrogen bonds. *Tetrahedron* **2006**, 62 (11), 2439-2463; (b) Lyons, T. W.; Sanford, M. S., Palladium-Catalyzed Ligand-Directed C–H Functionalization Reactions. *Chemical Reviews* **2010**, 110 (2), 1147-1169; (c) Kuhl, N.; Hopkinson, M. N.; Wencel-Delord, J.; Glorius, F., Beyond Directing Groups: Transition-Metal-Catalyzed CH Activation of Simple Arenes. *Angewandte Chemie International Edition* **2012**, 51 (41), 10236-10254.
62. (a) Engle, K. M.; Mei, T.-S.; Wasa, M.; Yu, J.-Q., Weak Coordination as a Powerful Means for Developing Broadly Useful C–H Functionalization Reactions. *Accounts of Chemical Research* **2011**, 45 (6), 788-802; (b) Neufeldt, S. R.; Sanford, M. S., Controlling Site Selectivity in Palladium-Catalyzed C–H Bond Functionalization. *Accounts of Chemical Research* **2012**, 45 (6), 936-946.
63. Emmert, M. H.; Cook, A. K.; Xie, Y. J.; Sanford, M. S., Remarkably High Reactivity of Pd(OAc)₂/Pyridine Catalysts: Nondirected C–H Oxygenation of Arenes. *Angewandte Chemie International Edition* **2011**, 50 (40), 9409-9412.
64. Kalyani, D.; Sanford, M. S., Regioselectivity in Palladium-Catalyzed C–H Activation/Oxygenation Reactions. *Organic Letters* **2005**, 7 (19), 4149-4152.
65. Murai, S.; Kakiuchi, F.; Sekine, S.; Tanaka, Y.; Kamatani, A.; Sonoda, M.; Chatani, N., Efficient catalytic addition of aromatic carbon-hydrogen bonds to olefins. *Nature* **1993**, 366 (6455), 529-531.
66. Leow, D.; Li, G.; Mei, T.-S.; Yu, J.-Q., Activation of remote meta-C-H bonds assisted by an end-on template. *Nature* **2012**, 486 (7404), 518-522.
67. Bag, S.; Patra, T.; Modak, A.; Deb, A.; Maity, S.; Dutta, U.; Dey, A.; Kancherla, R.; Maji, A.; Hazra, A.; Bera, M.; Maiti, D., Remote para-C–H Functionalization of Arenes by a D-Shaped Biphenyl Template-Based Assembly. *Journal of the American Chemical Society* **2015**, 137 (37), 11888-11891.
68. (a) Cho, S. H.; Kim, J. Y.; Kwak, J.; Chang, S., Recent advances in the transition metal-catalyzed twofold oxidative C-H bond activation strategy for C-C and C-N bond formation. *Chemical Society Reviews* **2011**, 40 (10), 5068-5083; (b) Hirano, K.; Miura, M., Direct Carbon-Hydrogen Bond Functionalization of Heterocyclic Compounds. *Synlett* **2011**,

2011 (03), 294-307; (c) Zhao, D.; You, J.; Hu, C., Recent Progress in Coupling of Two Heteroarenes. *Chemistry – A European Journal* **2011**, 17 (20), 5466-5492; (d) Fagnou, K., Mechanistic considerations in the development and use of azine, diazine and azole N-oxides in palladium-catalyzed direct arylation. (0340-1022 (Print)); (e) Beck, E. M.; Gaunt, M. J., Pd-catalyzed C-H bond functionalization on the indole and pyrrole nucleus. (0340-1022 (Print)); (f) Joucla, L.; Djakovitch, L., Transition Metal-Catalysed, Direct and Site-Selective N1-, C2- or C3-Arylation of the Indole Nucleus: 20 Years of Improvements. *Advanced Synthesis & Catalysis* **2009**, 351 (5), 673-714; (g) Seregin, I. V.; Gevorgyan, V., Direct transition metal-catalyzed functionalization of heteroaromatic compounds. *Chemical Society Reviews* **2007**, 36 (7), 1173-1193; (h) Bugaut, X.; Glorius, F., Palladium-Catalyzed Selective Dehydrogenative Cross-Couplings of Heteroarenes. *Angewandte Chemie International Edition* **2011**, 50 (33), 7479-7481; (i) Armstrong, A.; Collins, J. C., Direct Azole Amination: C-H Functionalization as a New Approach to Biologically Important Heterocycles. *Angewandte Chemie International Edition* **2010**, 49 (13), 2282-2285; (j) Brückl, T.; Baxter, R. D.; Ishihara, Y.; Baran, P. S., Innate and Guided C-H Functionalization Logic. *Accounts of Chemical Research* **2012**, 45 (6), 826-839; (k) Shul'pin, G. B., Selectivity enhancement in functionalization of C-H bonds: A review. *Organic & Biomolecular Chemistry* **2010**, 8 (19), 4217-4228.

69. Lane, B. S.; Brown, M. A.; Sames, D., Direct Palladium-Catalyzed C-2 and C-3 Arylation of Indoles: A Mechanistic Rationale for Regioselectivity. *Journal of the American Chemical Society* **2005**, 127 (22), 8050-8057.

70. Gorelsky, S. I.; Lapointe, D.; Fagnou, K., Analysis of the Palladium-Catalyzed (Aromatic)C-H Bond Metalation-Deprotonation Mechanism Spanning the Entire Spectrum of Arenes. *The Journal of Organic Chemistry* **2012**, 77 (1), 658-668.

71. Kharasch, M. S.; Isbell, H. S., THE CHEMISTRY OF ORGANIC GOLD COMPOUNDS. III. DIRECT INTRODUCTION OF GOLD INTO THE AROMATIC NUCLEUS (PRELIMINARY COMMUNICATION). *Journal of the American Chemical Society* **1931**, 53 (8), 3053-3059.

72. Lafrance, M.; Rowley, C. N.; Woo, T. K.; Fagnou, K., Catalytic Intermolecular Direct Arylation of Perfluorobenzenes. *Journal of the American Chemical Society* **2006**, 128 (27), 8754-8756.

73. Gorelsky, S. I.; Lapointe, D.; Fagnou, K., Analysis of the Concerted Metalation-Deprotonation Mechanism in Palladium-Catalyzed Direct Arylation Across a Broad Range of Aromatic Substrates. *Journal of the American Chemical Society* **2008**, 130 (33), 10848-10849.

74. Davidson, J. M.; Triggs, C., Reaction of metal ion complexes with hydrocarbons. Part I. 'Palladation' and some other new electrophilic substitution reactions. The preparation of palladium(I). *Journal of the Chemical Society A: Inorganic, Physical, Theoretical* **1968**, (0), 1324-1330.

75. Tan, Y.; Hartwig, J. F., Assessment of the Intermediacy of Arylpalladium Carboxylate Complexes in the Direct Arylation of Benzene: Evidence for C-H Bond Cleavage by "Ligandless" Species. *Journal of the American Chemical Society* **2011**, 133 (10), 3308-3311.

76. (a) Ishiyama, T.; Takagi, J.; Ishida, K.; Miyaura, N.; Anastasi, N. R.; Hartwig, J. F., Mild Iridium-Catalyzed Borylation of Arenes. High Turnover Numbers, Room Temperature Reactions, and Isolation of a Potential Intermediate. *Journal of the American Chemical Society* **2002**, *124* (3), 390-391; (b) Ishiyama, T.; Nobuta, Y.; Hartwig, J. F.; Miyaura, N., Room temperature borylation of arenes and heteroarenes using stoichiometric amounts of pinacolborane catalyzed by iridium complexes in an inert solvent. *Chemical Communications* **2003**, (23), 2924-2925; (c) Tajuddin, H.; Harrisson, P.; Bitterlich, B.; Collings, J. C.; Sim, N.; Batsanov, A. S.; Cheung, M. S.; Kawamorita, S.; Maxwell, A. C.; Shukla, L.; Morris, J.; Lin, Z.; Marder, T. B.; Steel, P. G., Iridium-catalyzed C-H borylation of quinolines and unsymmetrical 1,2-disubstituted benzenes: insights into steric and electronic effects on selectivity. *Chemical Science* **2012**, *3* (12), 3505-3515.
77. Cheng, C.; Hartwig, J. F., Rhodium-Catalyzed Intermolecular C–H Silylation of Arenes with High Steric Regiocontrol. *Science* **2014**, *343* (6173), 853-857.
78. Boller, T. M.; Murphy, J. M.; Hapke, M.; Ishiyama, T.; Miyaura, N.; Hartwig, J. F., Mechanism of the Mild Functionalization of Arenes by Diboron Reagents Catalyzed by Iridium Complexes. Intermediacy and Chemistry of Bipyridine-Ligated Iridium Trisboryl Complexes. *Journal of the American Chemical Society* **2005**, *127* (41), 14263-14278.
79. Saito, Y.; Segawa, Y.; Itami, K., para-C–H Borylation of Benzene Derivatives by a Bulky Iridium Catalyst. *Journal of the American Chemical Society* **2015**.
80. (a) Brown, J. M.; Gouverneur, V., Transition-Metal-Mediated Reactions for Csp²–F Bond Construction: The State of Play. *Angewandte Chemie International Edition* **2009**, *48* (46), 8610-8614; (b) Furuya, T.; Klein, J.; Ritter, T., Carbon-Fluorine Bond Formation for the Synthesis of Aryl Fluorides. *Synthesis* **2010**, *2010* (11), 1804-1821; (c) Furuya, T.; Kamlet, A. S.; Ritter, T., Catalysis for fluorination and trifluoromethylation. *Nature* **2011**, *473* (7348), 470-477.
81. (a) Noël, T.; Maimone, T. J.; Buchwald, S. L., Accelerating palladium-catalyzed C-F bond formation: use of a microflow packed-bed reactor. *Angewandte Chemie International Edition* **2011**, *50* (38), 8900-8903; (b) Maimone, T. J.; Milner, P. J.; Kinzel, T.; Zhang, Y.; Takase, M. K.; Buchwald, S. L., Evidence for in Situ Catalyst Modification during the Pd-Catalyzed Conversion of Aryl Triflates to Aryl Fluorides. *Journal of the American Chemical Society* **2011**, *133* (45), 18106-18109.
82. (a) Hull, K. L.; Anani, W. Q.; Sanford, M. S., Palladium-Catalyzed Fluorination of Carbon–Hydrogen Bonds. *Journal of the American Chemical Society* **2006**, *128* (22), 7134-7135; (b) McMurtrey, K. B.; Racowski, J. M.; Sanford, M. S., Pd-Catalyzed C–H Fluorination with Nucleophilic Fluoride. *Organic Letters* **2012**, *14* (16), 4094-4097.
83. Wang, X.; Mei, T.-S.; Yu, J.-Q., Versatile Pd(OTf)₂·2H₂O-Catalyzed ortho-Fluorination Using NMP as a Promoter. *Journal of the American Chemical Society* **2009**, *131* (22), 7520-7521.
84. Sladojevich, F.; Arlow, S. I.; Tang, P.; Ritter, T., Late-Stage Deoxyfluorination of Alcohols with PhenoFluor. *Journal of the American Chemical Society* **2013**, *135* (7), 2470-2473.
85. Fier, P. S.; Hartwig, J. F., Copper-Mediated Fluorination of Aryl Iodides. *Journal of*

the American Chemical Society **2012**, 134 (26), 10795-10798.

86. (a) Furuya, T.; Ritter, T., Fluorination of Boronic Acids Mediated by Silver(I) Triflate. *Organic Letters* **2009**, 11 (13), 2860-2863; (b) Tang, P.; Ritter, T., Silver-mediated fluorination of aryl silanes. *Tetrahedron* **2011**, 67 (24), 4449-4454.
87. Furuya, T.; Kaiser, H. M.; Ritter, T., Palladium-Mediated Fluorination of Arylboronic Acids. *Angewandte Chemie International Edition* **2008**, 47, 5993-5996.
88. (a) Fier, P. S.; Luo, J.; Hartwig, J. F., Copper-Mediated Fluorination of Arylboronate Esters. Identification of a Copper(III) Fluoride Complex. *Journal of the American Chemical Society* **2013**, 135 (7), 2552-2559; (b) Ye, Y.; Sanford, M. S., Mild Copper-Mediated Fluorination of Aryl Stannanes and Aryl Trifluoroborates. *Journal of the American Chemical Society* **2013**, 135 (12), 4648-4651.
89. (a) Powers, D. C.; Ritter, T., Palladium(III) in Synthesis and Catalysis. *Topics in organometallic chemistry* **2011**, 35, 129-156; (b) Mirica, L. M.; Khusnutdinova, J. R., Structure and electronic properties of Pd (III) complexes. *Coordination Chemistry Reviews* **2012**, 257, 299-314; (c) Lanci, M. P.; Remy, M. S.; Kaminsky, W.; Mayer, J. M.; Sanford, M. S., Oxidatively Induced Reductive Elimination from (tBu 2bpy)Pd(Me) 2: Palladium(IV) Intermediates in a One-Electron Oxidation Reaction. *Journal of the American Chemical Society* **2009**, 131 (43), 15618-15620; (d) Khusnutdinova, J. R.; Rath, N. P.; Mirica, L. M., The Aerobic Oxidation of a Pd(II) Dimethyl Complex Leads to Selective Ethane Elimination from a Pd(III) Intermediate. *Journal of the American Chemical Society* **2012**, 134 (4), 2414-2422; (e) Powers, D. C.; Ritter, T., Bimetallic Pd(III) complexes in palladium-catalysed carbon-heteroatom bond formation. *Nat Chem* **2009**, 1 (4), 302-309; (f) Powers, D. C.; Geibel, M. A. L.; Klein, J. E. M. N.; Ritter, T., Bimetallic Palladium Catalysis: Direct Observation of Pd(III)-Pd(III) Intermediates. *Journal of the American Chemical Society* **2009**, 131 (47), 17050-17051; (g) Powers, D. C.; Xiao, D. Y.; Geibel, M. A. L.; Ritter, T., On the Mechanism of Palladium-Catalyzed Aromatic C-H Oxidation. *Journal of the American Chemical Society* **2010**, 132 (41), 14530-14536; (h) Chuang, G. J.; Wang, W.; Lee, E.; Ritter, T., A Dinuclear Palladium Catalyst for α -Hydroxylation of Carbonyls with O₂. *Journal of the American Chemical Society* **2011**, 133 (6), 1760-1762; (i) Campbell, M. G.; Powers, D. C.; Raynaud, J.; Graham, M. J.; Xie, P.; Lee, E.; Ritter, T., Synthesis and structure of solution-stable one-dimensional palladium wires. *Nat Chem* **2011**, 3 (12), 949-953; (j) Powers, D. C.; Lee, E.; Ariafard, A.; Sanford, M. S.; Yates, B. F.; Canty, A. J.; Ritter, T., Connecting Binuclear Pd(III) and Mononuclear Pd(IV) Chemistry by Pd-Pd Bond Cleavage. *Journal of the American Chemical Society* **2012**, 134 (29), 12002-12009.
90. (a) Serguchev, Y. A.; Ponomarenko, M. V.; Lourie, L. F.; Fokin, A. A., Transannular additions of selectfluor and xenon difluoride: regioselectivity and mechanism. *Journal of Physical Organic Chemistry* **2010**, 24 (5), 407-413; (b) Nesterenko, A. M.; Ponomarenko, M. V.; Lur'e, L. F.; Serguchev, Y. A., Quantum-Chemical Study of the Mechanism and Regioselectivity of Transannular Cyclization of Dienes of the Bicyclo [3.3. 1] nonane Series Treated with Bromosuccinimide and F-TEDA-BF₄. *Theoretical and Experimental Chemistry* **2002**, 38 (3), 156-161; (c) Zhang, X.; Wang, H.; Guo, Y., Interception of the radicals produced in electrophilic fluorination with radical traps (Tempo, Dmpo) studied by electrospray ionization mass spectrometry. *Rapid Communications in Mass Spectrometry* **2006**, 20 (12), 1877-1882; (d) Zhang, X.; Liao, Y.; Qian, R.; Wang, H.; Guo, Y., Investigation of Radical Cation in Electrophilic Fluorination by ESI-MS. *Organic Letters* **2005**, 7 (18), 3877-3880; (e) Nyffeler, P. T.; Dur n, S. G.; Burkart, M. D.; Vincent, S. p. P.;

Wong, C.-H., Selectfluor: Mechanistic Insight and Applications. *Angewandte Chemie International Edition* **2005**, *44* (2), 192-212.

91. Furuya, T.; Benitez, D.; Tkatchouk, E.; Strom, A. E.; Tang, P.; Goddard, I., William A.; Ritter, T., Mechanism of C–F Reductive Elimination from Palladium(IV) Fluorides. *Journal of the American Chemical Society* **2010**, *132* (11), 3793-3807.

92. Taylor, R., *Electrophilic Aromatic Substitution*. John Wiley & Sons: West Sussex, England, 1990.

93. Mkhaliid, I. A. I.; Barnard, J. H.; Marder, T. B.; Murphy, J. M.; Hartwig, J. F., C–H Activation for the Construction of C–B Bonds. *Chemical Reviews* **2009**, *110* (2), 890-931.

94. (a) Romero, N. A.; Margrey, K. A.; Tay, N. E.; Nicewicz, D. A., Site-selective arene C–H amination via photoredox catalysis. *Science* **2015**, *349* (6254), 1326-1330; (b) Sibbald, P. A.; Rosewall, C. F.; Swartz, R. D.; Michael, F. E., Mechanism of N-Fluorobenzenesulfonimide Promoted Diamination and Carboamination Reactions: Divergent Reactivity of a Pd(IV) Species. *Journal of the American Chemical Society* **2009**, *131* (43), 15945-15951; (c) Wang, X.; Leow, D.; Yu, J.-Q., Pd(II)-Catalyzed para-Selective C–H Arylation of Monosubstituted Arenes. *Journal of the American Chemical Society* **2011**, *133* (35), 13864-13867.

95. Carey, F. A. S. R. J., *Advanced Organic Chemistry*. Fifth Edition ed.; Springer: New York, NY, 2007; Vol. 1.

96. Boursalian, G. B.; Ngai, M.-Y.; Hojczyk, K. N.; Ritter, T., Pd-Catalyzed Aryl C–H Imidation with Arene as the Limiting Reagent. *Journal of the American Chemical Society* **2013**, *135* (36), 13278-13281.

97. (a) Fischer, H.; Radom, L., Factors Controlling the Addition of Carbon-Centered Radicals to Alkenes—An Experimental and Theoretical Perspective. *Angewandte Chemie International Edition* **2001**, *40* (8), 1340-1371; (b) Wong, M. W.; Pross, A.; Radom, L., Comparison of the Addition of CH₃.bul., CH₂OH.bul., and CH₂CN.bul. Radicals to Substituted Alkenes: A Theoretical Study of the Reaction Mechanism. *Journal of the American Chemical Society* **1994**, *116* (14), 6284-6292; (c) Wong, M. W.; Pross, A.; Radom, L., Addition of tert-Butyl Radical to Substituted Alkenes: A Theoretical Study of the Reaction Mechanism. *Journal of the American Chemical Society* **1994**, *116* (26), 11938-11943.

98. (a) Parr, R. G.; Yang, W., Density functional approach to the frontier-electron theory of chemical reactivity. *Journal of the American Chemical Society* **1984**, *106* (14), 4049-4050; (b) Lewars, E., *Computational Chemistry*. Kluwer Academic Publishers: Norwell, Massachusetts, 2003; (c) Ayers, P. W.; Levy, M., Perspective on “Density functional approach to the frontier-electron theory of chemical reactivity”. *Theoretical Chemistry Accounts* **2000**, *103* (3-4), 353-360.

99. Traynham, J. G., Ipso substitution in free-radical aromatic substitution reactions. *Chemical Reviews* **1979**, *79* (4), 323-330.

100. (a) Pitts, C. R.; Bloom, S.; Woltornist, R.; Auvenshine, D. J.; Ryzhkov, L. R.; Siegler, M. A.; Lectka, T., Direct, Catalytic Monofluorination of sp³ C–H Bonds: A Radical-Based

Mechanism with Ionic Selectivity. *Journal of the American Chemical Society* **2014**, *136* (27), 9780-9791; (b) Michaudel, Q.; Thevenet, D.; Baran, P. S., Intermolecular Ritter-Type C–H Amination of Unactivated sp³ Carbons. *Journal of the American Chemical Society* **2012**, *134* (5), 2547-2550.

101. Cheng, Y.; Gu, X.; Li, P., Visible-Light Photoredox in Homolytic Aromatic Substitution: Direct Arylation of Arenes with Aryl Halides. *Organic Letters* **2013**, *15* (11), 2664-2667.

102. Allen, L. J.; Cabrera, P. J.; Lee, M.; Sanford, M. S., N-Acyloxyphthalimides as Nitrogen Radical Precursors in the Visible Light Photocatalyzed Room Temperature C–H Amination of Arenes and Heteroarenes. *Journal of the American Chemical Society* **2014**, *136* (15), 5607-5610.

103. (a) Citterio, A.; Gentile, A.; Minisci, F.; Navarrini, V.; Serravalle, M.; Ventura, S., Polar effects in free radical reactions. Homolytic aromatic amination by the amino radical cation, $\cdot\text{CnH}_{2n+1}\text{NH}_2$: reactivity and selectivity. *The Journal of Organic Chemistry* **1984**, *49* (23), 4479-4482; (b) Minisci, F., Novel Applications of Free-Radical Reactions in Preparative Organic Chemistry. *Synthesis* **1973**, (1), 1-24; (c) Minisci, F., Nuovi Processi per Introdurre l'azoto in Molecole Organiche con Reazioni Radicaliche: Azidazione e Amminazione. *La Chimica e l'industria (Milano)* **1967**, *49* (7), 705-719.

104. Taylor, R. D.; MacCoss, M.; Lawson, A. D. G., Rings in Drugs. *Journal of Medicinal Chemistry* **2014**, *57* (14), 5845-5859.

105. Fischer, C.; Koenig, B., Palladium- and copper-mediated N-aryl bond formation reactions for the synthesis of biological active compounds. *Beilstein Journal of Organic Chemistry* **2011**, *7*, 59-74.

106. Still, W. C.; Kahn, M.; Mitra, A., Rapid chromatographic technique for preparative separations with moderate resolution. *The Journal of Organic Chemistry* **1978**, *43* (14), 2923-2925.

107. Fulmer, G. R.; Miller, A. J. M.; Sherden, N. H.; Gottlieb, H. E.; Nudelman, A.; Stoltz, B. M.; Bercaw, J. E.; Goldberg, K. I., NMR Chemical Shifts of Trace Impurities: Common Laboratory Solvents, Organics, and Gases in Deuterated Solvents Relevant to the Organometallic Chemist. *Organometallics* **2010**, *29* (9), 2176-2179.

108. Evans, D. F., The determination of the paramagnetic susceptibility of substances in solution by nuclear magnetic resonance. *J. Chem. Soc.* **1959**, 2003-2005.

109. Pingping Tang and Jennifer Murphy are acknowledged for discovering the fluorination reaction and for performing much of the early reaction optimization.

110. Hall, D. G., *Structure, Properties, and Preparation of Boronic Acid Derivatives. Overview of Their Reactions and Applications*. Wiley-VCH Verlag GmbH & Co. KGaA: 2006.

111. Ortiz, B. W., F.; Yuste, F.; Barrios, H.; Sanchez-Obregon, R. Pinelo, L., A Convenient Synthesis of Methyl- and Isopropyl-Benzyl Ethers Using Silver(II) Oxide as Reagent. *Synth. Commun.* **1993**, *23* (6), 749-756.

112. Michal Szostak, M. S., and David J. Procter, Electron Transfer Reduction of Carboxylic Acids Using SmI₂–H₂O–Et₃N. *Organic Letters* **2012**, *14* (3), 840-843.
113. Jonathan W. Lockner, D. D. D., Rune Risgaard, and Phil S. Baran, Practical Radical Cyclizations with Arylboronic Acids and Trifluoroborates. *Organic Letters* **2011**, *13* (20), 5628-5631.
114. Michael Campbell is acknowledged for performing the vast majority of the mechanistic work for the fluorination reaction described in the following sections.
115. Thordarson, P., Determining association constants from titration experiments in supramolecular chemistry. *Chem. Soc. Rev.* **2011**, *40*, 1305-1323.
116. Frisch, M. J.; Trucks, G. W.; Schlegel, H. B.; Scuseria, G. E.; Robb, M. A.; Cheeseman, J. R.; Scalmani, G.; Barone, V.; Mennucci, B.; Petersson, G. A.; Nakatsuji, H.; Caricato, M.; Li, X.; Hratchian, H. P.; Izmaylov, A. F.; Bloino, J.; Zheng, G.; Sonnenberg, J. L.; Hada, M.; Ehara, M.; Toyota, K.; Fukuda, R.; Hasegawa, J.; Ishida, M.; Nakajima, T.; Honda, Y.; Kitao, O.; Nakai, H.; Vreven, T.; Montgomery, J., J A; Peralta, J. E.; Ogliaro, F.; Bearpark, M. J.; Heyd, J.; Brothers, E. N.; Kudin, K. N.; Staroverov, V. N.; Kobayashi, R.; Normand, J.; Raghavachari, K.; Rendell, A. P.; Burant, J. C.; Iyengar, S. S.; Tomasi, J.; Cossi, M.; Rega, N.; Millam, N. J.; Klene, M.; Knox, J. E.; Cross, J. B.; Bakken, V.; Adamo, C.; Jaramillo, J.; Gomperts, R.; Stratmann, R. E.; Yazyev, O.; Austin, A. J.; Cammi, R.; Pomelli, C.; Ochterski, J. W.; Martin, R. L.; Morokuma, K.; Zakrzewski, V. G.; Voth, G. A.; Salvador, P.; Dannenberg, J. J.; Dapprich, S.; Daniels, A. D.; Farkas, Ö.; Foresman, J. B.; Ortiz, J. V.; Cioslowski, J.; Fox, D. J. *Gaussian 09*, Gaussian, Inc.: Wallingford, CT, USA, 2009.
117. (a) Andrae, D.; Häußermann, U.; Dolg, M.; Stoll, H.; Preuß, H., Energy-adjusted ab initio pseudopotentials for the second and third row transition elements. *Theoretica chimica acta* **1990**, *77* (2), 123-141; (b) Andrae, D.; Häußermann, U.; Dolg, M.; Stoll, H.; Preuß, H., Energy-adjusted ab initio pseudopotentials for the second and third row transition elements: Molecular test for M₂ (M=Ag, Au) and MH (M=Ru, Os). *Theoretica chimica acta* **1991**, *78* (4), 247-266.
118. Ehlers, A. W.; Böhme, M.; Dapprich, S.; Gobbi, A.; Höllwarth, A.; Jonas, V.; Köhler, K. F.; Stegmann, R.; Veldkamp, A.; Frenking, G., A set of f-polarization functions for pseudo-potential basis sets of the transition metals Sc–Cu, Y–Ag and La–Au. *Chemical Physics Letters* **1993**, *208* (1–2), 111-114.
119. Hariharan, P. C.; Pople, J. A., The influence of polarization functions on molecular orbital hydrogenation energies. *Theoretica chimica acta* **1973**, *28* (3), 213-222.
120. Chemissan, 3.3; Skripnikov Leonid: <http://www.chemissian.com>, 2005-2012.
121. Dennington, R. I. K., T. A.; Millam, J. M. *GaussView*, 5.0.8; Semichem, Inc.
122. (a) Folgado, J. V.; Henke, W.; Allmann, R.; Stratemeier, H.; Beltran-Porter, D.; Rojo, T.; Reinen, D., Fluxionality in hexacoordinated copper(II) complexes with 2,2':6',2''-terpyridine (terpy) and related ligands: structural and spectroscopic investigations. *Inorganic Chemistry* **1990**, *29* (11), 2035-2042; (b) Mack, K.; Wünsche von Leupoldt, A.; Förster, C.; Ezhevskaya, M.; Hinderberger, D.; Klinkhammer, K. W.; Heinze, K., Effect of Chelate Ring Expansion on Jahn–Teller Distortion and Jahn–Teller Dynamics in Copper(II) Complexes.

Inorganic Chemistry **2012**, 51 (14), 7851-7858.

123. Gilicinski, A. G.; Pez, G. P.; Syvret, R. G.; Lal, G. S., On the relative power of electrophilic fluorinating reagents of the N–F class. *Journal of Fluorine Chemistry* **1992**, 59 (1), 157-162.

124. Gregory Boursalian is acknowledged for discovering the TEDA substitution of arene C-H bonds, for exploring and discovering most of the early substrates to form Ar-TEDAs, and for the entirety of the mechanistic analysis for the reaction.

125. Won Seok Ham is acknowledged for synthesizing many of the complex aryl TEDA products described below.

126. Won Seok Ham is acknowledged for synthesizing, isolating, and characterizing the majority of the aryl piperazines described below.

127. Aue, D. H.; Webb, H. M.; Bowers, M. T., Quantitative proton affinities, ionization potentials, and hydrogen affinities of alkylamines. *Journal of the American Chemical Society* **1976**, 98 (2), 311-317.